The University of
Nottingham

THE MORPHOLOGICAL, BIOLOGICAL AND GENETIC CHARACTERISTICS OF LOW NUCLEAR GRADE BREAST CARCINOMA AND THEIR PUTATIVE PRECURSOR LESIONS

TAREK MOHAMED A. ABDEL-FATAH, MD

Thesis submitted to the University of Nottingham for

the degree of Doctor of Philosophy

October 2009

"In recent times, however, Egypt and Arab World, which gave to Science Ibn-Sina (Avicenna), Ibn-Rushd (Averroës), Ibn-Hayan (Geber), Ibn-Haytham (Al-Hazen), and others, have had no prizes in science or medicine. I sincerely hope that this first one will inspire the young generations of developing countries with knowledge that it is possible to contribute to world science and technology. "

Ahmed Zewail

Nobel Prize 1999

Abstract

There is evidence to suggest that some special types of breast cancer including tubular and lobular carcinoma and their putative precursor lesions including atypical ductal hyperplasia (ADH), low grade ductal carcinoma in-situ (DCIS) and lobular neoplasia (LN) may consist in a family of interrelated lesions. Recently, an attention has been focused on the columnar cell lesion as an early non-obligate precursor lesion of breast cancer.

In this study we examined this hypothesis by identifying the morphological and biological characteristics of these lesions. In addition, we used high resolution array comparative genomic hybridization to identify the molecular genetic profiles of invasive lobular and tubular carcinoma and their matched coexisting precursor lesions to investigate their relationship and to provide insight into some of the earliest events leading to invasive breast cancer. Moreover, by validating aspects of our immunohistochemical and in situ hybridization expression data with high throughput tissue microarrays, we identified potential oncogenes and tumour suppressor genes that could potentially drive the progression of BC and have clinicopathological implications on BC. Subsequently, diagnostic, predictive and genetic classifications of breast cancer and their putative precursor lesions were developed.

In summary, our results suggest that 1) Tubular and lobular breast carcinoma arise as members of a low nuclear grade breast neoplasia (LNGBN) family, 2) CCLs are early non-obligate precursor components of the LNGBN family, 3) The common cell of origin of the LNGBN family may be the oestrogen receptor-alpha (ER α) positive luminal restricted progenitor cell (ER+/MUC1+ cells) of the terminal duct lobular unit that might acquire stochastic genetic and epigenetic changes that eventually lead to activation of the luminal "A" pathway, 4) Cyclin D1 and MDM4 are oncogenes that potentially lead to

activation of the luminal pathway and progression of the LNGBN family, 5) An alteration of E-cadherin (*CDH1*) appears to be a secondary event resulting in the characteristic morphology of both in situ and invasive lobular lesions, 6) A biological grading system dependent on the balance between Bcl2 protein expression and mitotic figures could accurately reclassify patients with intermediately differentiated, small early stage or ER α negative breast cancers into two groups of low versus high risk of death and recurrence, and 7) The functional status of p53 transcriptional pathways can be assessed using immunohistochemistry protein expression of p53 downstream/regulator genes to accurately discriminate between low and high grade breast carcinoma and to assist routine clinical decision-making.

Publications arising from this thesis

1. Abdel-Fatah TM, Powe DG, Agboola J et al. The Biological, Clinical and Prognostic Implications of *TP53* Transcriptional pathways in Breast Cancers. *J Pathol* 2009. [Epub ahead of print].
2. Lancashire LJ, Powe DG, Reis-Filho JS et al. A validated gene expression profile for detecting clinical outcome in breast cancer using artificial neural networks. Breast Cancer Res Treat 2009. [Epub ahead of print]
3. Abdel-Fatah TM, Powe DG, Hodi Z et al. Morphologic and Molecular Evolutionary Pathways of Low Nuclear Grade Invasive Breast Cancers and Their Putative Precursor Lesions: Further Evidence to Support the Concept of Low Nuclear Grade Breast Neoplasia Family. Am J Surg Pathol 2008; 32:513-523
4. Abdel-Fatah TM, Powe DG, Hodi Z et al. High frequency of coexistence of columnar cell lesions, lobular neoplasia and low grade ductal carcinoma in situ with invasive tubular carcinoma and invasive lobular carcinoma. Am J Surg Pathol 2007; 31:417-426

Abstracts arising from this thesis

1. Abdel-Fatah TM, Powe DG, Lambros M et al. Role of columnar cell lesions as precursors of some forms of invasive breast carcinoma: A new genetic map for the evolutionary pathway of low nuclear grade breast neoplasia (LNGBN) family. In: ASCO Breast Cancer Symposium 2009; 8-10 Oct 2009; San Francisco, USA. Abstract number 132. Available from: http://www.asco.org/ASCOv2/Meetings/Abstracts?&vmview=abst_detail_view&confID=70&abstractID=40035.
2. Abdel-Fatah TM, Powe DG, Ball GR et al. The need for a biologic grading system and its relationship to the current Nottingham histologic grading system (NGS). In: ASCO Breast Cancer Symposium 2009; 8-10 Oct 2009; San Francisco, USA. Abstract number 29. Available from: http://www.asco.org/ASCOv2/Meetings/Abstracts?&vmview=abst_detail_view&confID=70&abstractID=40039.
3. Abdel-Fatah TM, Powe DG, Lambros M et al. Use of high resolution array comparative genomic hybridization (aCGH) to identify mouse double minutes 4 (MDM4) as an early genetic change in breast cancer development: Evaluation of MDM4 as a prognostic and predictive marker.). In: ASCO Breast Cancer Symposium 2009; 8-10 Oct 2009; San Francisco, USA. Abstract number 32. Available from: http://www.asco.org/ASCOv2/Meetings/Abstracts?&vmview=abst_detail_view&confID=70&abstractID=40038.
4. Abdel-Fatah TM, Powe DG, Lambros M et al. High resolution array Comparative Genomic Hybridization (aCGH) of breast carcinoma identifies Mouse Double Minutes 4 (Mdm4) as one of the early genetic changes in breast cancer development: Mdm4 is a new independent prognostic and predictive marker [abstract]. In: National Cancer Research Institute (NCRI) Cancer Conference 2009; 4-7 Oct 2009; Birmingham, UK. NCRI; Oct 2009. Abstract BOA 2. Available from: www.ncri.org.uk/ncriconference/archive/2009/abstracts/pdf/BOA2.pdf

5. Abdel-Fatah TM, Powe DG, Ball GR et al. The need for a biological grading system and its relationship to the current Nottingham histological grading system (NGS) [abstract]. In: National Cancer Research Institute (NCRI) Cancer Conference 2009; 4-7 Oct 2009; Birmingham, UK. NCRI; Oct 2009. Abstract BOA 3. Available from: www.ncri.org.uk/ncriconference/archive/2009/abstracts/pdf/BOA3.pdf
6. Abdel-Fatah TM, Powe DG, Lambros M et al. Columnar cell lesions are the early precursors of some forms of invasive breast carcinoma: a new genetic map for the evolutionary pathway of low nuclear grade breast neoplasia (LNGBN) family [abstract]. In: National Cancer Research Institute (NCRI) Cancer Conference 2009; 4-7 Oct 2009; Birmingham, UK. NCRI; Oct 2009. Abstract B69. Available from: www.ncri.org.uk/ncriconference/archive/2009/abstracts/pdf/B69.pdf
7. Abdel-Fatah TM, Powe DG, Lambros M et al. High resolution array Comparative Genomic Hybridization (aCGH) of breast carcinoma identifies Mouse double minutes 4 (Mdm4) as one of the early genetic changes in breast cancer development – Mdm4 is a new independent prognostic and predictive marker. EJC Supplements 2009; 7: 270. Joint ECCO 15 – 34th ESMO Multidisciplinary Congress Berlin, 20–24 September 2009 Abstract Book.
8. Abdel-Fatah TM, Powe DG, Ball GR et al. The need for a biological grading system and its relationship to the current Nottingham histological grading system (NGS). EJC Supplements 2009; 7: 264. Joint ECCO 15 – 34th ESMO Multidisciplinary Congress Berlin, 20–24 September 2009 Abstract Book
9. Abdel-Fatah TM, Powe DG, Lambros M et al. Columnar cell lesions are the early precursors of some forms of invasive breast carcinoma – a new genetic map for the evolutionary pathway of low nuclear grade breast neoplasia (LNGBN) family. EJC Supplements 2009; 7: 312-313. Joint ECCO 15 – 34th ESMO Multidisciplinary Congress Berlin, 20–24 September 2009 Abstract Book
10. Abdel-Fatah TM, Powe DG, Ball GR et al. The need for a biological grading system and its relationship to the current Nottingham histological grading system (NGS). J Pathol on-line supplement 2009; 219: S1-S63 (2009). www3.interscience.wiley.com/journal/122597546/issue.
11. Abdel-Fatah TM, Powe DG, Lambros M et al. High resolution array Comparative Genomic Hybridization (aCGH) of breast carcinoma identifies Mouse double minutes 4 (Mdm4) as one of the early genetic changes in breast cancer development – Mdm4 is a new independent prognostic and predictive marker. J Pathol on-line supplement 2009; 219: S1-S63 (2009). www3.interscience.wiley.com/journal/122597546/issue.
12. Abdel-Fatah TM, Powe DG, Agboola J et al. New highlights of Biological, Clinical and Prognostic Implications of *TP53* Transcriptional Status in Breast Cancers. In: National Cancer Research Institute (NCRI) Cancer Conference 2008; 5-8 Oct 2009; Birmingham, UK. NCRI; Oct 2008. Abstract B69. Available from: www.ncri.org.uk/ncriconference/archive/2008/abstracts/C47.htm
13. Abdel-Fatah TM, Powe DG, Agboola J et al. New highlights of Biological, Clinical and Prognostic Implications of *TP53* Transcriptional Status in Breast Cancers. In: ASCO Breast Cancer Symposium 2008; 5-7 Sep 2008; Washington DC, USA. Abstract number 11. Available from: http://www.asco.org/ASCOv2/Meetings/Abstracts?&vmview=abst_detail_view&confID=588&abstractID=40350.
14. Abdel-Fatah TM, Powe DG, Agboola J et al. New highlights of Biological, Clinical and Prognostic Implications of *TP53* Transcriptional Status in Breast Cancers. J Pathol 2008; 216: S1-65

15. Abdel-Fatah TM, Powe DG, Hodi Z et al. Morphological and molecular evolutionary pathways of low and high grade breast cancers and their putative precursor lesions. EJC Supplements 2007; 5: 12-13.
16. Abdel-Fatah TM, Powe DG, Lambros MBK et al. Optimisation of DNA extraction and amplification from laser microdissected paraffin embedded breast carcinoma for array comparative genomic hybridization (aCGH): Problems and solutions. Virchow Archiv 2007; 451: 191.
17. Abdel-Fatah TM, Powe DG, Hodi Z et al. Morphological and molecular evolutionary pathways of low and high grade breast cancers and their putative precursor lesions. Virchow Archiv 2007; 451: 143.
18. Abdel-Fatah TM, Powe DG, Hodi Z et al. Morphological and molecular evolutionary pathways of low grade invasive breast cancers and Their Putative Precursor lesions: Further evidence to support the concept of a low grade breast neoplasia family. J Pathol 2007; 213: 5A
19. Abdel-Fatah TM, Powe DG, Hodi Z et al. Morphological and molecular evolutionary pathways of low grade breast cancers and their putative precursor lesions. 96th Annual Meeting of the United-States-and-Canadian-Academy-of-Pathology, Mar 24-30, 2007 San Diego CA, USA. Laboratory investigation 2007; 87: 22A
20. Powe DG; Ademola, M; Lambros, MBK, Tarek Abdel-Fatah et al. Genomic profiling of heterogonous metaplastic breast carcinoma (MBC) show clonal similarities between different lesion types but also distinct differences which might account for their morphological features. 96th Annual Meeting of the United-States-and-Canadian-Academy-of-Pathology, Mar 24-30, 2007 San Diego CA, USA. Laboratory investigation 2007; 87: 45A
21. Abdel-Fatah TM, Powe DG, Hodi Z et al. Immunoprofile of Invasive Tubular Carcinoma, Tubulolobular and Invasive Lobular Carcinoma and their Coexistent Putative Precursor Lesions. J Pathol 2006; 210: 1A-67A.
22. Abdel-Fatah TM, Powe DG, Hodi Z et al. Immunophenotype similarity and high frequency of co-existence of columnar cell lesions, lobular neoplasia, and low grade DCIS with invasive tubular carcinoma and invasive lobular carcinoma. EJC Supplements 2006;4:121-122
23. Abdel-Fatah TM, Powe DG, Hodi Z et al. High frequency of co-existence of columnar cell lesions, lobular neoplasia, and low grade DCIS with invasive tubular carcinoma and invasive lobular carcinoma. J Pathol 2006; 208: 1-35

Acknowledgements

I would like to express my deepest and sincere gratitude to my supervisor, Professor Ian O Ellis, Professor of Cancer Pathology, Pathology Department, University of Nottingham, Nottingham, UK, for his outstanding and unlimited support. His wide knowledge and his logical way of thinking have been of great value for me. His understanding, encouraging and personal guidance have provided the basis for the present thesis. His ideals and concepts have had a remarkable influence on my entire career in the field of breast cancer.

I am deeply grateful to my co-supervisor, DR. Des G Powe, PhD., Histopathology Department , Queen's Medical Centre, University of Nottingham, for his detailed and constructive comments and advice. He dedicated a lot of his time to direct and guide me through this work. His support was a cornerstone of this work.

I wish to express my warm and sincere thanks to DR Jorge S Reis-Filho and his colleagues at The Breakthrough Breast Cancer Research Centre, Institute of Cancer Research, London for his support and providing unlimited valuable experience and facilities for our work. It was a fruitful collaboration between his team and ours at Nottingham University.

I warmly thank Dr. Andrew Green, Senior Research Fellow, University of Nottingham for his valuable advice and friendly help.

During this work I have collaborated with many colleagues for whom I have great regard, and I wish to extend my warmest thanks to all those who have helped me with my work in the Department of Pathology in both Queen's Medical Centre and City Hospital Campus at Nottingham University, Pathology Department of Cambridge University and Histopathology and Molecular units at the Breakthrough Breast Cancer Research Centre, Institute of Cancer Research, London, UK.

I owe my thanks to my family in Egypt, my wife and my kids. They have lost a lot due to my research abroad. Without their encouragement and understanding it would have been impossible for me to finish this work.

My special gratitude is due to the Egyptian Government, National Liver Institute, and Minoufyia University, Egypt who provide the f financial support for my studentship and studies.

Tarek Abdel-Fatah

TABLE OF CONTENTS

LIST OF FIGURES

Number Page

LIST OF TABLES

Number Page

List of abbreviations

ADH	Atypical Ductal Hyperplasia
ALH	Atypical Lobular Hyperplasia
a CGH	array-Comparative Genomic Hybridization
AT	Adjuvant systemic Therapy
BC	Breast Cancer
BCSS	Breast Cancer Specific Survival
CCC	Columnar Cell Changes
CCH	Columnar Cell Hyperplasia
CCLs	Columnar Cell Lesions
CEP17	Centromere 17
CGH	Comparative genomic hybridization
CI	Confidence Intervals
CISH	Chromogenic In Situ Hybridisation
CK	Cytokeratin
CMF	Cyclophosphamide, Methotrexate, and 5-Fluorouracil
DAB	Diaminobenzidine
DCIS	Ductal Carcinoma In Situ
DFS	Disease Free Survival
DM	Distant Metastases
DSS	Disease Specific Survival
ER	Oestrogen Receptor
ER-α	Oestrogen receptor alpha
ESA	Epithelial Specific Antigen
EPG	Excellent Prognostic Group
FEA	Flat Epithelial Atypia
FISH	Fluorescence In Situ Hybridisation

G	Grade
GPG	Good Prognostic Group
HBEC	Human Breast Epithelial Cell
H&E	Haematoxylin and Eosin
HGBC	High Grade Breast Cancer
HNGBC	High Nuclear Grade Breast Cancer
HR	Hazard Ratio
HRP	Horseradish Peroxidase
HT	Hormonal Therapy
ICC	Invasive Cribriform Carcinoma
IDC	Invasive Ductal Carcinoma
IDC-NST	Invasive Ductal Carcinoma of No Special Type
ILC	Invasive Lobular Carcinoma
IHC	Immunohistochemistry
LCM	Laser Capture Micro-dissection
LGBC	Low Grade Breast Cancers
LN	Lobular Neoplasia
LNGBC	Low Nuclear Grade Breast Carcinoma
LOH	Loss of Heterozygosity
LPC	Laser Pressure Captured
LR	Local Recurrence
M	Mitotic Index.
M1	Low Mitotic Index
M2	Moderate Mitotic Index
M3	High Mitotic Index
MFS	Metastases Free Survival
mNPI	modified Nottingham Prognostic Index

MPG	Moderate Prognostic Group
NHSBSP	NHS Breast Screening Programme
NGS	Nottingham Grading System
NPI	Nottingham Prognostic Index
PCR	Polymerase Chain Reaction
PI	Proliferation Index
P	Percentage
P2	Moderate Nuclear Pleomorphism
P3	Marked Nuclear Pleomorphism
PR	Progesterone Receptor
PPG	Poor Prognostic Group
RMH	Royal Marsden Hospital
SMA	Smooth Muscle Actin
T	Tubule formation
TBS	TRIS/HC1 Buffered Saline
TC	Tubular Carcinoma
TDLUs	Terminal Duct Lobular Units
TEB	Terminal End Bud
TLC	Tubulolobular Carcinoma
TMA	Tissue Micro Array
TSG	Tumour Suppressor Gene
UK	United Kingdom
UEH	Usual Epithelial Hyperplasia
VPG	Very Poor Prognostic Group
WHO	World Health Organization

Chapter 1:

Introduction

Breast cancer (BC) is the third most common tumour in the world, representing 9% of the global cancer burden, and is the second most common cause of death from cancer in women [1-3]. Globally, there are more than 4.4 million women living with BC and annually there are 410,712 BC-related deaths [1-3]. According to American Cancer Society 2009 estimates [1] there will be 192,370 new cases of BC diagnosed as well as 62,380 additional cases of in situ. In developing countries, there are 514,072 incident cases and 220,648 BC deaths [3]. In Europe, 2006 estimates indicated 429,900 new cases of BC diagnosed and 131,900 BC-related deaths [4]. In the UK, annually there are 37,000 new cases diagnosed [5-8] and 11,000 deaths recorded each year [9].

BC is considered as a diverse group of diseases in terms of presentation, morphology and molecular profile. BC taxonomy divides BCs into tumours of special types; lobular (ILC), tubulolobular (TLC), tubular (TC), mucinous, papillary, cribriform (ICC), medullary, adenoid cystic, metaplastic, adenosquamous and squamous and ductal carcinoma of no special type (IDC-NST) [10]. It is now believed that the morphological difference between 'lobular' and 'ductal' 'carcinoma' results from secondary genetic/epigenetic changes rather than a difference in cell of origin as the current view is that most breast cancers arise from the terminal duct lobular unit (TDLUs) [11].

1.1 Normal breast tissue

The female breasts are modified sweat glands composed of lobes and lobules interspersed with adipose tissue and connective tissue. The mammary gland is organized into a tree-like structure composed of hollow branches which are started with 6-10 large ducts and ended by the TDLUs [12]. TDLUs have an inner "epithelial cell layer" that face the lumen and an outer "myoepithelial cell layer" which produces the basal lamina separating the mammary parenchyma from the stroma [13] (**Figure 1-1**).

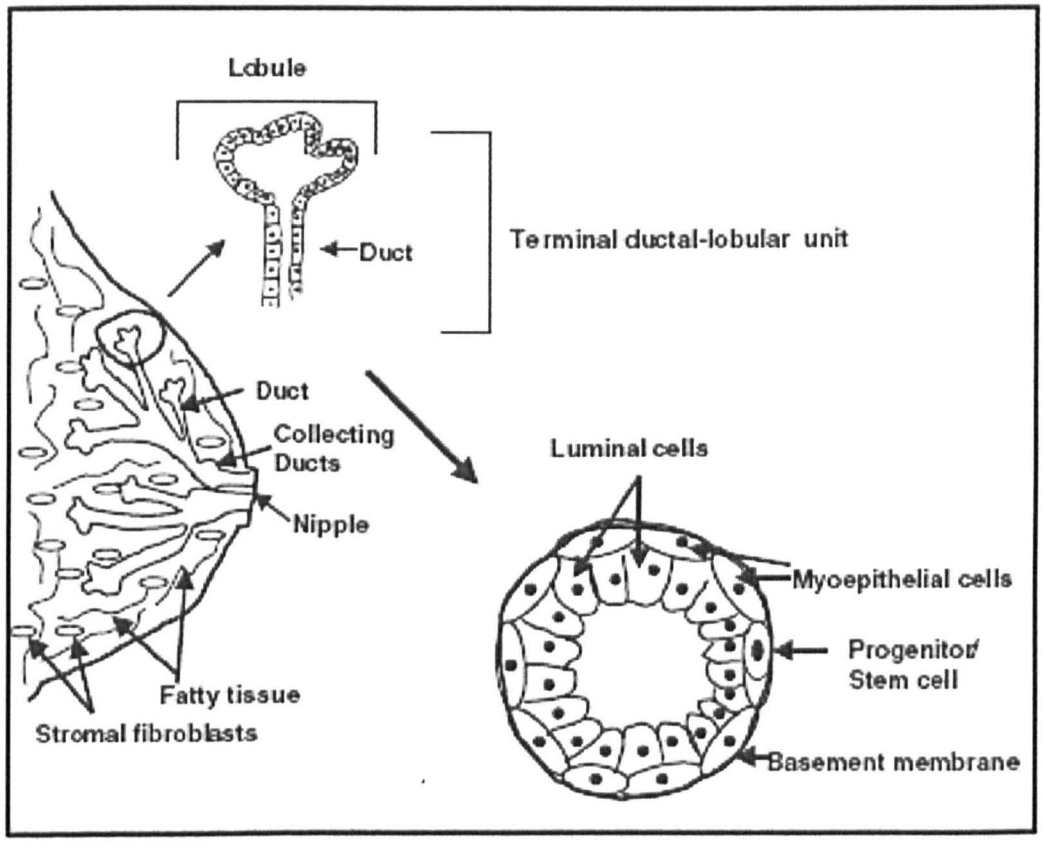

Figure 1-1: Structure of the normal breast tissue.

(Adapted from Dimri et al 2005 [12])

1.1.1 Developmental stages of the female breast

Intra-uterine development

During foetal development, the mammary gland epithelium is derived from the embryonic basal cells of the epidermis (the ectoderm) which from 28 weeks of intrauterine life, are rearranged into two cell layers - an inner luminal and a distinct outer basal cell layer [14]. The outer basal and inner luminal cell layers within the mammary epithelium express well defined immunophenotypes in vitro and vivo through the different stage of development of the breast [14]. All the epithelial cells of the breast bud retain the expression of cytokeratin 19 (CK19), but lose CK14 which is normally expressed in the epidermal basal cells [14]. The specialized stromal cells together with the outer basal cell layer of foetal breast between 16 and 23 weeks of age are strongly positive for Bcl2 protein [15]. From 28 weeks of intrauterine life, Bcl2 protein is expressed by the inner luminal epithelial cell layer while; outer basal myoepithelial cell layer becomes generally negative [16]. The vimentin is first expressed between 23 and 28 weeks in foetal breast and its expression is restricted to a few isolated suprabasal cells[14]. None of the outer basal myoepithelial cells is positive for vimentin [14]. None of the inner luminal epithelial cells is positive for CK18 or CK8. The proliferation index (MIB1), oestrogen receptor-alpha (ER α) and progesterone receptor (PR) are almost absent ($<1\%$) in foetal breasts and their expression (if any) restricted to the inner luminal epithelial cell layer [15]. The stromal cells show no expression of ER α or PR and display heterogeneous expression of both MIB1 and Bcl2[15].

During infancy

Within the infant breast, CK14 and SMA are expressed in the myoepithelial cells throughout the mammary tree from birth to 2 years. The epithelial cell layer is negative for both SMA and CK14. CK19 is uniformly expressed in the epithelial cell layer of infant

breast throughout the mammary tree. The epithelial cells show heterogeneous expression of CK18 and Bcl2. The proliferation rate, ER-α and PR are very low in infant breasts until puberty[13-15].

Adult breast

At the onset of puberty and under control of oestrogen and growth hormone, the immature mammary gland undergoes rapid growth and differentiation at the tip of the terminal end buds (TEBs) which are composed of outer cap cell layer and inner body cells (**Figure 1-2**) [16]. The cap cells have a phenotype that is intermediate between luminal and myoepithelial cells, as indicated by low expression of markers associated with both lineages (e.g. vimentin, smooth muscle actin (SMA) and MUC1 [16]. Subsequently, the cap cell layer can differentiate into myoepithelial or epithelial cells [16]. The TEBs are transient niche structures that disappear once the duct reaches the end of the fat pad [13-16]. In fact, the balance between the proliferation and apoptosis controls the development of TEBs which are characterised by high expressions of MIB1, ER, PR and Bcl2 [13-16]. Interestingly, in vitro and cell line culture studies have demonstrated that most of the proliferating cells (MIB1 positive cells) are ER-/PR- suggesting that the oestrogen hormone may stimulate the proliferation of ER negative cells by indirect mechanisms. For instance, estrogens by binding to ER+ cells might stimulate proliferation of the surrounding ER- cells through the induction of certain growth factors (para-crine mechanism) [17-18].

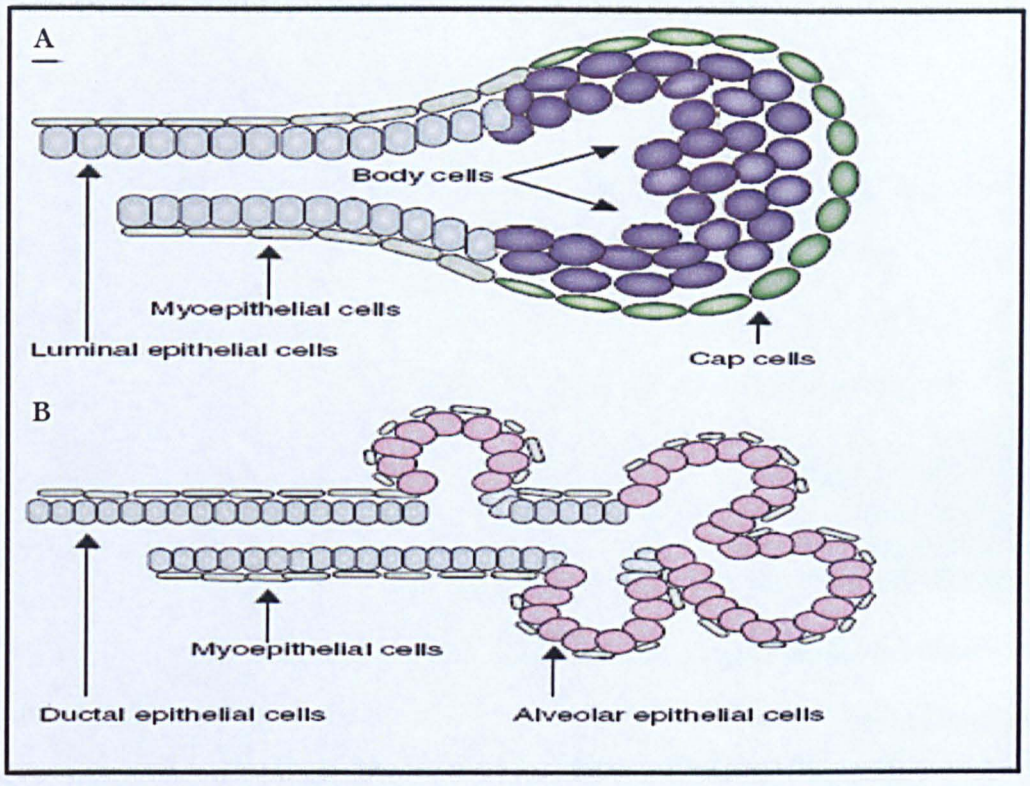

Figure 1-2: The terminal end bud (TEB).

The TEB appears at the onset of puberty, undergoing rapid growth and differentiation. (A): the structure of TEB: a cap cell layer surrounds the body cells. (B): The structure of fully differentiated terminal duct lobular unit (TDLU) during mid pregnancy. (Adopted from Wood et al 2005 [16])

1.1.2 Heterogeneity of Terminal Ductal Lobular Units (TDLUs)

The TDLU is heterogeneous morphologically, phenotypically and functionally. Morphologically, the luminal epithelial cell layer and myoepithelial cells may be either spindle in shape, cuboidal or low columnar depending on their location on the branching structure of the breast duct system and on the hormonal or menopausal status of the tissue [19]. Functionally, there are three epithelial cell types: a) the ductal cells are those that line the ducts of the mammary gland, b) the lobular cells are those that form secretory acinar structures at the end of each duct and c) alveolar cells are those that line the acinar structures during late pregnancy and produce milk proteins during the lactation period [16].

The structure of normal TDLUs varies considerably as a function of the hormonal status and they are grouped into four histological categories on a continuum of differentiation towards lactation [20,21].

Pre-menopausal TDLUs

TDLU TYPE 1 (LOB1)

TDLU type 1 (lob1) is the least differentiated structure of TDLU (TEB) and is more numerous in the breast of post-pubertal nulliparous women [20, 21]. It is noteworthy that in contrast to the overlapping myoepithelial cells of mammary ducts, the myoepithelial cell layer of TDLUs is a basket-like layer that allows some of the luminal epithelial cells to be in direct contact with the basement membrane and the surrounding stroma. Lob1 shows a relatively high proliferative rate and high expression of ER and PR [20, 21].but shows the lowest level of Bcl2 [14-15]. There is speculation that lob1 is the origin of atypical ductal hyperplasia and ductal carcinoma in situ [20]

TDLU TYPE 2 (LOB2)

TDLU type 2 is composed of more numerous ductules per lobule and exhibit a more complex morphology[20]. There is some speculation that atypical lobular hyperplasia (ALH) appears to arise directly within relatively well differentiated type 2 TDLU[20].

TDLU TYPE 3 (LOB3)

During the mid-cycle and 1st and 2nd trimesters of pregnancy, lob 1 and lob 2 rapidly progress to a more differentiated TDLU; lob 3 which is composed of more numerous and smaller alveoli per lobule[20].

TDLU TYPE 4 (LOB4)

During the last trimester of pregnancy the alveoli become distended and are fully differentiated structures and persist during lactation period. After weaning, all lob 4 structures regress reverting to lob 3 and lob 2[20].

There is a progressive decrease in the percentage of proliferating cells (MIB1 expressing cells) with the progressive maturation of lob 1 to lob 2, lob 3 and lob 4 [20-21]. The percentage of ER+ and PR+ cells is highest in lob 1 and progressively decreases in an inverse relationship to the degree of lobular differentiation [21]. The undifferentiated lob1 shows the lowest expression of Bcl2 but the fully differentiated lob 4 exhibits the highest expression of Bcl2[15, 16, 22]. In addition, the Bcl2 shows a marked cyclic variation with maximal expression at the mid-cycle (Lob 3) period and a sharp decrease at the end of the cycle [18].

Postmenopausal TDLUs (lob1)

After the menopause all remaining differentiated lobular structures (lob3 and lob2) regress, acquiring the appearance of the lob1 of nulliparous women from which they seem morphologically indistinguishable [20-21]. However, the proliferative activity and ER+ expression of lob 1 nulliparous women at menopause is at least 2-fold greater than of the lob 1 of parous women's breast [20-21]. Lob1 is more common in cancerous breast suggesting that it may preferentially give rise to early growth alterations with pre-malignant potential [20-21] such as columnar cell lesions.

Phenotypically, the mature differentiated epithelial and myoepithelial cells constitute >90% of the cells present in the TDLUs. A small number of small light undifferentiated electron-lucent cells have also been recognized in the suprabasal compartment of the epithelial cell layer and considered as candidate cells with stem and progenitor activities [23]. The fully differentiated myoepithelial cell exhibits many features of smooth muscle and expresses: myosin, smooth muscle actin (SMA), vimentin, neutral endopeptidase (CD10), p63, CK5/6 and CK14 [23-25]. The immunohistochemistry profiles of the epithelial and myoepithelial cells of the TLDU are summarized in **(Table 1-1)** [17-25]

It is noteworthy that in the breast pathology, the terms "basal" and "luminal" has acquired different meanings for each [19]. In one context, basal and luminal have become synonymous with breast myoepithelium and epithelial cell layer; respectively. In another context, luminal and basal define a specific subpopulation of "basal" cytokeratins (CK5/6 and CK14) and "luminal" cytokeratins (CK19 and CK18) expressing cells; respectively and are perceived to reside in the luminal epithelial cell layer of TDLUs [23-25]. Regarding breast cancer, "luminal" BC usually refers to ER+ positive cancer [26].

Table 1-1: Immunohistochemistry profile of the cells lining the luminal and myoepithelial cell layer of terminal duct lobular unit

Markers	Epithelial cells lining TDLUs				
	ER+ Differentiated luminal epithelial cell	ER- Differentiated luminal epithelial cell	ER- Differentiated basal epithelial cells	Stem/ progenitor cells	Differentiated myoepithelial cell
ER-α	+	-	-	+/-	-
CD133	+	-	-	-	-
P61	+	-	-	-	-
PgR	+	+/-	-	+/-	-
Bcl2	+	+/-	-	+/-	-
ESA	+	+	+	+	-
MUC1	+	+	-	-	-
CD24	+	+	+	+/-	-
CK19	+	+	-	+/-	-
CK18	+	+	-	+/-	-
CK5/6	-	-	+	+/-	+
CK14	-	-	+	+/-	+
CD44	-	-	-	+/-	+
CD10	-	-	+	+/-	+
SMA	-	-	-	-	+
Vimentin	-	-	+	-	+
P63	-	-	+	+/-	+
MIB1	-	+/-	+/-	+	-

1.2 Stem and progenitor cell concepts

1.2.1 Adult progenitor and stem cells

Adult stem cells are long-lived, generally quiescent cells that generate both new stem cells (self-renewal), and the different cell types of the tissue in which they exist (differentiation) [27]. The self-renewal of stem cells can be either asymmetric or symmetric. In asymmetric stem cell self-renewal, one of the two progeny is identical to the initial stem cell, whereas the other cell is a committed progenitor cell, which undergoes cellular differentiation [27]. The processes that regulate the balance between asymmetric and symmetric divisions of stem cells are poorly defined, but recent evidence indicates a role for p53 [27-28].

1.2.2 Mammary stem and progenitor cells

The ability of the mammary gland to regenerate through cycles of pregnancy, lactation and involution is attributed to normal breast stem cells [16]. Under the regulation of the systemic hormones, as well as local stromal epithelial interactions, these cells proliferate extensively differentiate during each pregnancy and lactation, and undergo apoptosis during mammary involution in pre-menopausal and post-menopausal periods [16-22].

By using different approaches, techniques and immunohistochemical markers, several models for breast progenitor and stem cells were proposed [16, 17, 23-40] however, these studies lack an in vivo validated xenotransplant assay[38]. As aforementioned, the earliest progenitor cells in the epithelial bud are CK19+, Bcl-2+, and ER- which differentiates into three pathways; one lineage acquiring basal markers (CK14, CK5/6) and the other acquiring luminal cell specific markers (CK18) or myoepithelial specific makers (SMA) [13-17]. These observations are consistent with the reports that considered CK19 and/or ER as markers for stem/progenitor cells [31, 33-36]. However, some investigators [27,32, 40] identified stem/progenitor cell populations by their expression of CK18 and CK14 (CK18+/CK14-,

CK18-/CK14+, CK18-/CK14- and CK18+/CK14+) while Böcker et al [23, 25] generated a different model in which the CK5+/CK18+ cells are adult stem/progenitor cells.

Stingl and colleagues [24, 37, 38] characterized the multipotent epithelial cells in the normal human adult breast. In their model, two distinct types of human breast epithelial cell progenitor population could be distinguished on the basis of their differential expression of the MUC1, CD10 and epithelial-specific antigen (ESA). MUC1+/CD10–/ESA+ progenitors (luminal restricted progenitors) expressed typical luminal epitopes (CK8/18+ and CK19+) and showed low levels of expression of myoepithelial/basal epitopes (CK14, CK5/6 and CD44v6). The second progenitor cell was MUC1–/CD10+/ESA+ (bipotent progenitor, or ductal progenitor) which generated mixed colonies of both luminal, basal, myoepithelial cells when seeded in two-dimensional and three-dimensional cultures [24, 37, 38].

1.2.3 Breast tumour stem cells

Cancer cells and normal stem/progenitor cells share the capacity for self-renewal, the ability to differentiate, active telomerase and anti-apoptotic pathways, increased membrane transport activity, anchorage independence and ability to migrate and form metastasis [27].

A subpopulation of highly tumorigenic breast cancer cells (CD44+ CD24-) was isolated from the bulk of human breast tumour cells [41, 42] and it was claimed that this subpopulation possesses stem cell characteristics. Analysis of gene expression profiles [42-44] showed that CD44+ CD24–cells from normal breast and breast cancers were more similar to each other than to CD24+ cells of the same tissue [17]. However, gene expression profiling of CD44+CD24- breast cancer cells compared to normal breast epithelium identified 186-genes which had a significant association with the invasiveness, poor outcome and basal-like tumour phenotype [42-44].

Taken together the published data[17-44] regarding breast stem/progenitor cells (**Figure 1-3**), we can postulate that:

1. There is a common breast stem cell that is perceived to reside in the suprabasal compartment of the epithelial cell layer. However, its nature and molecular characteristic remain elusive. This stem cell could be those cells which are ESA+, CD44+, CD24- and ER-[17, 24, 27, 29, 30, 38, 41-44].
2. There are at least 4 progenitor cells: one multilineage progenitor, 2 restricted luminal progenitors and one basal/myoepithelial progenitor cell and all of them are perceived to reside in the suprabasal compartment of the epithelial cell layer[17, 24, 27, 29, 30, 38].

   The multilineage progenitor cells are characterized by the expression of: ESA+, CK19+, CD10+, CK14+, CK5/6+, CK18/8-, MUC1-, ER-, CD133-, CD61- and could give rise to both luminal, basal and myoepithelial cells.

   According to the level of ER, CD133 and p61 expressions [17, 24, 27, 29, 30, 38], there are two luminal restricted progenitor cells that differentiate into ER+ and ER- luminal epithelial cells. ER+ luminal restricted progenitor cells have an ESA+, CK19+, CD24+, CK18/8+, MUC1+, ER+, CD133+, CD61+, CD10- , CK14-, and CK5/6- immunohistochemical profile. The ER- luminal restricted progenitor cell (alveolar progenitor cells) are ESA+, CK19+, CD24+, CK18/8+, MUC1+, ER-, CD133-, CD61-, CD10- , CK14-, and CK5/6- expressing cells. T

   he basal/myoepithelial restricted progenitor cells have an ESA-, CK19-, CD24-, CK18/8-, MUC1−, ER-, CD133−, CD61-, CD14+, CD10+ and CK5/6+ immunohistochemical profile and differentiate into myoepithelial cells (SMA+ and p63+).

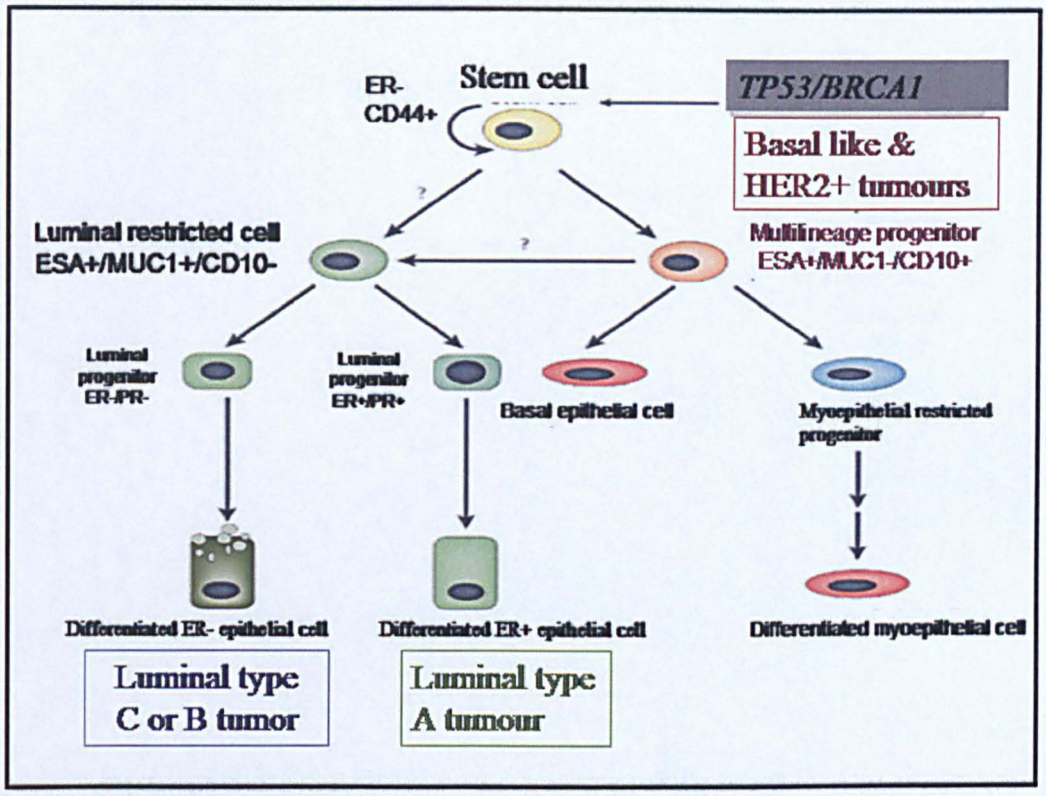

Figure 1-3: Stem cell and progenitor cells model of breast and cell of origin theory of breast tumour subtypes.

Adapted with modification from (Stingl J and Carlos C, 2007) [38].

1.3 Breast cancer evolution and progression

Gene expression array studies have shown the existence of at least five different BC subtypes, each with different clinical outcomes [45, 46] (**Figure 1-4**). These include luminal (A and B), basal, HER-2 and normal-like BC. The luminal subtype 'A' have higher levels of ER and a better survival outcome compared with luminal subtypes 'B'. The basal and HER2 subtypes are generally of higher grade than that of the luminal subtypes. According to Nielsen et al [26] the immunohistochemistry profile of basal like tumour (ER-, HER-2-, and either CK5/6+, CK14+ or EGFR+) is very similar to the immunohistochemistry profile of stem cell and basal cell of TDLUs of normal breast [17, 24, 26, 38]. Moreover, the immunohistochemistry profile of luminal "A" tumours was very similar to that of ER+ luminal restricted differentiated cells [17, 24, 26, 38]. These observations raise the following

question: 'Do different breast carcinoma subtypes as defined by gene expression arise from the normal cell equivalent like luminal, basal and possibly stem cell compartments that reside in the epithelial cell layer of TDLUs?' [17, 24, 26, 38] **(Figure 1-3)**

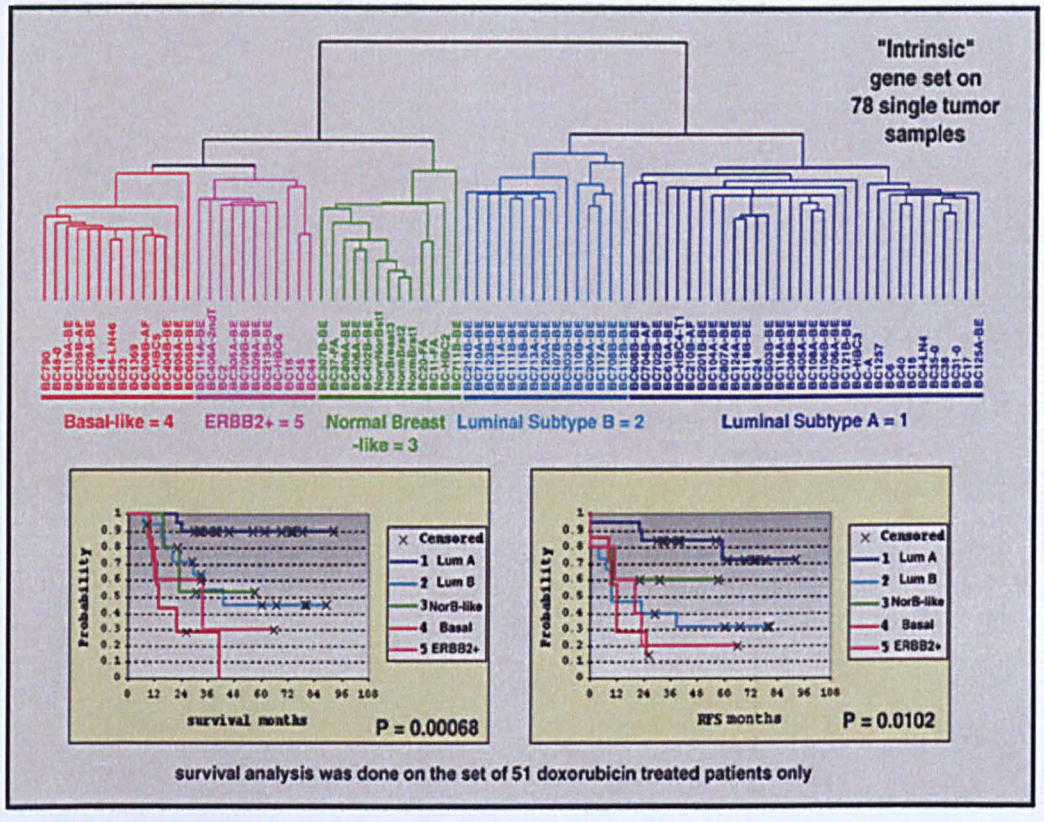

Figure 1-4: Classification of breast carcinoma according to gene expression signature.

(Adapted from Sorlie et al 2001 [46])

Interestingly, it has been demonstrated that the morphological and molecular patterns of BC were strongly related to the histological grade of breast cancer more than any other clinicopathological parameter or tumour intrinsic characteristic [47-52]. For instance, the evolutionary pathways of breast carcinoma can broadly be classified into a low and high grade route [52]. Low grade tumours have favourable prognosis, low proliferation rate, low apoptosis, glandular differentiation and fewer genetic changes compared to their high grade counterparts[52-53]. They are characterized by ER+, PR+, Bcl2+, wild type p53 and no

HER2-overexpression/amplification immunophenotype [52-55]. Moreover, they frequently show gain of 1q and loss of 16q[52-55]. In contrast, high grade tumours show a higher degree of nuclear atypia, and are more frequently negative for hormone receptors. Moreover, high grade tumours more commonly showed p53 mutation, triple negative (ER-/PR-/HER-2-) and basal like phenotypes[52-55]. They are genetically advanced lesions, showing a combination of recurrent genomic changes including loss of 8p, 11q, 13q, 14q; gain of 1q, 5p, 8q, 17q; and amplifications on 6q22, 8q22, 11q13, 17q12, 17q22–24, and 20q13 [52, 55-61].

It is known that the fate of any tumour reflects the molecular events acquired during its development. Accordingly, the morphological and clinical heterogeneity of any tumour including breast carcinoma is likely to derive from stochastic genetic and epigenetic events resulting in oncogenes activation and loss of tumour suppressor gene (TSG) function [27-30]. However, in contrast to the 'stochastic' model of ontogenesis [62, 63] where transformation results from random mutations and subsequent clonal selection, tumours nowadays are considered as a multi-step clonal disease and its progression is dependent on acquiring further genetic and epigenetic changes in the stem or progenitor cells [62]. In this model, cancer originates in tissue stem or progenitor cells probably through dysregulation of self-renewal pathways and this leads to expansion of these cell populations that may undergo additional genetic and epigenetic changes [27-30, 62-65]. The nature of the genetic and epigenetic changes, and the type of progenitor they target, probably contribute to the cellular/lesional heterogeneity found in BC[62].

1.4 Precursor lesions of breast carcinoma

The development of breast cancer involves a multi-step progression spanning from the normal TDLU, precursor lesions to invasive and metastatic disease. Frequently, pathologists observe a collection of co-existing subtle pathological changes representing 'precursor' lesions. These are challenging to identify, classify and manage and currently, we cannot predict which precursors will progress into cancer but studies suggest that between 1–30% lesions develop a subsequent tumour event within a decade [66, 67]. Moreover, autopsy studies have demonstrated that almost 20% of women with no overt symptoms are, in fact, harbouring pre-malignant lesions within their breast tissue that are not yet detected by mammograms or other techniques [68]. These data indicate that pre-malignant lesions are more common than originally appreciated but only a fraction of these women will ultimately develop invasive disease. Atypical ductal hyperplasia (ADH), atypical lobular hyperplasia (ALH), lobular carcinoma in situ (LCIS) and ductal carcinoma in situ (DCIS) have been proposed as precursor lesions of BC [66-67]. More recently, attention has been paid to a group of lesions called columnar cell lesions (CCLs) [69-71]. The frequent co-existence of CCLs with ALH/LCIS and low grade DCIS as well as overlapping morphological and immunohistochemical features with DCIS and low grade tumours suggest CCLs could be an early candidate precursor for the progression to low grade DCIS and invasive carcinoma [69-76]. However; the available biological and molecular data that support this hypothesis are limited.

1.4.1 Columnar cell lesions (CCLs)

CCLs represent a spectrum of lesions in the TDLUs of the breast which are characterized by dilatation of TDLUs and are lined by tall columnar cells with prominent apical cytoplasmic snouts (**Figure 1-5**), intraluminal secretion and calcification (**Figure 1-6**) and a varying degree of nuclear atypia and architecture complexity as described by Schnitt and Vincent-Salomon [69-71]. CCLs are increasingly recognised as a result of the widespread use of screening mammography and extensive investigation of radiological calcification [76]. They are considered as one of the most conflicting issues in breast pathology because there is no internationally accepted classification or terminology for this range of lesions, a limited number of cases that have been studied in a systemic fashion and the limited available data about these lesions [69].

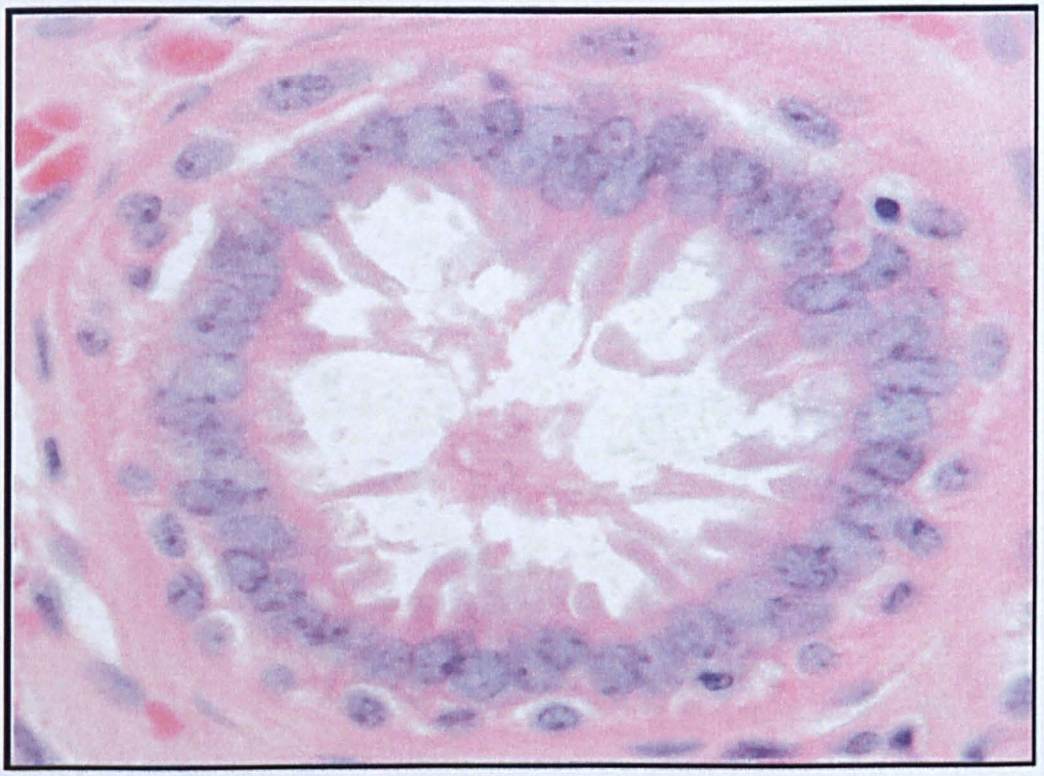

Figure 1-5: Columnar cell lesion showing apical snouts and intraluminal secretion

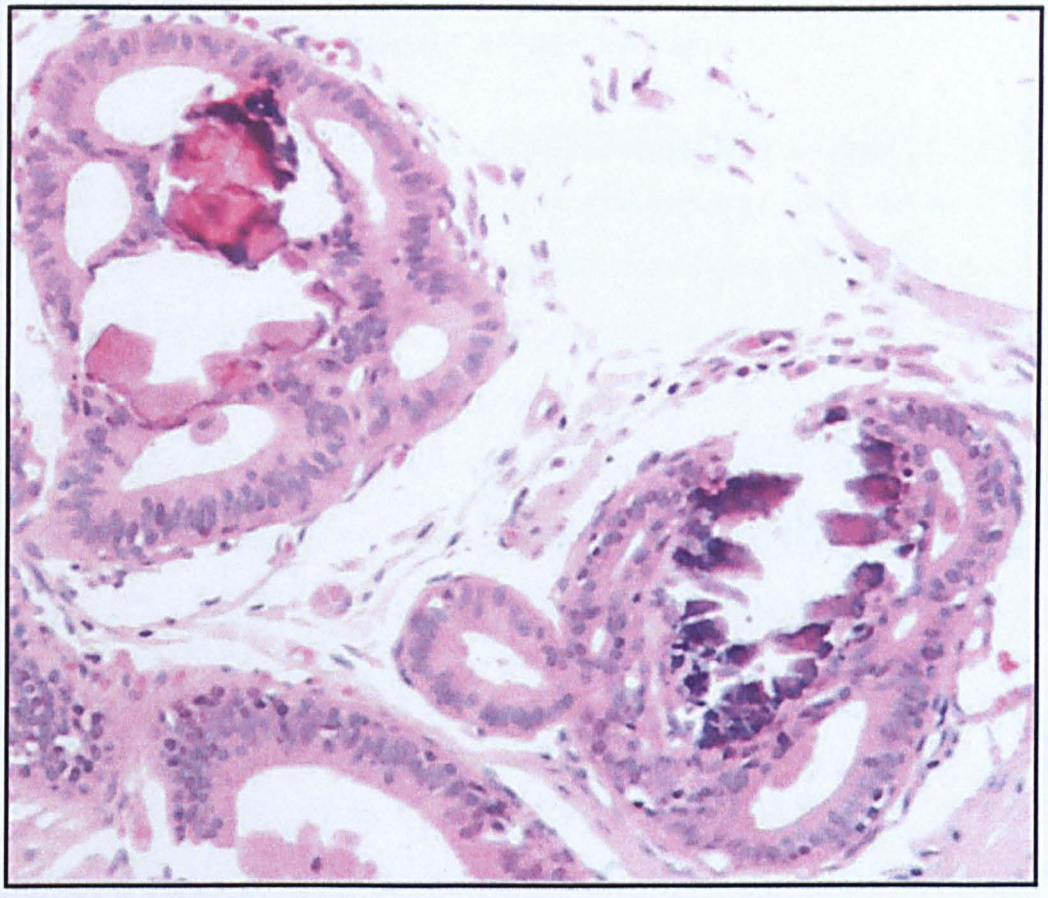

Figure 1-6: Columnar cell lesion showing complex architecture and intraluminal calcification

The CCLs have long been reported by pathologists under several names [69] including blunt duct adenosis, columnar cell metaplasia, atypical lobule, type A, hyperplastic terminal groupings, clinging carcinoma, columnar alteration of lobules, metaplasia cylindrique, columnar alteration with apical snouts and secretions, small ecstatic ducts lined by atypical ductal cells with apocrine snouts, atypical cystic duct, pretubular hyperplasia, atypical cystic lobules, ductal intraepithelial neoplasia of flat monomorphic type, unfolded lobules [69].

CCLs represent a spectrum which range from bland columnar cell changes (CCC) to columnar cell hyperplasia (CCH) with cytological atypia and architecture complexity. Based on recent classification of CCLs produced by Schnitt and colleagues [69], Simpson and colleagues [71] categorize CCLs as follows:

CCC (category 1)

CCC is the simplest form of CCLs and is a very frequent finding and as such has often been considered to be of negligible clinical significance misinterpreted as normal, or as microcystic lesions because of subtle or absence of cytological atypia. This lesion is characterized by variable dilatation of the TDLUs which are lined by one or two layers of cuboidal to tall columnar epithelial cells distributed in a relatively uniform pattern (**Figure 1-7**). The nuclei are uniform ovoid to elongated and oriented perpendicular to the basement membrane while the nucleoli are inconspicuous or absent. The nuclear cytoplasmic ratio is normal. Apical cytoplasmic snouts, luminal secretion and calcification may be present

CCC with cytological atypia (Category 6)

In this less common lesion, the cells showed mild to moderate cyto-nuclear atypia of a degree to cause concern but not amounting to flat DCIS (low grade atypia). This atypia may be extremely subtle. The nuclei are round to ovoid, mildly pleomorphic and hyperchromatic with inconspicuous basophilic nucleoli and increased nuclear cytoplasmic ratio. Sometimes the nuclei may show clumped chromatin or vesicular nuclei or prominent multiple nucleoli (**Figure 1-8**).

CCH (Category 2)

These comprise variably dilated TDLUs lined by columnar cells which have cytological features similar to those seen in CCC but show cellular stratification of more than two cell layers (**Figure 1-9**). The proliferating columnar cells may form small mounds, tufts or abortive micropapillations but true micropapillary structures lacking fibrovascular cores and epithelial bridges are not seen in this form. At present, this is considered to be equivalent to usual epithelial hyperplasia.

CCH with architectural atypia (Category 3)

These lesions show more complex architectural pattern in the form of well developed tufts, fronds, bulbous micropapillary, rigid cellular bridges, bars and arcades or punched-out fenestration with at least some evidence of cellular polarization within the micropapillations and bars or around fenestrations (**Figure 1-10**).

CCH with cytological atypia (category 4)

In these lesions the columnar cells show mild to moderate cytological atypia usually low grade but with no complex architecture. The degree of atypia is not sufficient to warrant a diagnosis of ADH or DCIS (**Figure 1-11**).

CCH with architectural and cytological atypia (Category 5)

These lesions show cytological and architecture atypia which are insufficient to warrant a diagnosis of ADH or DCIS (**Figure 1-12**).

Flat Epithelial Atypia (FEA)

FEA are lesions of the TDLUs in which the native epithelium is replaced by one (CCC with atypia) to several layers (CCH with atypia) of cells that show low grade cytological atypia. The term flat denotes the absence of more complex architectural patterns. While Flat DCIS is TDLUs which is lined by one or two cell layers with high grade cytological atypia and marked nuclear pleomorphism [77].

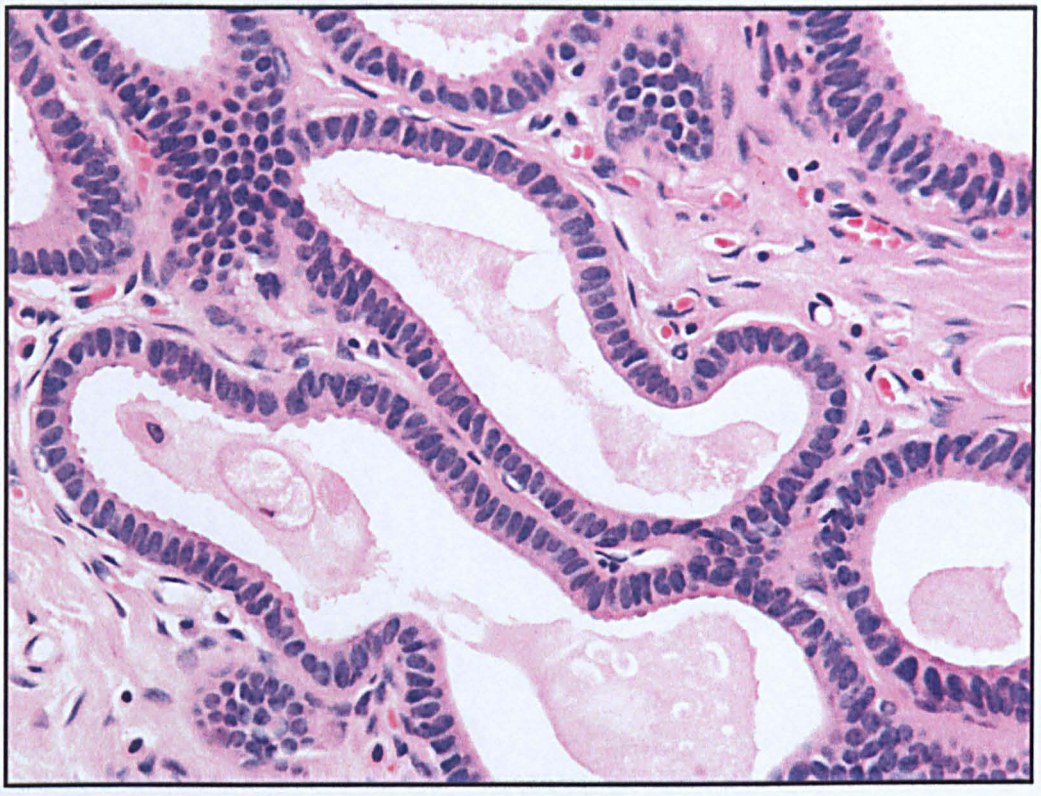

Figure 1-7: Columnar cell changes without cytological atypia

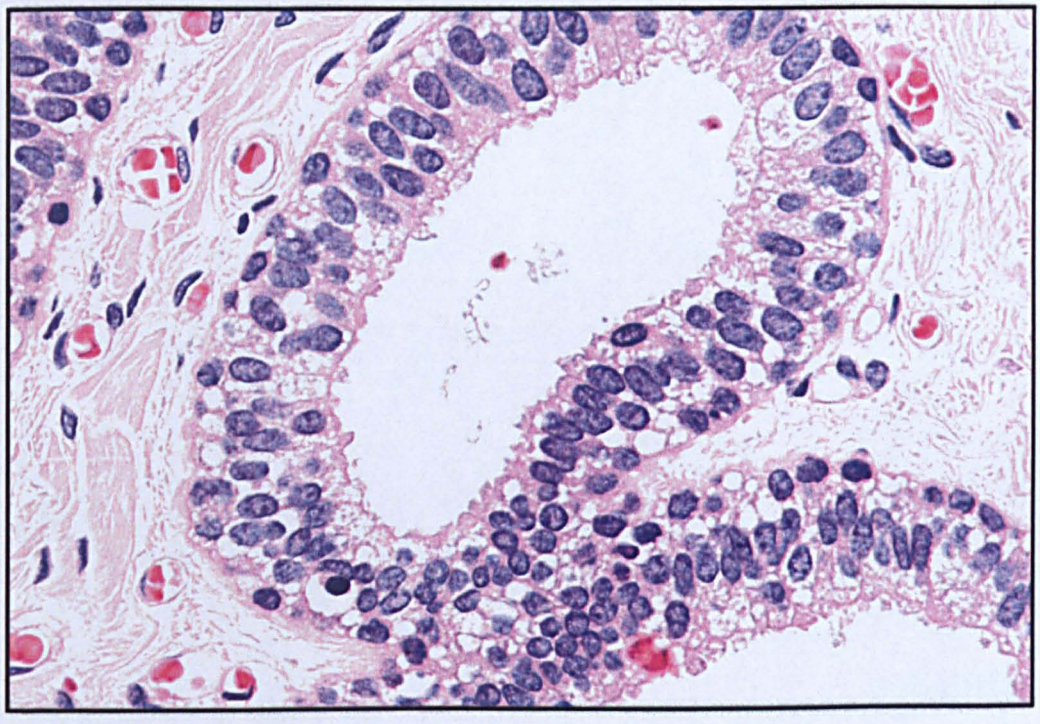

Figure 1-8: Columnar cell changes with cytological atypia

Figure 1-9: Columnar cell hyperplasia with cytological atypia

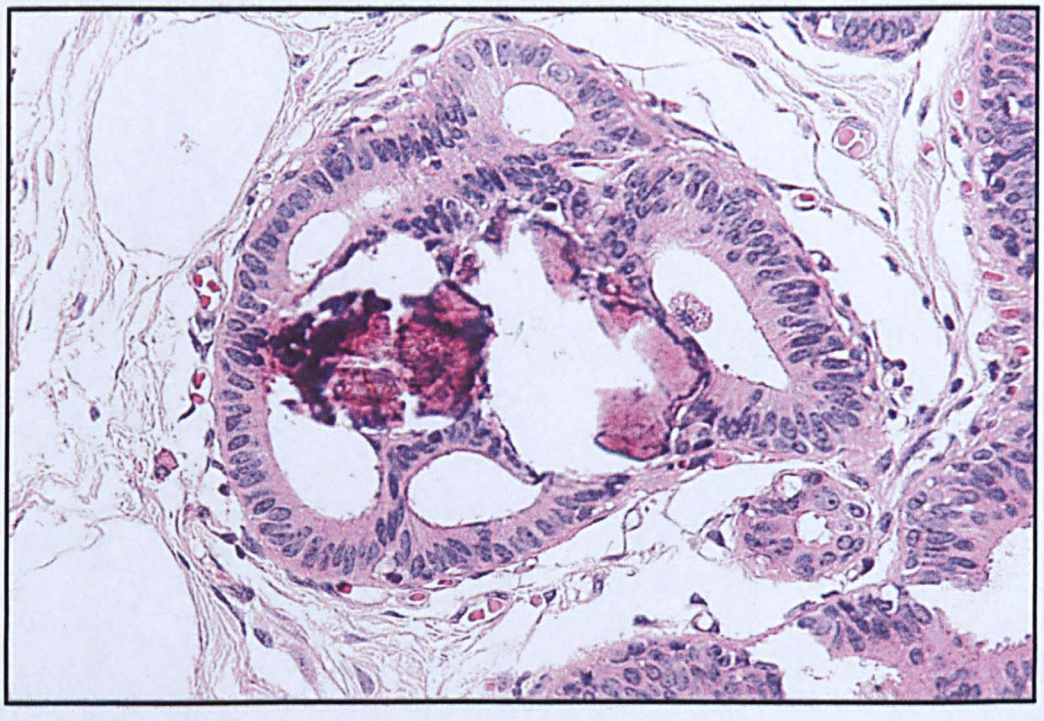

Figure 1-10: Columnar cell hyperplasia with complex architecture but without nuclear atypia

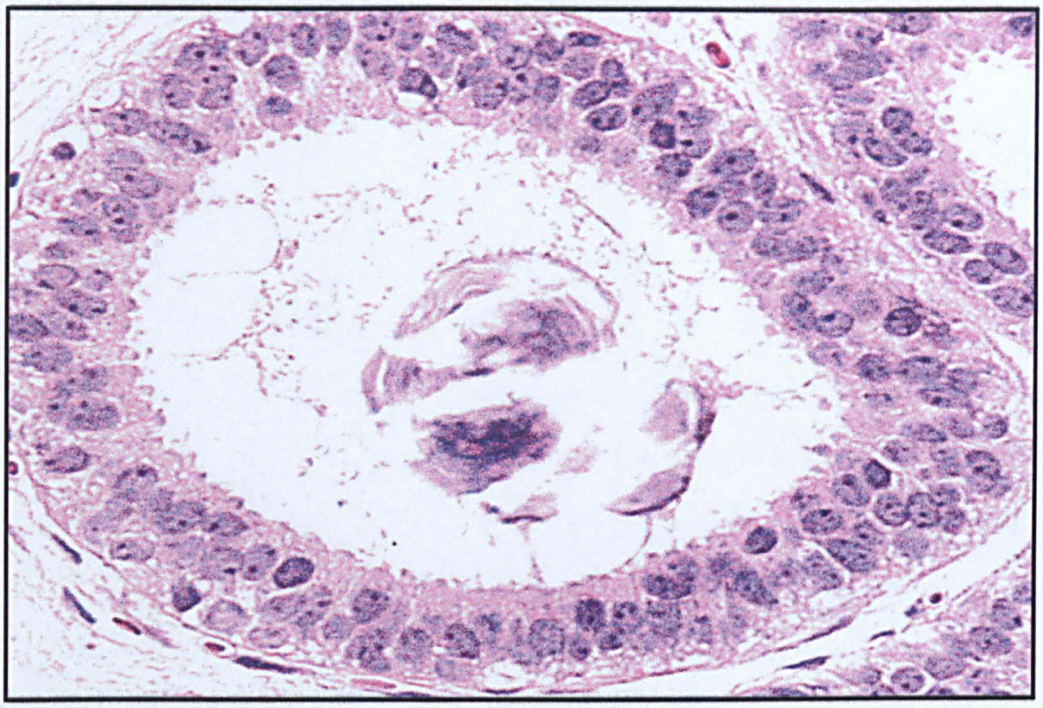

Figure 1-11: Columnar cell hyperplasia with cytological atypia

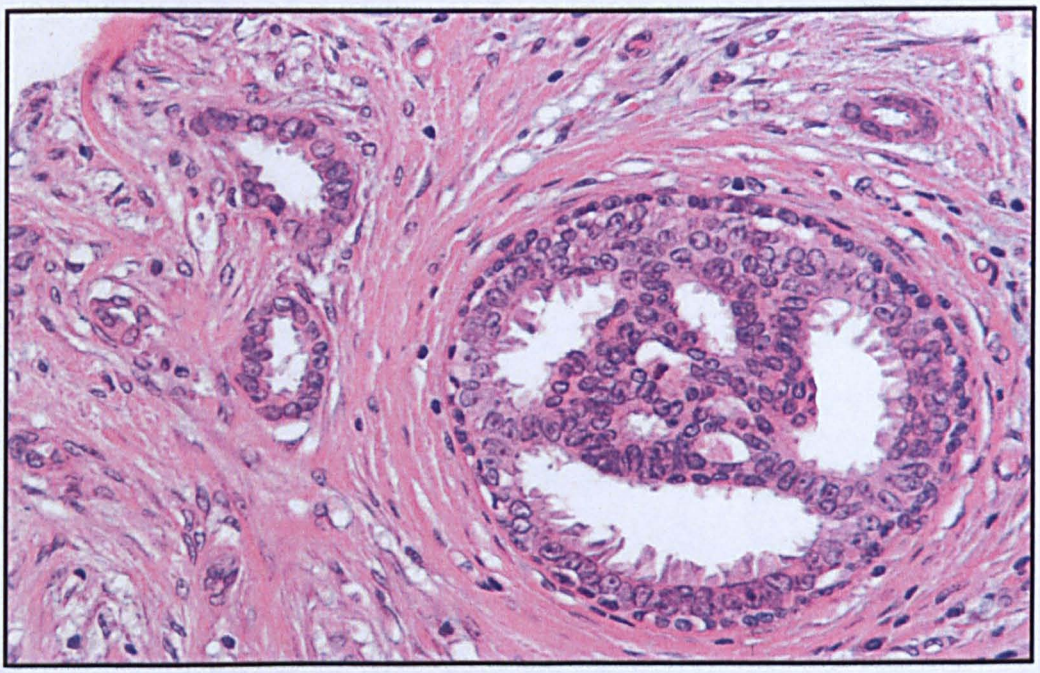

Figure 1-12: Columnar cell hyperplasia with cytological atypia and architecture atypia

1.4.2 Ductal carcinoma in situ

The cyto-morphologic and architectural criteria used to identify low grade DCIS and ADH are similar and distinction is primarily quantitative, based mainly on the extent of involvement. The ADH/DCIS results from a disruption in the architecture of the breast epithelium due to luminal epithelial cell proliferation in TDLUs that occur due to cell cycle dysregulation and imbalance between apoptosis and proliferation [78]. DCIS was categorized by architectural description into six groups: comedo (neoplastic cells surrounding a central area of necrotic debris), cribriform (radially oriented neoplastic cells forming glandular lumina), papillary (large papillations with fibrovascular stalks), solid (ductal filling with neoplastic cells), micropapillary (finger like papillary projections into dilated ductal spaces) and flat (absence of more complex architectural patterns) [77]. Also DCIS were categorized into three groups according to the nuclear grade (high, intermediate or low) [77].

High nuclear grade DCIS

Cells have pleomorphic, irregular spaced large nuclei exhibiting marked variation in size with irregular nuclear contours, coarse chromatin and prominent nucleoli. Nuclei are typically large and greater than three times the size of erythrocytes. Mitoses are usually frequent and abnormal forms may be seen [77]. This form of DCIS commonly shows negative expression of oestrogen receptor–α (ER-α) and Bcl2 and exhibited overexpression of HER-2 and p53 mutation [79-80]. Moreover, high grade DCIS commonly shows genetic changes similar to high grade BC including gain 17q, 11q 13, and 13q [81]. Some forms of DCIS showed basal like features CK5/6+, CK14+ and/or EGFR+[80].

Intermediate nuclear grade DCIS

The nuclei show moderate pleomorphism with lack the monotony of the small cell type and the nuclei are typically larger than those seen in low grade DCIS i.e., 2-3 times the size of erythrocyte. The nuclear cytoplasmic ratio is often high with 1-2 nucleoli. Intermediate grade DCIS showed combination of immunohistochemistry and genetic features of high and low DCIS [77-81].

ADH/Low nuclear grade DCIS

ADH/Low grade DCIS is composed of monomorphic evenly spaced cells with rounded, small centrally placed nuclei and inconspicuous nucleoli. Mitoses are few. ADH/Low DCIS commonly shows strong positive expression of ER and Bcl2 with absence of p53 mutation and HER-2-overexpression [77-81]. ADH/DCIS is associated with simplex array CGH profile with broad or whole arm loss of 16q and gain of 1q and 16p with absence or occasional amplification events [81].

1.4.3 Lobular neoplasia

For the purpose of this study, ALH and LCIS were grouped together as "lobular neoplasia" (LN). LN was characterized by round, cuboidal or polygonal with clear or light cytoplasm epithelial cell proliferation within terminal duct lobular units. The intraductal epithelial cells have small, round to oval nuclei with small inconspicuous nucleoli and bland cytology. The nuclear cytoplasmic ratio is high [77]. The cells similar to low DCIS were monotonous and evenly distributed but with poor cell cohesion and loss of E-cadherin [77]. This proliferation of neoplastic cells above the basement membrane undermined the normal lining epithelial cells. LN showed immunophenotype and genetic features very similar to low DCIS (**Table 1-2**)[81].

1.4.4 Usual epithelial hyperplasia (UEH)

UEH is be used to describe any intraluminal proliferation of a mixed cell population comprising epithelial cells, basal/myoepithelial cells and metaplastic cells showing no or only mild atypia [77].

Table 1-2: Summery of the characteristic features of low grade precursor lesions

Parameter	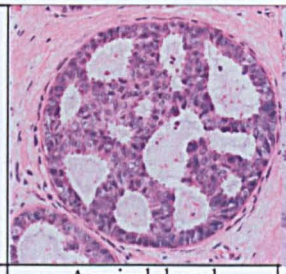		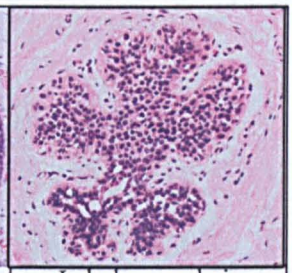
Lesion	Atypical ductal hyperplasia	Ductal carcinoma in situ	Lobular neoplasia
ER-α	+	+	+
PR	+	+	+
Bcl2	+	+	+
CK18/19	+	+	+
Cyclin D1	-	-	+
E-Cadherin	+	+	-
CK5/6	-	-	-
p53	-	-	-
HER-2 overexpression	-	-	-
Mitotic index	Low	Low	Low
Ploidy	Diploid or near diploid	Diploid or near diploid	Diploid or near diploid
Genetic changes	Few 1q+ and 16q	Few 1q+ and 16q	Few 1q+ and 16q
Amplification	Rare	Rare	Rare

Chapter 2:

Morphological evidence for the existence of a low nuclear grade breast neoplasia family: matched precursor and invasive lesions

2.1 Abstract

This study was undertaken to determine the morphological features and frequency of putative precursor lesions involved in the development of some pure forms of special type breast carcinoma. We reviewed 795 cases, comprising atypical ductal (ADH) and/or lobular hyperplasia (ALH) without coexisting invasive lesion (n=180); tubular carcinoma (TC); pure type (n=135), invasive cribriform carcinoma (ICC; n=20), tubulolobular carcinoma (TLC; n=20), low grade invasive ductal carcinoma of no special type (low grade IDC-NST; n=60), invasive lobular carcinoma (ILC); classical type (n=180) and high grade IDS-NST (n=200). The preinvasive cases were followed up for up to 20 years. The presence of pre-invasive lesions including columnar cell lesions (CCLs), usual epithelial hyperplasia (UEH), ductal carcinoma in situ (DCIS), and lobular neoplasia (LN) was determined. Oestrogen receptor (ER) and E-cadherin immunohistochemistry was performed.

About 11% of ADH and/or ALH without invasive lesions developed DCIS, LCIS and/or invasive lesions within 5-15 years. Ninety-five percent (95%) of pure tubular carcinomas had associated CCLs with the majority showing flat epithelial atypia (FEA). ADH/low grade DCIS was present in 89% patients. Co-localization of CCL, ADH/ low DCIS and

TC was seen in 85% of patients, all displaying the same cytologic-nuclear morphology in most cases. LN was seen in 16%. In ILC, 91% cases showed LN. CCL and DCIS were seen in 60% and 42% cases, respectively. E-cadherin was positive in TLC but reduced in TC and completely absent in ILC. In conclusion, our findings support the hypothesis that CCLs are associated with both tubular and lobular carcinoma, and that LN is involved in ILC development. Our observations suggest that these lesions represent family members of low nuclear grade precursor, in situ and invasive neoplastic lesions of the breast.

2.2 Introduction

Recent molecular studies in breast cancer have identified alterations associated with low and high grade tumours. Co-expression of the changes typically seen in low and in high grade carcinomas is rare, suggesting different evolutionary routes. The low grade tumours include tubular, cribriform, lobular and tubulolobular carcinoma and have a favourable prognosis, possibly a consequence of fewer genetic changes [71, 82]. The development of breast cancer is now believed to be a complex multi-step process originating in terminal duct lobular units (TDLUs) and progressing towards invasive cancer [11, 81]. Previously, four precursor lesions separating normal and malignant epithelium have been proposed: atypical ductal hyperplasia (ADH), atypical lobular hyperplasia (ALH), lobular carcinoma in situ (LCIS) and ductal carcinoma in situ (DCIS) [66-67]. Recent attention has focused on a fifth group of TDLU lesions called columnar cell lesions (CCLs). These lesions are increasingly detected by screening mammography because of the associated calcification. CCLs are a controversial and topical issue in breast pathology because there is currently no internationally accepted classification or terminology, and a restricted evidence base resulting from only a limited number of systematically studied cases. The frequent coexistence of CCL with ADH and/or low grade DCIS in the same breast **(Figures 2-1 and 2-2)** as well as overlapping morphological features with ADH and DCIS provides evidence for CCL being a candidate

precursor in the progression to low grade DCIS and invasive carcinoma [52, 71-73, 83-85]. Simpson et al (2005) [71] found that the morphologic classification of CCL closely mirrored the level of genetic instability seen with comparative genomic hybridization (CGH). To date, there have been no studies assessing and comparing the frequencies of putative precursor lesions found in association with different breast carcinomas. This study was undertaken to determine the morphological features and frequency of putative precursor lesions involved in the development of some pure forms of special types of breast carcinoma.

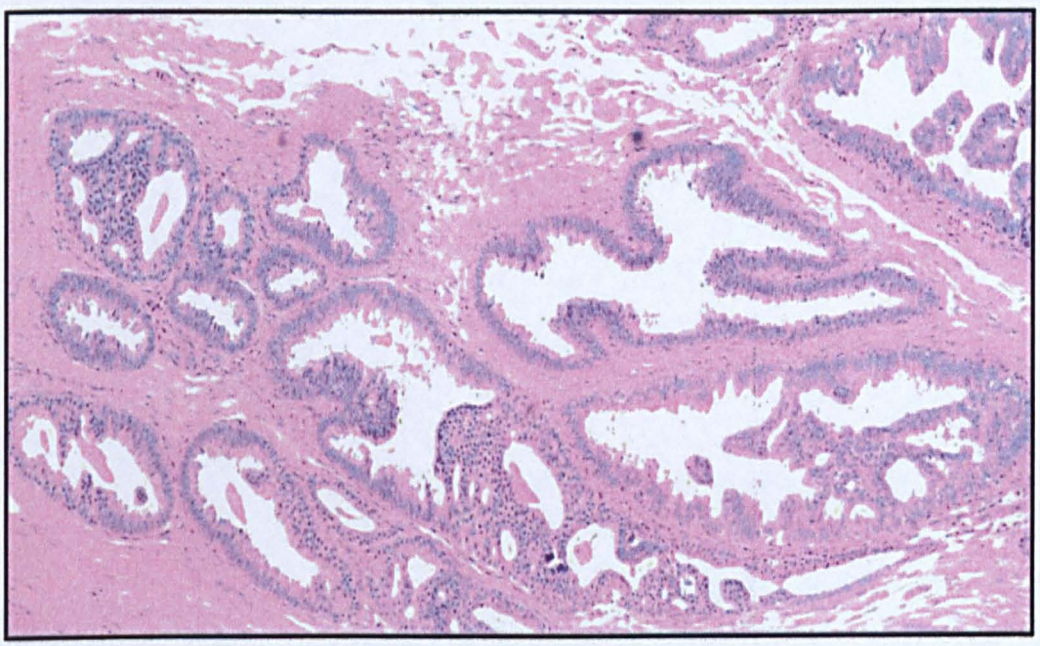

Figure 2-1: Atypical ductal hyperplasia on background of columnar cell lesions

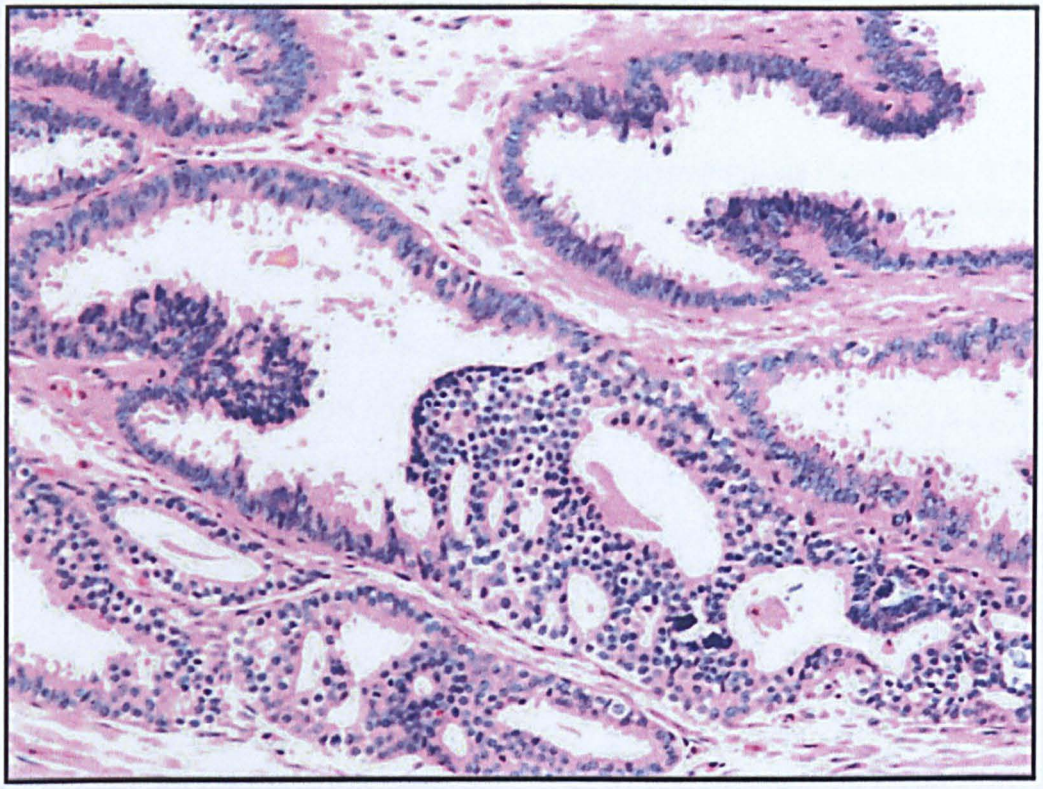

Figure 2-2: Atypical ductal hyperplasia partially lined by columnar epithelial cells showing apical snouts; high power (20X)

2.3 Material and Methods

2.3.1 Morphologic review

We accessed the Nottingham Tenovus Primary Breast Carcinoma Series data-base, Histopathology Department, City Hospital, for primary breast cancer cases diagnosed between 1986 and 2005. According to the WHO and UK guidelines [19, 20], we reviewed all the available haematoxylin and eosin (H&E) stained histological sections (average 20 slides/ case; range 12 to 46 slides/case) of 1) 180 successive pre-invasive cases not associated with invasive carcinoma including atypical ductal hyperplasia and/or atypical lobular hyperplasia, 2) 355 successive low/moderate grade special types BC (135 cases: pure tubular carcinoma, 180 cases ; invasive classic lobular carcinoma, 20 cases; invasive cribriform carcinoma and 20 cases of tubulolobular carcinoma) removed by simple mastectomy or wide local excision (WLE), 3) 60 successive cases of low grade invasive ductal carcinoma of no special type (IDC-NST) removed by simple mastectomy or WLE and 4) 200 successive cases of high grade (IDC-NST) cancer removed by simple mastectomy or WLE. As part of UK NHS Breast Screening Programme (NHSBSP) introduced in 1988, all 180 pre-invasive cases without cancer (unknown malignant potential category) were regularly checked up for any further pathological changes (follow-up up to 20 years).

In our study, pure TC was diagnosed with at least 90% tubule formation. The presence of invasive and pre-invasive lesions including columnar cell lesions (CCLs), usual epithelial hyperplasia (UEH), atypical ductal hyperplasia (ADH), ductal carcinoma in situ (DCIS), atypical lobular hyperplasia (ALH), and lobular carcinoma in situ (LCIS) was determined. For the purpose of our study ALH and LCIS were grouped together under lobular neoplasia (LN). A comprehensive morphologic review of CCLs was performed based upon an extended version [71] of the classification system outlined by Schnitt and Vincent-Salmon [69]. Subsequently, six categories were defined (**Figure 2-3**). Although simple cysts,

radial sclerosis, uncomplicated fibroadenomas, and sclerosing adenosis are common findings in breast biopsies, they have not been consistently linked to a clinically significant increased risk for breast cancer. For that reason, we will not include any of them in this study.

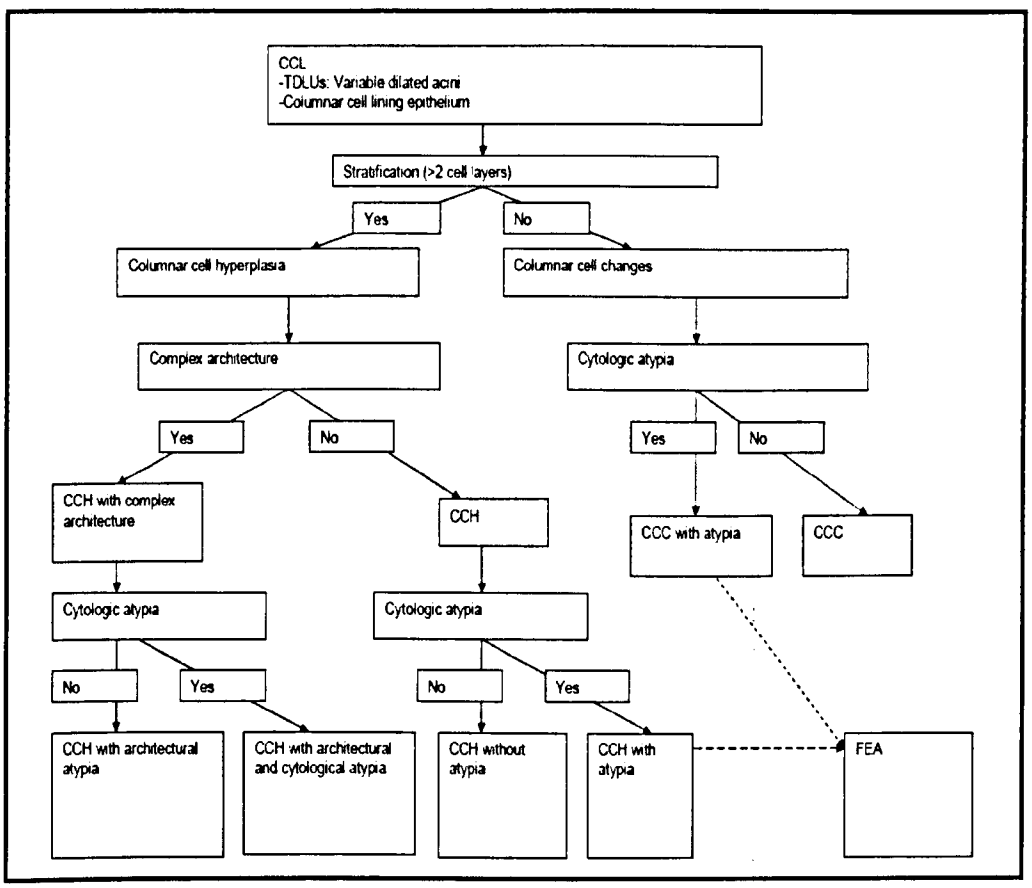

Figure 2-3: Classification of columnar cell lesions.

Columnar cell changes (CCC), columnar cell hyperplasia (CCH), flat epithelial atypia (FEA). Cytologic atypia criteria include round to ovoid, mildly pleomorphic and hyperchromatic nuclei with inconspicuous basophilic nucleoli, increased nuclear/cytoplasmic ratio. Complex architectural: micropapillae, tufts, fonds, arcades, rigid bridges, and punched out spaces.

2.3.2 Immunohistochemistry

Oestrogen receptor (ER) and E-cadherin (CDH1) immunohistochemistry was performed according to the labelled streptvidin-biotin-peroxidase complex method with citrate pH6.0

antigen retrieval using a TechMate 500 immunostainer (DakoCytomation) as previously described [87]. IHC was performed on 4um sections of formalin fixed paraffin wax embedded tissue specimen placed on TechMate glass slides (DakoCytomation, Cambs, UK). The sections were melted on a hot plate (58-60°C) for 10 minutes, dewaxed in xylene for 20 minutes, and then re-hydrated in 3 changes of descending graded alcohol for 1 minute each. Sections were pre-treated with microwave antigen retrieval using 0.1% citrate buffer, pH6 for 23 minutes. Slides were then transferred to a DAKO autostainer. Staining was done at room temperature as follows:

Slides were first incubated in buffer 1 (ChemMate) which contains goat serum for 20 minutes, followed by quenching of endogenous peroxidase activity by treatment with 0.1% H_2O_2 and then in the unconjugated primary antibody for 1 hour at room temperature. Therefore, slides were incubated in biotinylated secondary antibodies for 30 minutes and in horseradish peroxidase (HRP) StreptAvidin (DakoCytomation LSAB2 kit) for another 30 minutes. After that, slides were incubated in Diaminobenzidine (DAB) solution for 10 minutes. Then sections were counterstained in haematoxylin for 2 minutes, rinsed in tap water, dehydrated in ascending graded alcohol, then cleared in xylene and mounted in DPX.

Evaluation of results

Slides were evaluated under a light microscope with medium and high power magnification. Positive and negative controls were also evaluated to confirm the appropriate staining. Immunoreactivities were classified by estimating the percentage of cells showing characteristics staining, by estimating the intensity of staining and the location of staining cells either luminal or myoepithelial.

Negative and positive tissue controls

Negative control tissue sections were generated by omitting the specific primary antibody from the staining process. Positive tissue controls were processed by the same method as the stained sections.

Dilutions

The primary antibody dilutions used for ER was (1D5, 1:100, DakoCytomation) and for E-cadherin was (CDH1, 1:100, Zymed laboratories). These antibodies had previously been optimized in the Histopathology department, City Hospital, Nottingham. Only nuclear and membranous staining was considered for ER and E-cadherin scoring, respectively. For comparison with previous studies performed by Simpson et al 2005 [71], we evaluated the distribution of ER and E-cadherin in precursors lesions using a semi-quantitative five category score system: negative (-), ≤ 5% of cells stained; weak positive or reduced (+), 5% to 25% of cells stained; moderate positive (++), 25-50% of cells stained; strong positive (+++), ≥50% of cells stained.

Data were analysed using the statistical software package SPSS, (SPSS, version15 Chicago, IL). A Chi square test was used to compare the presence of CCLs, ADH, LN and DCIS in pure and mixed TC, tubulolobular and ILC. Results were considered significant if $p < 0.05$.

2.4 Results

2.4.1 Preinvasive cases

Eighty-two (46%), 71 (39%), and 27 (15%) patients were determined to have ALH, ADH and co-existence ADH and ALH; respectively, on the histological review of cases originally diagnosed as lesion with uncertain malignant potential. Notably, all the initial biopsies, showed in addition to ADH and/or ALH background of columnar cell lesions with and without atypia. The CCLs had morphological features and topographic distribution very similar to the associated ADH, and/or ALH. Follow up of these cases revealed that 19 cases (11%) subsequently developed invasive breast cancer (9 cases; 5%) and/or in-situ carcinoma (10 cases; 6%) within 5-15 years after the initial biopsy. The remaining 161 were followed up from 5-20 years and did not showed any significant pathological changes.

Two cases of the coexisting ADH/ALH cases (2/27; 7%) developed invasive carcinomas within 10 years which had two separate foci; one of low grade tubular carcinoma (T1, P2, M1) and the other focus of invasive classic lobular carcinoma grade 2 (T3, P2, M1). Twelve cases of the initial ALH cases (12/46; 26%) progressed into: classic ILC grade 2 (2 cases), tubulolobular carcinoma grade 1 (one case), LCIS with cribriform/micropapillary ADH/DCIS (5 cases) and exclusive LCIS (4 cases).

Five of the initial ADH cases (5/71. 6%) developed: tubular carcinomas grade 2 (2 cases), IDC-NST grade 2 (one case), IDC-NST grade 3 (one case) and DCIS grade 2 (one case) after 5 to 15 years.

The average interval to the subsequent carcinoma was the same in the ADH (10 years), ALH (8.8 years) and ALH/ADH (9.5 years) cases. The average interval to the subsequent DCIS and/or LCIS after the diagnosis of ADH (7.2 years) and/or ALH (6.5 years) was similar too. Thus, ALH tended to progress to LCIS which could progress to invasive

lobular carcinoma while ADH progressed into DCIS and therefore into ductal lineage pathways.

All subsequent carcinomas and their coexistent preinvasive lesions, except NST grade 3, showed cytoplasmic and nuclear morphological features very similar to the original preinvasive lesion. The initial preinvasive lesion of NST grade 3 was papillary ADH (ER+) which was detected in the subsequent biopsy adjacent and unrelated to the invasive carcinoma (ER-). While solid grade 3 DCIS (ER-) with morphological and topographic distribution very similar to the coexistence invasive NST grade 3 was detected.

Moreover, all ALH, LCIS and ILC showed negative expression of E-Cadherin. While all CCLs, ADH, DCIS, TC, IDC-NST, and tubulolobular lesions showed positive expression of E-cadherin. However, in three intraductal epithelial proliferative lesions lined by E-cadherin positive columnar cells with apical snouts focal islands of E-cadherin negative luminal epithelial cells were seen (**Figures 2-4 and 2-5**). Furthermore, in another two cases, some of the in situ components showed patchy expression of E-cadherin.

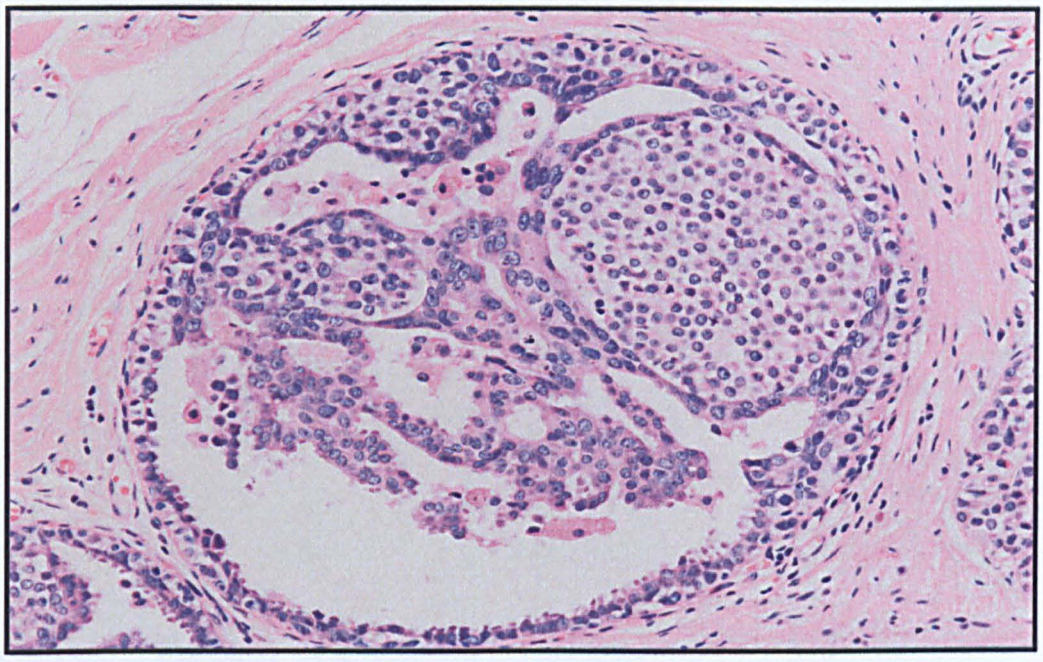

Figure 2-4: Duct lined by columnar cell epithelium with apical snouts spaces islands of pale lobular like cells.

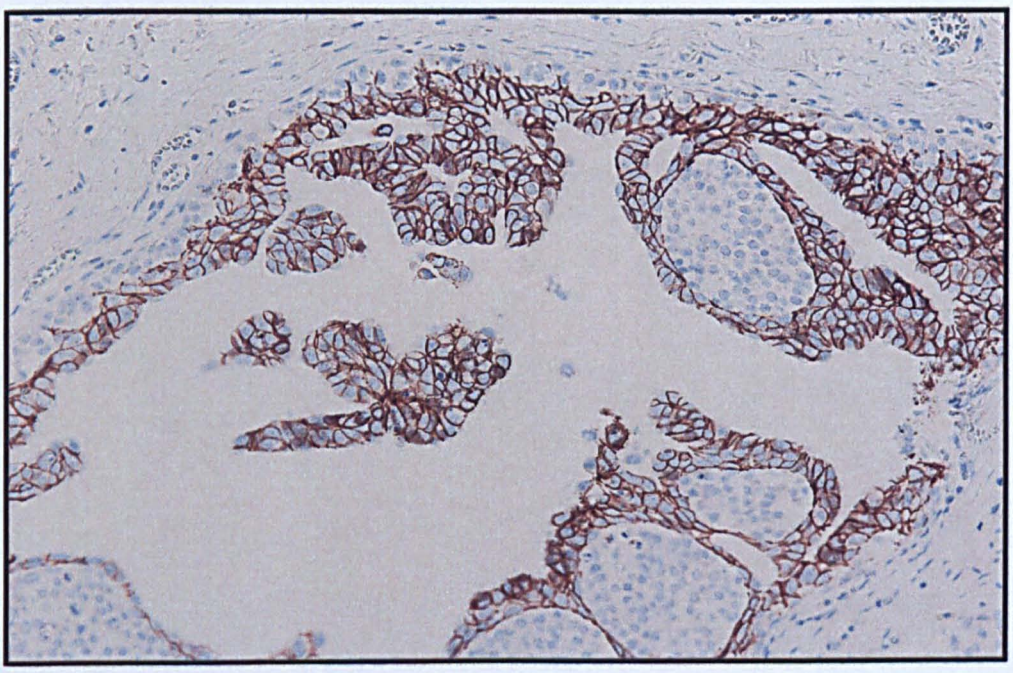

Figure 2-5: Duct lined by columnar cell epithelium showing positive expression for E-cadherin spaces islands of pale lobular like cells that showed no membranous expression of E-cadherin.

2.4.2 Tubular Carcinoma Pure type

The patients' characteristics are summarized in (**Table 2-1**). About 67% of patients were postmenopausal. All cases were well differentiated (grade 1; G1 with low mitotic index (M1). About 70% and 91% of cases showed moderate nuclear pleomorphism (P2) and >90% tubule formation (T1), respectively. Most tubular carcinomas were small in size (mean whole tumour size: 1.3 cm, range 0.2-3.6 cm). Only 15% and 6% showed local lymph node metastases and distant metastases, respectively. About 94% of cases were ER+. All cases were positive for E-cadherin but the majority showed reduced expression. CCLs were detected in 95% of cases (**Table 2-2 and Figure 2-6**). The CCLs were stratified into six types comprising CCH with cytologic atypia (77%), CCC with atypia (66%), CCC without atypia (57%), CCH with complex and cytologic atypia (27%), CCH with complex architecture (9%), CCH without atypia (7%) (**Figure 2-7 and Table 2-3**). Collectively, FEA was seen in 84% of pure tubular carcinomas. ADH/DCIS was present in 89% of patients; 65% low grade, 23% intermediate grade, 12% low to intermediate grade and none of high grade (**Figure 2-8**). ADH/DCIS was extensive (extending > 1 mm beyond the invasive component) in 47% and minimal in 53% cases. A cribriform growth pattern was present in 88% of DCIS cases while micropapillary, solid and flat growth patterns were present in 31%, 12% and 8% of ADH/DCIS patients, respectively (**Figure 2-9**). The triad of CCL, low/intermediate grade ADH/DCIS and tubular carcinoma was seen in 85% of cases. In most cases, the CCLs, DCIS, and tubular carcinoma displayed the same cytologic-nuclear morphology and were intimately associated with the same geographical distribution. UEH was detected in 18% of cases and when present, was associated with both CCLs and ADH/DCIS. LN was detected in 9/56 of cases (16%) but in the majority was present away from the invasive component. The triad of LN, ADH/DCIS and CCLs was seen in 16% of cases.

Table 2-1: Clinicopathological features of low nuclear grade breast carcinomas.

Parameter	Tubular Carcinoma "Pure"	Tubular carcinoma "Mixed"	Tubulolobular	ILC "Classical"
Mean age (years)	57	56	60	62
Mean tumour size(cm)	1.6	1.3	1.8	2.7
Histologic grade	G1	G1	G1	G2
Lymph node involvement (%)	2%	10%	25%	33%
E-Cadherin protein expression (%)	100%	100%	100%	0%
Estrogen receptor positive expression (%)	96%	100%	100%	90%
Mean Nottingham Prognostic index (NPI)	2.2	2.3	2.5	3.7

ER; oestrogen receptor, NPI; Nottingham Prognostic Index and ILC; invasive lobular carcinoma.

Table 2-2: Comparison of the frequency for putative precursor lesions in tubular, cribriform tubulolobular and classical invasive lobular carcinoma (ILC).

Lesions	Tubular carcinoma "Pure" (n= 135)		Invasive cribriform carcinoma (n= 20)		Tubulolobular carcinoma (n=20)		ILC "Classical" (n=180)		X^2
	n	%	N	%	n	%	n	%	
CCLs	128	95	18	90	17	86	108	60	.001**
DCIS	120	89	19	95	17	86	72	40	.001**
LN	22	16	4	20	11	57	162	90	.001**
HEU	24	18	6	30	3	14	45	25	0.568

* Chi-square tests showed highly significant differences when comparing the presence of columnar cell lesions (CCLs), ductal carcinoma in situ (DCIS) and lobular neoplasia (LN) in different tumour types. Hyperplasia of usual type (HEU) did not significantly differ between different cancer types.

** Statistical significant.

Table 2-3: Comparison of the frequency for different forms of CCLs in tubular, tubulolobular and invasive lobular carcinoma (ILC)

Lesions	Tubular carcinoma "Pure" (n= 135)		Invasive cribriform (n= 20)		Tubulolobular carcinoma (n=20)		ILC "Classical" (n=180)		X^2
	n	%	n	%	n	%	n	%	p
Columnar cell change	77	57	12	60	14	71	95	53	0.635
Columnar cell hyperplasia	9	7	4	20	8	42	97	54	.001*
Columnar cell hyperplasia with complex architecture	12	9	0	0	3	14	20	11	0.448
Columnar cell change with cytologic atypia	89	66	12	60	11	57	34	19	.001*
Columnar cell hyperplasia with cytologic atypia	104	77	11	55	17	86	95	53	.013
Flat epithelial atypia	113	84	14	70	17	86	97	54	.004*
Columnar cell hyperplasia with complex and cytologic atypia	36	27	6	30	7	36	16	9	.029*

* Statistically significant

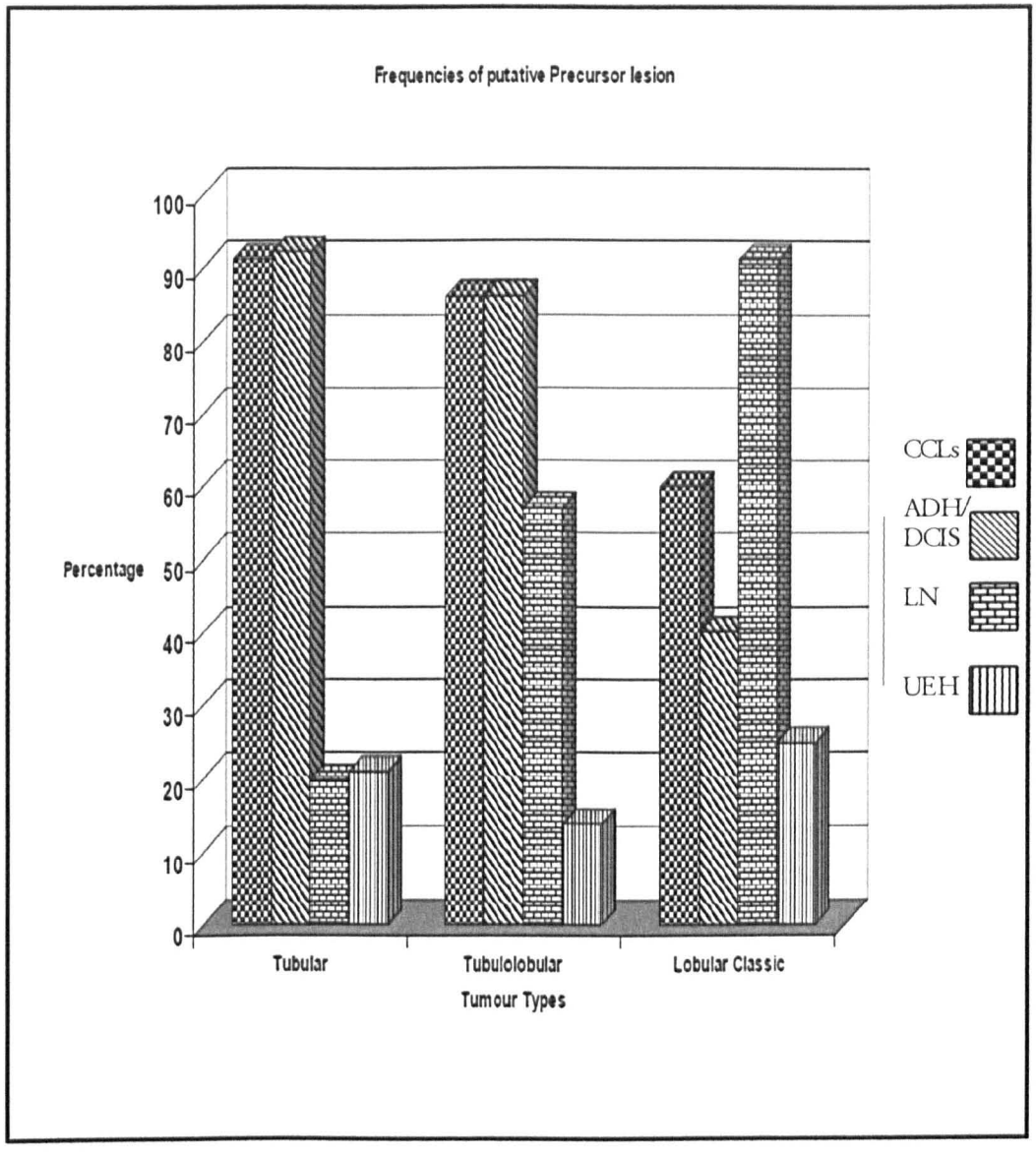

Figure 2-6: Frequency of columnar cell lesions (CCL), atypical ductal hyperplasia/ductal carcinoma in situ (ADH/DCIS), lobular neoplasia (LN) and usual epithelial hyperplasia among tubular carcinoma, invasive classic lobular carcinoma and tubulobular carcinoma.

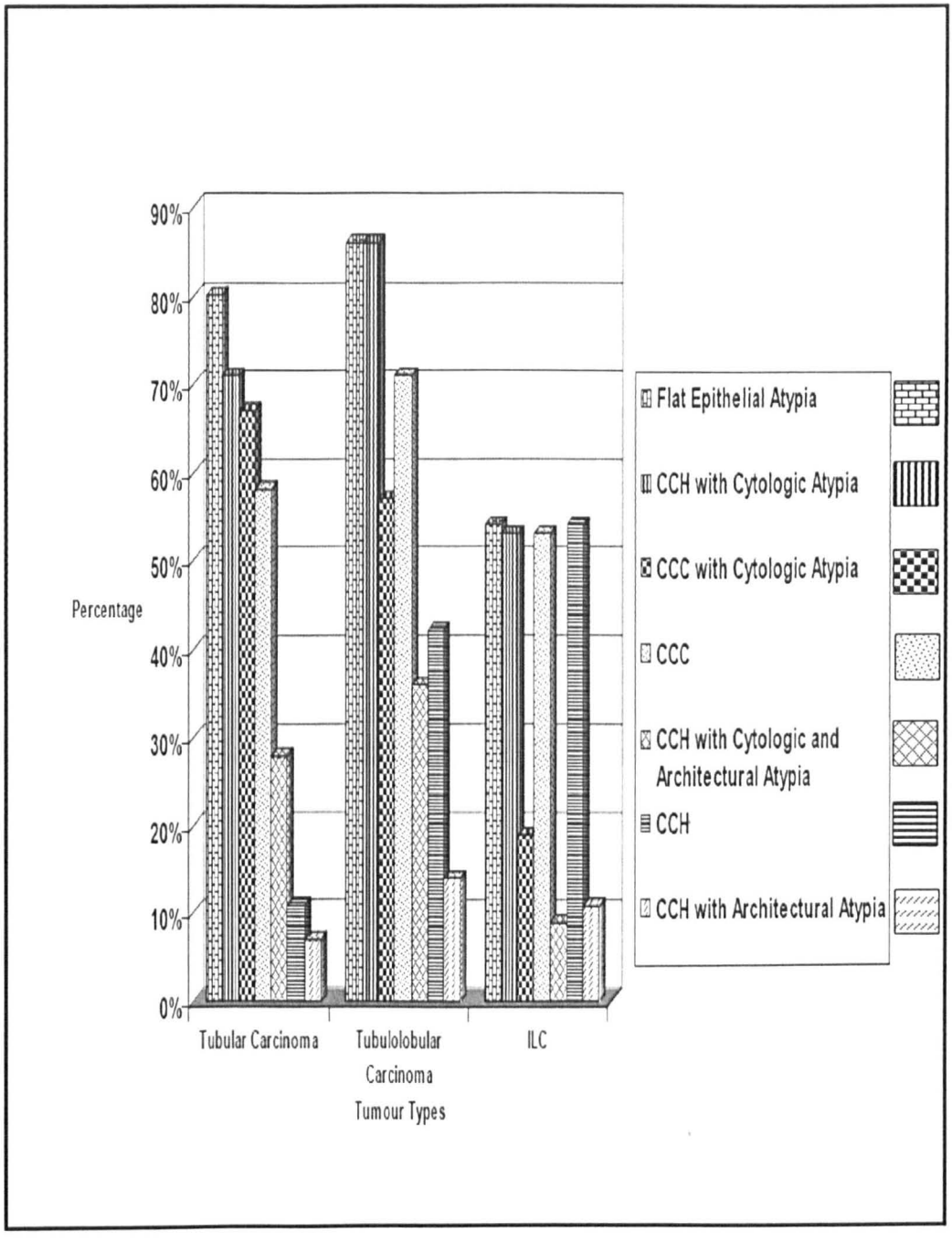

Figure 2-7: Frequency of different types of columnar cell lesions (CCLs) in tubular carcinoma, tubulolobular and invasive lobular carcinoma.

(CCC; columnar cell changes, CCH; columnar cell hyperplasia, FEA; flat epithelial atypia)

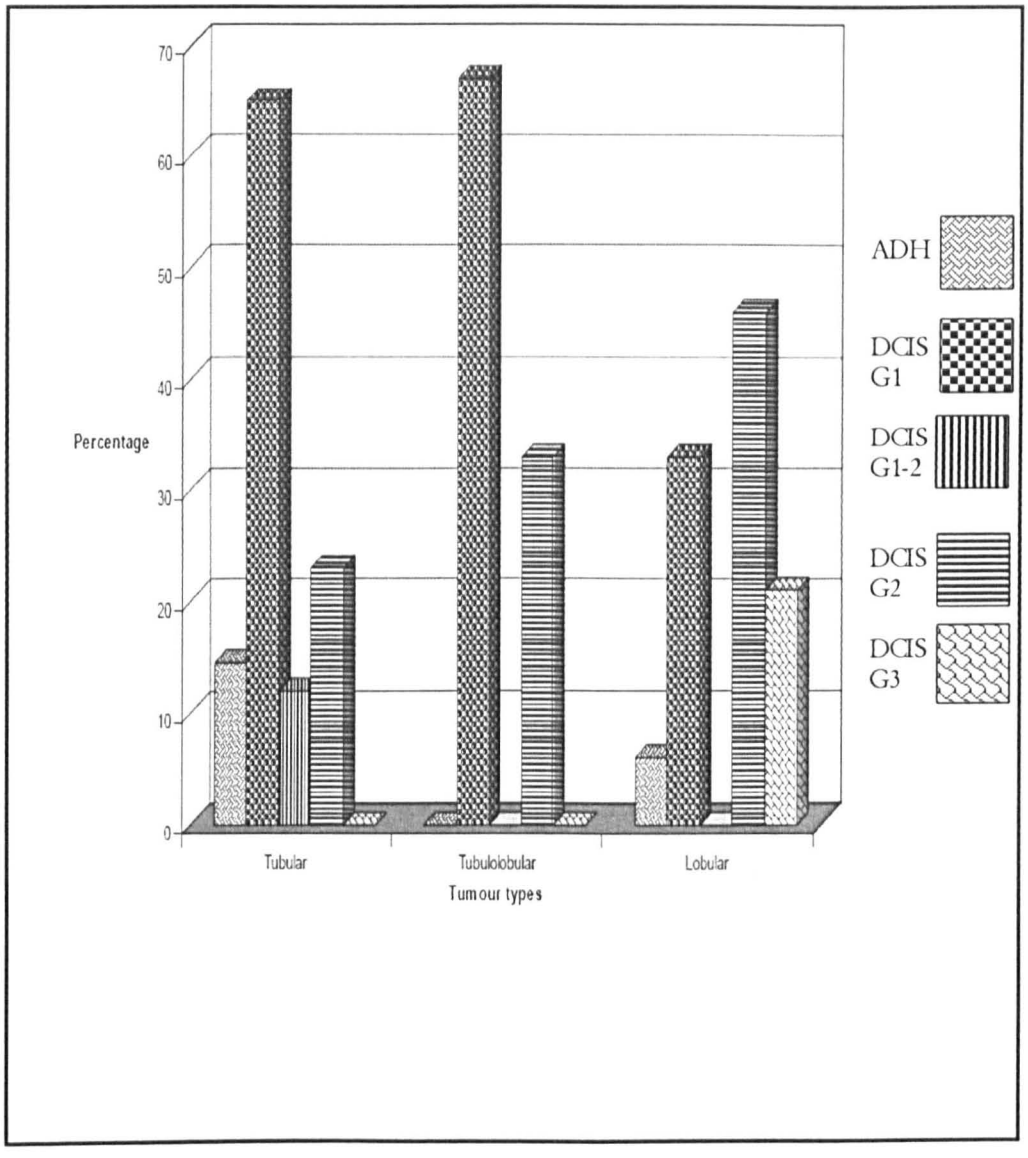

Figure 2-8: Frequency of different grades of DCIS in tubular, tubulolobular, invasive lobular carcinoma.

(G1; low grade, G2; intermediate grade, G3; high grade, CCLs; columnar cell lesions, DCIS; ductal carcinoma in situ, LN; lobular neoplasia, UH, usual epithelial hyperplasia)

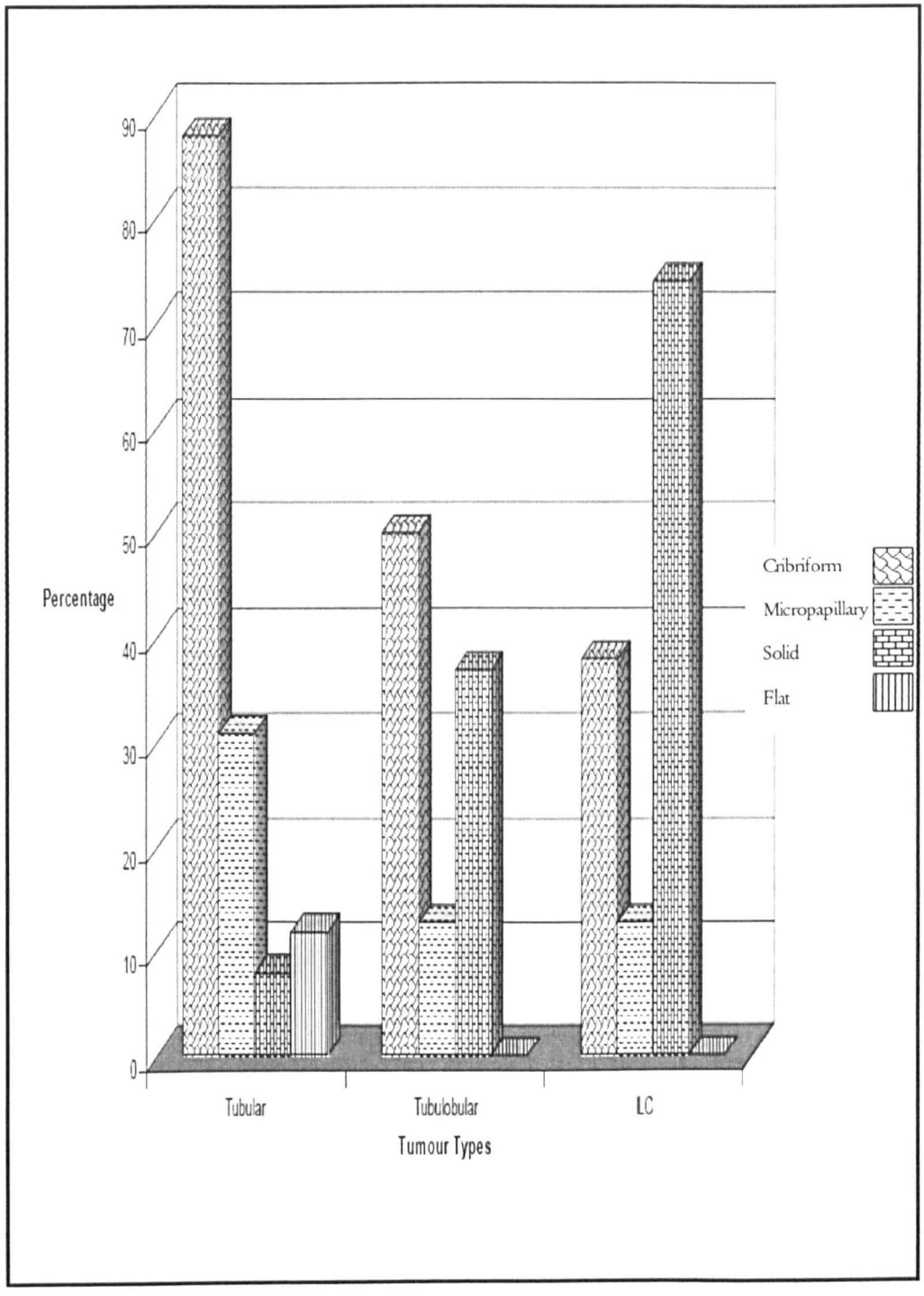

Figure 2-9: Frequency of different growth patterns of DCIS among tubular, tubulolobular, invasive lobular carcinoma. (ILC)

2.4.3 Invasive lobular carcinoma classic type

About 72% of patients were postmenopausal. About 95% were moderately differentiated (grade 2; G2) and 5% were well-differentiated (G1) with low mitotic index (97%; M1) and no tubule formation (T3; 96%). About 90% showed moderate nuclear pleomorphism. The mean whole tumour size was 2.1 cm (range; 0.13-5.5). Local lymph node metastases and distant metastases were detected in 41% and 24% of classic ILC. All ILC and LN showed no E-cadherin expression and 95% were ER+. No pre-invasive lesions were detected in 9% of cases while LN was seen in the remaining 91% of cases. ADH/DCIS was detected in 42% of cases, and was extensive in 33%. About 46% ADH/DCIS cases were of intermediate grade, 33% were low and 21% were high grade. Solid growth pattern ADH/DCIS was seen in 79% while cribriform and micropapillary growth pattern were seen in 38% and 13% of cases, respectively. CCLs were seen in 60% cases and all CCLs were associated with LN. ADH/DCIS, CCL and LN were present altogether in 23% of cases. The CCLs were stratified into six types including CCH without atypia (54%), CCC (53%), CCH with cytologic atypia (53%), CCC with atypia (19%), CCH with complex architecture (11%), CCH with complex and cytologic atypia (9%). UEH was diagnosed in 25% of cases.

2.4.4 Tubulolobular carcinoma

The mean whole tumour size was 1.8 cm. All cases were either well (75%) or moderately (25%) differentiated (G1) with low mitotic figure (M1). DCIS was seen in 86% of cases; 67% and 33% of low and intermediate grade respectively. A cribriform growth pattern was seen in 50% of DCIS while solid and micropapillary were seen in 37% and 12.5% of DCIS, respectively. CCLs were detected in 86% of cases; 45% of CCC with atypia, 29% of CCH, 14% of CCC and 14% of CCH with complex architecture. The triad of LN, DCIS and CCLs was seen in 56% of cases. UEH was diagnosed in 14% cases.

2.4.5 Cribriform carcinoma

About 63% of patients were postmenopausal. All cases were either well (81%) or moderately (19%) differentiated tumours with low mitotic index (M1). About 81% and 88% of cases showed moderate nuclear pleomorphism (P2) and tubule formation (T2), respectively. Mean whole tumour size was 1.8cm; range 0.6-4.8 cm. No vascular invasion, local lymph node metastases or distant metastases was recorded. All cases were ER+ and E-cadherin+. CCLs were detected in 90% of cases. Collectively, FEA was seen in 80% of cases. ADH/DCIS was present in 95% of patients; 85% of low grade/intermediate grade and 10% of high grade. A cribriform growth pattern was present in 90% of DCIS cases. In most cases, the CCLs, DCIS, and ICC displayed the same cytologic-nuclear morphology and were intimately associated with the same geographical distribution. UEH was detected in 20% of cases and when present, was associated with both CCLs and ADH/DCIS. LN was detected in 30% of cases.

2.4.6 IDC-NST low grade

About 65% of patients were post-menopausal. The mean whole tumour size was 1.6 cm (range 0.3-3.0 cm). All cases showed low mitotic index (M1), while about 80% showed moderate pleomorphism and tubule formation. Local lymph node metastases and distant metastases were recorded for 21% and 18% of cases, respectively. CCLs were detected in 82% of patients. CCLs were stratified as CCC with atypia (60%), CCC (60%), CCH with cytologic atypia (55%), CCH with complex and cytologic atypia (27%) and CCH without atypia (20%). ADH/DCIS was present in 87% of cases; 70% intermediate grade and 30% low grade. DCIS was extensive in 40% of cases. A cribriform growth pattern was present in 80% of DCIS cases while solid growth pattern was present in 40% of DCIS. UEH was detected in 42% of cases and all were associated with both CCLs and DCIS and were in the

same geographic regions. LN was detected in 23% of cases and was frequently localized away from the invasive component.

2.4.7 IDC-NST high grade

About 58% of patients were postmenopausal. About 90%, 95% and 85% showed high mitotic index (M3), marked pleomorphism (P3) and no tubule formation (T3), respectively. The mean whole tumour size was 2.2 cm (range; 0.16-6.5 cm). Local lymph node metastases, distant metastases and vascular invasion were detected in 41%, 41% and 37% of cases, respectively. About 50% and 95% were ER+ and E-Cadherin positive, respectively. No pre-invasive lesions were detected in 40% of cases while DCIS, UEH, CCLs and LN were seen in 60%, 33%, 10% and 5% of cases, respectively. Comedo and solid growth pattern were present in (70%) and (36%) of DCIS associated with high grade IDC while micropapillary and cribriform growth patterns were present in only 9% and 5% respectively. In most cases of high grade IDC, the DCIS lesions and invasive component displayed the same ER immunophenotype, cytologic-nuclear morphology and were intimately associated with the same geographical distribution.

2.5 Discussion

With ADH and lobular neoplasia, there is a 4 to 10 fold increase in the risk for subsequent invasive breast cancer over 15 to 30 years [66, 67]. In our study, we found 11% of ADH and/or ALH progressed into either in situ or invasive carcinoma which had the same topographic and morphological features similar to the initial lesion supporting the concept of a direct precursor product relationship [66, 67]. However this risk is spread over long periods, so that subsequent cancer can sometimes occur decades later as a result of the relatively low proliferative rate of ADH and LN. Interestingly, 10 cases of ADH and or ALH were associated with subsequent malignancy in other organ systems especially female genitourinary tract and gastrointestinal system which suggests that ADH/ALH could be a sign of a woman's increased risk for cancer either as a reflection of a genetic instability or as a part of common or general process that eventually lead to the development of particular form of human cancers e.g. ER signalling dysregulation.

To date, there has not been a comprehensive morphologic study comparing the association of different putative precursor lesions involved in the development of some special types of low grade and classical lobular breast carcinoma. Moreover, only a few studies have analysed the association of CCLs with tubular carcinoma [70, 72, 88]. CCLs consistently harbour recurrent chromosomal abnormalities suggesting they are clonal and neoplastic rather than hyperplastic proliferative lesions [71]. Some studies have shown that the sites and patterns of association of chromosomal alteration are similar to a range of precursor, in situ and invasive forms of breast cancer including ADH, ALH, low grade DCIS, LCIS, invasive low grade and lobular carcinoma [52, 67, 75, 76, 84, 89- 93] which led our group and others to speculate that these lesions form a family of related breast cancer and their precursor lesions (**Figure 2-10**).

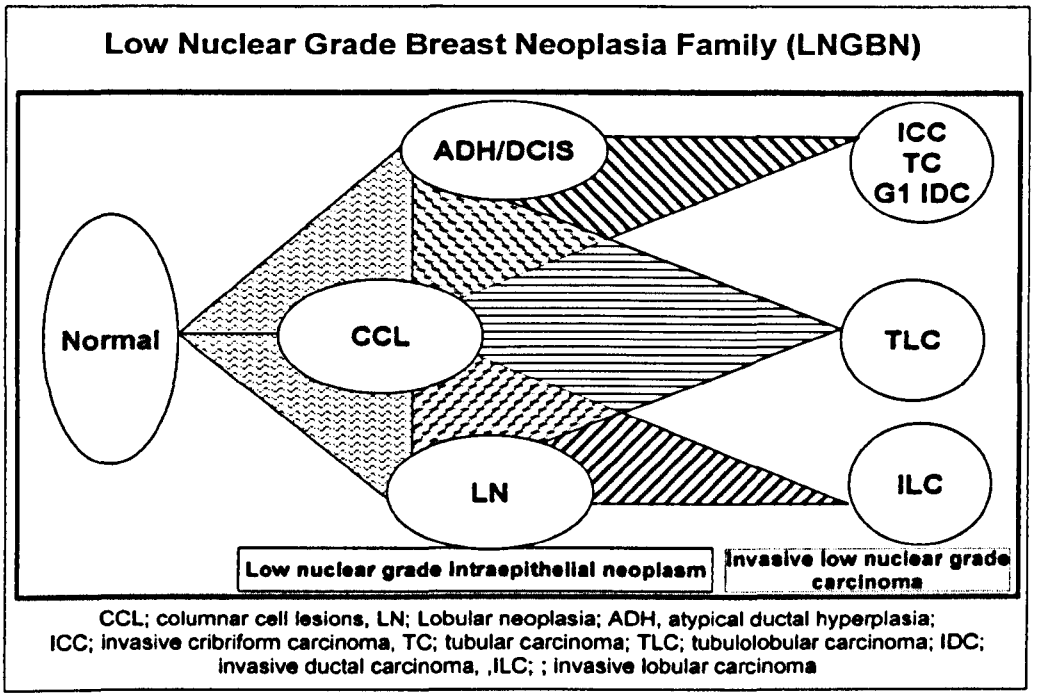

Figure 2-10: Evolutionary pathways of low grade breast neoplasia.

In tubular carcinoma, various names have been used synonymously to describe CCLs including atypical lobules type A [11], atypical cystic lobules [74], pre-tubular hyperplasia [85], small ectatic ducts lined by atypical ductal cells with apocrine snouts [72], monomorphic ductal neoplasia-flat type [75], columnar alteration with prominent apical snouts and secretions [70], clinging carcinoma [75] and flat epithelia atypia (FEA) [77]. These lesions were often reported at the periphery of, or within, TC. In our study of lesions associated with invasive carcinoma, we found a very high prevalence (95%) of CCLs in TC. Also, our study indicated that FEA (CCC with atypia and CCH with atypia) was the commonest form of CCL (80% of cases) in accord with other studies, [70, 72, 88] while CCH with or without complex architecture was rare. This interesting finding suggests that not all forms of CCLs are directly associated with tubular carcinoma implying that the acquisition of nuclear atypia and the more complex forms is a requirement for progression to invasive

carcinoma. Consequently, the type of CCLs could determine the type of invasive carcinoma formed. It has been reported that the genetic profile patterns seen in different forms of CCLs closely reflect the degree of proliferation and atypia indicating some of these lesions represent a morphologic biological and molecular continuum[71].

Previous studies have demonstrated a good correlation between the histological grade of DCIS and the grade of associated infiltrative component [88, 94]. Also, some studies have shown that cribriform and micropapillary growth patterns are closely associated with tubular carcinoma [70, 72]. Our results concur with these studies as we found the majority of DCIS lesions associated with low grade invasive carcinoma was low grade with a cribriform and/or micropapillary growth pattern, while the solid growth pattern was infrequent. We found the triad composed of CCLs, low grade DCIS and invasive carcinoma was present in 80% of tubular cases, showing similar, nuclear and cytoplasmic morphologic features and geographic location. We propose that FEA may develop into ADH and then low grade DCIS, particularly cribriform and micropapillary types, with the eventual progression to tubular carcinoma.

In agreement with other studies [74,76,88,95] we demonstrated that LN was present in approximately 16% of tubular cases with all LN lesions being associated with CCL and DCIS. This suggests DCIS and LN may in this situation have a relationship and form part of the precursor pathway to invasive tubular carcinoma. We speculate that they share a developmental lineage pathway from a common cell of origin giving rise to both CCLs, LN, and low grade ductal neoplasia (ADH and DCIS) dependant on acquisition of additional genetic alterations which influence morphological appearance and character such as E-cadherin loss.

Invasive lobular carcinoma of classical type share the low mitotic frequency and growth fraction seen in tubular carcinoma and low grade ductal carcinoma[46, 96] but are usually

moderately differentiated (histological grade 2) due to absence of tubule formation, larger in size, and have a higher tendency to metastasise to axillary lymph nodes. In contrast to TC, the overwhelming majority of LN and invasive lobular carcinoma are negative for the tumour suppressor gene E-cadherin [81, 97]. In our study all LN and classical ILC lesions were negative for E-cadherin protein expression. Furthermore, mutation analysis of the E-cadherin gene in adjacent in situ and ILC have revealed the same specific mutations in both lesions [97]. This provides compelling evidence for the precursor role of LCIS in ILC [97]. LN was present in 91% of classical ILC in the same geographic localization. In addition, we found LN occurred in isolation without any other putative lesions in only 21% of ILC. These findings further support the hypothesis that LN is a direct precursor for ILC, in agreement with others [66, 97]. Some investigators noted the higher co-existence of LN and FEA in the same surgical specimen, particularly in TC [76, 88, 95], but the co-existence of these precursors in ILC has not been reported. We found that CCLs and LN co-exist in 60% of ILC cases and the majority of these CCLs were CCH and FEA, particularly CCH with cytologic atypia. Also, we observed the combination of LN, CCLs, and DCIS in 23% of ILC. These observations when considered in the context of previous cytogenetic studies suggest that loss of normal E-cadherin gene expression is an early event and may switch on the development of lobular differentiation. We speculate that the particular evolutionary tumour pathway is dependent on the precise point when E-cadherin gene loss occurs; in ductal cancer, E-cadherin loss occurs at a later stage.

We found that tubulolobular carcinoma (TLC) had similar characteristics to TC including low tumour grade, size, ER and E-cadherin expression and relatively favourable prognosis. Compared to TC, TLC also showed a high co-existence and distribution of DCIS and CCLs shared with TC. However, TLC differed from TC in showing a higher tendency to metastasize to axillary lymph node, and also resembled ILC with a higher frequency of LN, solid DCIS and CCH lesions, all present in the same topographic regions as the invasive

component. Our findings support the hypothesis that TLCs are a distinct subtype of mammary carcinoma with morphologic and clinicopathological features overlapping those seen in tubular and invasive lobular carcinoma. The uniform positive expression of E-cadherin protein in TLC supports an alternative molecular derivation to classical lobular carcinoma, despite a dominant lobular growth pattern [98].

In summary, our findings support the hypothesis that CCLs are associated with pure and mixed forms of tubular carcinoma, and that LN is involved in ILC development. Co-existence of both LN and CCLs with invasive tubular and with lobular carcinoma was common. Our observations support the hypothesis that these lesions represent members of a family of low grade precursor, in situ and invasive neoplastic lesions of the breast. This hypothesis will be tested (Chapter 4) by performing molecular analysis of tubular and lobular carcinomas and their precursors (CCLs and FEA) to assess if they have direct evolutional links.

Chapter 3:

Molecular evidence to support the concept of a low nuclear grade breast neoplasia family

3.1. Abstract

In chapter 2, we provided morphological evidence showing a link between some precursor lesions and low nuclear grade breast carcinomas (LNGBC) especially tubular and classic lobular carcinoma. In this study, we aim to provide further immunophenotypic support to our proposed route of pathogenesis of LNGBC and their precursor lesions. Precursor lesions including columnar cell lesions (CCLs), atypical ductal hyperplasia (ADH), ductal carcinoma in situ (DCIS), usual epithelial hyperplasia, and lobular neoplasia (LN) were immunohistochemically compared with matching 'morphologically normal' terminal lobular duct units (TDLUs) and matching invasive carcinoma.

The epithelial cells in the putative precursor CCLs, flat epithelial atypia (FEA), ADH, LN, DCIS lesions and their co-existing LNGBC were negative for basal and myoepithelial markers, but positive for CK19/18/8, ER-α, Bcl-2, and cyclin D1. The ER-α/ER-β expression ratio increased during carcinogenesis, as did expression of cyclin D1 and Bcl-2. The p53 immunopositivity was found in 3% of LNGBC vs. 43% of high nuclear grade breast cancer (HNGBC), while ataxia telangiectasia mutated (ATM) expression was absent or reduced in 22% of LGNBC vs. 53% of (HNGBC) cases.

In summary, our findings support the concept that FEA is the earliest morphologically identifiable non-obligate precursor lesion of LNGBC. These may represent a family of precursor, in situ and invasive neoplastic lesions belonging to the luminal 'A' subclass of breast cancer. The balance between ER-α and ER-β expression may be important in driving

cyclin D-1 and Bcl-2 expression. ATM may be one of the alternative regulatory mechanisms to TP53 mutation or dysfunction in a subset of breast carcinoma. Our findings support the concept that progression of LNGBC "Luminal A" to HNGBC "Basal-like or HER-2+" phenotype is an unlikely biological phenomenon. Furthermore, we propose a model for the biological events that are associated with ER-α in the development of LNGBC.

3.2. Introduction

Breast cancers (BCs) are heterogeneous in their morphology, response to therapy and clinical course [19]. Molecular profiling studies have shown the existence at least five different BC subtypes, each with different clinical outcomes [45, 46]. The luminal subtype 'A' have higher levels of oestrogen receptor alpha (ER-α) and a better survival outcome compared with luminal subtypes 'B' [45, 46]. Moreover, there is convincing genetic evidence to suggest that the low grade (LGBC) and high grade (HGBC) breast cancers evolve through distinct evolutionary pathways [52, 57]. LGBCs are usually diploid/near-diploid and harbour recurrent loss of chromosome 16q and gains of chromosome 1q[54, 55]. In contrast, HGBCs are usually aneuploid with complex genetic profiles and infrequent deletion of 16q [54, 55]. In HGBCs, even when loss of 16q is present, the underlying genetic mechanism appears to be distinct from that seen in LGBCs [99].

In chapter 2 we adopted the concept of low nuclear grade breast neoplastic (LNGBN) family based on:

1) During follow up, some ADH and/or ALH progressed into invasive TC, TLC and/or classic ILC within 5-15 years of the initial diagnosis.
2) The similarity of the nuclear and cytoplasmic morphological features between some putative precursor lesions and their either co-exiting or consequent invasive carcinomas.
3) The intimate topographic distribution of some putative precursor lesions and their either co-existing or consequent invasive carcinoma
4) The significant coexistence of columnar cell lesions (CCLs), lobular neoplasia (LN) and atypical ductal hyperplasia/low grade ductal carcinoma in situ (ADH/low grade DCIS) with invasive tubular carcinoma (TC), tubulolobular carcinoma (TLC) and classic

invasive lobular carcinoma (ILC).

In this study, we expand our investigation to explore the immunohistochemical phenotype of the putative precursor lesions with both their related normal TDLUs and invasive cancers.

3.3. Materials and Methods

In this study, we included invasive TC (n=135), classic ILC (n=180), cribriform (ICC; n=20), TLC (n=20), mixed invasive tubular/classic lobular carcinoma (n=15) and 60 cases of invasive low grade ductal carcinomas of no special type (low grade IDC-NST) which were compared with high grade IDC-NST (n=670). Phenotype was assessed using immunohistochemistry (IHC) on tissue microarrays (TMA) and full face sections. Two TMAs sets were prepared as previously described [87]. Briefly, two representative areas from each lesion were carefully selected from haematoxylin-eosin stained sections of donor blocks. The H&E slide and its corresponding block were aligned then the selected marked area on the H&E slide was copied to the donor block using a marker pen. Blank paraffin blocks were used as recipient blocks for tissue cores. Paraffin wax was melted at 55-58°C and poured into a 5-10 mm thick moulds. A plastic cassette was placed on the surface of the melted paraffin then all were cooled and the mould was removed. Two core cylinders (0.6 mm diameter) were punched by using a tissue microarraying device (Beecher Instruments, Silver Spring, MD, USA) which was designed to make holes in the recipient blocks and to obtain cores from the donor blocks as previously described [87]. Then the punched cores were deposited and arrayed into the recipient blocks with 1 mm spacing distance between the two adjacent cores. About 450 different components (preinvasive and matching invasive carcinoma) of 150 TC and classic ILC cases were arrayed in TMA set

number 1. A second set of TMA containing unselected 2000 successive cases of invasive breast carcinoma was also used[87].

Four-um thick sections of the resulting microarray block were made and used for IHC analysis after transfer to glass slides.

To validate the use of the microarray for immunophenotyping, full face sections of 10 cases of each tumour type were stained and the protein expression levels of the 15 antibodies were compared for each lesion on the full face sections and on TMAs.

By using hierarchical clustering methodology of a large panel of well-characterized commercially available biomarkers related to epithelial cell lineage, differentiation, hormone and growth factor receptors and gene products known to be altered in some forms of breast cancer, Abd El-Rehim and her colleagues [87] identified 5 groups of breast cancer with distinct patterns of protein expression. In our study we have used the same panel of antibodies to immunophenotyping our lesions. In addition we explored the expression of selected proteins that are likely to play an important role in the pathogenesis of low grade breast cancer development such as Cyclin D1 (CCND1)[100], fragile histidine triad (FHIT)[101], ATM[101-102] and ER- β isoforms[103].

Subsequently, the TMAs, as well as 40 full face sections of benign preinvasive lesions not associated with invasive lesions, were immunohistochemically profiled for basement membrane components (laminin and collagen type IV), cytokeratins (CK19, CK18, CK8, CK14, CK5.6), hormone receptors (ER-α and ER- β 1), putative tumour suppressor genes (FHIT, ATM, BRCA1, p53 and E-cadherin), apoptosis/cell cycle regulator (Bcl2 and cyclin D1), and proliferation index (MIB1) markers to immunohistochemically phenotype the different lesion types (**Tables 3-1 and 3-2**).

In addition, normal breast tissue comprising 40 biopsy specimens removed from patients (age range 25-60 years; 20 cases premenopausal and 20 cases postmenopausal) that underwent reduction mammoplasty, primarily for cosmetic reasons, were histologically examined and immunohistochemically profiled. All normal control patients were free of breast cancer in both breasts and had no previous medical history of breast cancer. Immunostaining was performed as previously described in Chapter 2 (section 2.3.2). Positive and negative (omission of the primary antibody and IgG-matched serum) controls were included in each run.

Table 3-1: Types and number of breast lesions (n=1605) included in this study

Type of lesions	Number of lesions	
Invasive lesions	(n= 1185)	
▪ Tubular carcinoma		135
▪ Classic invasive lobular carcinoma		180
▪ Tubulolobular carcinoma		20
▪ Mixed invasive tubular and classic lobular carcinoma		15
▪ Invasive cribriform carcinoma		20
▪ Invasive low grade ductal Carcinoma		60
▪ Invasive High grade ductal Carcinoma		670
Pre-invasive Lesions adjacent to invasive	(n=255)	
▪ Columnar cell changes (CCC)		49
▪ Columnar cell hyperplasia (CCH)		43
▪ Flat epithelial atypia (FEA)		40
▪ Atypical ductal hyperplasia/low grade ductal carcinoma in situ (ADH/low DCIS		40
▪ Lobular neoplasia (LN)		39
▪ Usual epithelial hyperplasia (UEH)		44
Pre-invasive Lesions not associated with invasive	(n=120)	
▪ Columnar cell changes (CCC)		20
▪ Columnar cell hyperplasia (CCH)		20
▪ Flat epithelial atypia (FEA)		40
▪ Atypical ductal hyperplasia/low grade ductal carcinoma in situ (ADH/low DCIS		20
▪ Lobular neoplasia (LN)		20
▪ Usual epithelial hyperplasia (UEH)		20
Normal Terminal Duct Lobular Units(TDLUs) adjacent to invasive	(n= 65)	
Normal TDLUs from reduction breast specimen	(n= 40)	
▪ Premenopausal		20
▪ Postmenopausal		20

Table 3-2: Primary antibodies, clone, source and optimal dilution used for immunohistochemistry.

Antibody	Clone	Source	Dilution	Pre-treatment	References
Mouse MAb anti p53	DO7	Novocastra	1: 50	MAR	87, 102, 104, 105, 106, 107
Mouse MAb anti-Bcl2	124	Dako-Cytomation	1:100	MAR	87, 104 106, 107
Mouse MAb anti-BRCA1	MS110	Oncogen Research	1:150	MAR	87, 102, 104, 106, 107
Rabbit MAb anti-ATM	Y170	Abcam	1:100	MAR	102, 104
Mouse MAb anti-vimentin	Vim 3B4	Dako-Cytomation	1:250	MAR	104, 106
Mouse MAb anti-CK19	BCK 108				87, 104
Mouse MAB anti-CK7/8	CAM 5.2				87, 104
Mouse MAb anti-Ck18	DC10	Dako-Cytomation	1:100	MAR	87, 104
Mouse MAb anti-ER-α	1D5	Dako-Cytomation	1:200	MAR	87, 104, 107
Mouse MAb anti-PR	PR	Dako-Cytomation	1:150	MAR	87, 104, 107
Mouse MAb anti-Ck14	LL002	Novocastra	1:40	MAR	87, 104, 107
Mouse MAb anti-Ck5/6	D5/161B4	Chemicon	1:60	MAR	87, 104, 107
Mouse MAb anti-β2	57/3	Serotec	1:10	MAR	108
Mouse MAb anti-β1	14C8	Gene Tex	1:100	MAR	108
Rabbit antihuman HER-2	polyclonal	Dako-Cytomation	1:100	No treatment	104, 107, 109
Mouse MAb anti-Ki-67	MIB1	Dako-Cytomation	1:300	MAR	104, 107
Mouse MAb anti-SMA	1A4	Dako-Cytomation	1:200	MAR	87
Rabbit MAb anti-cyclin D1	SP4	Lab vision	1:200	MAR	100
Mouse MAb anti-E-cadherin	HERCD-1	Zymed Laboratories	1:100	MAR	87
Rabbit polyclonal ant-FHIT	ZR44	Zymed Laboratories	1:600	MAR	87

ATM: ataxia telangiectasia mutated; BRCA1: Breast cancer 1, ER: oestrogen receptor, PR; progesterone receptor, Ck: cytokeratin, SMA; smooth muscle actin, MAb: Monoclonal antibody.

3.3.1 IHC scoring and evaluation

The immunohistochemistry staining was evaluated by estimating the percentage (%) of cells showing characteristic staining (from undetectable level or 0% to homogenous staining or 100%), by estimating the intensity (I) of staining (1, weak staining; 2, moderate staining; or 3, strong staining), and by determining topographical localization (membranous, nuclear, or cytoplasmic). The IHC staining was semi-quantitatively scored by 2 pathologists using both Allred and H-scores as previously described [86, 87, 110]. For H-score assessment, 10 fields were chosen at random at x 20 magnification and the staining intensity was scored as 0, 1, 2, or 3 corresponding to the presence of negative, weak, intermediate, and strong brown staining, respectively. The total number of cells in each field and the number of cells stained at each intensity were counted. The average percentage positive was calculated and the following formula was applied: H-score = (% of cells stained at intensity category 1 x 1) + (% of cells stained at intensity category 2 x 2) + (% of cells stained at intensity category 3 x 3). A score between 0 and 300 was obtained where 300 was equal to 100% of tumour cells stained strongly (3 +). For quick score, the percentage of cells stained at the most frequent intensity was counted and given a score (0 = 0%, 1 < 1%, 2 = 1-10%, 3 = 11-33%, 4 = 34-46%, 5 = 67-100%), as was their intensity (1 = weak, 2 = moderate, 3 = strong). The total of the two scores gives the overall Allred score between 2 to 8 (by definition, there is no Allred score of 1). The intensity of staining (0-3) and percentage of tumour cells with unequivocal nuclear staining for Ki-67 (MIB1), ATM and BRCA1 was recorded semi-quantitatively (0, no staining; 1, ≤10%; 2, 11-25%; 3, 26-50%; 4, 51-75%, 5; >75%) [102, 104]. Cytoplasmic staining was scored for Bcl2, cytokeratin (CK 5/6, CK8/18, CK19 and, CK7/8), smooth muscle actin (SMA), and vimentin and the intensity of staining (0-3) and the percentage of positive cells were recorded [87, 104, 106, 107].

Immunoreactivity for all antibodies was separately assessed in both epithelial and myoepithelial cells when present.

The expression in tumours and putative precursor lesions was compared to those of the adjacent TDLUs. In normal TDLUs and precursor lesions the expression of different biological markers was quantified by estimating the percentage of positive cells as follow (0= none, 1=< 1%, 2=1% to 10%, 3=11% to 33%, 4=34% to 66%, 5=67% to 90%, 6=91%-99% and 7=100%) [104]. The expression of CK19, CK7/8, CK18, CK5/6, CK14, SMA, and vimentin was evaluated for cytoplasmic staining with a cut off point selected at 10% determined by reference to the histogram.

The H-score was used to categorise cytoplasmic FHIT staining using the following thresholds: strong expression (H-score= 210-300); moderate (H-score = 110-209); mild (H-score of < 110) and complete loss (P<20%). H-scoring was selected because it had been shown previously to be an appropriate technique for assessing FHIT to determine clinical outcome in breast cancer[87].

For invasive breast lesions, we used the H-score to assess membranous E-cadherin staining: complete loss was defined by staining in less than 10% of the cells while, positive expression was further categorised into reduced (H-score ≤100) and normal (H-score >100). However, in Chapter 2 we used a different scoring system for E-Cadherin as proposed by Simpson et al 2005 [71] to detect subtle changes among precursor lesions in breast tissue samples.

Only nuclear reactivity was considered for ER-α and ER-β and both were scored as continuous variables (percentage of positive cells) and using the Allred score with positive expression defined as staining in ≥10% cells or Allred score >2 as cut-offs as previously determined.[86, 108, 110].

For p53 and cyclin D1, nuclear expression was categorized as follows: 0: no staining; 1: staining in <1% of cells; 2: staining in ≥ 1% and < 10% cells; 3: staining in ≥10% and < 50% cells; 4: staining in ≥ 50% [100]. p53 positivity was further subdivided into negative (score 0 or 1), borderline positive (score 2) and definite positive (scores 3 or 4)[100]. For cyclin D1, positive expression was defined as staining in 10% or more of the cells [100]. For MIB-1, the proliferation index (PI) was determined for each case by calculating the percentage of positive cell nuclei. PI was stratified into low: <10% cells stained; intermediate: 10-30% cells stained; high: ≥30% cells stained [100]. For ATM, we considered lesions with <75% positive cells [102] as showing reduced expression, while all others were classified as normal expression.

HER-2 expression was assessed according to the new ASCO/ CAP guidelines [109] by using IHC and fluorescence in situ hybridisation (FISH). Membrane IHC expression of HER-2 was scored according to the Herceptest guidelines [109] and FISH was performed using a HER-2 and a centromere 17 (CEP17) specific probe (Vysis, IL, USA), according to the supplier's instructions. A positive HER-2 result is IHC staining of 3 (uniform, intense membrane staining of 30% of invasive tumour cells) or FISH amplified (ratio of HER-2 to CEP17 of 2.2) and a negative HER-2 is an IHC staining of 0 or 1 (no or faint incomplete membrane staining) or FISH ratio of less than 1.8. Equivocal for HER-2 is defined as either IHC 2 or FISH ratio of 1.8-2.2.

3.3.2 Statistical analysis

Associations between clinicopathological variables were performed using either Pearson's Chi-square test, Fisher's exact test or Mann-Whitney U analysis where appropriate, using SPSS software (SPSS, Chicago, IL). Where appropriate, X^2 test for trend, Student's t test and ANOVAs one way test were used. To assess intra-lesional differences for markers producing multiple outcomes, the Kruskal-Wallis test was used. The correlation between

different target antibodies within each lesion type was determined using the Spearman test. All tests were two-sided unless otherwise stated, with a confidence interval of 95%. Significant p value was <0.05.

3.4. Results

3.4.1 Immunohistochemical profile of TDLUs

TDLUs comprise two cell layers: an outer basal (myoepithelial cells) and inner luminal cell layers (epithelial cells) surrounded with complete intact basement membrane showing strong positive complete laminin and collagen IV staining. In the TDLUs (associated with and without invasive lesions), all epithelial cells showed staining for one or more of the luminal cytokeratin, CK19, CK18, and CK8. A small proportion (<5%) of these epithelial cells co-expressed CK5/6, CK14 and/or vimentin. None of the epithelial cells showed any staining for SMA. The myoepithelial cells showed strong positive staining for SMA, vimentin, CK5/6 and CK14.

In TDLUs, 5-50% of luminal epithelial cells showed nuclear staining for ER-α. The expression of ER-α was significantly lower in TDLUs in pre-menopausal than in postmenopausal of both cancer-free cases (6% vs. 35%; p=0.0001) and adjacent to cancer (23% vs. 45%; p=0.0001), respectively. The expression of ER-α was significantly higher in

TDLUs adjacent to preinvasive lesions with and without invasive lesions than in TDLUs of cancer free cases in both postmenopausal and premenopausal samples (p=0.001), (**Tables 3-3 and 3-4**). None of the myoepithelial cells in TDLUs showed positive ER-α. On the contrary, ER-β1 was expressed in both luminal and myoepithelial cells; >90% of luminal epithelial and myoepithelial cells expressed ER-β1. The staining pattern was identical in TDLUs of normal control tissue from breast reduction specimens and in TDLUs adjacent

to tumour. In addition, no significant difference between the expression of ER-β1 in premenopausal and postmenopausal cases was detected (**Tables 3-3** and **3-4**).

In TDLUs of premenopausal breast reduction specimens, only a few luminal epithelial cells showed a strong Bcl-2 positivity (<10%), whereas strong Bcl-2 staining was found in 40% and >80% of luminal epithelial cells lining TDLUs of postmenopausal reduction specimens and TDLUs surrounding preinvasive/invasive cases, respectively ((**Tables 3-3** and **3-4**).

CCND1 expression was very low (<10%) in the luminal epithelial cells both pre- and post-menopausal TDLUs either of reduction breast specimens, preinvasive or of invasive carcinoma samples (**Tables 3-3** and **3-4**).

The proliferation index (MIB1) was higher in premenopausal than in postmenopausal TDLUs of reduction breast specimen (2.5% vs. 0.5%). All TDLUs associated with low grade invasive tumours showed low MIB1 (<10%) however, the expression of MIB-1in cases associated with preinvasive invasive lesions was significantly higher compared to reduction specimens.

The epithelial cells lining the TDLUs showed positive expression of FHIT, ATM, BRCA1, and E-Cadherin protein, and negative expression of p53 regardless of the menopausal and malignancy status.

Table 3-3: The average proportion scores* of different biological markers in different breast lesions not associated with invasive tumours.

Markers	TDLUs (pre Menopause	TLDU Post Menopause	UEH	CCC	CC H	FEA	ADH/ DCIS	LN
ER-α	+2	+4	+3	+6	+6	+6	+6	+6
ER-β1	+6	+6	+5	+5	+4	+4	+4	+4
MIB1 (%)	2.5	0.5	2.5	0.6	5	6.4	7	4
Bcl2	+1	+3	+3	+6	+6	+7	+7	+7
Cyclin D1	+1	+2	+2	+2	+3	+3	+3	+3
CK19/19/8	+6	+6	+4	+7	+7	+7	+7	+7
CK5/6	+2	+2	+5	+1	+1	0	0	0
Vimentin	+1	+1	+4	0		0	0	0

* Average proportion score representing the estimated proportion of positive cells

(0; none, 1; <1%, 2; 1-10% 3; 11=33%, 4; 34-66%, 5; 67-90% 6; 91-99%, 7; 100)

Table 3-4: The average positive cells of different biological markers in terminal duct lobular unite (TDLUs).

Markers	TDLUs (pre-menopause %	TDLU Post-menopause Post-Menop %	TDLU Adjacent to preinvasive lesion without invasive %	TDLU Adjacent to invasive cancer %
ER-α	6	35	42	45
ER-β1	93	91	91	89
MIB1 (%)	2.5	0.5	1.2	1.1
Bcl2	7	40	75	80
Cyclin D1	1	7	6	6

3.4.2 Immunohistochemical profile of usual epithelial hyperplasia

UEH showed intact basement membrane and extensive expression (>50% of luminal epithelial cells) of both basal cytokeratin (CK5/6 and CK14), vimentin, ATM, FHIT and BRCA1 (**Figure 3-1**). However, no UEH epithelial cells showed SMA expression. In addition, the epithelial cells lining UEH showed heterogeneous (mosaic like) expression of luminal cytokeratin (CK19, CK18 and CK8), ER-α, ER-B, and Bcl2. No expression of cyclin D1 or p53 was noticed in any of UEH.

3.4.3 Immunohistochemical profile of CCLs lesions

All forms of CCLs showed complete strong positive staining for both laminin and collagen type VI. The majority of epithelial cells (>95%) lining CCC and CCH showed strong positive expression of luminal cytokeratin (CK19, CK18 and CK8) and lack expression of basal CKs (CK5/6 and CK14), SMA and vimentin. While the neoplastic cells of the FEA and CCH with both cytological and architecture atypia showed homogenous expression of the luminal CKs and consistently lacked expression of basal/ myoepithelial markers (**Tables 3-3 and 3-4**). The epithelial cells of all forms of CCL were strongly positive for ER-α, ER-B, and Bcl2. However, ER-α expression was relatively lower in the epithelial cell lining of CCC in lesions without invasion (75%) than in CCC adjacent to invasive lesions (90%). The epithelial cell lining of CCH, FEA, and CCH with cytological and architecture atypia showed strong and diffuse positivity for ER-α. None of the CCLs showed either HER-2 overexpression or p53 positive expression. All CCLs were positive for BRCA1 and ATM.

In addition, the epithelial cell population of CCC, CCH, and FEA, with and without either preinvasive or invasive carcinoma were almost exclusively composed of Bcl-2

positive cells and the expression was strong to moderate (I = 3 or 2). Some CCC (39%), CCH (61%), and 76% of FEA showed positive expression of cyclin D1. All CCC and CCH, and the majority of FEA (92%) showed a low proliferation index (<10%).

3.4.4 Immunohistochemical profile of LNGBC

All tumor types belonging to LNGBC (low grade IDC, TC, TLC, ICC and ILC) showed strong positive expression of ER+ and luminal CKs (CK19+, CK18+ and CK8+) and displayed negative expression of both basal CKs (CK14 and CK5/6), vimentin and SMA compared to HGNBC. Although the tubules of TLC and TC and ICC lack the myoepithelial cell layer, they demonstrated discontinuous weak laminin staining at the interface with the stroma. While HNGBC and classic ILC and cord like structure of TLC showed no staining at all of either collagen IV or laminin.

Most LNGBC (93%) showed very low proliferation index (<10%) compared to HNGBC (>50% positive cells). Neither HER-2 overexpression nor HER-2 gene amplification was detected in any of the precursor lesions and their associated invasive LGBC/ILC; while 11% of HNGBC showed HER-2 overexpression **(Table 3-5)**

ATM expression was absent or reduced in all ICC, 22% of TC, 25% of TLC, 33% of low grade IDC-NST and 40% of ILC compared to 53% of HNGBC. In cases showing coexistent FEA and/or in situ carcinoma with the invasive component, ATM expression was identical in both lesions. No positive nuclear expression of p53 was detected in ICC (0%), TC (0%), and TLC (0%), ILC (2%) and low grade IDC (3%) compared to 44% of HGNBC. BRCA1 negative expression was very rare in ILC (1%), ICC (0%), and TLC (0) and uncommon in TC (13%).

Table 3-5: Summary of immunohistochemical expression of different target antibodies in and invasive classic lobular carcinoma

Antibodies	TC (n=135)		ICC (n=30)		Low grade IDC (n=60)		TLC (n=20)		Classic ILC (n=180)		X^2 P
	(n)	(%)	(n)	(%)	(n)	(%)	(n)	(%)	(n)	(%)	
CK19	135	100	30	100	60	100	20	100	180	100	NS
CK7/8	135	100	30	100	60	100	20	100	180	100	NS
CK18	135	100	30	100	60	100	20	100	180	100	NS
SMA	1	0.7	0	0	2	3	0	0	1	.06	NS
Vimentin	1	0.7	0	0	2	3	0	0	1	.06	NS
CK5/6	1	0.7	0	0	0	0	0	0	2	1.2	NS
CK14	1	0.7	0	0	0	0	0	0	2	1.2	NS
ER-α	132	98	30	100	56	93	20	100	168	93	NS
ER-β	131	97	30	100	58	97	20	100	160	89	0.01*
p53	3	3	0	0	2	3.3	0	0	6	3.3	NS
c-erbB-2	0	0	0	0	0	0	0	0	0	0	
E-Cadherin (Loss)	2	1.5	0	0	2	3.3	1	10	160	89	0.001*

There was no significant difference between the expression of luminal CKs, myoepithelial and basal markers, hormonal receptors, HER-2 and p53 in TC, cribriform, low grade IDC, TLC and classic ILC.

* E-Cadherin and ER-β showed significant difference between LGBC and ILC.

LGBCs: low grade breast carcinomas; ICC: invasive cribriform carcinoma; CK: cytokeratin; EGFR: epidermal growth factor receptor; ER-α: oestrogen receptor alpha; ER-β: oestrogen receptor beta; IDC: invasive ductal carcinoma; ILC: invasive lobular carcinoma; TC: tubular carcinoma; TLC: tubulolobular carcinoma.

3.4.5 Lobular differentiation

All TDLUs, UEH, CCC, CCH, FEA, ADH/low grade DCIS showed normal expression of E-cadherin while LN was E-cadherin negative. The majority of TC, cribriform carcinoma, low and high grade IDC, and TLC, differed from the majority of ILC in being positive for E-cadherin (**Tables 3-6 and 3-7**). In TLC, both tubules and cord like cells were positive for E-cadherin. In contrary to TLC, the separate foci of lobular carcinoma in mixed tubular/classic ILC tumours showed complete loss of E-cadherin

3.4.6 Evidences of progression of CCLs to invasive carcinoma

All the precursor lesions including CCLs, DCIS and LN showed positive expression of luminal CKs (CK19, CK18 and CK 8) and negative expression of CK14, CK5/6, vimentin and SMA identical to matching or consequent invasive carcinoma. The ER-α and Bcl2 expressions were significantly higher in all forms of CCLs (CCC, CCH, and FEA) than in adjacent TDLUs in samples with and without invasive cancers.

The percentage of ER-β1 positive cells significantly decreased ($P < 0.001$) in all forms of CCL (CCC: 80%, CCH: 75%, FEA: 60%) compared to matching TDLUs.

The ratio of ER-α positive/ER-β1 positive cells progressively increased from normal (0.3) to CCC (1.13) to CCH (1.58), to FEA/ADH/low grade DCIS (1.7) to their co-existing invasive low grade nuclear tumours (3.3) and it was statistically significant ($p = 0.01$). In invasive high nuclear grade IDC, the mean of ER-α positive/ER-β1 positive cells ratio was 4.3.

There was a significant stepwise increase in the percentage of cyclin D1 positive cells from normal to CCC to CCH/FEA to ADH/low grade DCIS to invasive carcinoma ($p=0.001$, Kruskal-Wallis test), **(Figure 3-2)**.

There was a positive correlation between the level of ER-α expression and both Bcl-2 and cyclin D1 in the progression from normal to invasive tumours ($p=0.001$).

Proliferation rate was significantly elevated in CCH (5%), FEA (6.4%), ADH/DCIS (7%) and LN (4%) as compared with TDLUs (1.1%), UEH (2.5%) and CCC (1.5%) in both cancer-free and cancer samples **(Tables 3-4, 3-5 and 3-7)**.

The epithelial cells lining the TDLUs and CCC showed strong uniform expression of FHIT protein regardless of the malignancy status. 80% of low nuclear grade carcinoma showed a reduced expression of FHIT in which there was a progressive loss of FHIT in the associated putative precursor lesions. In invasive HNGBC showing co-existence in situ carcinoma, p53, FHIT and ATM expression was identical in both lesions.

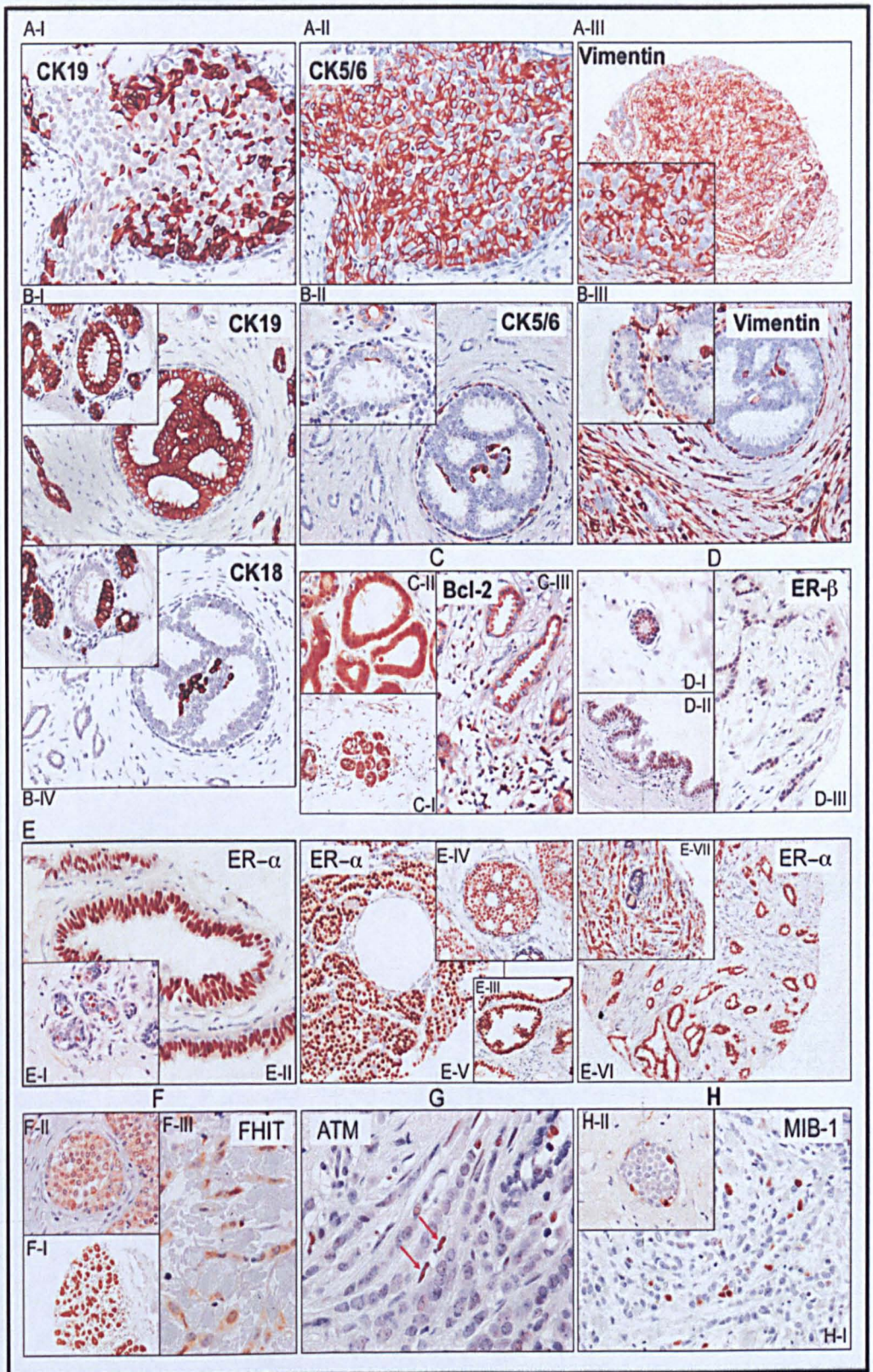

Figure 3-1: Immunohistochemical expression of different target antibodies in different low grade breast neoplastic lesions.

Figures (1 AI–III) show an example of usual epithelial hyperplasia (UEH) exhibiting heterogeneous expression for CK19 (AI) and extensive expression of CK5/6 and vimentin (AII, AIII). Figures (1 BI-IV) show an example of flat epithelial atypia (FEA) with (main fig) and without (inset) complex architecture associated with invasive tubular carcinoma (TC) (main fig). This case showed homogenous expression of CK19 (B I) and lack of expression of CK5/6 (B II) and vimentin (B III). Although the expression of CK19, CK8 and CK18 similar in almost all lesions in our series, in this example (B IV) the majority of neoplastic in FEA and TC were negative for CK18. Bcl-2 expression is shown in figures (1 C I-III). The epithelial cells (ECs) in the terminal duct lobular units (TDLUs) (C I) and FEA (C II) showed strong expression for Bcl-2, whereas TC (C III) showed moderate expression of Bcl-2. Figures (1 D I-III) demonstrates levels of expression of oestrogen receptor-β (ER-β1) in a typical case and shows that all ECs in TDLUs (D I) were positive for ER-β. The percentage of ER-β1positive cells decreased in columnar cell hyperplasia (D II) and the associated TC (D III). Oestrogen alpha (ER-α) expression is showing in fig (1 E I-VII). Only occasional ECs in normal TDLUs (E I) showed positive nuclear stained for ER-α while the majority of ECs in columnar cell changes were positive for ER-α (E II). A case with FEA (E III), ADH/low grade DCIS (E IV) and lobular neoplasia (LN) (E V) uniformly displayed strong nuclear expression for ER-α Similarly, in the invasive tumours the majority of the neoplastic cells were positive for ER-α with a moderate to weak staining intensity. (E VI TC, E VII invasive lobular carcinoma). FHIT expression is shown in figures (1 F I-III). ECs lining the TDLUs (F I) showed a strong uniform expression of FHIT protein. Progressive loss of FHIT in the associated LN (F II) and ILC (F III) were seen. ATM expression is shown in figure 1 (G) in an example of ILC which showed negative expression of ATM while the stromal fibroblasts showed characteristic nuclear positive staining (red arrows). Growth fraction assessed using MIB-1 staining, figure 1 (H I–II), generally showed low levels as illustrated in a case of ILC (H I) with associated LN (H II).

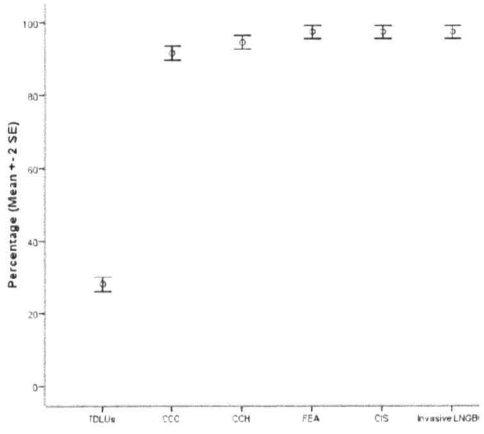
Percentage (Mean +- 2 SE)
100
80
60
40
20
0
TDLUs
CCC
CCH
FEA
CIS
Invasive LNGBC

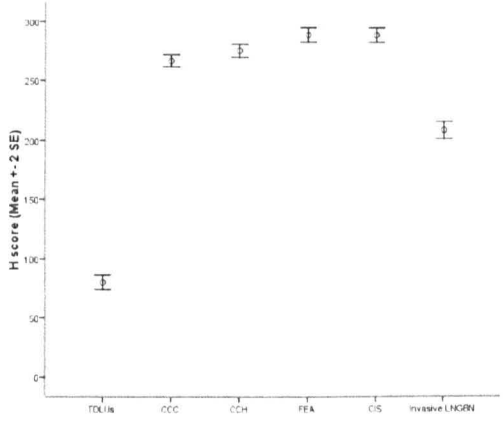
H score (Mean +- 2 SE)
300
250
200
150
100
50
0
TDLUs
CCC
CCH
FEA
CIS
Invasive LNGBC

A

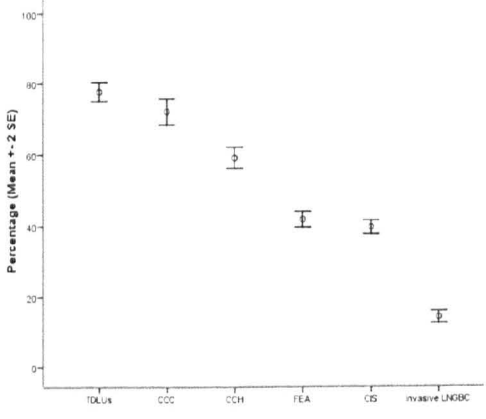
Percentage (Mean +- 2 SE)
100
80
60
40
20
0
TDLUs
CCC
CCH
FEA
CIS
Invasive LNGBC

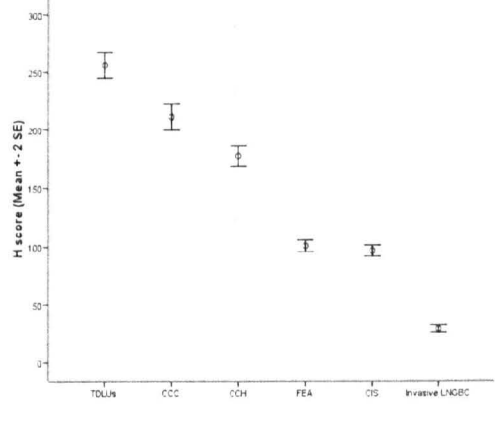
H score (Mean +- 2 SE)
300
250
200
150
100
50
0
TDLUs
CCC
CCH
FEA
CIS
Invasive LNGBC

B

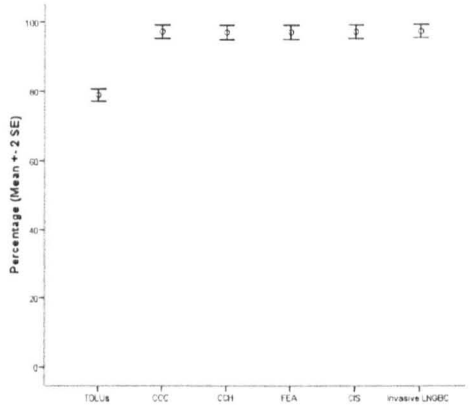
Percentage (Mean +-2 SE)
TDLUs
CCC
CCH
FEA
DIS
Invasive LNGBC

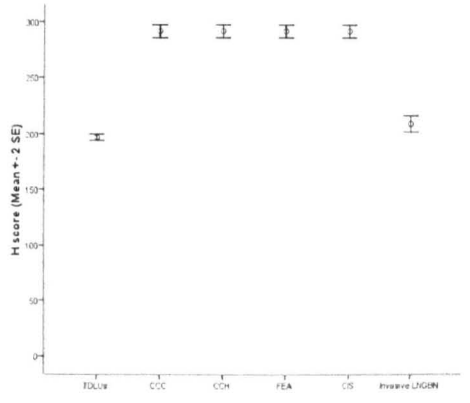
H score (Mean +-2 SE)
TDLUs
CCC
CCH
FEA
DIS
Invasive LNGBC

C

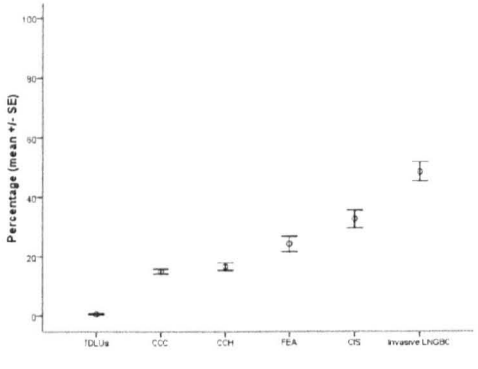
Percentage (mean +/- SE)
TDLUs
CCC
CCH
FEA
DIS
Invasive LNGBC

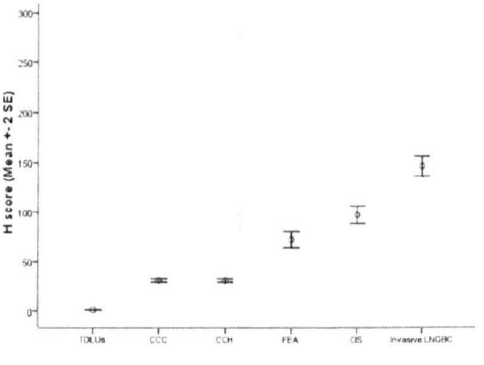
H score (Mean +-2 SE)
TDLUs
CCC
CCH
FEA
DIS
Invasive LNGBC

D

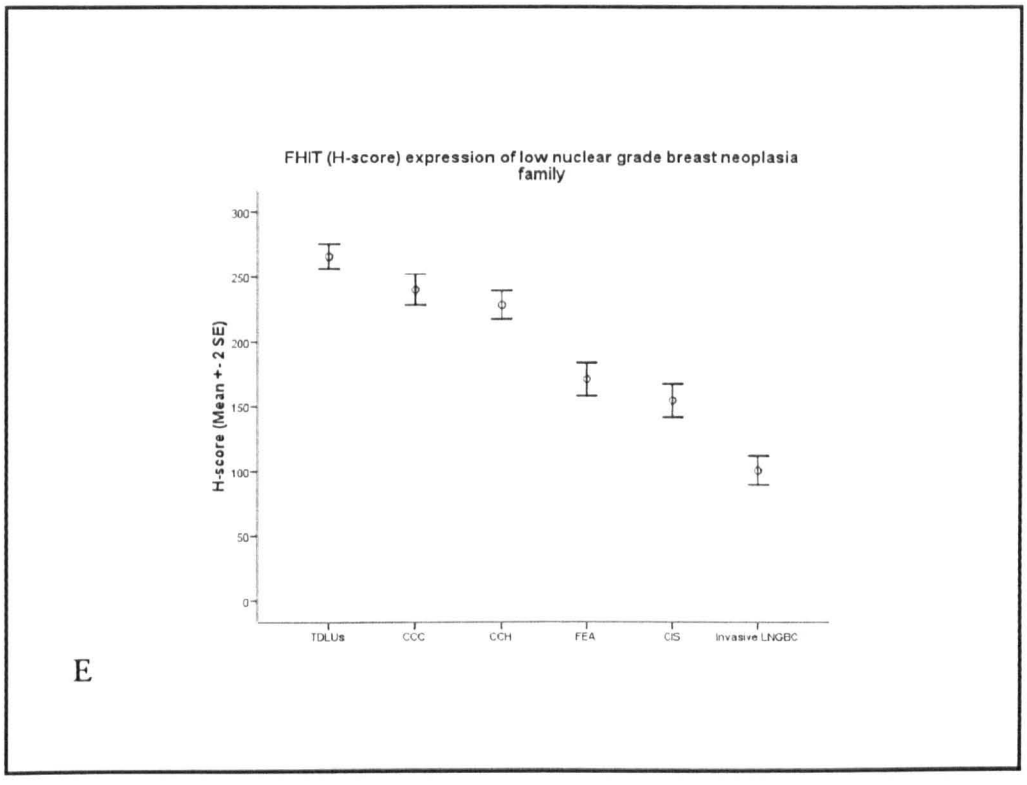

Figure 3-2: Comparison between the percentage of positive cells (left) and H-score (right) for oestrogen receptor-α (A), oestrogen receptor-β (B), Bcl2, (C), Cyclin D1 (D) in samples belonging to the low nuclear grade breast neoplasia family including normal terminal duct lobular units (TDLUs), columnar cell changes (CCC), columnar cell hyperplasia (CCH), flat epithelial atypia (FEA), carcinoma in situ (CIS) and invasive low grade breast carcinomas (LGBCs). Only the H-score was used to assess FHIT (E).

Table 3-6: Comparison of immunohistochemical expression of different target antibodies amongst low grade breast carcinoma (LGBC), invasive lobular carcinoma (ILC) and high grade invasive.

Family	Antibodies	Expression	LGBC (n=415)		High grade IDC (n=670)		X^2 p
			n	%	N	%	
Luminal CKs	CK18/8/19	Positive	415	100	516	77	0.001*
High molecular weight cytokeratin	CK5/6	Positive	3	0.7	168	25	0.001*
	CK14	Positive	3	0.7	154	23	0.001*
Myoepithelial Markers	SMA	Positive	3	0.7	80	12	0.001*
Hormone Receptors	ER-α	Positive	336	95	288	43	0.001*
	ER-β1	Positive	311	75	496	74	NS
Tumour Suppressor	p53	Positive	11	3	295	44	0.001*
	BRCA1	Loss	21	5	188	28	0.001*
	ATM	Loss	91	22	355	53	0.001*
	E-cadherin	Loss	166	40		14	0.001*
EGFR family	c-erbB-2	Overexpression	0	0	17	28	0.001*
Proliferation index	Ki67	High PI (>10%)	17	4	536	65	0.001*
Mesenchymal marker	positive	0	0	0	141	21	0.001*

Table 3-7: Proliferation index (PI) of normal terminal duct-lobular units, breast cancer precursors and invasive lesions.

MIB-1 PI	TDLUs	UEH	CCC	CCH	FEA	ADH/ low grade DCIS	G1/G2 Invasive
Range	0-9.9	0-9.9	0-9.9	0-9.9	0-20	0-30	0-36
Mean ±SD	1.1±2.1	1.6±3.2	1.5±2.3	5±3.8	6.42±4.9	7.1±8.3	9.1±10.8
Low PI (%)	100	100	100	100	93.5	89	87.3
Intermediate PI (%)	0	0	0	0	6.5	11	8.7
High PI (%)	0	0	0	0	0	0	4

ADH: atypical ductal hyperplasia; CCC: columnar cell change; CCH: columnar cell hyperplasia; DCIS: ductal carcinoma in situ; FEA: flat epithelial atypia; LN: lobular neoplasia; TDLU: terminal duct-lobular unit; UEH: usual epithelial hyperplasia.

3.5. Discussion

In this study, we expanded our investigation to explore the immunohistochemical phenotype of the putative precursor lesions and related cancers and to test the hypothesis of whether low grade IDC, TC, invasive cribriform carcinoma (ICC), TLC and classic ILC carcinomas share a common phenotype supporting their direct evolutionary links to CCLs, particularly flat epithelial atypia (FEA). Furthermore, we postulate a model for the biological events that are associated with ER-α in the development of pure invasive low nuclear grade carcinoma.

Low grade IDC, TC, invasive cribriform carcinoma, classic ILC and TLC all have a relatively favourable prognosis, possibly due to high levels of differentiation which may be the consequence of fewer genetic aberrations. In Chapters 2 and 3, we reported a high frequency of co-existence of CCLs, ADH/low grade DCIS and LN, with TC, TLC and ILC, respectively suggesting that these lesions form a family of low nuclear grade precursor, in situ and invasive neoplastic lesions of the breast. In this report, we provide further evidence supporting the hypothesis that CCLs are the precursor of LNGBC using an immunophenotyping approach encompassing expression of cytokeratin, cell proliferation/differentiation markers and a number of putative tumor suppressor genes (TSGs).

Our results call into question the role of UEH as a BC precursor. Firstly, UEH only shows a low relative risk (1.5 times) of subsequent carcinoma development [66]. Although some studies [89, 111], demonstrated similar copy number changes in UEH and DCIS, Simpson et al (2005) [71] differentiated UEH from some forms of CCLs, and found no or only few and apparently random chromosomal changes in agreement with other studies [112, 113]. Furthermore, UEH does not fit well on the histological continuum to invasive BC [66] and no

association between the presence of UEH and LGBC was observed in previous chapter. In this study, we found that UEH showed extensive expression for CK5/6, CK14 and vimentin and heterogeneous expression for ER, Bcl-2, FHIT, cyclin D1 and CK19/18/8. In contrast, FEA, ADH/low grade DCIS, and LN were consistently negative for CK5/6, CK14 and vimentin and positive for ER-α, Bcl-2, cyclin D1, and CK19/18/8. The latter phenotype was shared with their co-located LGBC lesions. The immunophenotype of UEH infers that this lesion either is unrelated to or is a side branch of the LNGBC evolutionary pathway [52]. Based on the morphological, immunohistochemical and molecular genetic data, we favour the former interpretation and believe that the vast majority of UEHs are not precursor lesions of LNGBC.

Presently, cancer is perceived as a clonal disease that depends on multiple genetic mutations in division-competent stem and progenitor cells [62]. After transformation, these cells can become neoplastic due to deregulation of self-renewal, differentiation, membrane transport activity, telomerase activity and anti-apoptotic pathways, resulting in the ability to migrate and metastasise [62]. Subsequently, the heterogeneity of BCs may derive from inherent differences in the underlying originator cell population and/or result from stochastic genetic and epigenetic events causing different combinations of oncogene activation and loss of tumour suppressor gene (TSG) function in normal breast stem or committed progenitor cells [27-30, 63-65].

Several models of stem and progenitor cells of the breast have recently been put forward as we mentioned previously in chapter 1. Whilst some suggested that the earliest progenitor cells in the epithelial bud are negative for basal cell markers and CK8/18, but positive for CK19 and Bcl-2, others suggested the stem cells are positive for CK5/6 and negative for CK19. However, some investigators suggested the existence of two distinct epithelial progenitor cell types [37-38]. According to the latter, one of the precursor cells has a luminal

phenotype (CK8/18+, CK19+, MUC1+, ESA+, CD10-, CK14- and CK5/6-) and a second comprises bipotent progenitor cells (MUC1- /CD10+ /ESA+) with potential to generate mixed colonies of both epithelial cells and myoepithelial cells. In agreement with this proposal, some researchers [31, 34] proposed that the CK19+ and ER+ positive cells, respectively, were the progenitor cells in their model of human breast progenitors.

It has been shown that oestrogen can indirectly induce proliferation and inhibit apoptosis, resulting in cell proliferation and growth [114]. In our study, we found that a high percentage of contiguous cells in CCLs expressed ER-α with a progressive increase in CCH, and rising even further with the appearance of atypia, in agreement with a previous study [115]. In contrast, normal breast tissue showed ER-α positive epithelial cells surrounded by ER-α negative cells, indicating proliferation of ER-positive cells in both precancerous and cancerous breast lesions [34]. Our findings could be interpreted as evidence in support of the hypothesis that the ER+ luminal restricted progenitor (ER+, MUC1+, CK8/18+ and CK19+) cells -as we have shown in the introduction- could be the cell of origin that give rise to the LNGBC family or families and their precursors. However, there are several lines of evidence to suggest that the final phenotype of the tumour should not be regarded as a mere reflection of that of its progenitor cell phenotype [116, 117]. This is also exemplified in the mouse model developed by McCarthy and colleagues [118], where the authors inactivated Brca1 and tp53 in the epithelial cells of mouse mammary gland and the animals developed basal-like cancers.

In accord with others [103, 108, 119], we have found that ER-α/ER-β1 expression ratios increased from normal towards the invasive tumours, supporting the hypothesis that ER-α and ER-β-specific pathways may have an important role in this process [120]. It has been suggested that the ER-β1 gene may have tumour suppressive functions [121]. ER-β1 may

regulate ER-α-mediated transcriptional activation, providing protection against ER-α induced hyper-proliferation [114].

We found the expression level of the known ER-α responsive gene cyclin D1, increased in a stepwise manner from normal to CCLs to invasive lesions [122, 123]. In agreement with others [124, 125], we found positive and negative correlations between cyclin D1 with ER-α and ER-β1 respectively, suggesting that these receptors may oppose each other for regulating cell proliferation via cyclin D1 [126]. Epithelial Bcl-2 expression declined from precursor to LNGBC, as previously reported [127, 128]. Strong Bcl-2 expression was associated with ER-α positivity, low MIB-1 expression, an absence of p53 mutation and low level of HER-2 expression.

We investigated the presence of a number of putative TSGs in our family of precursor and LNGBC to assess their involvement at different stages of carcinogenesis. In LGBCs, deletion of chromosome 11q23-25, containing ataxia telangiectasia mutated (ATM), is common [102]. ATM phosphorylates p53 causing its stabilisation which is required for cell cycle arrest, DNA repair, or apoptosis. A reduction in ATM protein and mRNA levels has been reported in invasive BCs [101, 129]. In our study, 22% of FEA, ADH/low grade DCIS, LN and LNGBC showed low or absent ATM expression compared to normal TDLUs. Moreover, concurrent positive expression of Bcl-2 and lack of p53 nuclear expression were found in cases with low or absent expression of ATM. In leukaemia, ATM has been shown to represent an alternative regulatory mechanism of TP53 mutation [130] and it is not known if it has a similar function in breast cancer.

The function of BRCA1 is still unknown but it is proposed to be a TSG with transcriptional activity; it is involved in cell proliferation processes of mammary epithelial cells in response to hormonal stimulation, in apoptosis, control of recombination, and genome integrity after

binding to proteins involved in these activities. In accordance with other studies [101, 102] we found that BRCA1-associated BCs were associated with HNGBC, high PI, high frequencies of high p53 protein expression, loss of ATM and negativity of ER.

In vivo animal studies support a tumour suppressor role for fragile histidine triad (FHIT) [131]. We found reduced FHIT levels in the majority of CCH, FEA, ADH/low grade DCIS, LN and the associated invasive lesions, in accordance with others [101]. Importantly, we noted an inverse correlation between FHIT and Bcl-2, cyclin D1, and ER-α expression supporting its role in the development of LNGBC.

E-cadherin (CDH1) is a TSG localised on chromosome 16q21 and is frequently lost in ILC. Our results demonstrate that whilst CCLs, ADH/low grade DCIS, TC, ICC, low grade IDC, and TLC are positive for E-cadherin, LN and ILC lack expression of this tumour suppressor gene and adhesion molecule. Our observations support the idea that loss of normal CDH1 gene expression may switch on the development of lobular differentiation [52, 60].

In summary, our findings demonstrate that FEA, ADH/low grade DCIS, LN and invasive low grade breast cancers have remarkably similar immunophenotype and that this phenotype is distinct from that seen in high grade breast cancers. Given that the morphological and immunohistochemical features of FEA cells are almost identical to those seen in ADH/ low grade DCIS and LN, and that the molecular genetic changes of FEA are similar to those found in matched low grade breast cancers [71], our findings suggest that FEA is a common non-obligate precursor of LGBC and ILC. Taken together, these lesions may represent a family of precursor, in situ and invasive neoplastic lesions belonging to the luminal 'A' subclass of BC. Furthermore, our findings demonstrate that the balance between ER-α and ER-β expression may be important in driving cyclin D1 and Bcl-2

expression, that p53 inactivation and HER-2 overexpression/ HER-2 gene amplification are uncommon phenomena in this family of lesions.

Chapter 4:

The need for a biological grading system and its relationship to current Nottingham Histological Grading System (NGS)

4.1 Abstract

In chapter 3 we found that the low nuclear grade breast neoplasia family including tubular carcinoma and invasive classic lobular carcinoma is characterized by low mitotic index and positive expression of Bcl2. In this study, we hypothesised that the interaction between mitotic index (M) and Bcl2 accurately discriminates between low and high-grade breast cancer (BC) and provides a more objective measure of clinical outcome than histological grade especially for patients with intermediate histological grade, small size or oestrogen receptor (ER) negative cancers.

A well characterised series of 1650 BC with long term follow-up was immunohistochemically profiled for Bcl2. Mitotic index (M) was assessed according to Nottingham Grading System (NGS): M1: <10 mitoses; M2: 10 to 18 mitoses; M3: > 18 mitoses. Results were validated in an independent series of patients (n=245) uniformly-treated with adjuvant anthracycline-based chemotherapy. Subsequently, BC were classified according to the combined M/Bcl2 profile and compared to NGS.

In multivariate Cox regression models including validated prognostic factors, the subgroups defined by M/Bcl2 profile remained significantly associated with patients' outcome but also performed better than lymph node status and tumour size. Incorporation of the M/Bcl2 profile into the Nottingham Prognostic Index (NPI) accurately reclassified twice as many

patients into the excellent prognosis group, improving decision-making for which patients should be spared systemic adjuvant therapy. Patients with M2-3/Bcl2- and M3/Bcl2+ (high risk) had a 2-3 fold increase in the risk of recurrence when treated with either adjuvant hormone therapy or anthracycline-based chemotherapy than those with M1/Bcl2± and M2/Bcl2+ (low risk) (HR= 3.4 (2.8-5.6); $p<0.0001$ and HR=2.3 (1.2-4.3); $p=0.0009$).

In conclusion a grading system defined by mitotic counting and Bcl2 expression accurately reclassified patients with NGS-G2, small size cancers or ER negative into two groups: low risk (NGS-G1 like) versus high risk (NGS-G3 like) of both BC mortality and recurrence, improving prognosis and therapeutic planning.

4.2 Introduction

The Elston-Ellis modified Scarff-Bloom-Richardson grading system (aka, Nottingham Grading System; NGS) is one of the most widely used methods of breast carcinoma (BC) grading [132]. NGS provides a consistent prognostic tool which has been validated in multiple independent studies [133]. One of the main limitations of NGS, however, is that 30%-60% of BCs are still classified as grade 2 (G2), which is a category with ambiguous clinical significance due to its intermediate risk of recurrence [134]. Furthermore, for statistical analysis, G2 cancers are often combined together with either G3 or G1, rendering interpretation of the results challenging and leading to a debate of whether grade should play a role in therapeutic planning [135]. Furthermore, it has been argued that NGS has little or no prognostic role in either early stage small tumours or in oestrogen receptor (ER-) negative subgroup [136].

In previous chapters, we proposed that some special types of BC including invasive classic breast carcinoma (grade 2) and tubular carcinoma (grade 1) constitute a biologically related neoplastic family named "low nuclear grade breast carcinoma (LNGBC)" [104]. Our LNGBC proposal is based not only on the clinical outcome [10] but also on the remarkable similarity of the morphological, immunophenotypic, and reported molecular genetic characteristics [52]. Among the biological characteristic features of this family were low mitotic index (M) and Bcl2 positivity (Bcl2+); (**Figure 4-1**).

In this study, we explore the hypothesis that a grading system based on balance between "M" as a proliferation marker and "Bcl2" as a cell cycle/apoptosis regulator would be capable of accurately discriminating between low and high-grade tumours and providing a more objective and clinically valuable measure of tumour grade with prognostic significance

for invasive BC in general and particularly in moderately differentiated, small and ER negative (ER-) cancers.

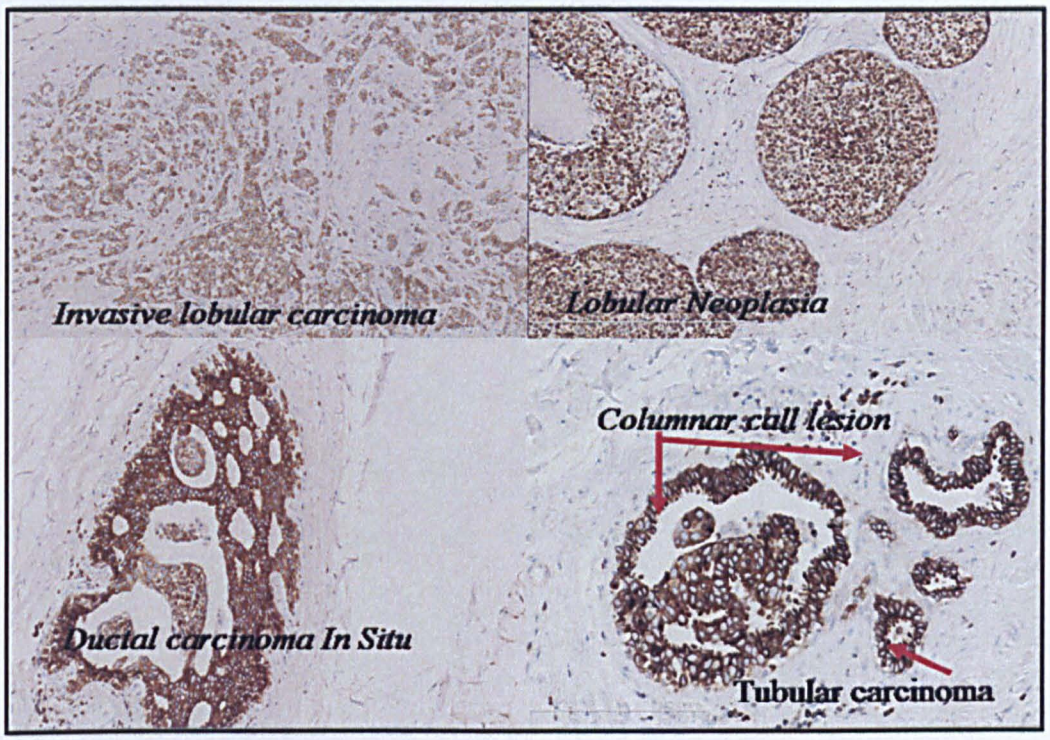

Figure 4-1: Low nuclear grade breast neoplasia family showed strong positive expression of Bcl2

4.3 Patients and Methods

We studied a series of primary operable invasive BC derived from the Nottingham Tenovus Primary Breast Carcinoma Series of women age ≤70 years, Nottingham City Hospital (1989-1999). 1650 consecutive cases were informative and included in this study as they had complete clinical, therapeutic and biological data available. The clinicopathological characteristics of our cohort are summarised in (**Table 4-1**).

Tumour grade and mitotic index data were assessed by experienced pathologists with strict adherence to the NGS [132] protocol. M was assessed at the periphery of the tumour and scored according to the observed frequency dependent on the field area of the objective lens used, for example as follows: M1 = Low, if <10 mitoses, M2 = medium, if 10 to 18 mitoses and M3 = high, if >18 mitoses (per 10 high-power fields with field-diameter; 0.56 mm). The Nottingham Prognostic Index (NPI) was calculated using the following equation: NPI =0.2 tumour size (cm) + grade (1 to 3) + LN score (1 to 3) [137]. Six NPI groups are recognised according to NPI: an Excellent Prognostic group (EPG); 2.08 to 2.4, Good (GPG); 2.42 to 3.4; Moderate I (MPG I) 3.42 to 4.4, Moderate II (MPG II); 4.42 to 5.4, Poor (PPG); 5.42 to 6.4 and very poor (VPG); 6.5–6.8.

Table 4-1: Clinicopathological characteristics of Nottingham whole cohort

Variable	n*	Cases (%)
Menopausal status	1650	
Pre-menopausal		612 (37.0)
Postmenopausal		1038 (63.0)
Tumour Grade (NGS)	1650	
G1		306 (18.5)
G2		531 (32.2)
G3		813 (49.3)
Lymph node stage	1650	
Negative		1056 (64.0)
Positive (1-3 nodes)		486 (29.5)
Positive (>3 nodes)		108 (6.5)
Mitotic activity	1650	
M1 (low; mitoses <10)		617 (37.4)
M2 (medium; mitoses 10-18)		300 (18.2)
M3 (high; mitosis >18)		733 (44.4)
Survival at 20 years	1650	
Alive and well		1055 (64.0)
Dead from disease		468 (28.4)
Dead from other causes		127 (7.6)
Adjuvant systemic therapy (AT)	1602	
No AT		665 (42)
Hormone therapy (HT)		642 (41)
Chemotherapy		307 (20)
Hormone + chemotherapy		46 (3)
Tumour type	1650	
Ductal no special (NST)		940 (57)
Tubular mixed		295 (18)
Tubular pure		54 (3)
ILC classic		100 (6)
Other types of ILC		122 (7)
Medullary carcinoma		41 (3)
Others		98 (6)
Tumour size (cm)	1650	
T1 a + b (≤1.0)		187 (11)
T1 c (>1.0 - 2.0)		868 (53)
T2 (>2.0-5)		5729 (35)
T3 (>5)		16 (1)

* Number of cases for which data were available.

Adjuvant systemic therapies (AT) were scheduled on the basis of prognostic and predictive factor status including NPI [137], oestrogen receptor-α (ER-α) status, and menopausal status. Patients with NPI ≤3.4 did not receive AT. Hormonal therapy (HT) was prescribed to patients with ER-α+ tumours and NPI >3.4. Pre-menopausal patients with NPI >3.4 were candidates for CMF (Cyclophosphamide, Methotrexate, and 5-Flourouracil) chemotherapy. Conversely, postmenopausal patients with (NPI >3.4 and ER-α+) were offered HT, while ER-α- patients received CMF if fit.

Exploratory subgroup analysis of the M/Bcl2 surrogates was also performed in AT untreated lymph node negative patients.

4.3.1 Clinical outcomes of M/Bcl2 profile in specific AT settings

To evaluate whether the different M/Bcl2 subgroups had different clinical outcomes in specific AT settings, we investigated the clinical outcome of 474 and 295 of Nottingham high risk patients (NPI >3.4 and ER+) and (NPI >3.4 and pre-menopausal) who had HT and CMF based chemotherapy, respectively. In addition, we compared the survival of high risk AT-treated patients to those of AT untreated for each M1/Bcl2 subgroups.

4.3.2 Validation Study

We also used an independent series of 245 invasive BC diagnosed and managed at the Royal Marsden Hospital (RMH) between 1994 and 2000 (Breakthrough series). Patients were selected on the basis of being eligible for therapeutic surgery and receiving standard anthracycline-based AT. All patients were primarily treated with surgery followed by anthracycline-based chemotherapy. HT was prescribed for patients with ER+ tumours (tamoxifen alone in 96.4% of the patients for the available follow-up period). Complete follow-up was available for 244 patients, ranging from 0.5 to 125 months (median = 67

months, mean = 67 months). The characteristics of this cohort are described elsewhere [107] and summarised in **(Table 4-2)**. It should be noted that any differences between Nottingham population and RMH/Breakthrough series may be a reflection of the different treatment protocols that were used. For instance most of RMH/Breakthrough cases of larger size and higher stage as it is composed solely of patients who received AT.

4.3.3 Survival data

Survival data including BC survival time (BCSS), disease-free survival (DFS), and development of loco-regional and distant metastases (DM) were maintained on a prospective basis. BCSS was expressed as the number of months from diagnosis to the occurrence of BC related-death. DFS was defined as the number of months from diagnosis to the occurrence of local recurrence (LR), local LN relapse or DM relapse. DM-free survival (MFS) was defined the number of months from diagnosis to the occurrence of DM relapse.

4.3.4 Immunohistochemistry (IHC) assay

In both Nottingham and Breakthrough series, tumours were arrayed in tissue microarrays (TMAs) constructed with 2 replicate 0.6 mm cores for each marker. The TMAs were immunohistochemically profiled for Bcl2 and a panel of other antibodies. Details of antibodies, antigen retrieval, immunohistochemical methods were summarized in **(Table 4-3)**. A cut-off for Bcl2 was selected at 10% as previous described[106].

To validate the use of TMAs for immunophenotyping, full-face sections of 20 cases were stained and the protein expression levels of the different antibodies were compared. The concordance between TMAs and full-face sections was excellent (kappa=0.8).

Positive and negative (omission of the primary antibody and IgG-matched serum) controls were included in each run.

HER-2 expression was assessed according to the new ASCO/ CAP guidelines [109] (**Table 4-4**) using IHC and fluorescence in situ hybridisation (FISH); FISH was performed for HER-2 IHC score 2+ cases using a HER-2 probe and a centromere 17 (CEP17) specific probe (Vysis, IL, USA), according to the supplier's instructions.

For the Breakthrough TMA, immunohistochemistry was performed with antibodies raised against the following markers: Bcl2, ER, progesterone receptor (PR), HER-2, EGFR, CK 5/6, CK 14, CK 17, Cyclin D1, KI67, p53, and topoisomerase II α, as reported elsewhere [137]. TMA sections were also subjected to chromogenic in situ hybridisation (CISH) with SpotLight probes for CCND1, MYC, HER-2, TOP2A, and chromosome 8 centromere as previously reported [138].

The immunohistochemical scoring for Bcl2 and mitotic count was performed by at least three observers, who were blinded to the results of the patients' outcome in two different settings. There was excellent intra and inter-observer agreements ($k > 0.8$; Cohen's κ and multi-rater κ tests, respectively).

Table 4-2: Clinicopathological characteristics of the RMH/Breakthrough series

Variable	RMH/Breakthrough Series (n=245)	
	n*	Cases (%)
Menopausal status		
Pre-menopausal		NA
Postmenopausal		NA
Tumour histological grade	240	
G1		23 (10)
G2		69 (29)
G3		148 (62)
Lymph node stage	237	
Negative		38 (35)
Positive		154 (65)
Survival **	244	
Alive and well		179
Dead from disease		42
Dead from other causes		NA***
Adjuvant systemic therapy (AT)	245	
No AT		0 (0)
Hormone therapy (HT) alone		0 (0)
Chemotherapy alone		53 (22)
Hormone + chemotherapy		192 (78)
Tumour size (cm)	243	
T1		127 (52)
T2 (>2.0-5)		100 (41)
T3 (>5)		16 (7)

*Number of cases for which data were available.

** Survival data for Nottingham/Tenovus series were available for up to 20 years and for RMH/Breakthrough series for up to 10 years.

***: Deaths of causes other than breast cancer were censored at last follow up.

Table 4-3: Primary antibodies, clone, source, optimal dilution and scoring system used for each immunohistochemical marker

Antibody	Clone	Source	Dilution	Cut-offs	Ref.
Mouse MAb anti p53	DO7	Novocastra	1: 50	10%	87, 102,-107
Mouse MAb anti-Bcl2	124	Dako-Cytomation	1:100	10%	87, 104, 106, 107
Mouse MAb anti-BRCA1	MS110	Oncogen Research	1:150	25%	87, 102, 104, 106, 107
Rabbit MAb anti-ATM	Y170	Abcam	1:100	25%	102, 104
Mouse MAb anti-CK19	BCK 108	Dako-Cytomation	1:100	10%	87, 104
Mouse MAb anti-CK18	DC10	Dako-Cytomation	1:100	10%	87, 104
Mouse MAb anti-CK7/8	CAM 5.2	Becton Dickinson	1:10	10%	87, 104
Mouse MAb anti-CK5/6	D5/16134	Dako-Cytomation	1:100	10%	87, 104
Mouse MAb anti-CK14	LL002	Novocastra	1:60	10%	87, 104
Mouse MAb anti-E-cadherin	HECD-1	Zymed Laboratories	1:100	10%	87
Mouse MAb anti-Ki-67	MIB1	Dako-Cytomation	1:100	10%	104, 107
Mouse MAb anti-ER-α	1D5	Dako-Cytomation	1:100	10%	87, 104, 107
Rabbit antihuman HER-2		Dako-Cytomation	1:100	see text	104, 107, 109
Mouse MAb anti- P21	EA10	Abcam	5ug/ml	10%	104,106, 107, 139
Mouse MAb anti- P27	SX53G8	Dako-Cytomation	1:50	10%	104, 106, 107

All sections were pre-treated with microwave antigen retrieval using 0.1% citrate except those for c-erbB2 did not pre-treat.

ATM: ataxia telangiectasia mutated; BRCA1: Breast cancer 1, early onset; CK: cytokeratin; ER-α: oestrogen receptor alpha; c-erB2, human epidermal growth factor receptor 2. MAb: Monoclonal antibody.

Table 4-4: HER-2 expression according to ASCO/ CAP guidelines

HER-2 Status	Criteria
Positive	o IHC staining 3+: uniform, intense membrane staining of >30% of invasive tumor cells (or) o HER-2:CEP17 FISH ratio >2.2
Equivocal	o IHC staining 2+: complete membrane staining that is either non-uniform or weak in intensity but with obvious circumferential distribution in at least 10% of cells (or) uniform, intense membrane staining of ≤30% of invasive tumor cells (or) o FISH ratio of 1.8-2.2
Negative	o IHC staining 0 or 1+: no or faint incomplete membrane staining) (or) o FISH ratio HER-2:CEP17 FISH ratio <1.8

HER-2, human epidermal growth factor receptor 2; IHC, immunohistochemistry; FISH, fluorescent in situ hybridisation; CEP17, centromere 17 specific probe

4.3.5 Statistical analysis

Data management and analysis were performed using both SPSS software (SPSS, version16 Chicago, IL) and STATA software (STATA, version 10, StataCorp LP, Texas, USA). Where appropriate, Pearson's Chi-square, Fisher's exact, x2 for trend, Student's t and ANOVAs one way tests were used. Cumulative survival probabilities were estimated using the Kaplan–Meier method and differences between survival rates were tested for significance using the log-rank test. Multivariate analysis for survival was performed using the Cox hazard model. The proportional hazards assumption was tested using standard log-log plots. When appropriate, variables were assessed in univariate analysis as a continuous and categorical variable and the two models were compared using an appropriate likelihood ratio test. Hazard ratios (HR) and 95% confidence intervals (95% CI) were estimated for each variable. All tests were two-sided with a 95% CI and a p value <0.01 was considered significant. For multiple comparisons, p values were adjusted according to Holm-Bonferroni correction method.

4.4 Results

4.4.1 Clinicopathological importance of Bcl2 expression

Positive expression of Bcl2 showed a significant inverse association with increasing NGS grade, mitotic index and pleomorphism and a significant positive association with glandular (tubule) differentiation. In addition, Bcl2 expression was significantly associated with other favourable clinicopathological features including small tumour size, low NGS grade, low LN stage, CK18+, CK19+, CK8+, ER+, PR+, AR+, and absence of both p53 mutation, HER-2 overexpression and basal CKs (CK5/6 and CK14), **(Table 4-5)**.

4.4.2 Survival analyses

Both histological grade and Bcl2+ expression were strongly associated with an adverse outcome at 10 years with a significant increase in the hazard of death, recurrence and DM in both the whole cohort, AT untreated LN negative subgroups, and in ER+/HT treated patients. However, in ER negative tumours, NGS was not significantly associated with patient outcome **(Table 4-6)**. Bcl2 and NGS independent association with outcome was confirmed in multivariate Cox-regression analysis of the whole cohort, AT untreated LN negative subgroup, and in ER+/HT treated patients **(Table 4-7)**.

Table 4-5: The association between Bcl2 expression and other clinicopathological variables

Variable	Bcl2 Expression		X^2
	Bcl2+ (N=1045) n (%)	Bcl2- (N=605) n (%)	*P*
Size			3.5E-6*
≤2cm	714 (68)	344 (57)	
>2cm	331 (32)	261 (43)	
Lymph node Stage			
Negative	697 (67)	359 (59)	5.0E-7*
Positive (1-3 nodes)	305 (29)	181 (30)	
Positive (>3 nodes)	43 (4)	65 (11)	
Grade**			1.1E-49*
G1	279 (27)	27 (4.5)	
G2	389 (37)	142 (23.5)	
G3	377 (36)	436 (72)	
Mitotic Index			1.1E-52*
M1 (low; mitoses <10)	521 (50)	96 (16)	
M2 (medium; mitoses 10-18)	202 (19)	98 (16)	
M3 (high; mitosis >18)	322 (31)	411 (68)	
Pleomorphism			5.7E-38*
1 (small-regular uniform cells)	38 (4)	9 (2)	
2 (Moderate variation)	534 (51)	122 (20)	
3 (Marked variation)	473 (45)	474 (78)	
Tubule formation			2.9E-22*
1 (>75% of definite tubule)	97 (9)	5 (1)	
2 (10%-75% definite tubule)	395 (38)	159 (26)	
3 (<10% definite tubule)	553 (53)	441 (73)	
p53 (+)	120 (13)	193 (35)	2.9E-14*
p21(+)	401 (50)	136 (28)	3.7E-14*
p27 (+)	312 (50)	75(19)	2.3E-23*
BRCA1 (-)	113 (14)	127 (27)	2.8E-9*
HER-2(+)	37(4)	85 (16)	1.9E-14*
ER(+)	868 (87)	253(43.5)	2.2E-14*
PR(+)	699 (72)	159 (28)	3.2E-14*
CK5/6(+)	101(10)	161(28)	1.6E-14*
CK18(-)	52(6)	102 (19)	1.0E-15*
Basal-like phenotype (+)	59 (6)	154(28)	8.3E-15*
Triple negative phenotype (+)	76 (7.5)	220 (40)	2.8E-14*

* Statistically significant; **: grade as defined by NGS; BRCA1: Breast cancer 1,early onset; HER-2: human epidermal growth factor receptor 2: ER: oestrogen receptor, PR: progesterone receptor; CK: cytokeratin; Basal-like: ER-, HER-2 and positive expression of either CK5/6, CK14 or EGFR; Triple negative: ER-/PgR-/HER-2-.

Table 4-6: Univariate survival analysis of whole patients' cohort and of both patients who did not receive any systemic adjuvant therapy and ER negative subgroups at 10 years

Variables	Whole patients cohort (n=1650)		No adjuvant therapy (n=673)		ER negative patients (n=454)	
	HR (CI 95%)	*P*	*HR (CI 95%)*	*P*	*HR (CI 95%)*	*P*
Grade**		4.8E-26*		1.2E-15*		0.126
G1	1		1		1	
G2	2.3 (1.5-3.3)		2.2 (1.4-3.6)		0.99 (0.4-2.6)	
G3	4.7 (3.3-6.8)		5.5 (3.5-8.8)		1.70 (0.7-3.7)	
Lymph node stage		3.08E-46*		2.7E-7*		7.7E-12*
Negative	1		1		1	
1-3 nodes	1.8 (1.4-2.1)		2.3 (1.4-3.8)		1.5 (1.1-2.2)	
>3 nodes)	5.8 (4.4-7.5)		5.1 (2.4-11.0)		4.5 (3.0-6.8)	
Size (>2cm)	2 (1.6-2.4)	1.0E-13*	1.8 (1.3-2.7)	0.002*	1.6 (1.2-2.2)	0.002*
Bcl2 (-)	2.8 (2.4-3.4)	5.8E-29*	3.7 (2.7-5.1)	6.7E-15*	2.0 (1.3-2.9)	0.001*
HER-2 (+)	2.0 (1.5-2.7)	1.3E-6*	2.1 (1.1-3.8)	0.016*	1.3 (0.9-1.9)	0.187
P53 (+)	2.0 (1.6-2.4)	1.5E-10*	1.9 (1.2-0.5)	0.005*	1.2 (0.9-1.6)	0.243
ER (+)	0.6 (0.5-0.7)	5.6E-9*	0.4 (0.3-0.5)	2.0E-7*	NA	NA
PR (+)	0.6 (0.5-0.7)	2.1E-9*	0.4 (0.3-0.7)	6.3E-6*	1.1 (0.7-1.7)	0.768
CK5/6 (+)	1.5 (1.2-1.9)	1.7E-4*	1.8 (1.3-2.7)	0.002*	1.3 (0.9-1.7)	0.111

* Statistically Significant. HR: Hazard ratio; CI: confident interval; **: grade as defined by NGS; HER-2: human epidermal growth factor receptor 2; ER: oestrogen receptor; PR: progesterone receptor.

Table 4-7: Prognostic independence of histological grade and Bcl2 expression using multivariate Cox regression

Variable	HR(95% CI)	P
Whole patients cohort (n=990)		
Grade*		4.8-5*
1	1	
2	2.267(1.601-3.212)	
3	2.811(1.963-4.025)	
Lymph node Stage		2.7E-20*
Negative	1	
Positive (1-3 nodes)	1.7 (1.4-2.2)	
Positive (>nodes)	4.5 (3.3-6.1)	
Size	1.37 (1.2-1.6)	1.1E-5*
Bcl2 (-)	2.3 (1.6-3.4)	2.5E-8*
Oestrogen receptor (+)	1.3 (0.9-1.7)	NS
Progesterone receptor (+)	0.97 (0.7-1.3)	NS
P53 (+)	1.4 (1.1-1.8)	0.006*
HER-2 (+)	1.5 (1.1-2.0)	0.012*
ER negative subgroup (n=454)		
Lymph node Stage		
Negative	1	6.6E-12*
Positive (1-3 nodes)	1.5 (1.1-2.1)	
Positive (>nodes)	4.6 (3.0-7.0)	
Size (>2cm)	1.5 (1.1-2.0)	0.013*
Bcl2 (-)	2.0 (1.4-3.0)	3.0E-4*

* Statistically Significant; **: grade as defined by NGS; HR: Hazard ratio; CI: confident interval; HER-2: human epidermal growth factor receptor 2; ER: oestrogen receptor; PR: progesterone receptor.

4.4.3 Relative prognostic importance of the three components of NGS

The prognostic relevance of the three components of NGS i.e. mitoses, tubule formation and pleomorphism was evaluated in univariate and multivariate analysis. The mitotic index was found to be the principal prognostic component of NGS in the whole cohort (**Table 4-8**) and was further confirmed in both AT untreated-LN negative, ER+/HT treated and ER negative subgroups as well. In addition, substitution of histological grade by its three components in the multivariate regression analysis including validated prognostic markers showed that only mitotic index remained an independent predictor of outcome in the final models. Moreover, although NGS did not show any significant association with clinical outcome in the ER negative subgroup, mitotic index did retain significance in the multivariate analysis (**Table 4-9**).

Table 4-8: Multivariate analysis using Cox model for the three components of Nottingham grading system

Variables	Disease Specific Survival		Disease Free Survival	
	HR (CI 95%)	*P*	*HR (CI 95%)*	*P*
Mitotic activity		8E-12*		1.4E-6*
M1 (low; mitoses <10)	1		1	
M2 (medium; mitoses 10-18)	2.32 (1.68-3.22)		1.58(1.24-2.03)	
M3 (High; mitosis >18)	3.46 (2.50-4.80)		2.00 (1.55-2.57)	
Tubule Formation		0.02800*		0.42800
1 (>75% of definite tubule)	1		1	
2 (10%-75% definite tubule)	2.40 (1.03-5.61)		1.31 (0.82-2.10)	
3 (<10% definite tubule)	2.84 (1.23-6.64)		1.36 (0.85-2.19)	
Nuclear pleomorphism (variation in size and shape)		0.92800		0.87100
1 (small, regular uniform)	1		1	
2 (moderate variation)	0.87 (0.37-2.03)		1.14 (0.61-2.13)	
3 (marked variation)	0.85 (0.35-2.03)		1.10 (0.58-2.10)	

* Statistically significant

Table 4-9: Multivariate Cox Hazard analysis of the components of the Nottingham Grading System (NGS), Bcl2 expression and clinicopathological variables.

Variable	HR(95% CI)	*P*
Whole patient cohort (n=1650)		
Mitotic activity		7.0E-5*
M1 (low; mitoses <10)	1	
M2 (medium; mitoses 10-18)	2.0(1.3-2.9)	
M3 (high; mitosis >18)	2.3(1.6-3.4)	
Tubule Formation		0.235
1 (>75% of definite tubule)	1	
2 (10%-75% definite tubule)	2.1 (0.8-5. 5)	
3 (<10% definite tubule)	2.3 (0.9-5.9)	
Nuclear pleomorphism (variation in size and shape)		0.200
1 (small, regular uniform)	1	
2 (moderate variation)	0.4 (0.2-1.1)	
3 (marked variation)	0.4 (0.2-1.1)	
Lymph node stage		2.3E-20*
Negative	1	
Positive (1-3 nodes)	1. 7 (1.3-2.1)	
Positive (>3 nodes)	4. 5 (3.2-6.1)	
Size	1. 3 (1.2-1.5)	6.2E-6*
Bcl2 (-)	1. 9 (1.5-2.5)	1.0E-7*
ER (+)	1. 2(0.9-1.7)	0.149
PR (+)	0. 97(0.7-1.3)	0.860
P53 (+)	1.4 (1.1-1.8)	0.009*
HER-2 (+)	1.5 (1.1-2.0)	0.012*
ER- subgroup (n=355)		
Lymph node Stage		
Negative	1	8.3E-8*
Positive (1-3 nodes)	1.3 (0.9-2.0)	
positive (>3 nodes)	4.2 (2.5-6.8)	
Size	1.2 (1.1-1.5)	0.007*
Bcl2 (-)	2.0 (1.2-3.1)	0.001*
M1 (low; mitoses <10)	1	0.032*
M2 (medium; mitoses 10-18)	3.2 (1.3-8.4)	
M3 (high; mitosis >18)	1.9 (0.8-4.3)	

*Statistically Significant. HER-2; human epidermal growth factor receptor2

4.4.4 Prognostic significance of combined M/Bcl2 profiles

Multivariate Cox regression models were used to assess and compare the prognostic performance of M/Bcl2 profiles to that of validated prognostic indicators assessed in the total patient cohort and was further confirmed in AT untreated LN negative patients, and in those with ER+ disease who received HT.

We found that the M/Bcl2 profile was significantly associated with DSS, DFS and DM along with LN status and tumour size. In the ER negative disease, M/Bcl2 distinguished between patients with low risk from those with high risk independently on stage and size (Table 4-10).

4.4.5 Prognostic significance of M/Bcl2 profiles in small early stage (N0, T1) tumours

We investigated the clinical outcome of 522 patients with early stage small tumours (lymph node negative with primary tumour size ≤ 2cm) from the Nottingham series who did not receive any AT (**Figure 4-2**). Consistent with the findings in the other groups, patients with M1-2/Bcl2+ or M1/Bcl2- phenotypes displayed a better prognosis than cases with M2-3/Bcl2- or M3/bcl2+ (HR; 5.3, CI 95%; 3.5-8.0, p=6.7 E-15). In the multivariate analysis, M/Bcl2 was the only independent prognostic factor in this subgroup (**Table 4-11**).

Table 4-10: Multivariate analysis using Cox regression in whole patients' cohort, in patients who did not receive any systemic adjuvant therapy and ER- subgroups.

Variables	Overall Survival		Disease Free Survival	
	HR (CI 95%)	*P*	*HR (CI 95%)*	*P*
Whole Cohort (n=1650)				
MI/Bcl2 profiles		7.5E-16*		1.0E-11*
M1/Bcl+	1		1	
M1/Bcl2-	2.5 (1.4-4.3)		2.3 (1.5-3.4)	
M2/Bcl2+	1.3 (0.8-2.2)		1.2 (0.8-1.7)	
M2/Bcl2-	6.0 (3.8-9.3)		3.4 (2.4-4.9)	
M3/Bcl2+	2.9 (2.0-4.3)		1.7 (1.3-2.3)	
M3/Bcl2-	4.2 (2.8-6.3)		2.4 (1.8-3.3)	
Lymph node stage		6.2E-20*		1.4E-17*
Negative	1		1	
Positive (1-3 nodes)	1.7 (1.3-2.1)		1.3 (1.1-1.6)	
Positive (>3 nodes)	4.4 (3.2-6.0)		3.6 (2.7-4.8)	
Size	1.3 (1.2-1.5)	2.4E-6*	1.2 (1.1-1.3)	0.001*
p53 (+)	1.4 (1.1-1.8)	0.008*	1. 3 (1.1-1.6)	0.02*
HER-2 (+)	1.4 (1.1-1.9)	0.02*	1.4 (1.1-1.9)	0.01*
ER (+)	1.2 (0.9-1.6)	0.202	1.3 (1.0-1.6)	0.074
PR (+)	0.96(0.7-1.3)	0.784	1.0 (0.8-1.2)	0.829
No adjuvant therapy (n=673)				
Mitoses/Bcl2 Profiles		1.6E-4*		1.2E-5*
M1/Bcl+	1		1	
M1/Bcl2-	1.3 (0.5-3.0)		2.1 (1.5-4.2)	
M2/Bcl2+	2.8(1.3-6.1)		2.5 (0.8-2.4)	
M2/Bcl2-	2.4 (1.0-5.5)		4.9 (2.6-9.2)	
M3/Bcl2+	6.5 (3.0-14.4)		2.1 (1.1-4.0)	
M3/Bcl2-	3.7 (1.7-8.3)		2.8 (1.5-5.3)	
Lymph node stage		0.002*		0.003*
Negative	1		1	
Positive (1-3 LNs)	3.0 (1.6-5.7)		1.9 (1.1-3.3)	
Positive (>3 nodes)	3.1 (0.9-11.27)		4.7 (1.6-13.2)	
Size	1.3 (0.9-1.7)	0.092	1.4 (1.1-1.7)	0.008*
P53+	0.7 (0.4-1.3)	0.291	1.2 (0.7-1.9)	0.559
HER-2	0.9 (0.5-1.8)	0.840	1.1 (0.6-2.0)	0.652
ER	0. 6 (0.3-1.1)	0.111	1.2 (0.7-2.0)	0.500
Progesterone receptor	0. 98 (0.5-1.8)	0.949	0.9 (0.6-1.4)	0.675
ER- subgroup (n=355)				
Mitoses/Bcl2 Profiles		0.002*		5.0E-4
M1/Bcl+	1		1	
M1/Bcl2-	1.8 (0.4-8.9)		2.9 (0.7-13.2)	
M2/Bcl2+	1.7 (0.3-8.7)		3.1 (0.7-13.8)	
M2/Bcl2-	7.3 (2.0-25.6)		8.9 (2.6-30.7)	
M3/Bcl2+	2.0 (0.6-6.8)		2.5 (0.8-8.4)	
M3/Bcl2-	3.4 (1.1-10.7)		4.4 (1.4-13.8)	
LN Stage		9.4E-8*		1.8E-8
Negative	1		1	
Positive (1-3 nodes)	1.3 (0.4-2.0)		1.1 (0.7-1.6)	
Positive (>3 nodes)	4.1 (2.5-6.8)		4.0 (2.5-6.4)	
Size	1.3 (1.1-1.6)	0.005*	1.4 (0.96-1.4)	0.143

* Statistically significant. HER-2; human epidermal growth factor receptor 2

Table 4-11: Prognostic independence of combined mitotic index (MI)/BcL2 profile using multivariate analysis using Cox model of patients with small early stage tumour who did not receive any adjuvant therapy (n=522 cases)

Variables	Disease Specific Survival		Disease Free Survival	
	HR (CI 95%)	*P*	*HR (CI 95%)*	*P*
Mitotic index/Bcl2-		3.0E-8*		1.5E-9*
M1/Bcl2+	1		1	
M1/Bcl2-	1.7 (0.7-4.0)		2.0 (1.1-3.4)	
M2/Bcl2+	1.2 (0.5-3.0)		1.9 (1.1-3.3)	
M2/Bcl2-	9.5 (4.4-20.3)		6.0 (3.2-11.3)	
M3/Bcl2+	6.8 (3.0-15.3)		6.2 (3.3-11.6)	
M2/Bcl2-	4.3 (1.8-11.5)		3.5 (1.6-11.3)	
ER (+)	0.6 (0.3-1.3)	0.212	1.2 (0.7-2.2)	0.560
PgR (+)	0.8 (0.5-1.5)	0.588	0.6 (0.4-0.9)	0.041
P53 (+)	0.5 (0.3-1.1)	0.096	0.8 (0.4-1.5)	0.502

* Statistically significant. ER; oestrogen receptor, PgR; progesterone receptor

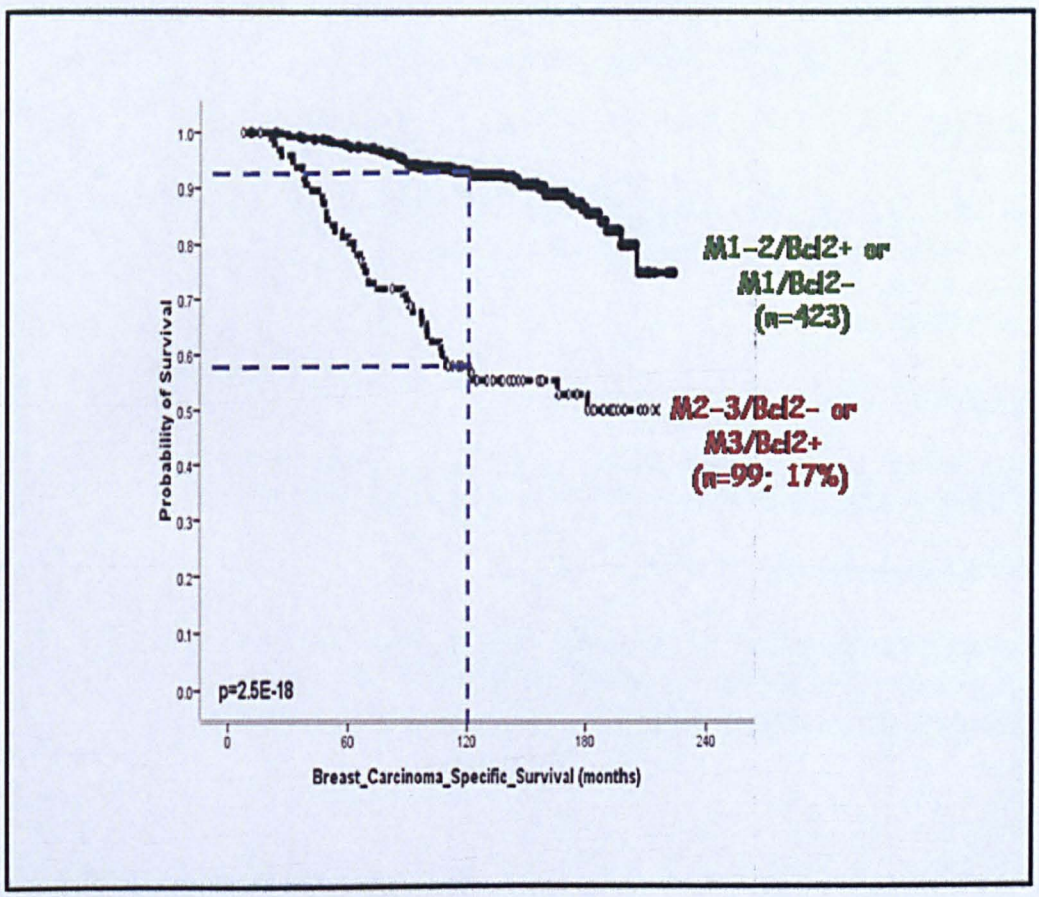

Figure 4-2: Disease specific survival (DSS) of early stage small tumours stratified by MI/Bcl2 expression profile

4.4.6 Clinical outcome of M/Bcl2 in different adjuvant therapy settings

HT-treated cases of Nottingham series with M2-3/Bcl2- and M3/Bcl2+ showed 2.5-4.0 fold increase in the risk of death (HR: 4.3, 95% CI: 2.8-6.6, p=8.2E-12), recurrence (HR: 2.7, 95% CI: 1.9-3.7, p=3.9E-9) and DM (HR: 3.3, 95% CI: 2.2-4.7, p=2.5E-10) compared with those of M1-2/Bcl2+ and M1/Bcl2- phenotype.

Poor outcome of BC with M2-3/Bcl2- and M3/Bcl2+ phenotypes was further confirmed in Breakthrough series which comprises patients that were uniformly treated with anthracycline based chemotherapy. In this cohort, patients with M2-3/Bcl2- and M3/Bcl2+ showed 2.5 fold increase in the risk of death (HR: 2.5, 95% CI: 1.1-5.6, p=0.03), recurrence (HR: 2.3, 95% CI: 1.2-4.3, p=0.009) and DM (HR: 2.5, 95% CI: 1.2-5.1, p=0.017) compared with those of M1-2/Bcl2+ and M1/Bcl2- phenotype.

4.4.7 Re-stratification of patients' outcomes according to M/Bcl2

Good clinical outcome (Low risk; NGS-G1-like prognosis, n=723; 43%)

The survival curves and clinicopathological features of M1/Bcl2+ phenotype of either NGS-G1 (279/521; 54%) or NGS-G2 (241/521; 46%) were identical (log-rank test, p=NS) showing low risk of death, recurrence and DM (**Figure 4-3**). Similarly, the survival and clinicopathological characteristics of M2/Bcl2+ either of NGS-G2 (147/202; 73%) or of NGS-G3 (55/202; 27%) were indistinguishable and showed low risk of death, recurrence and DM (**Figure 4-3**). The 10-year survival probability of AT-untreated LN negative patients with M1/Bcl2+ and M2/Bcl2+ was 94% and 92%, respectively which is indistinguishable from that of both NGS-G1 (95%) and an age-matched female population without BC. However; M1-2/Bcl2+ tumours included over twice (723/1650; 43%) as many patients as NGS-G1 (306/1650; 19%; Fisher's exact test $p<0.0001$). These results suggest that the M1-2/Bcl2+ phenotypes more accurately identify patients with low risk than NGS-G1 and we referred to this as NGS-G1-like prognosis.

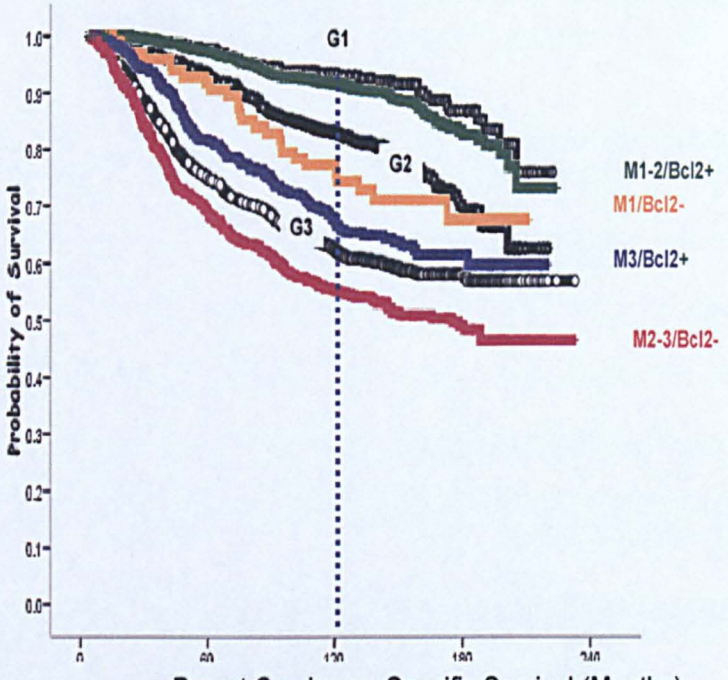

Clinical outcome	NGS	MI/Bcl2 profile
Good prognosis	G1 (19%)	M1-2/Bcl2+(44%)
Intermediate prognosis	G2 (32%)	M1/Bcl2- (6%)
Poor prognosis	G3 (49%)	M3/Bcl2+ (19%)
		M2-3/Bcl2- (31%)

Figure 4-3: Disease specific survival (DSS) of different M/Bcl2 profiles of whole breast cancer cohort compared to Nottingham grading system (NGS).

Intermediate clinical outcome (Intermediate risk; NGS-G2-like prognosis, n=96; 5.8%)

M1/Bcl2- tumours with either of NGS-G1 (27/96; 28%) or NGS-G2 (69/96; 72%) had survival curves and clinicopathological features indistinguishable from NGS G2 (i.e. NGS-G2-like) AT untreated LN negative patients with M1/Bcl2- phenotype had 86% 10-year survival probability which is equal to that of NGS-G2 (i.e. intermediate risk). Thus M/Bcl2 profile reduced the percentage of cases with intermediate prognosis from 32% to only 6% and >80% of them was either invasive ductal of no special type or mixed tumours.

Poor clinical outcomes (High risk; NGS-G3-like prognosis, n=831; 50%)

The 10-year survival probability of AT untreated LN negative patients with M2/Bcl2-, M3/Bcl3- and M3/Bcl2+ phenotypes was 50%, 54% and 68%; respectively while that of NGS-G3 was 62%. M2/Bcl2- tumours displayed poor prognosis similar to those of M3/Bcl2- which showed a significant worse clinical outcomes and more aggressive clinicopathological features than those of M3/Bcl2+ (**Table 4-12**).

Table 4-12: Clinicopathological comparison between M3/Bcl2- and M3/Bcl2+ phenotype of high Nottingham grade system (NGS 3)

Variable	NGS G3		*P*
	M3/Bcl2+ (N=322) n(%)	M3/Bcl2- (N=403) n(%)	
Size (>2cm)	151 (47)	193 (48)	0.8160
Lymph node (+)	138 (43)	165 (41)	0.575
P53 (+)	97 (30)	181 (45)	1.3E-4*
P21	161(50)	97 (24)	7.8E-11*
P27	119(37)	52 (13)	4.4E-9*
BRCA1 (-)	71 (23)	133 (33)	0.004*
HER-2(+)	32 (10)	72 (18)	0.004*
ER(+)	235 (73)	113 (28)	1.7E-14*
PR(+)	170 (53)	68 (17)	1.8E-14*
CK5/6(+)	60 (18)	133 (33)	1.1E-5*
Ck18(-)	48 (15)	105 (26)	<0.001*
Basal-like (+)	37 (14)	145 (36)	<0.0001*
Triple negative phenotype (+)	45 (17)	204 (50)	<0.0001*

* Statistically significant. BRCA1: Breast cancer 1 early onset; HE-R2; human epidermal growth factor receptor 2; ER: oestrogen receptor; PR: progesterone receptor: CK: cytokeratin; Basal like: ER-, HER-2 and positive expression of CK5/6, CK14 or EGFR; Triple negative: ER-/PR-/HER-2-

.

4.4.8 M/Bcl2 profiles accurately relocated the clinical outcomes of NGS

NGS-G1 clinical outcomes

Although all NGS-G1 tumours showed low M (M1), Bcl2 expression divided NGS G1 into two subgroups with distinct clinical outcomes (**Figure 4-4 and Table 4-13**). The M1/Bcl2- tumours (27/306; 9%) had a 3-4 fold increased risk of death, relapse and DM compared to M1/Bcl2+ (279/306; 91%).

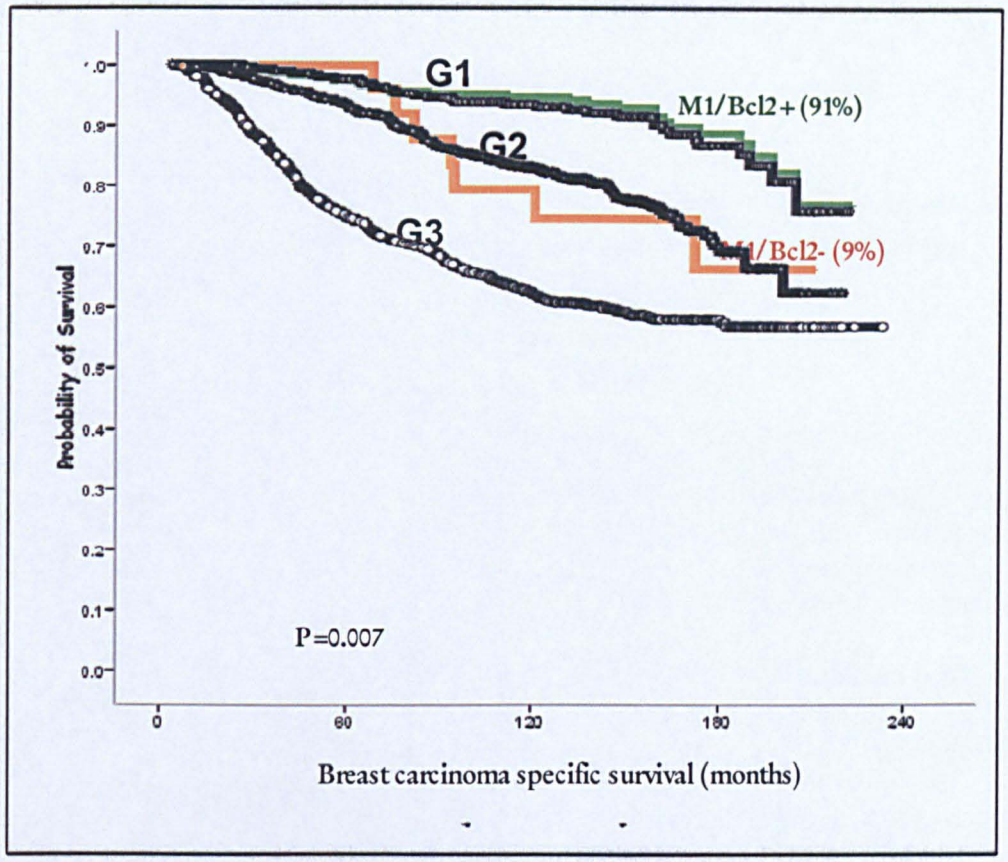

Figure 4-4: Disease specific survival curve of Nottingham grade 1 (NGS-G1) stratified by combined mitotic index (M)/Bcl2 profile

M/Bcl2 profile identifies prognostically relevant subgroups of NGS-G3

NGS G3 tumours with a Bcl2- phenotype had a 2-fold increase risk of death (HR: 1.7; 95% CI: 1.4-2.1; p=4.4E-6), relapse (HR: 1.6; 95% CI: 1.3-1.9; p=3E-5) and DM (HR: 1.5; 95% CI: 1.2-1.9; p=2E-4) compared with Bcl2+ cases. However, M/Bcl2 profiles reclassified tumours with NGS-G3 into three clinicopathological subgroups (Table3-12): NGS-G3 with M2/Bcl2+ phenotype (55/813; 7%) showed good clinical outcome identical to that of NGS-G1 while NGS-G3 with either M2/Bcl2- (33/813; 4%), M3/Bcl2+ (322/813; 40%) or M3/Bcl2- (403/813; 49%) retained poor outcome and aggressive characteristics of NGS-G3 (**Figure 4-5**). However, NGS-G3 with M2-3/Bcl2- showed a worse

clinicopathological outcome compared to those of NGS-G3 with M3/Bcl2+. Similar associations between the groups defined by M and Bcl2 and outcome were found in the analysis of the AT-untreated LN-negative subgroup.

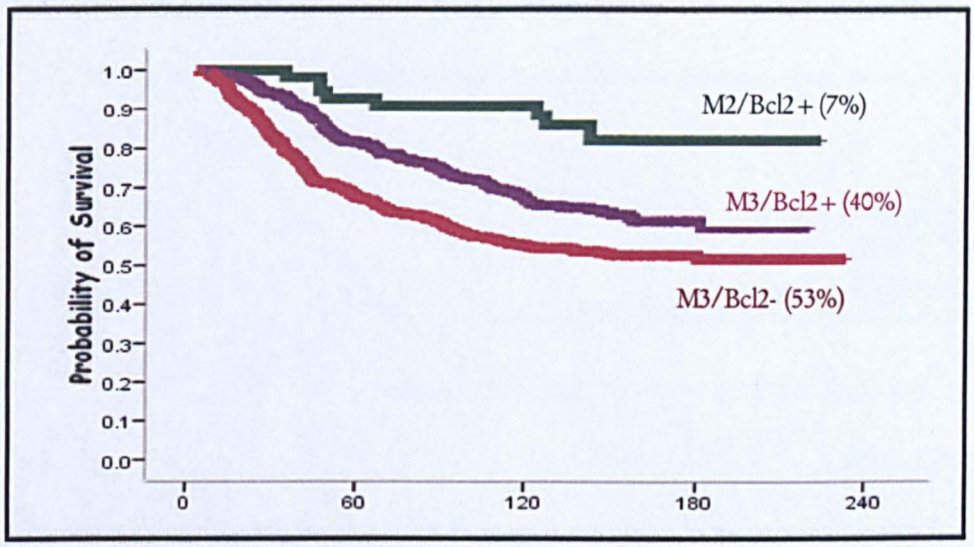

Figure 4-5: Disease specific survival curve of Nottingham grade 3 (NGS-G3) stratified by mitotic index (M)/Bcl2 profile

M/Bcl2 profile identifies NGS-G2 tumours with; good and poor clinical outcomes

Bcl2 expression divided the NGS grade 2 group into two clinical different subgroups: Bcl2- cases (142/531; 27%) had 3-fold increase risk of death (HR: 3.6; 95% CI: 2.5-5.42; p=3E-12), disease relapse (HR: 2.5; 95% CI: 1.8-3.3; p=1.2E-9) and DM (HR: 3.0; 95% CI: 2.2-4.2; p=3.9E-11) compared with Bcl2+ cases (389/531; 73%). We explored the clinical significance of M/Bcl2 profile of NGS-G2 patients (**Figure 4-6**) in the whole cohort, in AT-untreated LN-negative patients, in those with ER+ tumours who received HT and in patients with ER-negative tumours. We found that only M1/Bcl2- (69/531; 13%) of NGS-G2 retained the intermediate prognosis of NGS-G2. Moreover, 87% of NGS-G2 was

reclassified into either good (74%) or poor (13%) prognosis. Notably, no significant difference was observed between NGS-G2 with either M1/Bcl2+ (242/531; 46%) or M2/Bcl2+ (147/531; 28%) and NGS-G1 survival curves, or the NGS-G2 with either M2/Bcl2- (65/531, 12%) or M3/Bcl2- (6/531; 1%) and NGS-G3 curves.

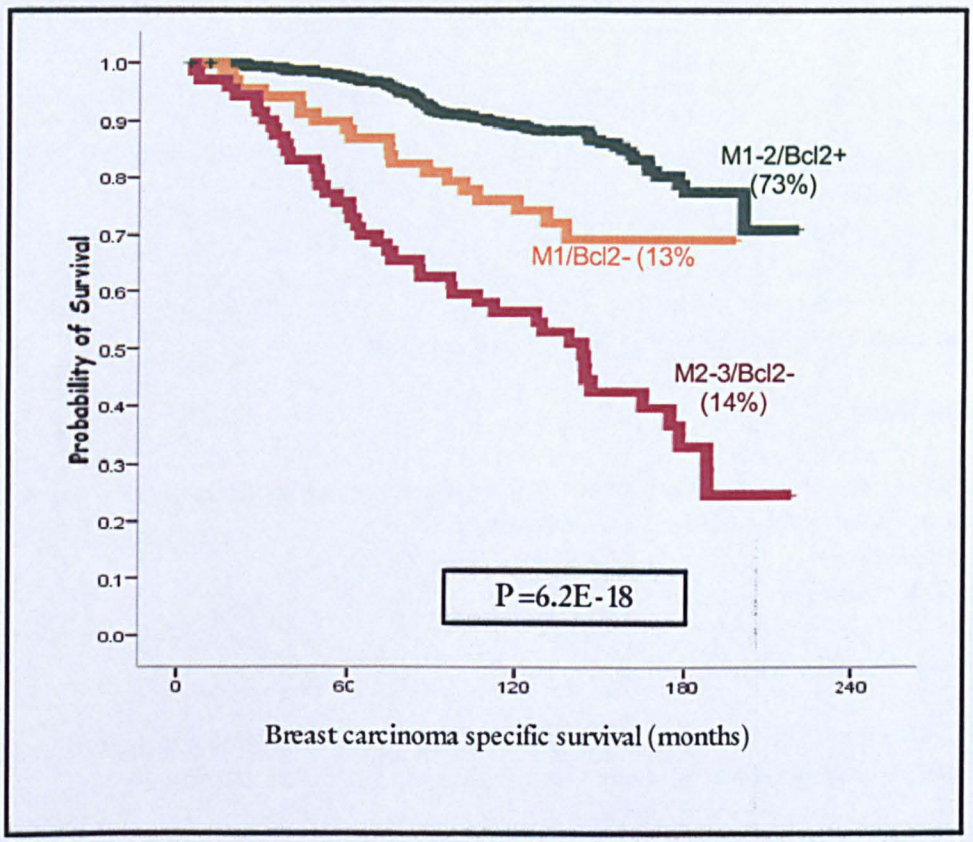

Figure 4-6: Disease specific survival curve of NGS G2 stratified by combined mitotic index (M)/Bcl2 profile

Table 4-13: Univariate analysis to determine risk of each class of combined mitotic index/Bcl2 profile within histologic grade 1 (A), grade 2 (B) and grade (C)

Risk group	MI/Bcl2 profile	Disease specific survival		Disease free survival		Distant metastases-related survival	
		HR (95% CI)	p	HR (95% CI)	p	HR (95% CI)	p
A) Grade 1							
Low risk	MI/Bcl2+	1	0.003*	1	5.0E-6*	1	1.7E-4*
High risk	MI/Bcl2-	3.3 (1.5-7.4)		3.4 (2.0-5.6)		3.7	
B) Grade 2							
Low	MI/Bcl2+	1		1		1	
	M2/Bcl2+	0.98 (0.6-1.7)	0.937	1.1 (0.8-1.6)	0.566	1.2 (0.7-1.9)	0.484
Intermediate	M2/Bcl2+	2.2 (1.2-3.8)	0.007*	1.7 (1.1-2.6)	0.023*	2.1 (1.3-3.5)	0.003*
High	M2/Bcl-	5.1 (3.2-8.2)	8.3E-12*	3.7 (2.5-5.3)	2.6E-11*	4.3 (2.8-6.7)	1.4E-11*
	M3/Bcl2-	5.8 (2.0-16.6)	0.001*	5.4 (2.2-13.4)	3.0E-4*	4.6 (1.6-12.8)	0.004*
C) Grade 3							
Low	M2/Bcl2+	1		1		1	
High	M3/Bcl2+	2.7 (1.3-5.6)	0.006*	1.9 (1.1-3.4)	0.018*	2.0 (1.1-3.7)	0.017*
	M2/Bcl2-	5.2 (2.3-12.0)	9.8E-5*	3.4 (1.7-6.7)	4.1E-4*	3.4 (1.6-7.0)	0.001*
	M3/Bcl2-	4.0 (2.0-8.3)	1.0E-4*	2.7 (1.6-4.7)	2.8E-4*	2.8 (1.6-5.0)	0.001*

* Statistically significant

4.4.9 M/Bcl2 profile improves prognosis by NPI

We investigated whether incorporating the M/Bcl2 profile, instead of NGS, into NPI could improve patient's stratification. A simplified substitution of NGS by M/Bcl2 profile: score 1: NGS-G1-like phenotype, score 2: NGS-G2-like phenotype, and score 3: NGS-G3-like phenotype was explored and a modified NPI (mNPI) score was derived. The survival of patients stratified into risk groups was then compared between original NPI and mNPI. As shown in (**Figure 4-7**), the survival curves of the NPI and mNPI displayed a moderate agreement (k=0.58). Importantly however, the number of patients identified as part of the excellent prognostic groups (EPGs; NPI≤2.4) was increased 2-fold when AT-untreated LN-negative patients were stratified by mNPI as compared to NPI (366 vs. 198 patients, respectively. Thus twice as many patients could be accurately classified into EPG by mNPI suggesting use of the M/Bcl2 profile could have clinical benefit through more accurate classification of patients into prognostic classes and in particular, identifying a greater proportion of patients who could potentially be spared AT. Moreover, evaluation of tubular formation and pleomorphism used in the NGS is subjective, leading to inconsistency. Therefore, including M/Bcl2 profile instead of tubular formation and pleomorphism in mNPI could render it a more objective system compared to the classic NPI..

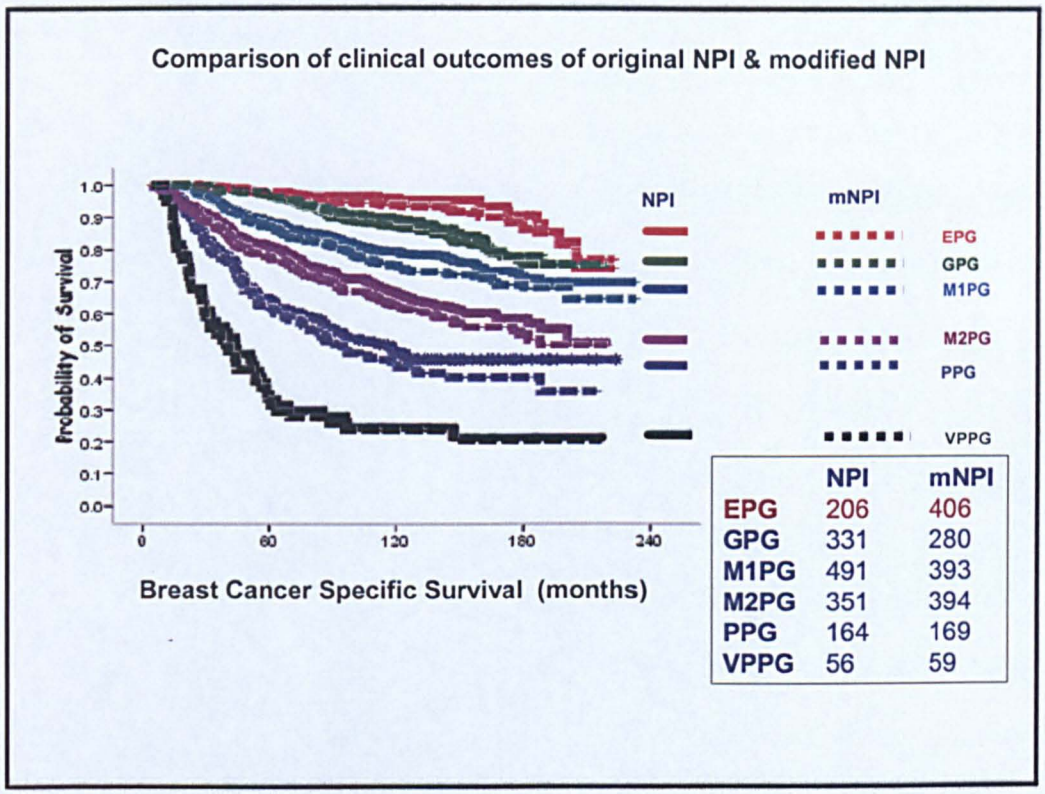

Figure 4-7: Stratification of patients' risk by classic Nottingham Prognostic index (NPI) and modified (m) NPI and Kaplan-Meier disease specific survival (DSS) curves.

4.5 Discussion

Histological grade has been shown to be underpinned by distinct transcriptomic patterns [48-50]. In fact, genetic grade signatures developed to recapitulate NGS-G1 and NGS-G3 BCs have been shown to be able to stratify NGS-G2 tumours into NGS-G1-like and G3-like cancers [48-51]. In agreement with these studies, we found by using a simple objective M/Bcl2 profile that BC with intermediate prognosis is rarer than previously assumed with only 6% instead of 32% of BC retaining the intermediate clinical outcome of NGS-G2. The prognostic performance of M/Bcl2 profile was found to be independent of LN status, tumour size and ER status suggesting that it can substantially contribute to patient prognosis. In addition, by using M/Bcl2 profiles, about twice as many patients could be accurately classified into the EPG by mNPI improving identification of patients that could be spared of or who require systemic AT thus reducing potential harm due to over- and under treatment.

Meta-analysis of publicly available gene expression data demonstrated that most of the genes associated with histological grade are involved in cell cycle regulation, proliferation, apoptosis, p53 and ER signalling networks [49-51, 133, 135, 140, 141, 142, 143]. In agreement with these studies, we found that the mitotic figure recognition as a reflection of growth fraction was the most important prognostic factor among the 3 morphologic features of NGS. In addition, we confirmed that Bcl2 expression is strongly associated with tumour differentiation and is an independent prognostic factor [14, 141, 144]. There are several lines of evidence to suggest that Bcl2 plays a central role in breast morphogenesis, BC tumourigenesis, and that it may be employed to improve on the prognostic methods for the management of BC patients [14, 138 144-148]. Furthermore, Bcl2 is as a direct downstream responsive gene of ER and p53 and plays a crucial role in their molecular network with respect to BC development [14, 144-147]. Bcl2 also confers survival advantage to tumour cells by

prolonging cell cycle at G0/G1[29] (anti-proliferative) and by simultaneously extending cell survival (anti-apoptotic). In this context, the M/Bcl2 profile is actually a phenotypic profile that bears biological significance. For example, tumours with the M1-2/Bcl2+ profile showed low levels of expression of the growth fraction marker MIB1 and high level of expression of the G0/G1 regulatory proteins p21 and p27, implying that the proliferative capacity is lowered as these cells exit cell cycle into quiescent (G0), senescent out-of-cycle states. Given that engagement of the somatic differentiation programme is coupled to G1 arrest and cell cycle withdrawal into the out-of-cycle state, this phenotype could be considered to represent well differentiated forms of BC[149]. It is noteworthy that acquisition of Bcl2 expression could create a restrictive environment for the expansion of these neoplastic cells. In addition given that most M1-2/Bcl2+ cases are ER+/PR+ thus this phenotype is likely to be identifying the low proliferation end of the spectrum of ER+/PR+ cancers.

On the other hand, most of the neoplastic cells (>50%) of M2-3//Bcl2- tumours are actively replicative and show the lowest level of both p21 and p27 and highest frequency of p53 nuclear expression, and BRCA1 and ATM down-regulation, as defined by immunohistochemistry, compared to other phenotypes, indicating an active cell cycle progression with arrested tumour differentiation [148]. Moreover this high proliferative capacity is coupled with high levels of apoptosis due to absence of Bcl2 reflecting an increased cell turnover. Furthermore, this phenotype was associated with ER-/PR- indicating hormone independence and resulting in resistance to HT [147].

Whether grade is a continuum through which BC progresses or merely the end point of distinct genetic pathways has been debated. It is not clear whether BC develops along two (grades 1 versus 3) or three (grades 1 versus 2 versus 3) distinct pathways. In our study, the large majority of BC cases are either low (NGS-G1-like) or high (NGS-G3-like) grade

supporting the genetic pathways model of grade origin [52, 134, 104]. Tumours with intermediate prognosis (NGS-G2-like) may arise as homogenous tumours that are truly borderline between low and high grade, or could rather reflect a heterogeneous composition of both low and high grade cell types[48, 50]. Genetic analysis of NGS-G2 cancers suggests the majority of these tumours constitute the end of the spectrum of NGS G1 cancers as they often harbour deletion of 16q and gains of 1q, which are both typical of low grade BC [57].

Interestingly, we found that LNGBN tumours belonged to the NGS-G1-like phenotype and were either arrested in G0/G1 or out-of-cell cycle state. On the contrary, most basal-like and HER-2+ tumours were NGS G3-like phenotypes with actively progressive cell cycle suggesting that once BC is committed to a specific evolutionary/molecular pathway, progression or cross over to other high grade pathways would be an unlikely biological phenomenon. However, progression within biological class e.g. luminal "low grade" to luminal "high grade" is a possibility[140] and could be due to acquisition of additional genetic or epigenetic aberrations (e.g., p53 mutation, gene amplifications), which lead to more active cell cycle progression and increased proliferation.

In conclusion, here we described a grading system based on the balance between mitotic frequency and Bcl2 expression which is an independent predictor of outcome in a population based cohort. This system accurately reclassified patients with NGS-G2, small early stage BC and ER- into two groups with high versus low risks of death and recurrence, and also identified prognostically significant subgroups in a cohort of patients treated with adjuvant anthracycline-based chemotherapy. The use of this simple and objective grading system instead of NGS may help improve on the prognostic ability of current algorithms for clinical decision making (e.g. NPI).

Chapter 5:

A new genetic map for the evolutionary pathway of the low nuclear grade breast neoplasia (LNGBN) family

5.1 Abstract

In previous chapters, we have shown morphological and immunohistochemical evidence to suggest that a number of low nuclear grade invasive breast cancers (LNGBC) including invasive tubular and lobular carcinoma and their putative precursor lesions: columnar cell lesions (CCLs), low grade ductal carcinoma in-situ (DCIS) and lobular neoplasia (LN) may comprise a family of interrelated lesions.

In this study, we identified the molecular genetic profiles and potential evolutionary pathogenetic pathways of matched co-existing lesions belonging to the LNGBN family to support their common cell of origin.

Twenty cases of invasive LNGBCs and their matched coexisting CCLs, DCIS and LN were laser microdissected from formalin fixed paraffin embedded tissues (FFPET). The isolated non-amplified-DNA was subjected to high-resolution array-Comparative Genomic Hybridization (aCGH; 32 Kb BAC-array platforms, Breakthrough Breast Cancer Research Centre). Results were validated using chromogenic in situ hybridization (CISH) and immunohistochemistry. Comparative analysis was performed on aCGH datasets derived from independent BC series of 64 high grade invasive ductal carcinoma of no special type (IDC-NST) cases and 171 unselected series of BC in which the results were validated by gene expression array.

We observed that lesions from the same patient displayed remarkably similar patterns of genetic aberrations (Pearson's correlations 0.55-0.89; $p<0.00001$). All CCLs, low grade DCIS, LN and their matching invasive carcinoma harboured gain/amplification of 1q and loss of 16q. In addition in situ and matching invasive components displayed additional genetic aberrations at one of 16p13.3, 11q13.1-q14.1, 17q25.3, 19p13.3. Amplification of cyclin D1 was confirmed as a target gene by using CISH. The MDM4 gene on 1q32 was confirmed as an early genetic change using IHC and gene expression in three independent data sets. Moreover, prognostic and predictive implications of MDM4 overexpression were proved in a large data set with long term follow up.

In conclusions, our results suggest that 1) Tubular, and lobular carcinomas have a remarkable similarities in their genomic plots supporting the proposal that they comprise a family of low nuclear grade breast neoplasia (LNGBN), 2) The recurrent genetic changes associated with CCLs support that the CCLs are clonal disease., 3) The CCLs are non-obligate precursor components of the LNGBN family, 4) The low nuclear grade breast neoplasia family commonly shows gain/amplification at 1q21.4 (MUC1 locus), 5) The ER+ luminal restricted progenitor cell of TDLUs (ER+/MUC1+/CK18) could be the common cell of origin of LNGBN family, 6) Cyclin D1 and MDM4 are oncogenes that could drive the progression of the LNGBN family, 7) Such stochastic genetic hits could be responsible for the activation of the luminal 'A' pathway in ER+ progenitor cells, 8) An alteration of E-cadherin (CDH1) appears to be a secondary event resulting in the characteristic morphology of both invasive and in situ lobular lesions.

5.2 Introduction

It is known that the progression and clinicopathological outcome of any tumour reflects the molecular events acquired during its development [150]. Accordingly, the morphological and clinical heterogeneity of any tumour including breast carcinoma (BC) is likely to derive from stochastic genetic and epigenetic events resulting in oncogene activation and loss of tumour suppressor gene (TSG) function [29]. However, currently the precise cell lineages involved in the earliest oncogenic events involving progenitor transformation and formation of precursor lesions en route to invasive cancer development is not known. Indeed, the molecular basis of breast tumourigenesis is poorly understood and this is possibly a reflection of a) our inability to study the earliest stages (CCLs, ADH, DCIS and LN) of progression, b) the complexity and heterogeneity of breast tissue and c) the microscopic size and limited extent of the pre-invasive lesions in pathological specimens.

Indeed, besides increasing our understanding of breast tumourigenesis, studying the detailed molecular profiling of early stages of breast cancer could improve on diagnostic decision-making and provide advice on the optimal treatment of these lesions, including identifying targets for the development of selective customised therapies. Consequently, unnecessary side-effects associated with over-treatment could be avoided and health economic cost efficiencies could be achieved through targeted treatment.

Recently, comparative genomic hybridization (CGH) technique has been expanding our knowledge about tumour pathogenesis as it allows for genome wide detection of deletions and gain/amplifications in a single hybridization [151] and for studying the genetic changes of some precursor lesions [58, 89, 112, 113, 152] facilitated by using laser capture microdissection (LCM), and polymerase chain reaction (PCR) amplification [152, 153]. The results have widened and even changed our understanding of human cancer development and progression [152].

For instance, recent molecular studies imply that the low and high grade forms of both invasive breast cancers and ductal carcinoma in situ are distinct entities[154] and that progression from low to high grade is rare [26, 52, 58, 61, 81]. Moreover, some CGH [26, 52, 58, 61, 81] and gene expression data [155] show that invasive tubular carcinoma and ADH/low grade DCIS are more closely related to invasive lobular and lobular neoplasia, respectively, than to invasive ductal carcinoma and high grade DCIS, respectively [154]. For instance, high grade DCIS and high grade BCs are genetically advanced lesions, showing a complex recurrent genomic rearrangements including loss of 8p, 11q, 13q, 14q; gain of 1q, 5p, 8q, 17q; and amplifications on 6q22, 8q22, 11q13, 17q12, 17q22–24, and 20q13, while most of low/intermediate grade DCIS and BC showed an increased frequency of losses of 16q and 1q [26, 52, 58, 61, 81].

As have been shown in Chapters 2 and 3, we found that the columnar cell lesions (CCLs), flat epithelial atypia (FEA), lobular neoplasia (LN), atypical ductal hyperplasia/low grade ductal carcinoma in situ (ADH/low grade DCIS), invasive tubular carcinoma (TC), tubulolobular carcinoma (TLC) and classic invasive lobular carcinoma (ILC) not only have the same patterns of associated topographic distribution but also have remarkable morphological and immunohistochemical similarity. Subsequently, we have proposed that they may constitute a family of related low nuclear grade precursor, in situ and invasive neoplastic lesions collectively called the "LNGBN".

In this study, by using high resolution aCGH, we aim to identify the molecular genetic profiles of this group of lesions and to recognise the potential evolutionary pathogenetic pathways of LNGBN that support their common cell of origin.

5.3 Material and Methods

Twenty cases of invasive tubular and lobular carcinoma and their matched coexisting CCLs, DCIS and LN were laser microdissected from formalin fixed paraffin embedded tissues (FFPET). The isolated non-amplified-DNAs were subjected to high-resolution array-Comparative Genomic Hybridization (aCGH; 32 Kb BAC-array platforms, Breakthrough Breast Cancer Centre, London), (**Figure 5-1**).

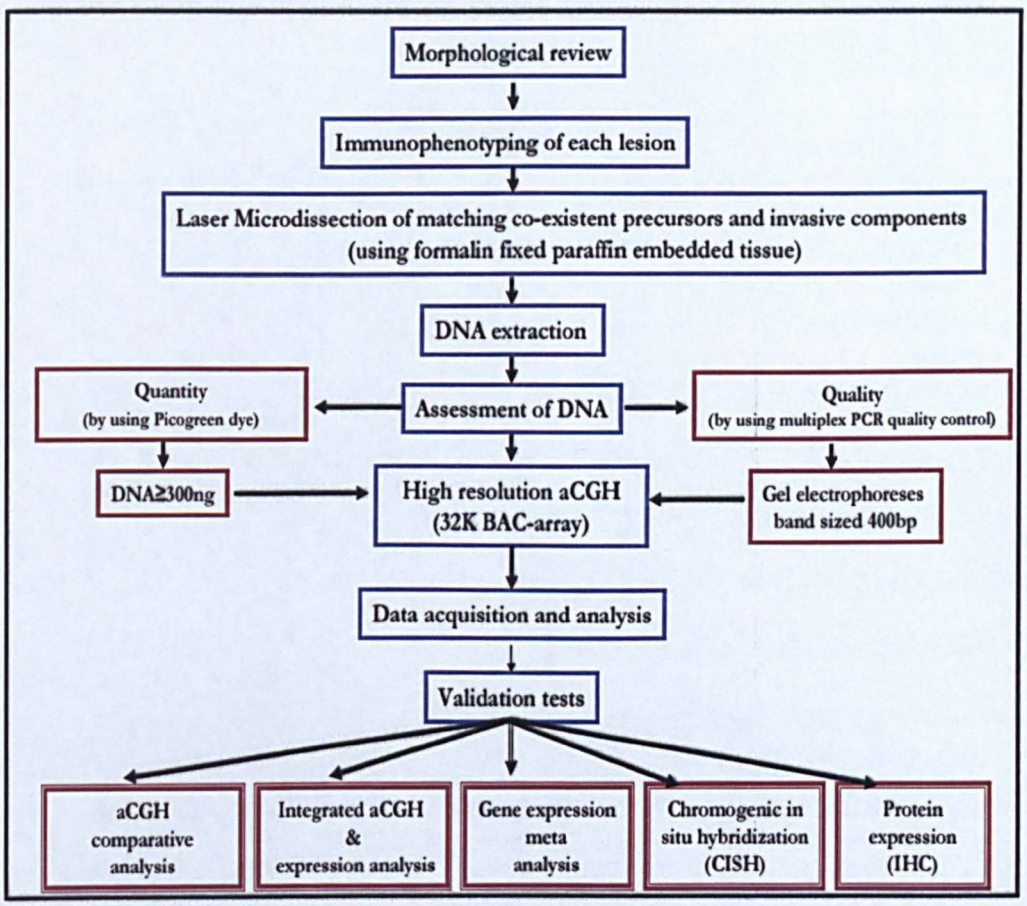

Figure 5-1: An overview of the techniques and methods used for array comparative genomic hybridization (aCGH).

5.3.1 Comparative Genomic Hybridization

Introduction

The principle of CGH is that the tumour (test) and normal (reference) genomic DNAs are labelled respectively with red and green fluorescent dye [156]. Each labelled DNA is subjected to competitive hybridization to either normal metaphase chromosomes (chromosome or M CGH) [156], or DNA fragments (DNA microarray CGH) [157]. DNA fragments which have been spotted onto glass microscope slides using robotic devices may be oligonucleotides (ROMA CGH) [158], complementary DNA (c-DNA array) [159] or genomic clone e.g., bacterial artificial chromosomes (BACs); matrix array CGH [160] **(Figure 5-2 and Table 5-1)**. Hybridization of repetitive sequences is blocked by addition of Cot-1 DNA. The ratio of red and green fluorescent signals in paired samples are measured along the longitudinal axis of each chromosome providing a cytogenetic representation of DNA copy number changes in the tumour compared to normal sample [161]. Chromosomal regions involved in deletion or amplification in test DNA appear red or green, respectively, but chromosomal regions that are equally represented in test and reference DNAs appear yellow i.e., no copy number changes [161] **(Figure 5-3)**. Measurement of ratio of the test to reference is performed using a digital image analysis system. In array CGH the resolution in detecting segmental copy number changes is limited only by the distance between and the size of the genomic DNA segments spotted on the array [161, 162].

Advantages of aCGH

The main advantage of CGH is the whole genome screening which is faster and less laborious than low throughput methods such as (PCR and FISH) [154-162]. Moreover, by using array CGH, the segmental amplification of whole chromosome arms, terminal deletions,

and discrete, high magnitude copy number gains and losses up to 16Kb are easily detected.[158-162]

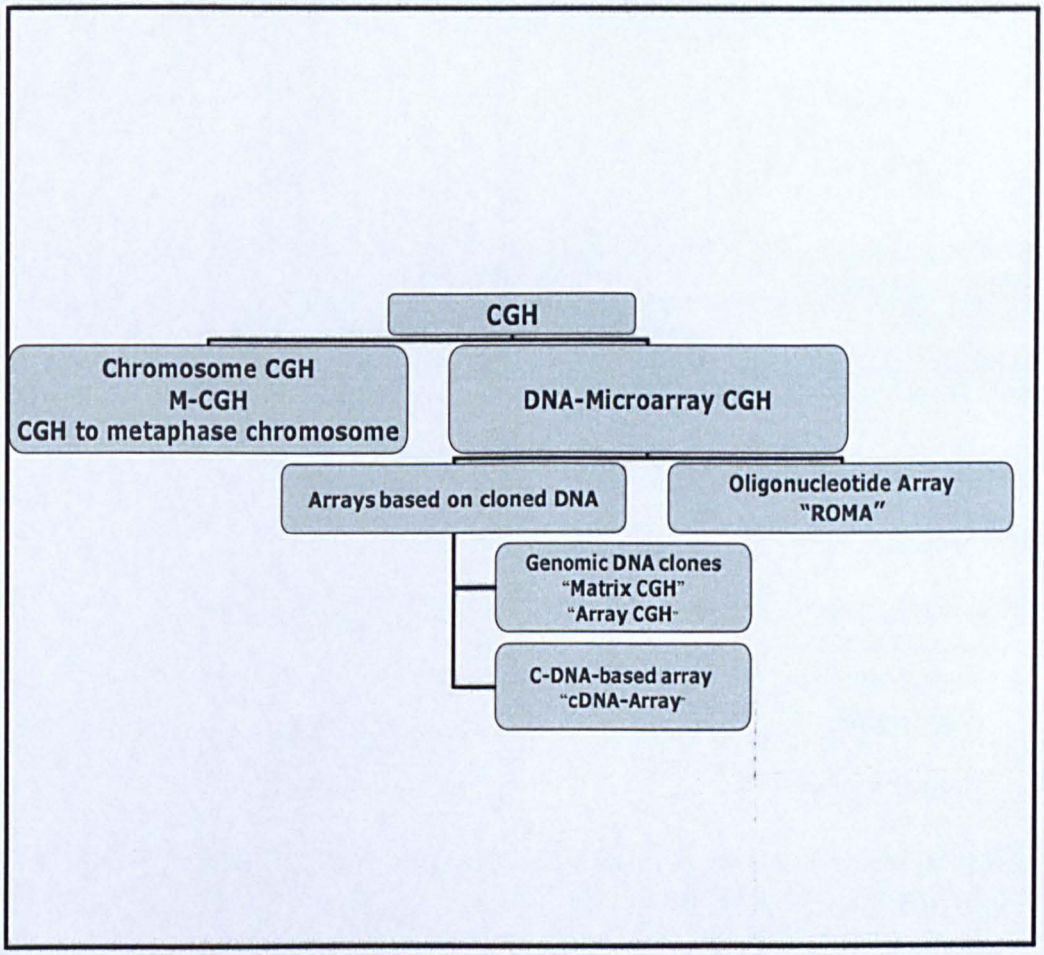

Figure 5-2: Types of comparative genomic hybridization

Table 5-1: Comparison between different types of comparative genomic hybridization (CGH)

Characters	m-CGH	c-DNA CGH	Array-CGH
Targets	Metaphase chromosomes	c-DNA sequences typically only 0.5-2 kb in size	Genomic clones: ▪ YAC (0.2-2 Mb) ▪ BAC(up to 300 Kb) ▪ P1 (~70-100 kb) ▪ PAC (~130-150 kb) ▪ Cosmid (~30-45 kb)
Resolution	10Mb for loss and 2 Mb for gain	High resolution up to 0.5 Kb	High resolution up to 16Kb
Advantages	1- Whole genome screening capability 2- Increasing our understanding of tumour biology and progression.	1- High resolution 2- Straightforward and automated analysis.	As c-DNA CGH plus Uniformity of hybridization Signal fidelity
Limitations	Low resolution and the need for experience in cytogenetic	Low complexity of the target c-DNA sequences leads to High false positive and negative rates (15%) and reduced signal sensitivity	Expensive hardware and soft ware

YAC: yeast artificial chromosome; BAC: bacterial artificial chromosome: PAC: plasmid artificial chromosome

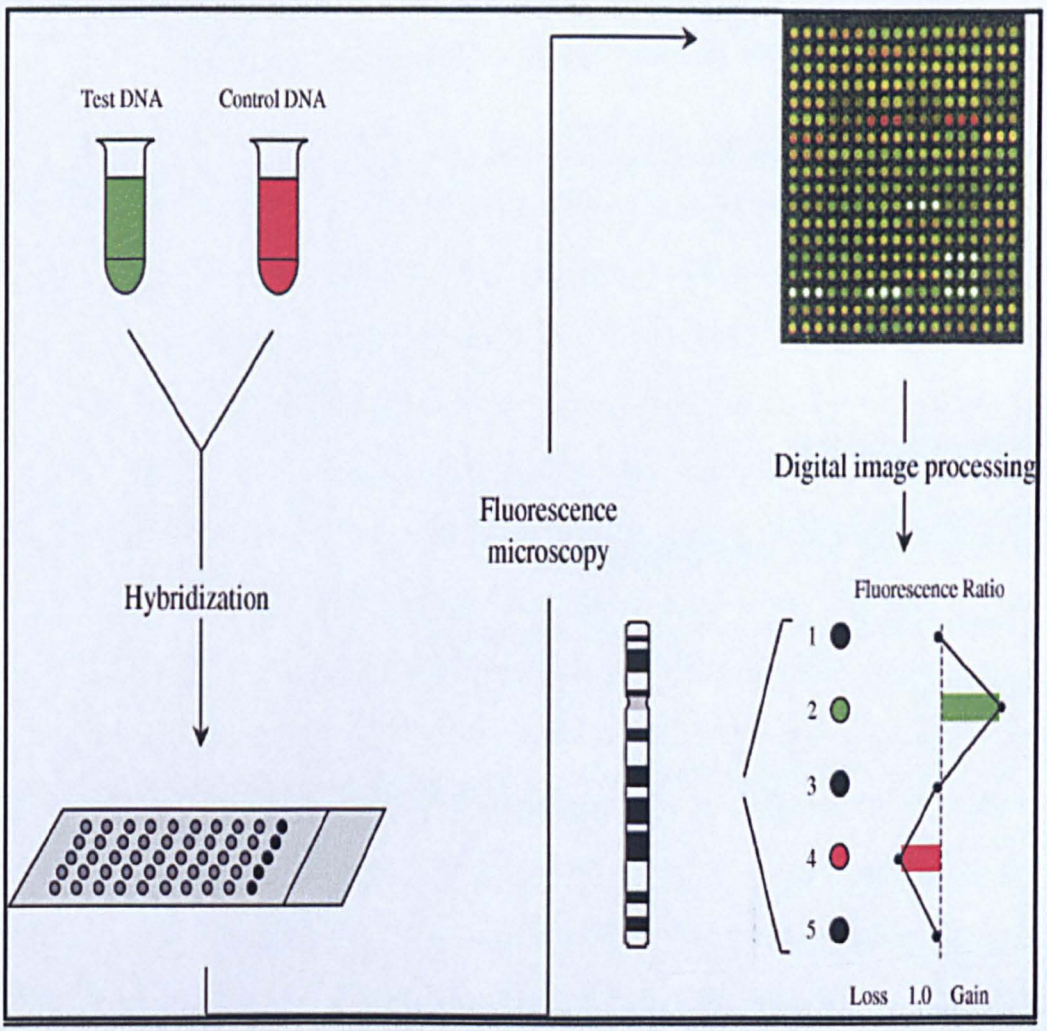

Figure 5-3: Schematic overview of the microarray-based comparative genomic hybridization technique.

Test and control DNA are labelled with a green and red fluorochrome, respectively. Both DNAs are hybridized to cloned DNA fragments that have been spotted in triplicate on a glass slide (the array). Images of the fluorescent signals are captured and analyzed. Red spots indicate loss of test DNA, green spots indicate gain of test DNA, and yellow spots indicate the presence of equal amounts of test and control DNA (Adapted from Oostlander et al 2004 [162])_

Limitations of aCGH

One of the main limitations of the BAC array CGH is that regions not represented on an array are not assayed [162-164]. Subsequently, smaller or larger deletions or duplications will not be identified because this tool only interrogates gains and losses of chromatin approximating the size of a BAC clone (16 to 200 kb). Moreover, epigenetic changes, balanced chromosomal rearrangements translocation (reciprocal translocations, Robertsonian translocations, and inversions), mitochondrial DNA defects, point mutation, origin of translocation events or complex chromosomal rearrangements can not be detected by using CGH technique [156-164] . Moreover, additional validation tests of the results either by using gene expression array, fluorescent in situ hybridization (FISH), chromogenic in situ hybridization (CISH) or immunohistochemistry (IHC) are required to pinpoint the genes involved [154-164]. Other molecular techniques such as spectral karyotyping (SKY) or muti-colour chromosome painting strategies could be used in conjunction to aCGH to detect reciprocal translocation or subtle rearrangements [162-165]. However, even with these recognized constraints, array CGH has the potential to identify twice as many chromosome abnormalities as other techniques [165].

Challenges facing our aCGH experiment for analysis of LNGBN family

TISSUE MATERIAL

The successful rate of aCGH using high molecular weight DNA samples i.e., frozen or cell line is high in most cases [157-165]. However, for the purpose of our study, we could not use DNA derived from either frozen breast cancer tissue or cell lines for many reasons. First, there is no cell lines derived from columnar cell lesion or low grade neoplastic lesions such as tubular carcinoma. Second, laser microdissection of frozen section is very difficult technically as we should work very quickly against very poor visualization which will lead to inevitable errors, inaccuracy and impurity of the highly selected target lesions. Last but not

least, most of our lesions are minute in size and no frozen materials were available for most of them. Subsequently, using DNA derived from formalin fixed paraffin embedded tissue (FFPET) was inevitable. In fact, the successful rate of getting informative aCGH results from FFPET is very challenging and it is mainly due to a) fragmentation of DNA (quality of DNA), b) presence of formaldehyde cross-links of DNA and c) the relative large amount of DNA that is required (500ng-2ug quantity) [166, 167].

However, applying aCGH using DNA derived from FFPET has many advantages especially for the purpose of our study 1) DNA is stable for many years, 2) it allows us to use the huge clinicopathological and clinical data available, 3) it allows us to compare the genetic changes of the different matching lesions with different histological and phenotypic characteristics, 4) a successful aCGH requires chopped DNA rather than intact DNA, and 5) FFPET- sections are compatible and easy to use with laser microdissection with high resolution of the histological details of different lesions[14-15]. Moreover, recently a few number of studies succeeded to apply CGH on tissue derived from FFPET and their results were encouraging [154, 166, 168-170].

QUALITY OF DNA

As aforementioned, one of the major limitations of getting informative aCGH results from FFPET is the quality of DNA. Because aCGH experiments are very tedious and expensive, using unsuitable DNA is a big problem as some tumours may have too degraded DNA that is unsuited for aCGH analysis even with repeating the experiment using fresh sections [154, 166-170]. The integrity of DNA depends on several factors: a) sample type, b) sample age, c) storage conditions, d) handling methods, e) fixation conditions (timing of the fixation, fixation materials, and the duration of the fixation) and f) DNA isolation methods [154, 166-170]. In fact, some cases may have degraded DNA more than others due to unknown causes [166]. Subsequently, scanning the FFPET archival blocks to identify which blocks

contain high quality DNA that is suitable for aCGH is essential [166]. For that reason, we adopted the recent published multiplex PCR quality control protocol [166] for scanning more than 75 cases of low grade breast carcinoma. In addition the quality and size of the isolated DNA samples were evaluated by using 1% gel electrophoreses and NanoDrop spectrophometer (NanoDrop Technologies, Wilmington, USA) [170].

QUANTITY OF DNA

The amount of extracted DNA was measured using a NanoDrop spectrophometer however, we and others [167] found that using the NanoDrop spectrophometer to measure the very tiny amount of DNA isolated from FFPET is not suitable as the NanoDrop spectrophometer reading is up to 10-times higher than using a double stranded DNA (dsDNA) binding dye e.g. picogreen. The explanation for this difference is the NanoDrop spectrophometer detects both single-stranded and double stranded DNA and most of our DNAs isolated from FFPE samples were denatured and single-stranded. As aCGH require dsDNA, we used picogreen dye to quantify our DNA samples [167].

Because our target lesions are very small and the thickness of FFPET is small too, normally 5-10 microns thick, the amount of DNA retrieved is minute. For that reason during the optimization process for our aCGH experiment, different methods of DNA amplification were compared to produce DNA of adequate quantity and quality.

For instance we have used GenomiPhi™ DNA amplification kit (25-6600-01, GE Healthcare, USA), Restriction and Circularization-Aided Rolling Circle Amplification (RCA-RCA) method [171], GenomePlex complete Whole Genome Amplification kit (Sigma WGA2; Sigma-Aldrich, USA) and GenomePlex complete Whole Genome Amplification for single cells (Sigma WGA4; Sigma-Aldrich, USA) according to manufacture's instructions. We did the experiments on 3 microdissected cases with different DNA

template concentrations starting from 5ng, 10, 15, 20, 30, and 50 ng for each method. According to DNA measurements and multiplex PCR quality control we found that the GenomePlex Complete Whole Genome Amplification for single cells (Sigma WGA4) with starting DNA from 20 ng gave the highest DNA yield with DNA fragment ≥300bp. Although we succeeded in performing aCGH experiments using this amplification method, we were not able to get informative results -even after repeating the experiment- due to the presence of high background noise. In addition, to avoid any possibility of biases that could arise from the amplification [165-167] of such low concentration especially for lesions that we expected to have very few genetic changes; we decided to use non-amplified DNA for our aCGH experiments which was laborious.

5.3.2 Methods

Immunohistochemical phenotyping

Four um thick sections of each case were subjected to immunohistochemistry with a panel of antibodies against CK18, CK19, CK8, CK5/6, CK14, EGFR, PR, ER-α, ER-β1, MUC1, Cyclin D1, p53, MDM2, MDM4, SMA, Vimentin, Bcl2, E-Cadherin, and HER-2 as previously described in chapter 3. All markers were scored by two pathologists, blinded to the results of the aCGH, expression array and CISH analysis. Utilising the criteria of Nielsen et al [26] all of our samples had a luminal phenotype.

Laser microdissection

In this study we used a laser microdissection technique to obtain highly pure populations of breast lesion cells from invasive and precursor lesions, devoid of normal epithelial or surrounding stromal cells, which might confound the genetic analysis [153]. We used two systems of laser microdissection. In Histopathology, Queen's Medical Centre, Nottingham, we used a PALM Microbeam Laser Capture Microdissector (PALM AG, Berndried,

Germany; www.palmmicrolaser.com). At the Breakthrough Breast Cancer Research Centre, Institute of Cancer Research, London, the PixCell II Laser Capture Microdissection system (Arcturus Biosciences, Genetic Research Instrumentation Ltd, Braintree, UK) was used [172].

Briefly in both systems, at least 15 consecutive 10 um paraffin embedded tissue full face sections from each cases were a) de-paraffinized twice for 5 min in xylene, b) re-hydrated in 100%, 96% and 70% molecular ethanol for 30 second each, c) incubated overnight in 1M NaSCN at 37°C to remove DNA cross-links, d) rinsed twice 10 min in 1 x PBS at room temperature, e) stained by fresh purified 1% nuclear fast red to identify lesions details and finally h) completely air-dried as previous described [166]. Under direct microscopic visualization, the target neoplastic epithelium cells have been microdissected. For PALM Microbeam laser capture microdissection, sections were directly transferred to ultra-violet (UV)-cross-linked PEN membrane PALM membrane slides. The neoplastic cells under laser pressure were captured (LPC) into collection tubes (PALM) [153]. Using PixCell II Laser Capture Microdissection system, sections were mounted directly on the glass slides and the pulsed low-power IR laser beam was focused producing one of three manual interchangeable predefined laser spot size (7.5, 15 and 30 um) [172]. The special cap (CapSure TM LCM) which is covered by thin thermoplastic film was positioned directly on the tissue. With each pulse of the laser beam, the thermoplastic sheet is melted and the target tissue glues onto the film. The target tissue was separated and capture by lifting the cap from the slide [172]. When completed, the thin film was carefully peeled and transferred into an Eppendorf tube under DNase-free and RNase-free conditions. The estimated purity of captured target cells was 100% for precursor lesions (columnar cell lesions, DCIS and LN) and 95% for invasive TC and ILC. At least 100,000 neoplastic cells (60,000,000 um2) were microdissected per each lesion (**Figures 5-4 and 5-5**).

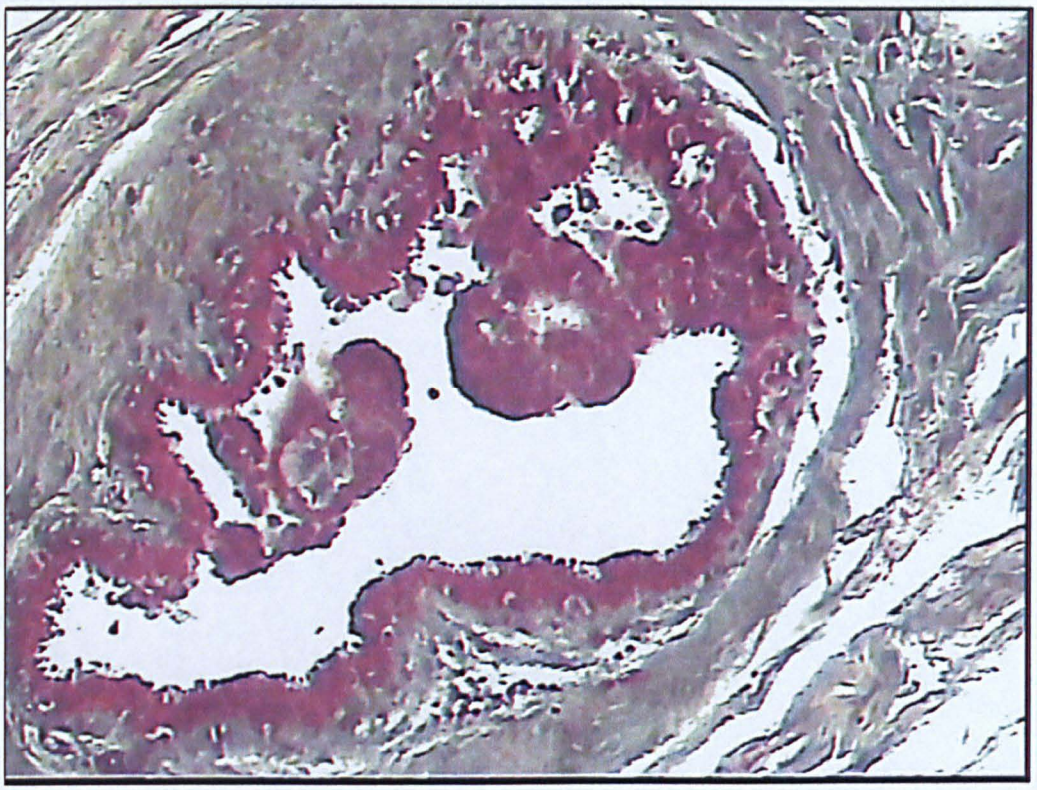

Figure 5-4: Nuclear fast red staining section showed columnar cell lesion before laser microdissection

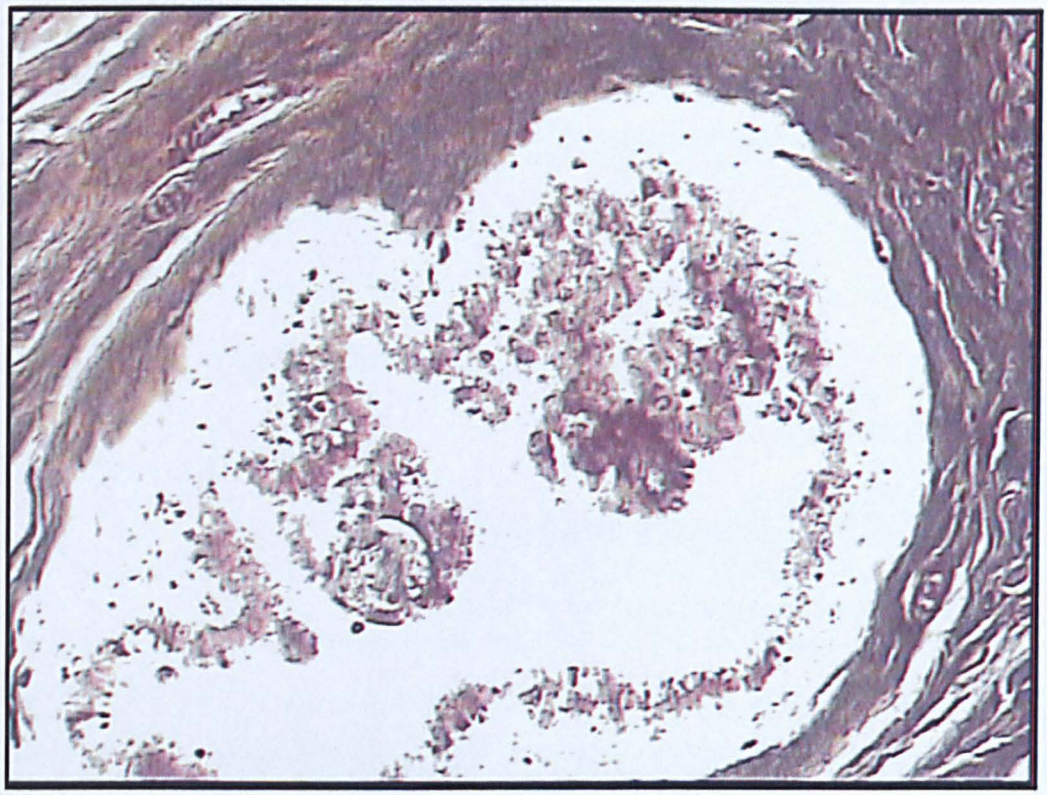

Figure 5-5: Columnar cell lesion after laser microdissection dissection by using PixCell II Laser Capture Microdissection system.

DNA extraction

DNA was extracted using a QIAamp DNA FFPE Tissue Kit (Qiagen, cat. 56404) adapted to LMD samples. After microdissection, the DNA was extracted in 180 ul Qiagen ATL buffer and incubated overnight with 20 ul proteinase-K (20mg/ml stock) by shaking at 450 rpm, at 56°C. Another dose (20 ul) of proteinase-K was added after 18 hours [166]. After total proteinase-K incubation of ~22h or until the sample has been completely lysed, the samples were incubated at 90°C for no more than 1 hour to inactivate the proteinase-K and to reverse the formaldehyde modification of DNA. Then 2 µl of RNase A (100 mg/ml) was added to obtain RNA-free genomic DNA and the samples were incubated for 2 min at room temperature. DNA extraction and purification proceeded according to the manufacturer's instructions (Qiagen, cat. 56404). Subsequently, the DNA yield was

measured with the PicoGreen® assay according to the manufacturer's instructions (Invitrogen, Paisley, UK) and DNA fragment size distribution was assessed by 1% agarose gel electrophoresis. The DNA purity and quality were assessed by NanoDrop spectrophometer (NanoDrop Technologies, Wilmington, USA). High quality pure DNA samples should have an A260/A280 nm ratio of 1.8-2.0 and an A260/A230 nm ratio ≥ 2.0 by NanoDrop spectrophometer [170].

Assessment of DNA quality

DNA integrity which is the cornerstone for successful CGH analysis was tested using a multiplex PCR technique as described by van Beers EH and his colleagues 2006 [166]. Briefly, 100 ng of DNA was analysed in a PCR reaction that was performed with four primer sets. The four primer sets produce 100, 200, 300 and 400 bp non-overlapping fragments of GAPDH gene (chromosome 12) in a master mix reaction (10mM Tris-HCl pH 8.8, 1.5 mM Mgcl2, 75mM, KCl, 0.2mM dNTPs, 1U Taq DNA polymerase; Invitrogen cat. 18038-26). Ten ul of PCR products were assessed on a 1.5% agarose gel. Samples with DNA fragments sized 400 bp were selected for downstream aCGH experiments, catalogued and stored at -80°C (**Figure 5-6**).

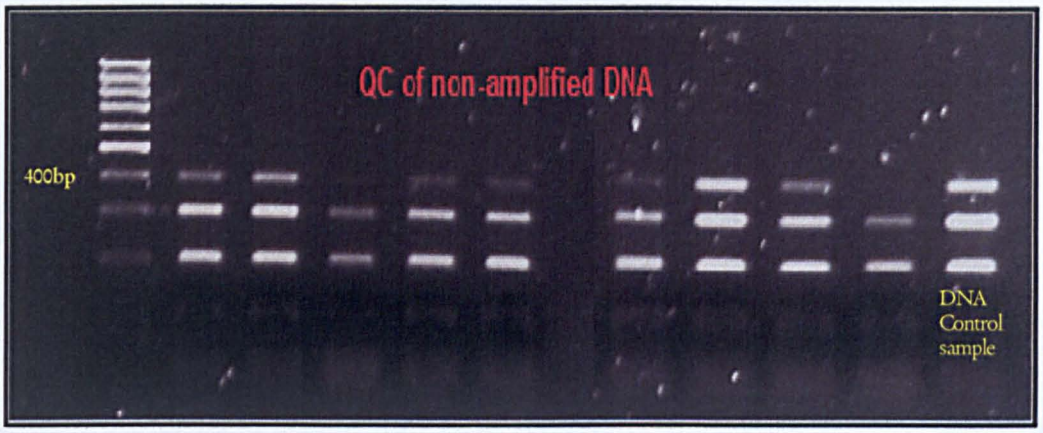

Figure 5-6: Assessment of formal fixed paraffin embedded tissue DNA integrity by multiplex PCR quality control (QC) technique.

This gel electrophoresis shows that DNA products of at least 400bp in size (maximum product size achievable with the chosen primers) was obtained

Microarray-Based Comparative Genomic Hybridization (aCGH)

NUMBER AND TYPES OF LESIONS

Twenty-one lesions were tested 6 tubular carcinoma, 3 invasive lobular carcinoma, 4 ductal carcinoma in situ, 4 lobular neoplasia, 2 flat epithelial atypia, and 2 columnar cell lesion without atypia, out of 42 microdissected lesions yielded DNA of sufficient quantity and quality for aCGH analysis.

CGH PLATFORM

The aCGH platform used for this study was constructed at the Breakthrough Breast Cancer Research Centre and comprises 32 000 BAC clones (CHORI) tiled across the genome and spotted onto Corning GAPSII-coated glass slides (Corning, NY, USA). Previous studies have shown that the robustness and resolution of this type of BAC array platform were comparable with high density oligonucleotide arrays [140, 173]. Moreover the small target size of oligonucleotides reduces effectiveness of oligonucleotide arrays with degraded FFPET-

DNA and increases the susceptibility to cross hybridization with multiple genomic loci leading to poor signalling [174].

NORMAL REFERENCE DNA

Normal DNA extracted from blood lymphocytes pooled from 24 females and scanned for normal variation polymorphism [140].

DNA LABELLING AND ARRAY HYBRIDIZATION

As previously described [138, 140] , by default, Cy3 and Cy5 conjugated dCTP were used to label at least 300 ng of tumour (test) and 300 ng normal female (reference) DNA, respectively (GE Healthcare Life Sciences, Buckinghamshire, United kingdom, cat number PA55321) by using a BioPrime DNA labelling System random primers solution (Invitrogen Life Technology; cat number 18094-011) according to the manufacturer's protocol, modified to incorporate 1.0mM Cy dye, 0.6 Mm dCTP and 1.2 mM dATP, dGTP, and dTTP and subsequently incubated overnight (16-18h) at 37°C. After removal of unincorporated nucleotides by using MinElute Reaction Cleanup (Qiagen, Crawley, United Kingdom; cat number 28004), Cy3-labeled test and Cy5-labeled reference DNAs were mixed together and ethanol precipitated with 100 ug of human Cot-1 DNA (Invitrogen Life Technology, cat number 15279011) and 3 M sodium acetate (pH 7). Then the pellets were re-suspended in 45 ul hybridization buffer (50% deionised formamide, 10% (w/v) dextran sulphate, 2 x SSC, 2% SDS, 20 ug Yeast RNA). The labelled DNA was denatured at 70 °C for 15 min followed by 30 min reannealing at 37°C to allow blocking of repetitive sequences by human Cot-1 DNA. Subsequently, DNA samples were hybridized to high resolution DNA microarray cooperative genomic hybridization slides comprising 32,000 BAC spots for 18 hours at 37°C as previously described [138, 140].

WASH

After hybridization, the cover slips were removed by washing slides in 2× SSC/1% SDS for 15 min at 45°C followed by washing of the slides in 50% deionised formamide 2× SSC for 15 min at 45°C. Finally, washing in 2× SSC/1% SDS for 30 min at 45°C and twice in 0.2 × SSC for 15 min at room temperature was followed. The arrays were dried by centrifugation at 2000 rpm for 2 min.

DATA ACQUISITION

Following hybridization and washes, slides were scanned using a DNA Microarray Axon 4000B Scanner (Axon Instruments, Burlingame, CA, USA) and the Fluorescent images (TIFF images) were processed using GenePix Pro 5.1 image analysis software (Axon Instruments). Per array, a GenePix results file (Microsoft Excel) with the extracted Cy3 and Cy5 spot and background raw intensities was been generated. The karyotype for each lesion was underwent cluster analysis to identify distinct groups and primary data analysis and normalization carried out using Microsoft Excel file.

DATA ANALYSIS

Cases with >10% of clones missing and clones where data were not available in 10% of cases were excluded. The log2 ratios were normalized for spatial and intensity-dependent biases using a two-dimensional local regression followed by a BAC-dependent bias correction as previously described [138, 140]. BAC clone replicate spots were averaged across dye-swap experiments after exclusion of poorly reproducible replicates (SD > 0.2) and excessively flagged clones (>70% of samples). Results were analysed using plots of log2-transformed normalized Cy5:Cy3 intensity ratios against clone position. Polymorphic BACs identified in an analysis of 50 male: female and female: female hybridizations were filtered out. This left a final dataset of 30,606 clones with unambiguous mapping

information according to GENCODE project; Ensembl release 56-Sept 2009 © WTSI / EBI WTSI / EBI of the human genome (http://www.ensembl.org). Each of the 30,606 BACs defines a genomic region starting from the end position of the previous non-overlapping clone on the array to the start position of the next contiguous, non-overlapping array clone. These genomic regions were defined because any deletion or gain/amplification seen for a clone may extend beyond the clone, and thus the extent of change was determined by the next unaffected clone on the array in both directions [59, 138, 140].

Data were smoothed using the circular binary segmentation (cbs) algorithm [175]. A categorical analysis was applied to each clone on the array after classification as gain, loss, or no-change according to their smoothed log2 ratio values. Smoothed log2 ratio values less than - 0.12 were categorized as losses; those greater than 0.12 as gains; and those in between as unchanged. Amplifications were defined as smoothed log2 ratio values greater than 0.45. These threshold values were chosen to correspond to three standard deviations (SD) of the normal ratios obtained from the filtered clones mapping to chromosomes 1-22, assessed in comparisons between DNA extracted from a pool of male and female blood donors as described before.

Data processing and analysis were carried out in R 2.0.1 (http://www.r-project.org/) and BioConductor 1.5 (http://www.bioconductor.org/), using modified versions of the packages aCGH, marray and aws.

Copy number changes were categorized as gains, losses or amplifications according to the aforementioned thresholds for each clone before using Fisher's exact test with adjustment for multiple testing using the step-down permutation procedure maxT providing strong control of the family-wise type I error rate (FWER) [59, 138, 140, 175] to identify statistically significant differences between the genomic profiles of different lesions. A false discovery rate-adjusted $p < 0.05$ was considered significant.

aCGH comparative analysis

Comparative analysis was performed with publicly available aCGH datasets derived from 64 high grade breast cancers cases [140] and 171 unselected series of BC (Gene expression Omnibus (GEO), series accession number GE8757) in which the aCGH results were validated by gene expression [176] **(Table 5-2)**.

HIGH GRADE BREAST CANCER CASES

As previously described [139], sixty-four consecutive grade III invasive ductal carcinomas were retrieved from University Hospital La Paz (UHLP), Madrid, Spain.

Eight-μm thick frozen sections of 64 grade III tumours were microdissected using needle to obtain a percentage of tumour cells in the remaining tissue greater than 90% [138, 140]. DNA was extracted as previously described [138, 140]. RNA was extracted using Trizol according to manufacturers' instructions (Invitrogen, UK) and quantified using the Agilent 2100 Bioanalyzer with RNA Nano LabChip Kits (Agilent Biosystems). The final dataset comprised 48 cases and were subjected to 32K BAC as described before [138, 140].

Gene expression profiling was performed using the Illumina human WG6 version 2 expression array according to the manufacturer's protocol. Briefly 200ng of each RNA sample was amplified using the Illumina Totalprep RNA amplification kit following the manufacturer's instructions (Ambion, UK). Labelled cRNA was subsequently hybridised to Illumina Sentrix-human 6 version 2 expression bead-chips. Full details on RNA amplification and hybridisation can be found at www.illumina.com. Raw gene expression values were robust-spline normalised using the Bioconductor lumi package (http://www.bioconductor.org/packages/2.3/bioc/html/lumi.html) in R. Genes were mapped to their genomic location using the lumiHumanAllv2 annotation database available

from Bioconductor. Only Illumina transcript probes with detection p-values <0.01 in >25% of samples were included; this resulted in a dataset of 12,699 transcriptionally regulated probes with accurate and unequivocal mapping information. Gene-expression data are publicly available at ArrayExpress http://www.ebi.ac.uk/microarray-as/ae/ (accession number: E-TABM-543).

UNSELECTED BREAST CANCER CASES

Primary breast tumour specimens were obtained from the Nottingham Tenovus Primary Breast Cancer Series. DNA was extracted using the Promega DNA Wizard kit (Promega, UK) according to manufacturer's instructions. Labelled DNAs were hybridized to a customized oligonucleotide microarrays containing 30,000 60-mer oligo probes [176], for which 27,801 unique map positions were defined (Human Mar. 2006 assembly (hg18)). The median interval between mapped elements was 39.4 kb, 75% of intervals were less than 104.2 kb and 95% were less than 402 kb. The raw and mode-normalized data for the 171 tumours are available from NCBI's GEO [176] under the series accession number GSE8757.

113 out of the 171 breast tumours were also profiled on Agilent gene expression arrays [176] in which gene-dosage levels to gene expression were evaluated using Wilcox on test to evaluate the significance of the association between copy number and aberrant expression.

Table 5-2: Summery of material and methods used in this study

Experiment		Group (1)	Group (2)	Group (3)
Morphology	Breast lesions	Low nuclear grade invasive carcinoma and matching preinvasive including: tubular carcinoma and invasive lobular carcinoma.	High grade invasive ductal carcinoma no special type	Unselected series of invasive carcinoma
Array CGH	No. of invasive cases	20	64	171
	Type of fixation	Formalin Fixed Paraffin Embedded	Frozen	Frozen
	Type of dissection	Laser microdissection	Needle micro-dissection	Full section
	DNA	Non-amplified	Amplified	Non-amplified
	Resolution	32Kb	32Kb	<100Kb
	Platform	BAC aCGH platform	BAC aCGH	Oligonucleotide
Gene expression	no of case	NA	48 cases	113 cases
	Platform	NA	Illumina human WG6 version 2	Agilent gene
Immunohistochemistry (IHC)	No. of cases	145	NA	1081
	Type of tissue	Full face and TMA	NA	TMA
Clinical follow		NA	NA	Yes

Validation tests for MDM4 as a target oncogene in breast cancer

As we have shown in Chapter 2, more than 97% of low grade breast cancer had wild type p53 suggesting that the p53 pathway is inactivated by alterations other than mutation of TP53 itself [102, 177-180]. Among these, alterations of MDM4 overexpression/amplification were found. MDM4 binds to p53 and thereby inactivates the function of p53 as a transcriptional activator of other genes[181]. Mice knockout studies suggest that MDM4 has been shown to negatively regulate the p53 pathway[181]. More recently, Danovi et al[182] found that MDM4 was amplified in 5% of human primary breast cancers, all of which retained wild-type p53. Moreover, MDM4 was also amplified in MCF-7, an ER+ breast cancer cell line harbouring wild-type p53[181]. In addition, artificial overexpression of MDM4 led to immortalization of primary mouse embryonic fibroblast and neoplastic transformation[182]

The human MDM4 gene has been mapped to chromosome 1q32 region which is frequently amplified in low grade breast cancers. Recent studies have proposed that MDM4 is one of the target amplified genes on 1q32 in up to 65% of malignant gliomas and urinary bladder carcinoma, detected by aCGH[183]. Subsequently, we hypothesised that it may be a candidate oncogene in BC and we tested this hypothesis at several levels.

INTEGRATED ARRAY CGH AND EXPRESSION ANALYSIS

To determine whether MDM4 gene copy numbers correlated with MDM4 mRNA expression levels, cbs-smoothed aCGH data were used to assign the median aCGH states for MDM4 using the median values for all BACs which overlap with the genomic position of MDM4. This resulted in a 1:1 matrix of expression data and aCGH values used in correlations. Pearson correlations were performed between mRNA expression log intensity values and median cbs-smoothed ratios derived from aCGH analysis for each gene. P values for each test were adjusted with Benjamini and Hochberg multiple P-value adjustment [175].

To determine whether MDM4 is consistently overexpressed when amplified, a Mann Whitney U test was performed and adjusted with Benjamini and Hochberg multiple P-value adjustment. An adjusted p value of <0.05 was considered significant.

MDM4 PROTEIN EXPRESSION USING IMMUNOHISTOCHEMISTRY

Immunohistochemistry for MDM4 (affinity purified rabbit anti-HdmX/MDM4 clone, IHC-00108, 1:250, Bethyl Labs)[183] was performed on 20 full face section of LNGBC cases and 2 sets of TMAs as described before in Chapter 3. The first TMA set include 140 cases of low nuclear grade breast carcinoma and their matched co-existing precursor lesions as described in Chapter 2. The second data set included a series of primary operable invasive BC derived from the Nottingham Tenovus (Nottingham/Tenovus) Primary Breast Carcinoma Series of women age ≤ 70 years, Nottingham City Hospital (1989-1999). Out of 1,200 tumours consecutively accrued, 1,081 cases were included in this study based on the following inclusion criteria i) complete clinical and therapeutic data available and ii) successful staining for MDM4. The clinicopathological characteristics and survival data of this cohort were previously described in Chapter 3. Median follow up was 111 months (range 1 to 233).

Positive control and negative controls (omission of the primary antibody and IgG-matched immune serum) were included in each slide run. MDM4 immunohistochemical intensity and percentage of positive cells were scored by two pathologists. Only nuclear staining was considered specific[183]. The analysis was performed blinded to the results of the patients' outcome. Statistical analysis was described in chapter 3.

Validation tests for Cyclin D1 (*CCDN1*)

IMMUNOHISTOCHEMISTRY FOR PROTEIN EXPRESSION

Immunohistochemistry for cyclin D1 (SP4, 1:50, Neomarkers, UK) was performed as previously described in chapter 2. Cyclin D1 immunohistochemical intensity and distribution were semi quantitatively scored by two pathologists as described in chapter 2. Only nuclear staining was considered specific. The analysis was performed blinded to the results of the aCGH and CISH results.

CHROMOGENIC IN SITU HYBRIDISATION

As previously described [138, 140], CISH for *CCND1* was performed using the ready-to-use digoxigenin-labelled SpotLight cyclin D1 amplification probe (Zymed, South San Francisco, CA). Heat pre-treatment of deparaffinised sections consisted of incubation for 15 min at 98°C in CISH pre-treatment buffer (SPOT-light tissue pre-treatment kit, Zymed) and digested with pepsin for 7 min at room temperature according to the manufacturer's instructions. An appropriate *CCND1* gene-amplified breast tumour control was included in the slide run. CISH experiments were analysed by two pathologists. Only unequivocal signals were counted. Signals were evaluated at 400 and 630 magnification and 60 morphologically unequivocal neoplastic cells were counted for the presence of the gene probe signals. Amplification was defined as >5 signals per nucleus in more than 50% of cancer cells, or when large gene copy clusters were seen [138, 140]. The scoring was evaluated with observers blinded to the results of the aCGH and immunohistochemical analysis.

Published copy number and gene expression data bases

We have accessed and mined the following database:

- http://projects.tcag.ca/variation/ (for copy number polymorphism)

- http://www.ensembl.org (for location of genes)
- http://www.Oncomine.org (for Meta-analysis of publicly available gene expression data)

5.4 Results

21 lesions belonging to 10 cases were successfully analyzed for copy number changes by using aCGH.

5.4.1 Analysis of case 1 (invasive lobular carcinoma)

Morphology

Haematoxylin and eosin staining of full face sections showed columnar cell changes, flat epithelial atypia (**Figure 5-7**), low/intermediate grade ductal carcinoma in situ [micropapillary (**Figures 5-8 and 5-9**) and cribriform pattern], duct spaces lined by columnar cells showing nuclear atypia and apical snout with intraductal islands of paler cells of lobular neoplasia morphology, ducts spaces an admixture of DCIS with islands of lobular neoplasia (**Figures 5-10 and 5-11**); intimately admixed DCIS and LCIS, expanded lobules showing features typical of lobular carcinoma in situ (**figures 5-12 and 5-13**) and tiny focus of invasive classic lobular carcinoma (**Figure 5-14**). These lesions had the same topographic distribution and cytoplasmic and nuclear features.

Immunohistochemical profile

The aforementioned lesions showed strong positive staining for CK18+, CK19+, CK8+, ER+ (**Figures 5-15 and 5-16**), PR+, Bcl2+ (**Figures 5-17, 5-18, 5-19 and 5-20**) , cyclin D1+, MUC-1+ and negative expression for p53, CK5/6, and CK14 with no HER-2 over-expression. E-Cadherin immunohistochemistry staining showed strong membrane positive reactivity in the CCLs, FEA and DCIS component and negativity in both ILC focus and LCIS component in the pure and admixed areas.

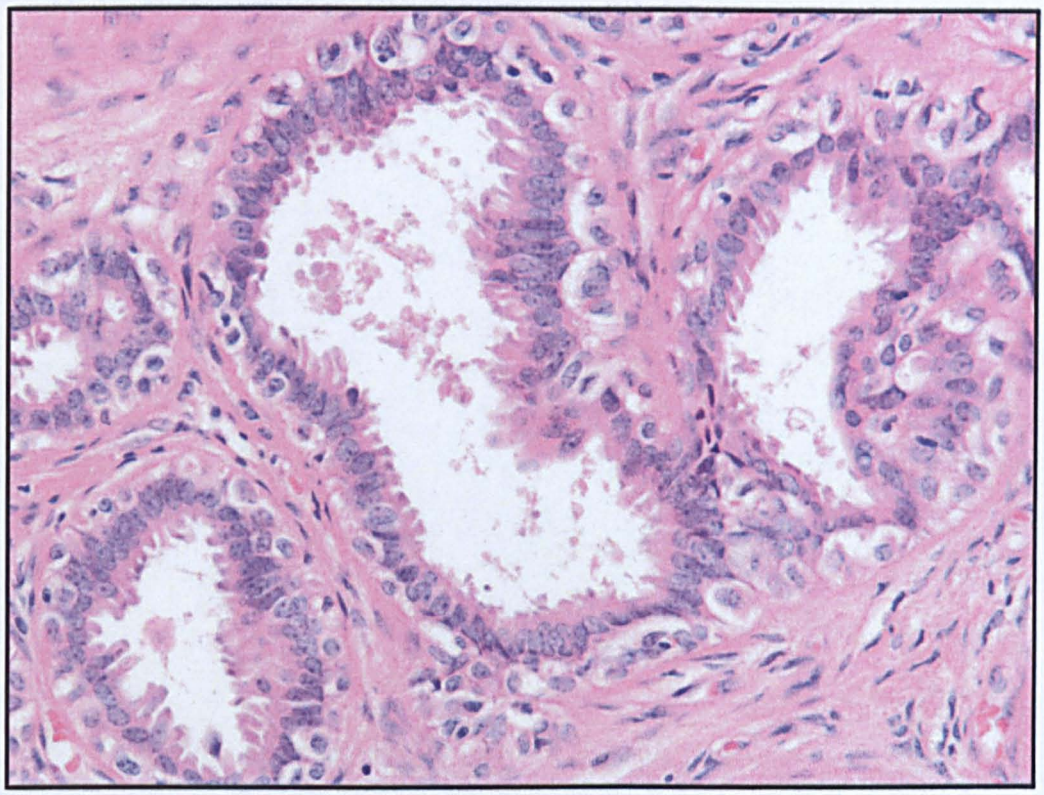

Figure 5-7: Columnar cell lesion from case 1 (H & E)

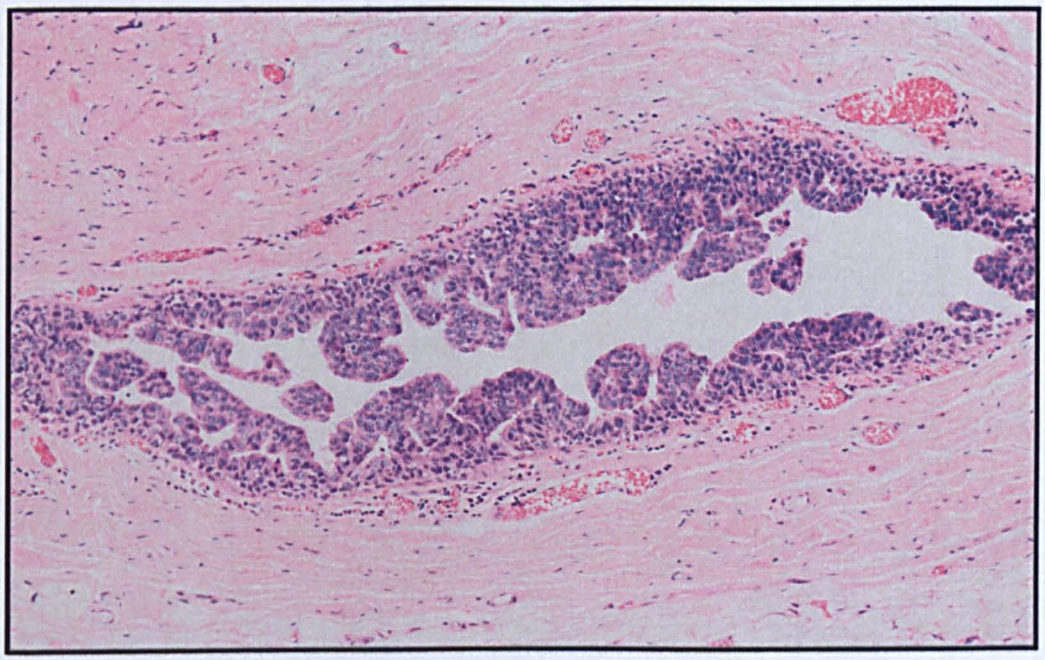

Figure 5-8: Ductal carcinoma in situ from case 1 (H&E)

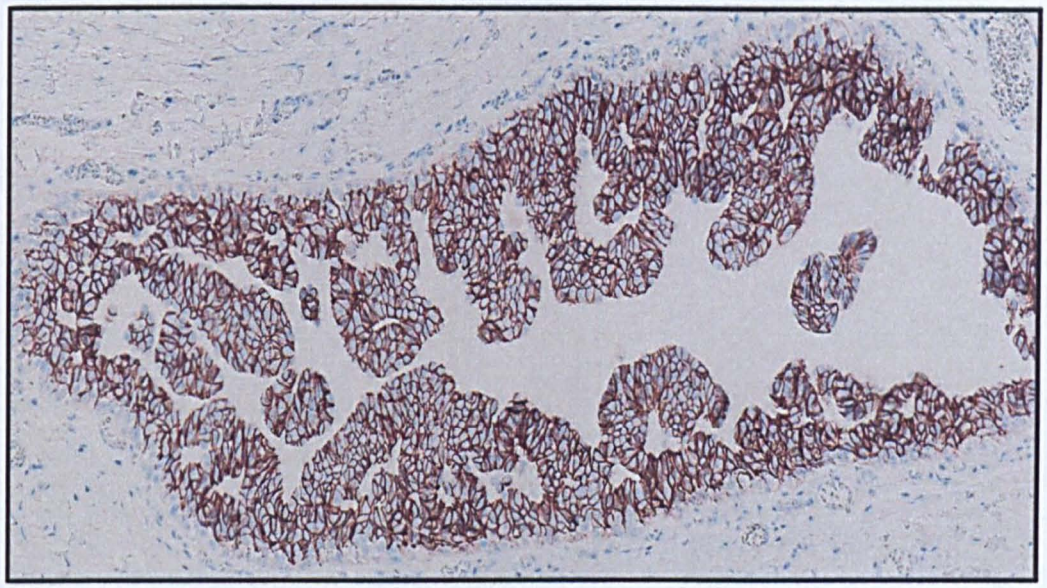

Figure 5-9: Ductal carcinoma in situ showing positive expression of E-cadherin

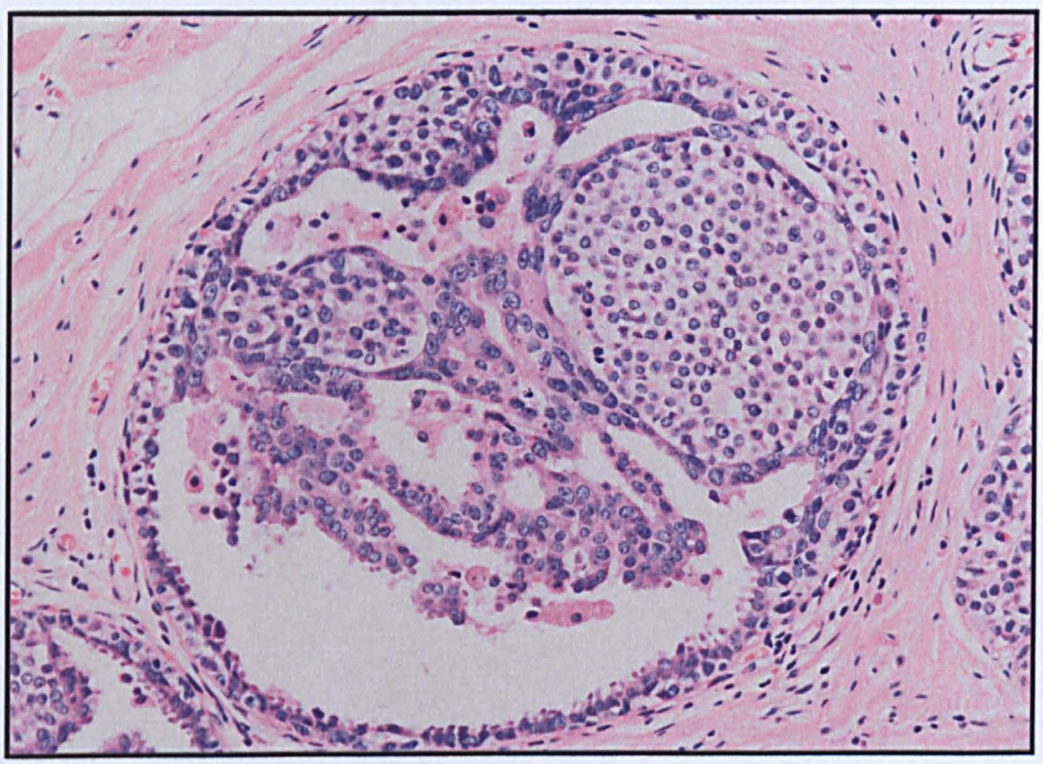

Figure 5-10: Duct spaces lined by columnar cells showing nuclear atypia and apical snout with intraductal islands of paler cells of lobular neoplasia morphology

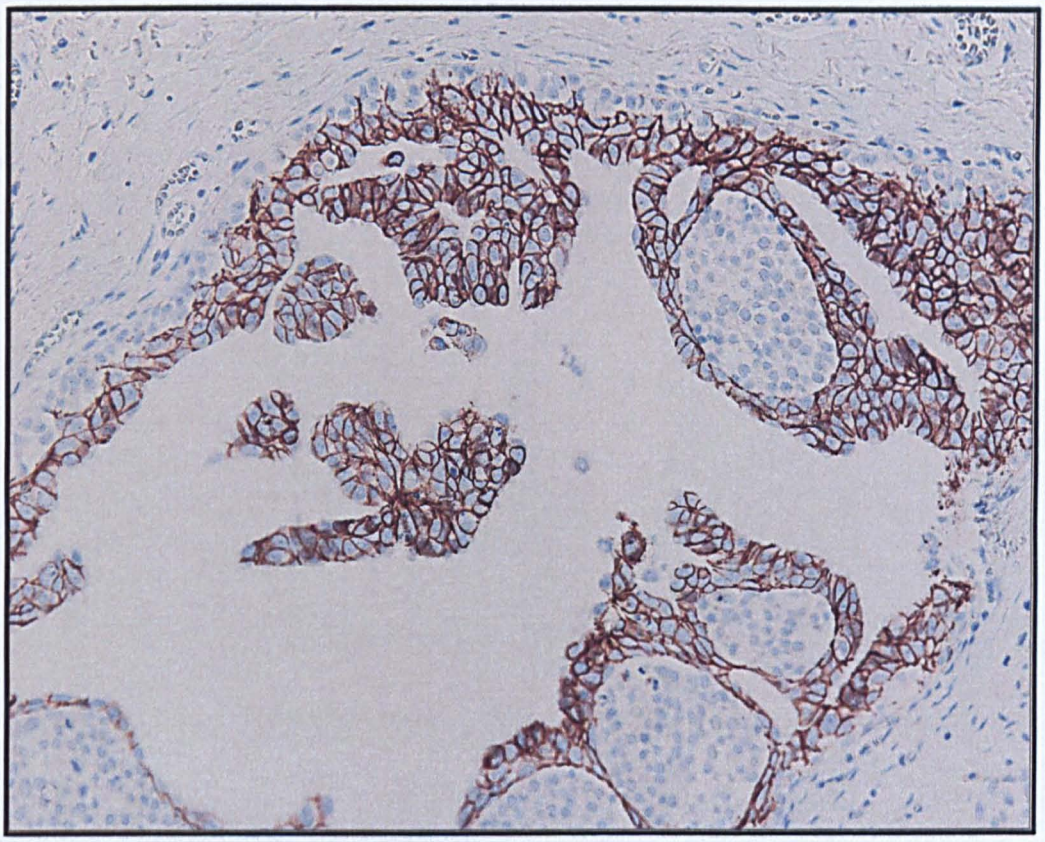

Figure 5-11: A duct spaces an admixture of DCIS (E-Cadherin positive) with islands of E-cadherin negative lobular neoplasia (intimately admixed DCIS and LCIS).

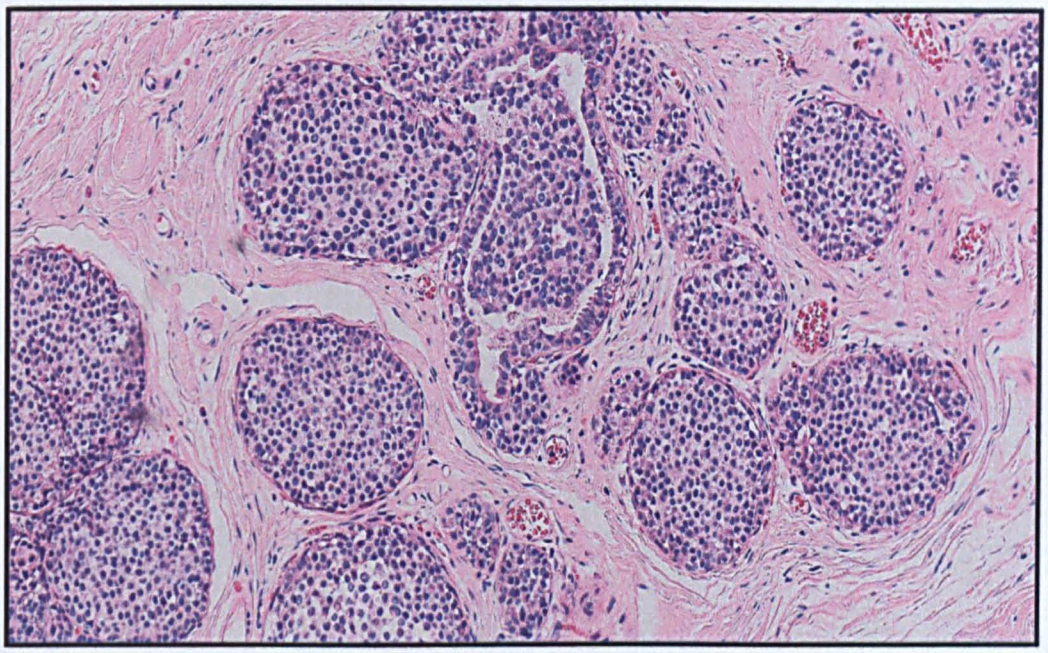

Figure 5-12: Expanded lobules showing features typical of lobular carcinoma in situ (H&E)

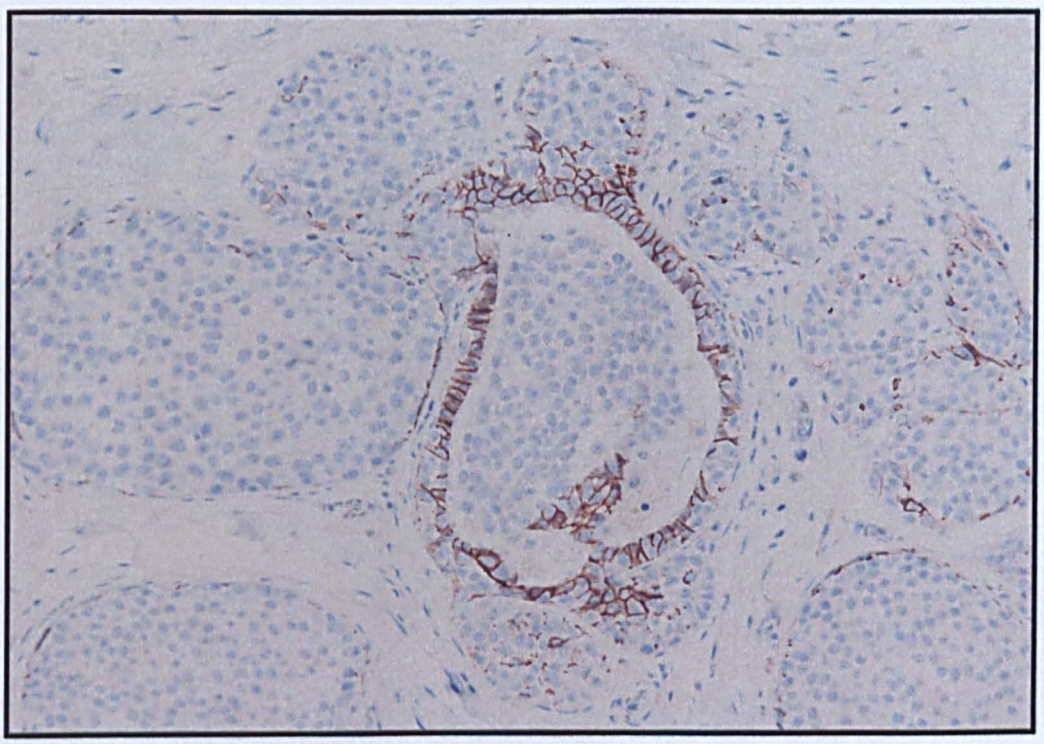

Figure 5-13: Lobular carcinoma in situ showing negative expression of E-cadherin

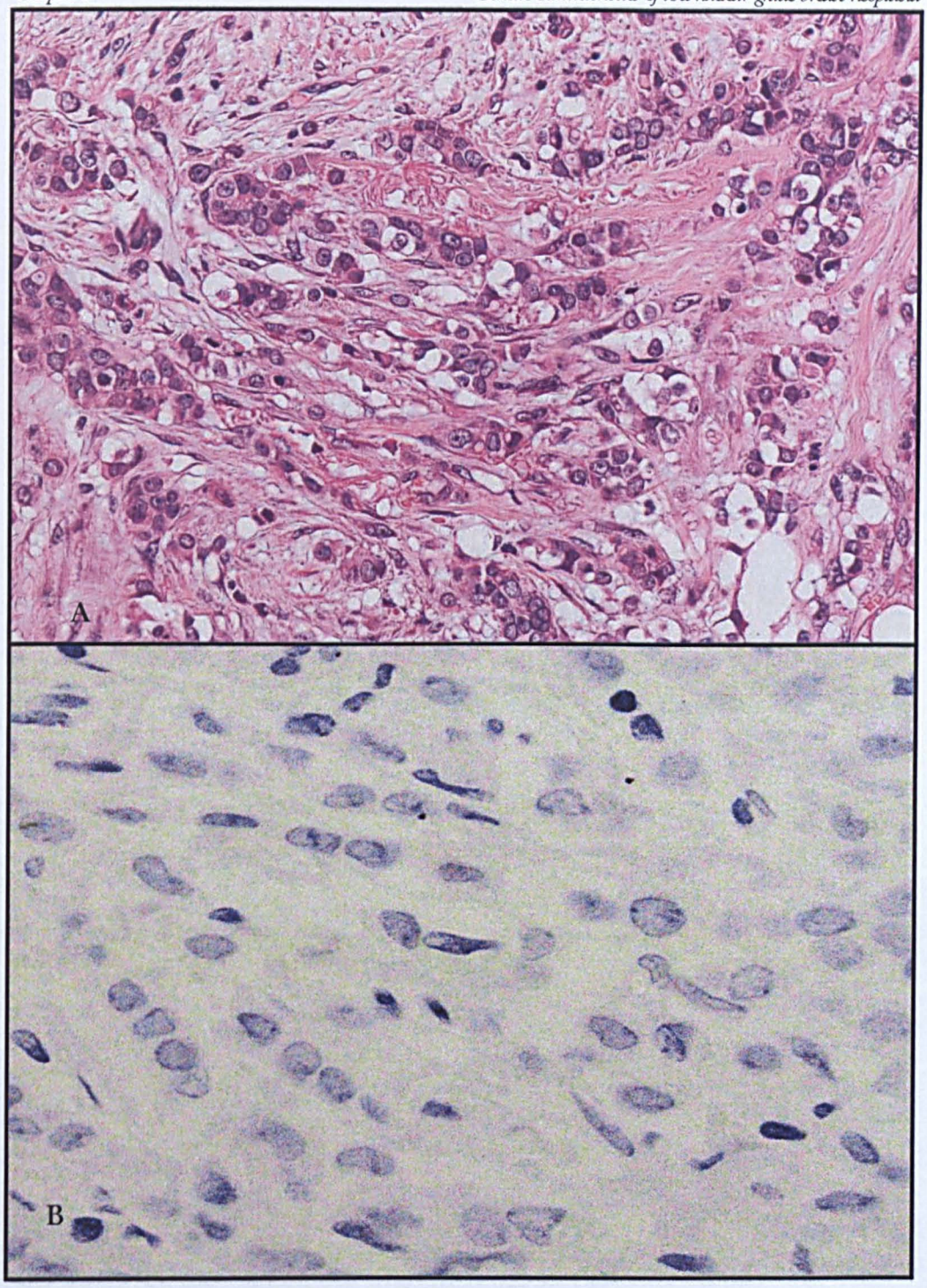

Figure 5-14: A: H&E section showing classic cord like structure of invasive lobular carcinoma (ILC). B: ILC showing negative E-cadherin expression

Figure 5-15: Columnar cell change lesions showing positive expression of oestrogen receptor nuclear staining

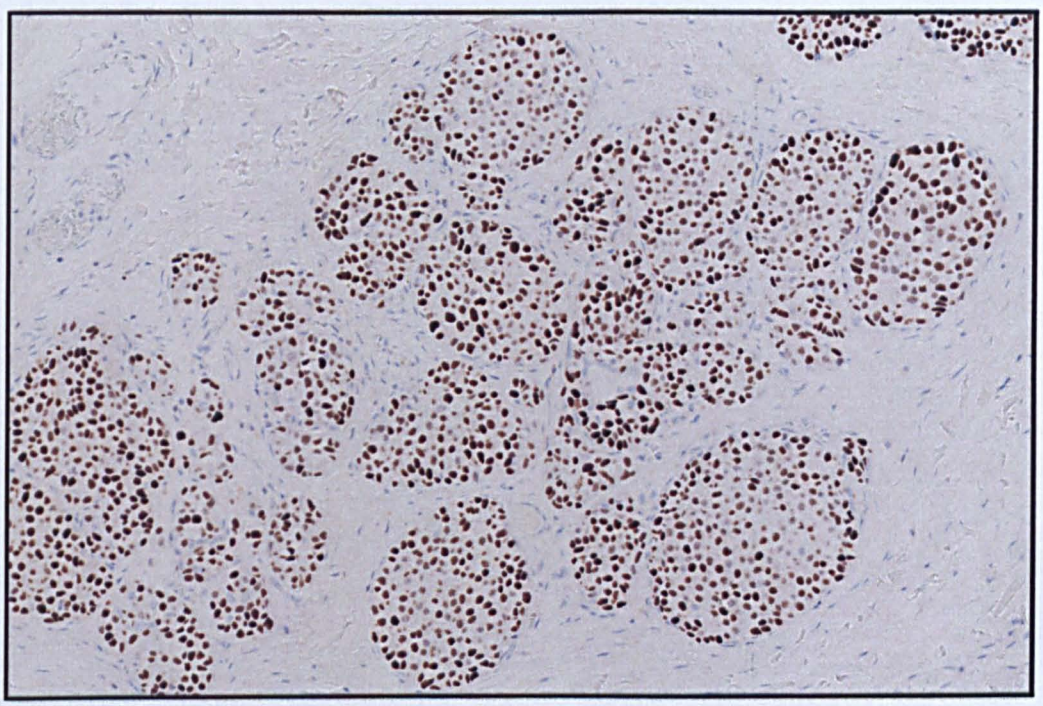

Figure 5-16: Lobular neoplasia lesions showing positive expression of oestrogen receptor nuclear staining

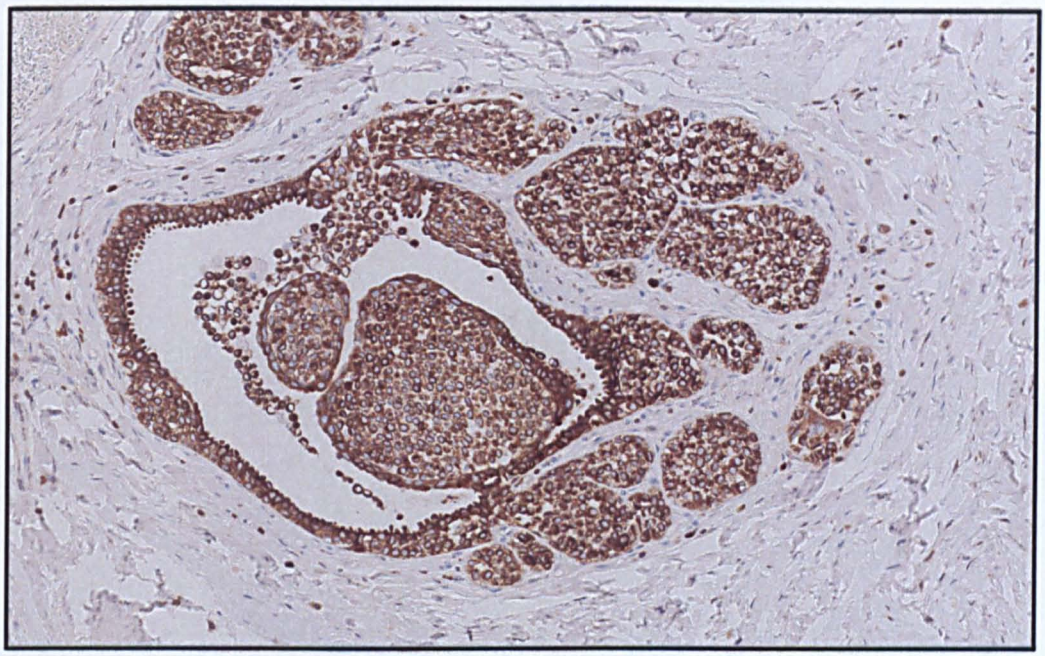

Figure 5-17: Lobular neoplasia showing strong positive cytoplasmic positive expression of Bcl2.

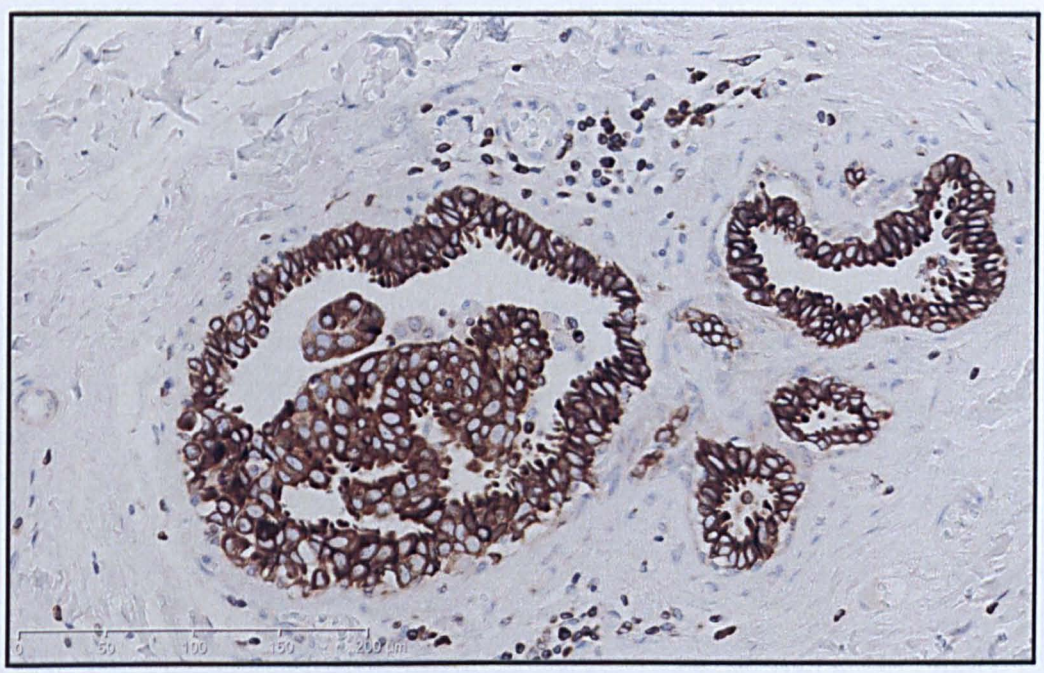

Figure 5-18: Columnar cell lesions showing strong positive cytoplasmic expression of Bcl2

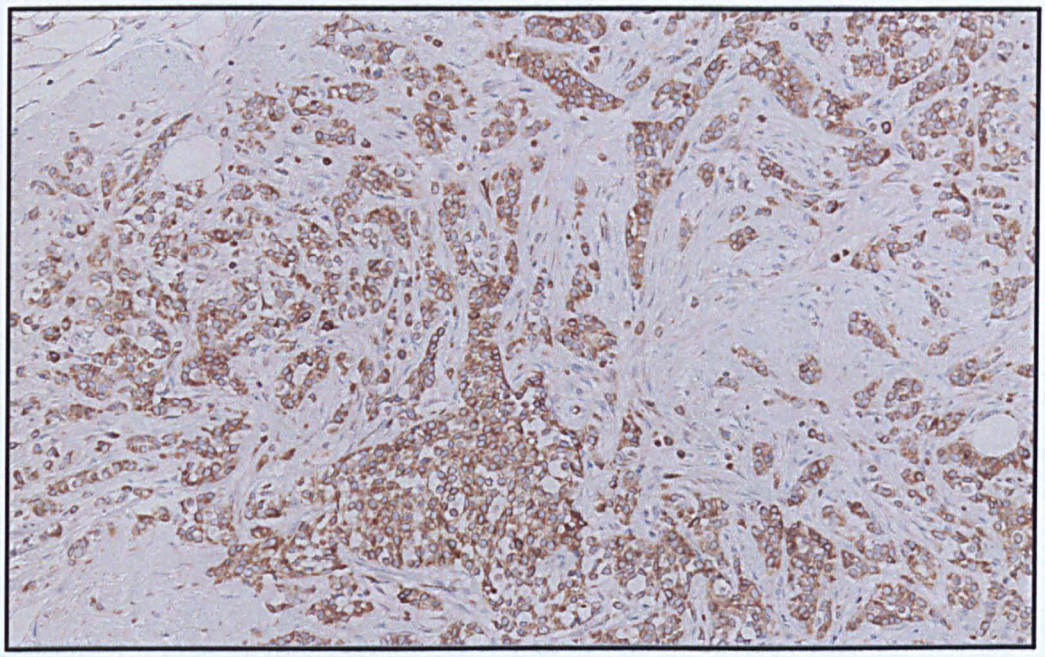

Figure 5-19: Invasive lobular carcinoma showing positive Bcl2 expression

Figure 5-20: Columnar cell lesions showing positive Bcl2.

Genome profiles

Four components were separately laser microdissected including FEA, DCIS, LN and ILC; however, the microdissected ILC did not yield DNA of sufficient quantity for aCGH.

According to the genomic patterns described by Hicks et al [55], all lesions were of simplex pattern, characterized by broad segments of duplications and deletions comprising part or entire chromosome arms (1q+, 11q22- and 16q-) with occasional amplifications. A comparison between distinct morphological components of case 1 (FEA, DCIS and LN) in a pairwise fashion revealed that they shared strikingly similar genomic profiles (**Figures 5-21, 5-22 and 5-23 and Table 5-3**). Pearson's correlation performed with normalized Log2 ratios showed the following corrections: FEA vs. DCIS: r=0.647; FEA vs. LN, :r=0.434 and DCIS vs. LN: r=0.802. The common genetic changes among FEA, DCIS and LN were gains of 1p36.31, 1q21.1-44 (1q+), 3p21.31-p21.1, 5q35.2-35.3, 11q13.3-11q13.4, 15q11.2, 18q21.1 and 19p13.2 and losses of 1p34.3, 11q22.3 and 16p11.2-q24.3 (16q-). Amplifications of 11q13.3-11q13.4 (*CCND1*) and 19p13.2 (*ADAMS10*) were common between DCIS and LN. LN showed additional amplification at 11p15.1 and 11q13.1-11q13.3 while DCIS showed exclusive amplification at 8q22.1.

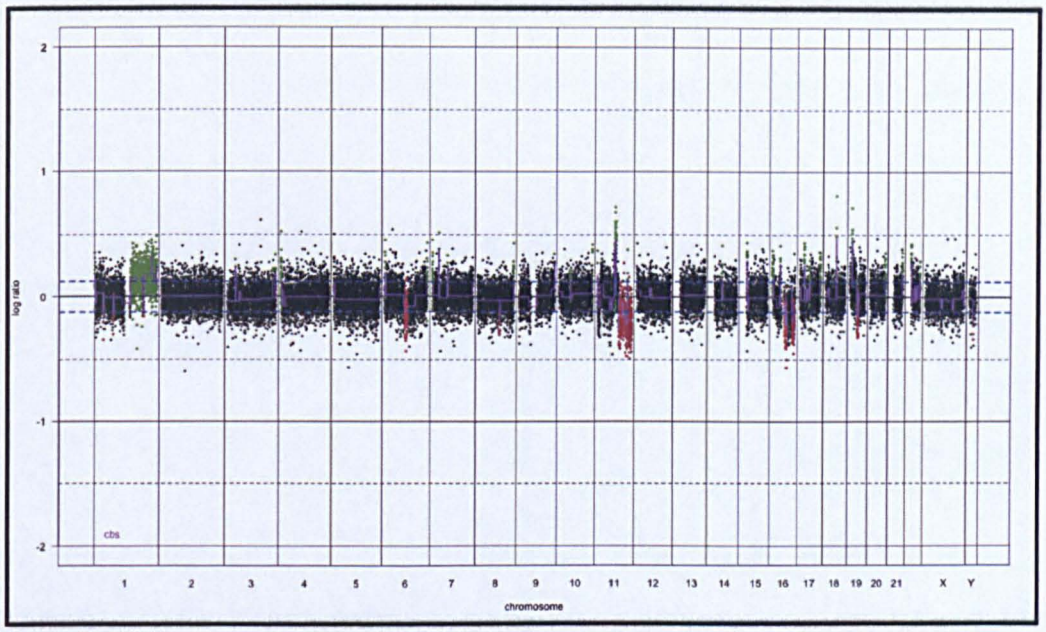

Figure 5-21: Genome plot of flat epithelial atypia which has been dissected from case 1 showing gain of 1q, 11q, 18q and 19p,and loss of 11q, 16q and 19q

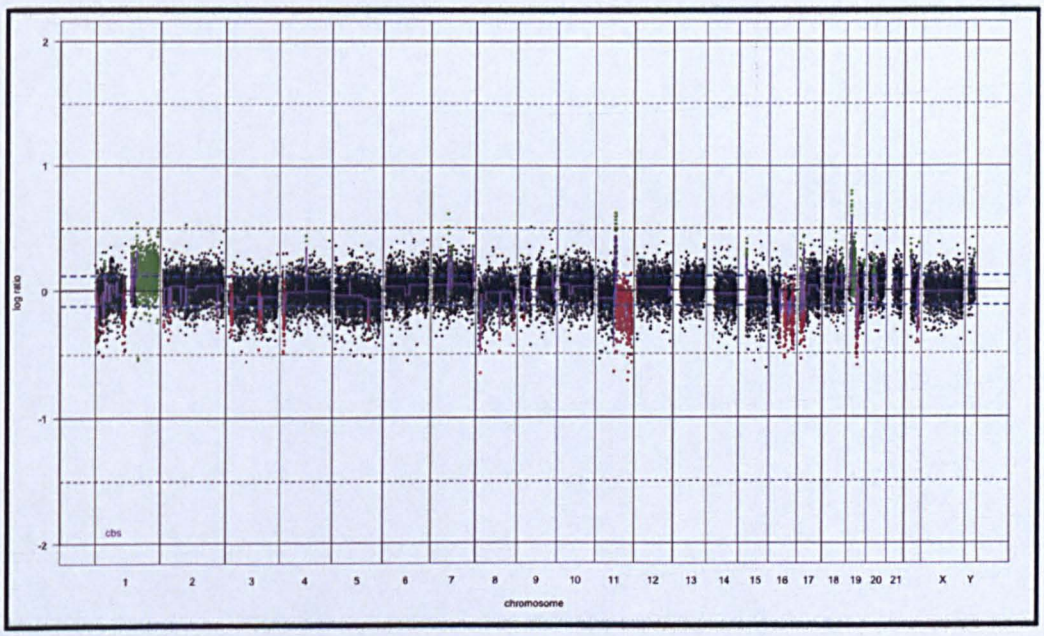

Figure 5-22: Genome plot of ductal carcinoma in situ from case 1 showing gain/amplification of 1q, 11q and 19p and loss of 11q, 11q and 19q.

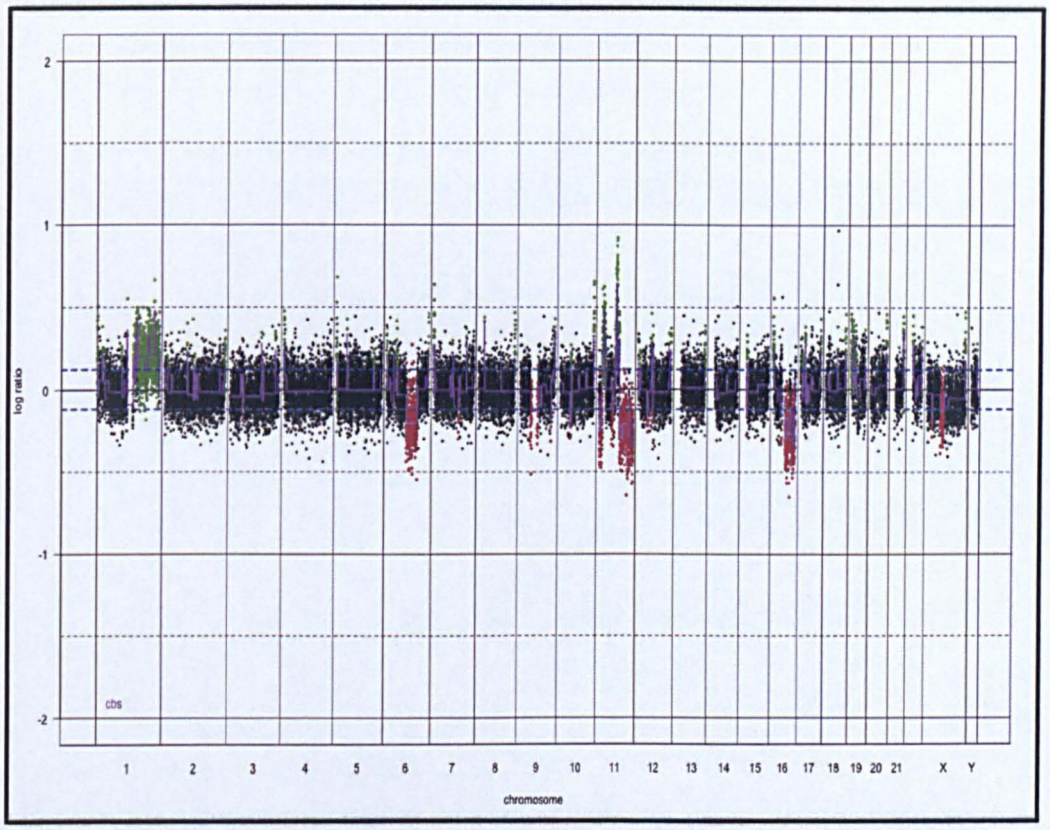

Figure 5-23: Genome plot of lobular neoplasia that laser micro-dissected from case 1 showing gain/amplification of 1q, 11p, 11q, 16p and 19p and loss of 6q, 11q and 16q.

Table 5-3: Genetic changes of different components of case number 1: columnar cell lesion (CCL-1), ductal carcinoma in situ (DCIS-1) and lobular neoplasia (LN-1).

chrom	map	Cytogenetic Band	CCL-1	DCIS-1	LN-1
1	1:2277295..2485326	p36.33-p36.32		GAIN	GAIN
1	1:2697923..3757389	p36.32	LOSS		GAIN
1	1:4114075..5665582	p36.2	LOSS		
1	1:5873942...6950771	p36.31	GAIN	GAIN	GAIN
1	1:34515166..35375482	p34.3	LOSS	LOSS	LOSS
1	1:144452745..246624589	q21.1-q44	GAIN	GAIN	GAIN
2	2:10092490..10269500	2p25.1			GAIN
2	2:10224532..10608610	2p25.1			GAIN
3	3:46851921..53308680	p21.31-p21.1	GAIN	GAIN	GAIN
3	3:125828183..129284640	p21.31-p21.1			GAIN
3	3:183258533..195960808	q26.33-q29		GAIN	
4	4:9371304....23169797	p16.2-p15.2	LOSS		
5	5:43351415..43702315	5p12			GAIN
5	5:176368478..180676573	q35.2-q35.3	GAIN	GAIN	GAIN
6	6:42373615..44434337	p21.1			GAIN
6	6:57335587...58075261	p11.2	LOSS	LOSS	
6	6:80657246..92946437	q14.1-q16.1		LOSS	LOSS
7	7:61091237..62439460	q11.1-q11.21	GAIN	GAIN	
7	7:72815547..75193290	q11.22-q11.23	GAIN		
8	8:6755220..8042158	p23.1	LOSS		
8	8:21864085..23175482	p21.3-p21.2			GAIN
8	8:143743728..144743580	q24.3		GAIN	GAIN
9	9:39131199...71033904	p13.1-q12			LOSS
9	9:130513305..138069659	q33.1-q34.3	GAIN		GAIN
10	10:38598310...43015352	p11.21-q11.21			LOSS
10	10:43498972..44019673	q11.21		GAIN	GAIN
11	11:4551894...8684969	p15.5-p15.4			LOSS
11	11:17520419..19540446	p15.1			AMP
11	11:49003873..49980055	p11.2-q12.1			LOSS
11	11:60166833..61767307	12q2			GAIN
11	11:64845754..68578000	11q13.1-11q13.3		GAIN	AMP
11	11:68523084..71362638	11q13.3-11q13.4	GAIN	AMP	AMP
11	11:80636716..108525726	11q14.1-q22.3		LOSS	LOSS
11	11:108450613..108525726	11q22.3	LOSS	LOSS	LOSS
12	12:5972109..7247166	p13.31			GAIN
12	12:48027380..55251462	q13.11-q13.2			GAIN
12	12:121193338..125667418	q24.23-q24.31			GAIN
14	14:50264879..51754207	q22.1		GAIN	
15	15:20829066..22596193	q11.2	GAIN	GAIN	GAIN
16	16:11139..31764125	p13.3-p11.2-p11.2-q11.2		GAIN	GAIN
16	16:48900991..84593836	p11.2-q24.3	LOSS	LOSS	LOSS
17	17:2256623..5083694	p13.3-p13.2	GAIN		
17	17:6879623..8614953	p13.2-p13.1	LOSS		GAIN
17	17:16917282..18377155	p11.2	GAIN	GAIN	
17	17:36690553..49204340	q12-q21.33		GAIN	
18	18:44404930..44713872	q21.1	GAIN	AMP	GAIN
18	18:74032492..74812028	q23			GAIN
19	19:8649225..8687198	p13.2 (ADAM S10)	GAIN	AMP	AMP
19	19::9074066..19919144	p13.2-13.11	GAIN		GAIN
19	19:28680998..32819119	p12-q13.11	LOSS	LOSS	
21	21:43466719...45929047	q22.3			GAIN

Validation of *CCND1* as a target candidate gene

Immunohistochemistry and CISH analysis of full face sections revealed amplification and overexpression of *CCND1* in all co-existing lesions including columnar cell changes, flat epithelial atypia, low/intermediate grade ductal carcinoma in situ (micropapillary and cribriform pattern), duct spaces lined by columnar cells with intraductal islands of lobular neoplasia morphology, intimately admixed DCIS and LCIS, expanded lobules showing features typical of lobular neoplasia and invasive classic lobular carcinoma (**Figures 5-24, 5-25, 5-26, 5-27, 5-28, 5-29, 5-30 and 5-31**). This finding was compatible with what we have already demonstrated in Chapter 3 concerning role of *CCND1* in the development of LNGBN family.

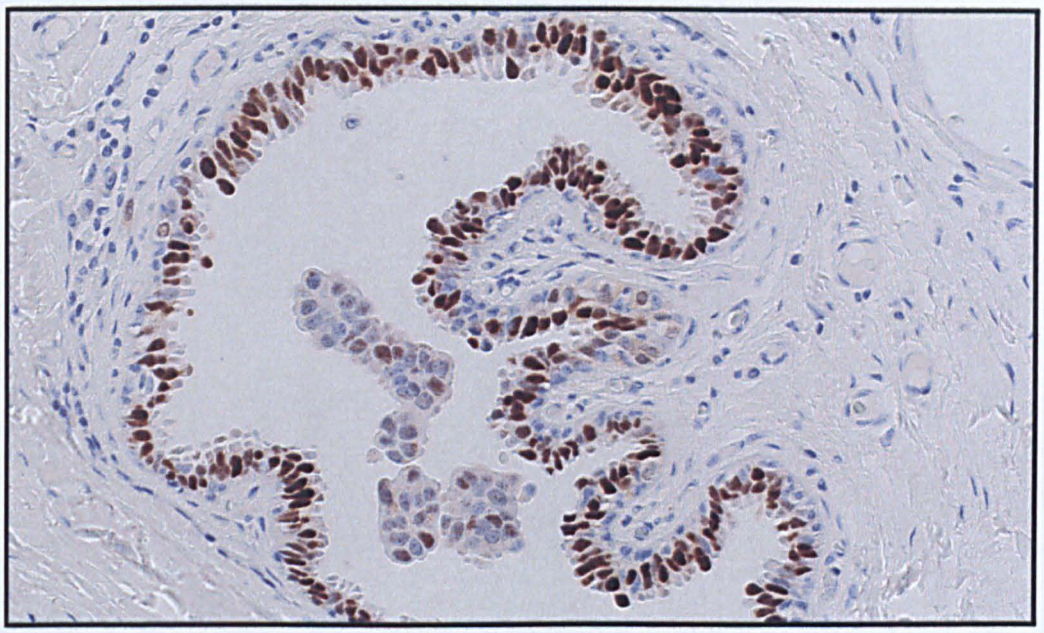

Figure 5-24: Columnar cell change lesion showing positive nuclear Cyclin D1 IHC staining

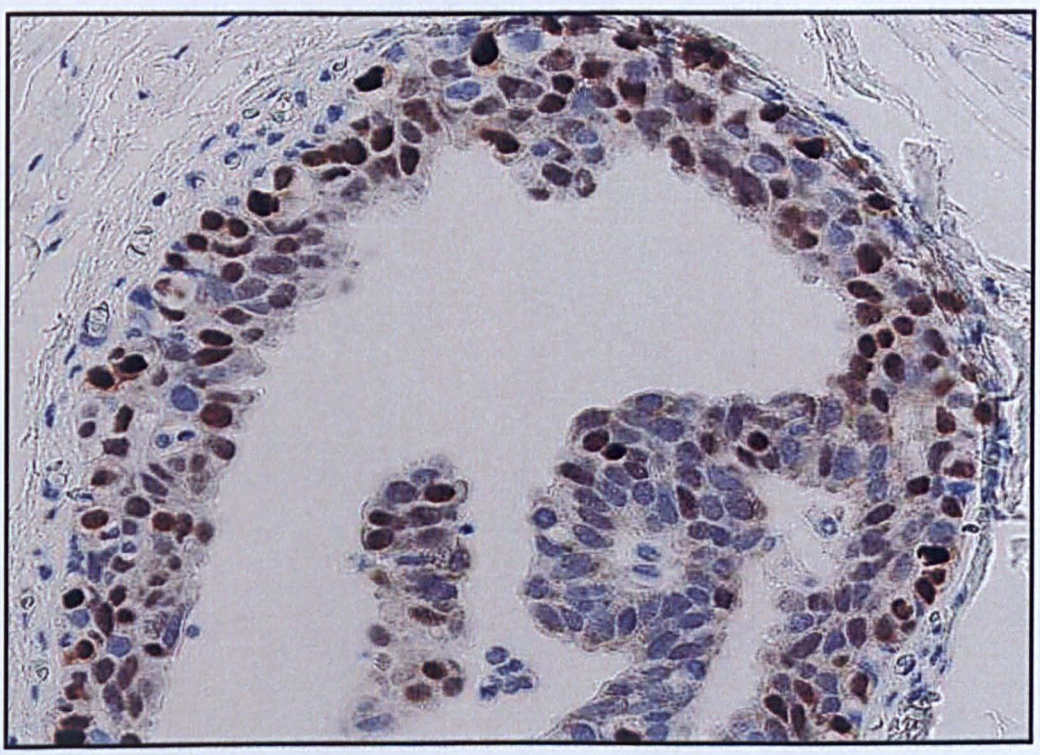

Figure 5-25: Atypical ductal hyperplasia s showing positive nuclear Cyclin D1 IHC staining

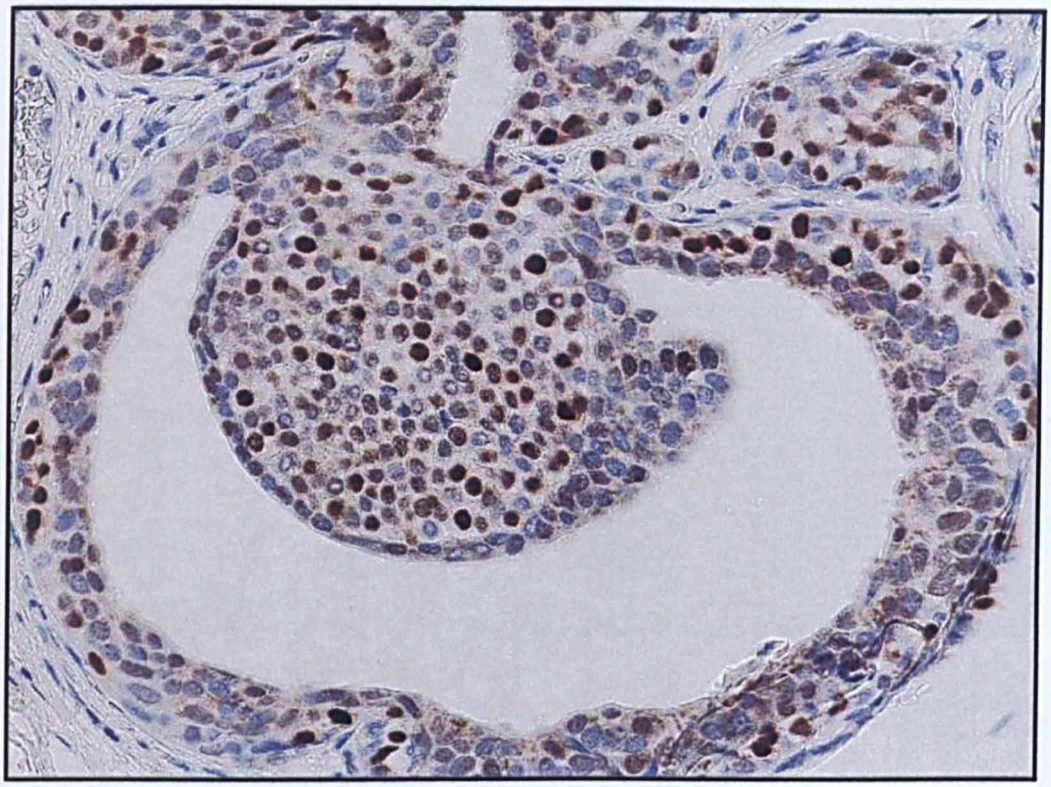

Figure 5-26: A duct spaces lobular neoplasia showing positive nuclear Cyclin D1 IHC staining

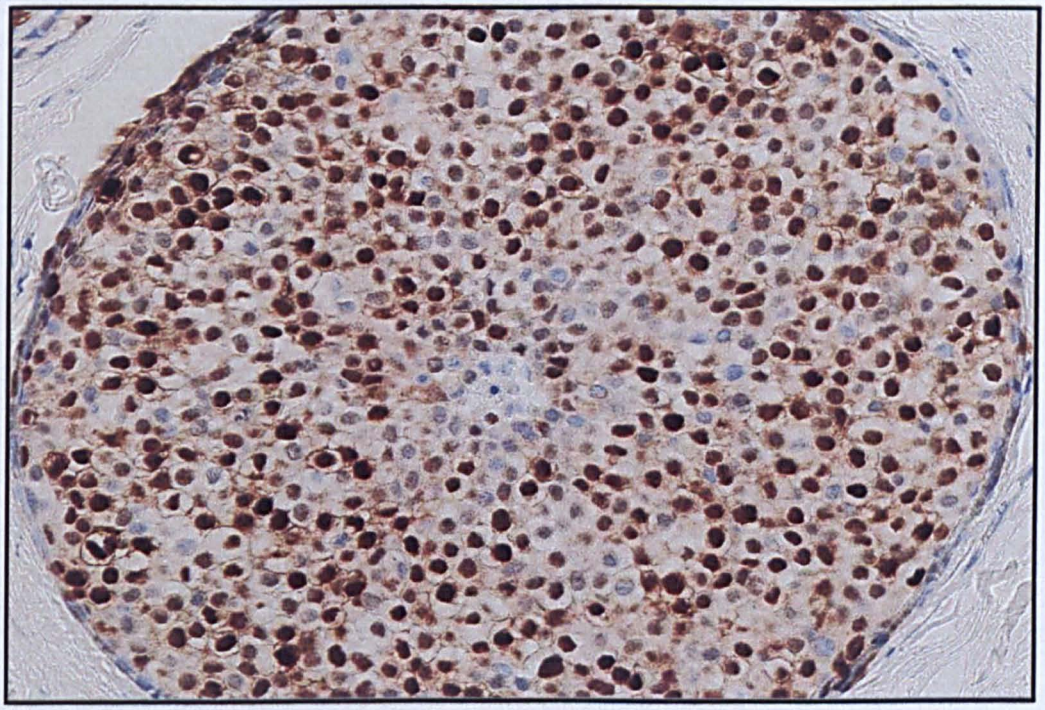

Figure 5-27: lobular neoplasia showing positive nuclear Cyclin D1IHC staining

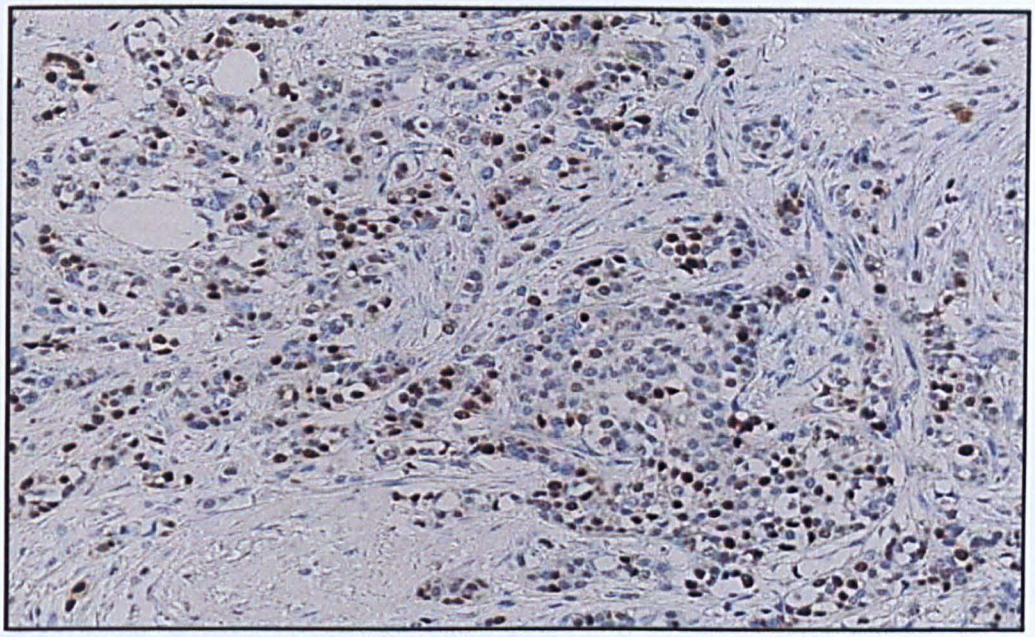

Figure 5-28: Invasive lobular carcinoma showing positive nuclear Cyclin D1 IHC staining

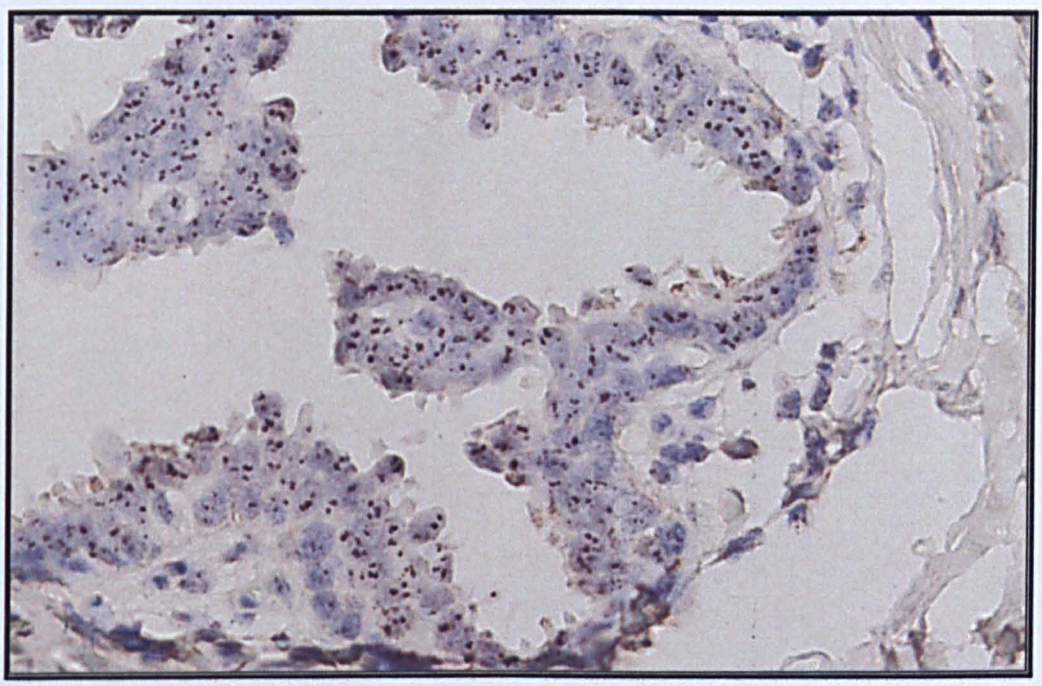

Figure 5-29: Flat epithelial atypia showing amplification of Cyclin D1 (*CCD1);* chromogenic in situ hybridization

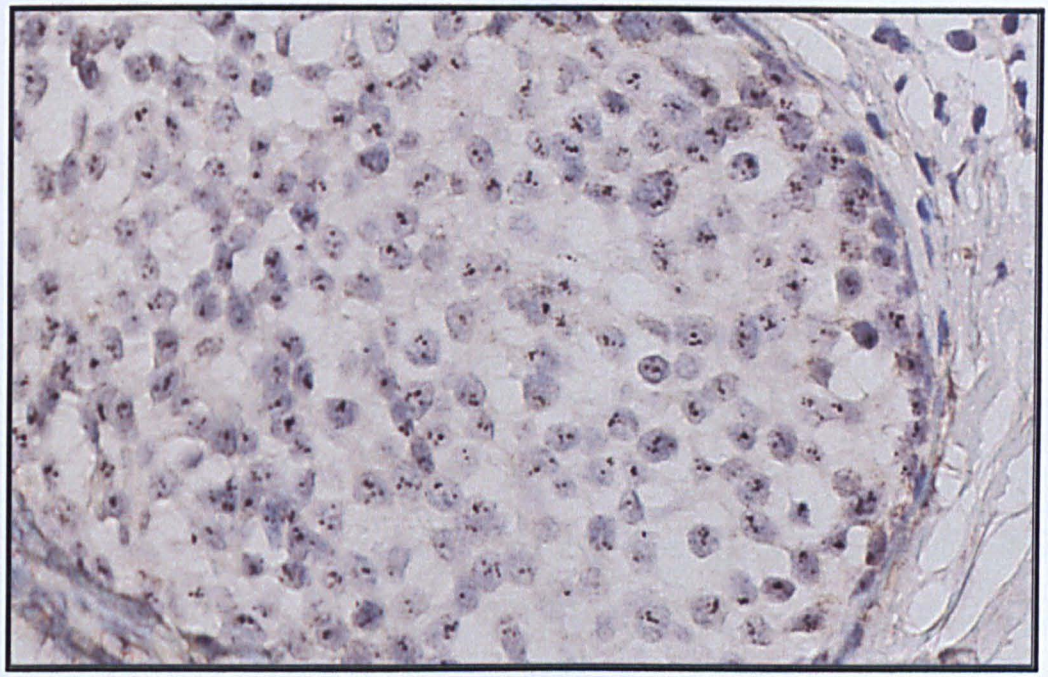

Figure 5-30: Lobular neoplasia showing amplification of Cyclin D1 (CCD1); chromogenic in situ hybridization (low power).

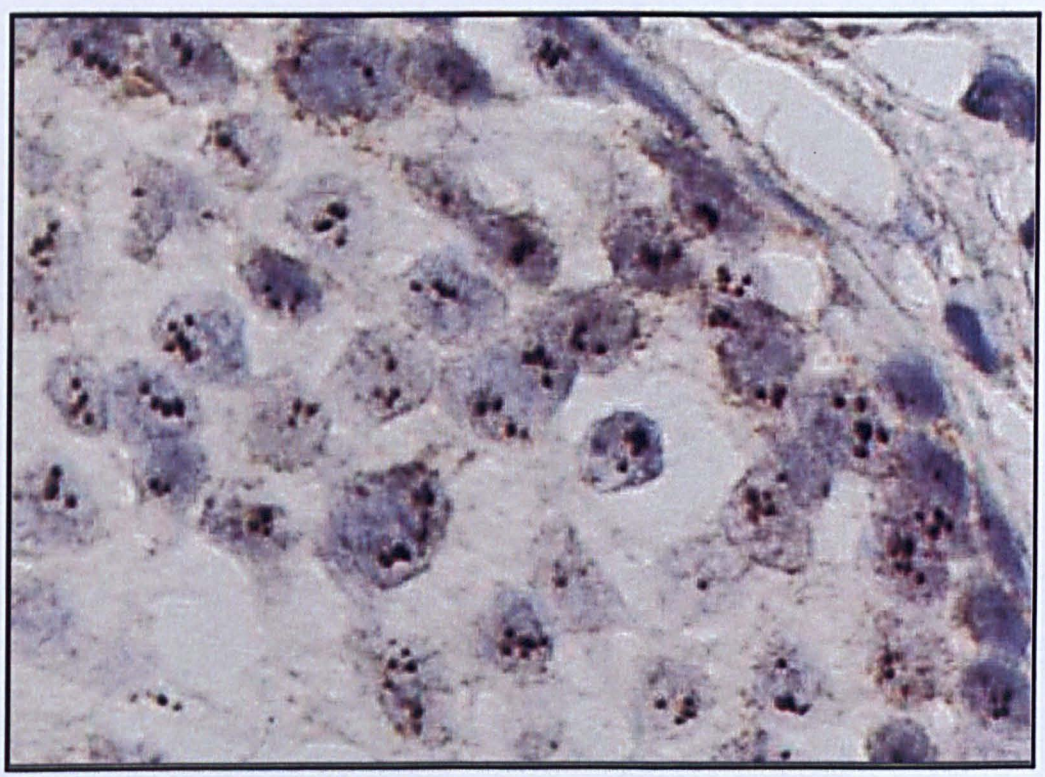

Figure 5-31: Lobular neoplasia showing amplification of Cyclin D1 (CCD1); chromogenic in situ hybridization (high power).

5.4.2 Analysis of case 2 (mixed tubular carcinoma)

Morphology

This is an example of mixed tubular carcinoma in which about 80% of the tumour showing tubules formation at the centre and 20% of solid sheets with less occasional tubules at the periphery of the tumour. A range of preinvasive lesions including columnar cell lesions, usual epithelial hyperplasia (UEH) and ductal carcinoma in situ (mainly cribriform pattern) was noticed. These lesions had same topographic distribution and cytoplasmic and nuclear features.

Immunohistochemical profile

The aforementioned lesions showed strong positive staining for CK18+, CK19+, CK8+, ER+, PR+, Bcl2+, MUC-1+ and negative expression for p53, CK5/6, and CK14 with no HER-2 over-expression. E-Cadherin immunocytochemistry staining showed strong membrane positive reactivity in all of them.

Genome profiles

Four components were laser microdissected separately including CCC with atypia, DCIS, and invasive tubular carcinoma (one sample from the centre of the tumour and the other from the periphery).

The genomic patterns of all lesions (**Figures 5-32, 5-33, 5-34 and 5-35 and Table 5-4**) were of simplex pattern, characterized by broad segments of duplications and deletions comprising part (16p13-q11+ and 20p13.3-q13.33), entire chromosome arms (whole 1q+ arm, whole 13q+ arm and whole 16q- arm) and whole chromosome (loss of whole chromosome 22) with occasional amplifications. A comparison between the distinct morphological components of case 2 (CCL, DCIS, invasive from centre and invasive from

periphery) in a pairwise fashion revealed that they shared strikingly similar genomic profiles; Pearson's correlation performed with normalized Log2 ratios revealed *r* values of CCLs vs. DCIS: r=0.661; CCLs vs. invasive from centre: r=0.695; CCLs vs. invasive from periphery: r=0.681; DCIS vs. invasive from centre: r=0.933; DCIS vs. invasive from periphery: r=0.931 and invasive from centre vs. invasive from periphery: r= 0.954. The common genetic changes among CCLs, DCIS and invasive components were gains of 1p36.31, 1q21.1-44 (gain of whole long arm; 1q+), 3p21.31-p2.1, 5q35.2-35.3, 13q34, 16p13.3-q11.2, 20p13-q13.33 and losses of 1p36.32, 1p35.3-35.2, 1p34.3, 4p16.2-14.2, 6p11.2, 8p23.1, 15q11.1-15q1, 16p11.2-q24.3, 19p12-q13.11, and whole chromosome 22. Amplifications of 5q13.2, 13q14.3 (*DLEU1, RNASEH2B and GUCY1B2*) and 17q12-21.33 were noticed in the invasive component from the periphery of the tumour. In addition, all samples showed high gain in 1q12 and 1q+ especially at 1q32.1-32.2.

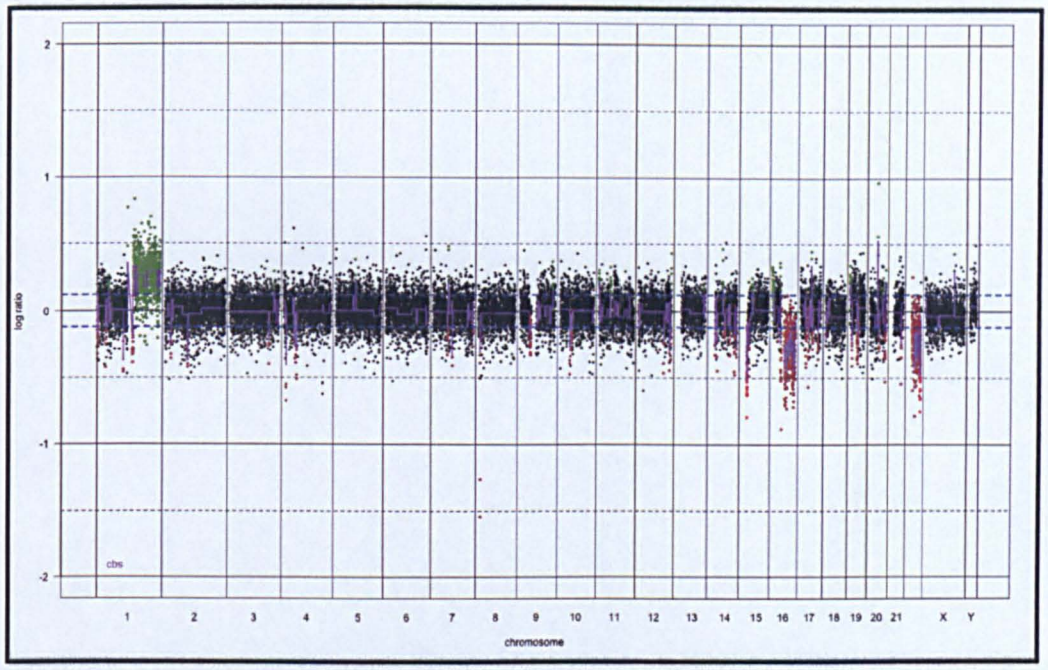

Figure 5-32: Genome plot of columnar cell lesion which has been dissected from case 2 showing gain of 1q and 20q and loss of 1p, 15p, 16q, 19p and 22q

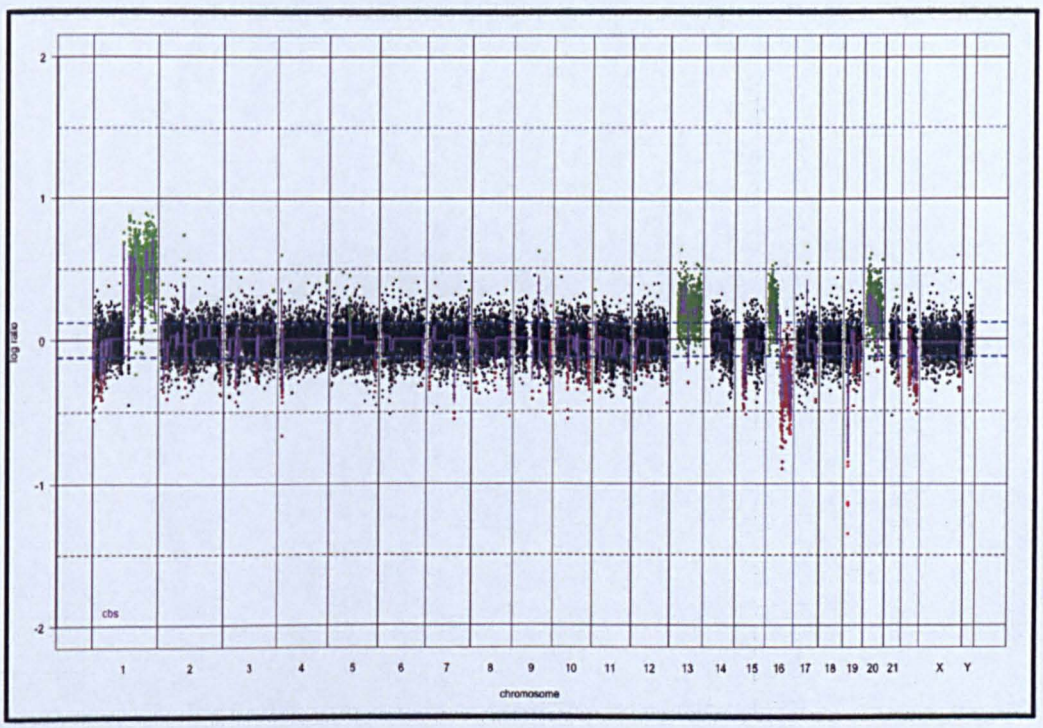

Figure 5-33: Genome plot of ductal carcinoma in situ which has been dissected from case 2 showing high gain of 1q, 13q, 16p and 20 and loss of 1p, 15p, 16q, 19p and 22q

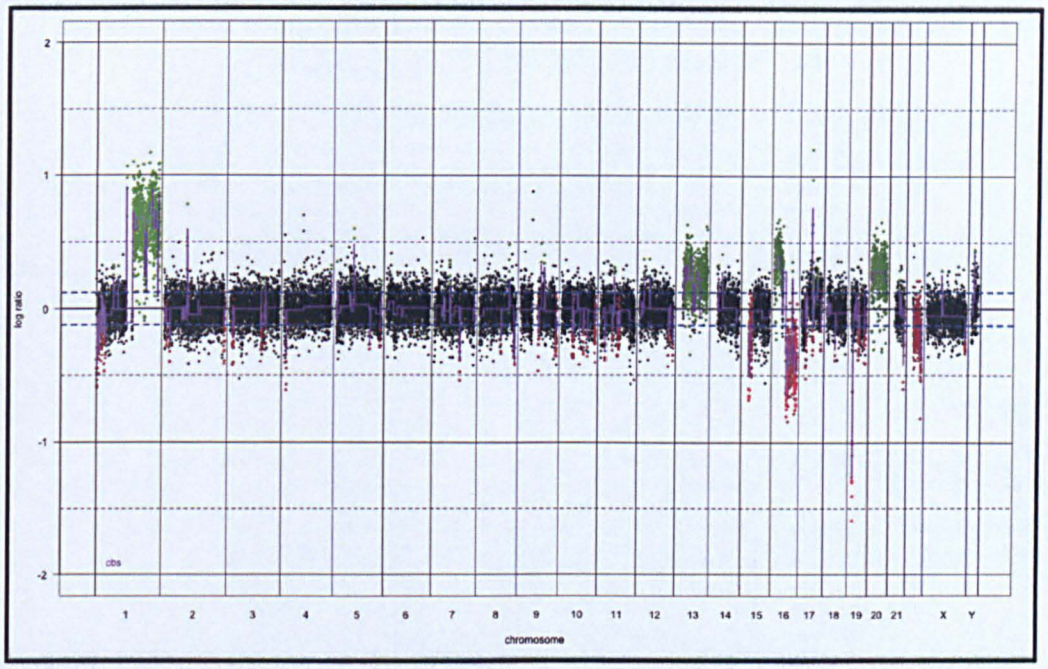

Figure 5-34: Genome plot of invasive tubular carcinoma from the centre which has been dissected from case 2 showing high gain of 1q, 13q, 16p and 20 and loss of 1p, 15p, 16q, 19p and 22q

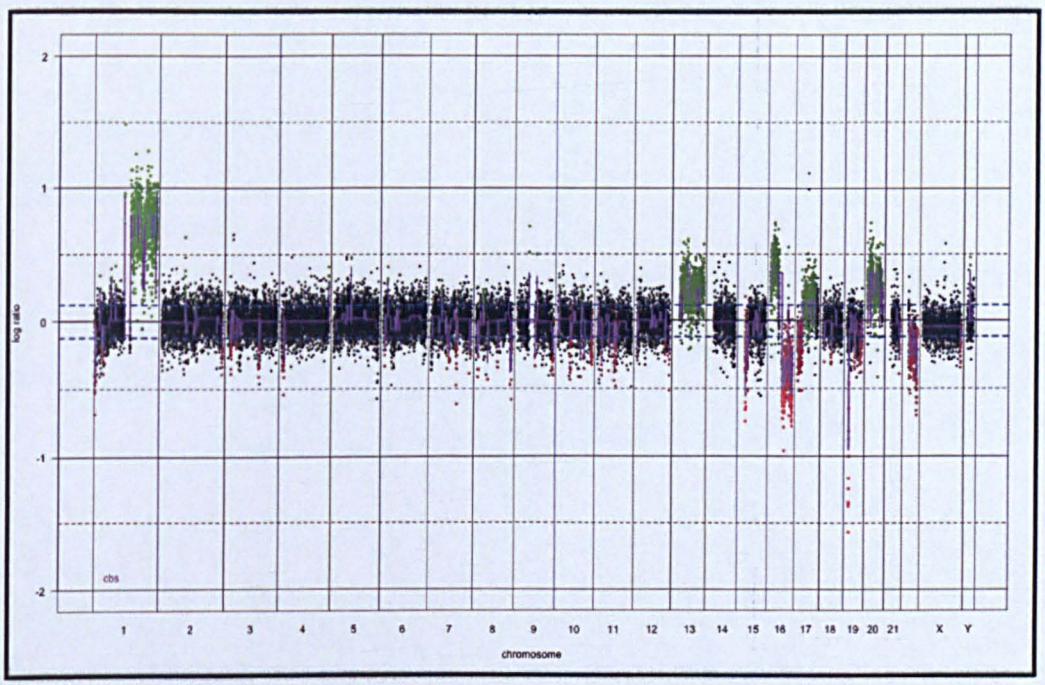

Figure 5-35: Genome plot of invasive tubular carcinoma from the periphery which has been dissected from case 2 showing high gain of 1q, 13q, 16p and 20 and loss of 1p, 15p, 16q, 19p and 22q

Table 5-4: Genetic changes of different components of case 2: columnar cell lesions (CCL), ductal carcinoma in situ (DCIS), and tubular carcinoma (TC)

chrom	map	Cytogenetic Band	CCL-2	DCIS-2	TC-2 cenreal	TC-2 periphery
1	1:2697923..3757389	p36.32	LOSS	LOSS	LOSS	LOSS
1	1:4114075..5665582	p36.2	LOSS	LOSS	LOSS	LOSS
1	1:5873942...6950771	p36.31	GAIN	GAIN	GAIN	GAIN
1	1:29549713..31394713	p35.3-p35.2	LOSS	LOSS	LOSS	LOSS
1	1:34515166..35375482	p34.3	LOSS	LOSS	LOSS	LOSS
1	1:104025830..104426934	p21.1	LOSS			
1	1:120436410..120650514	p12	GAIN	High gain	High gain	High gain
1	1:144452745..246624589	q21.1-44	GAIN	High gain	High gain	High gain
3	3:46851921..53308680	p21.31-p21.1	GAIN	GAIN	GAIN	GAIN
4	4:9371304..23169797	p16.2-p15.2	LOSS	LOSS	LOSS	LOSS
5	5:65203593..68826309	q12.3		GAIN		
5	5:69035579..70388712	q13.1-q13.2		GAIN	GAIN	AMP
5	5:176368478..180676573	q35.2-q35.3	GAIN	GAIN	GAIN	GAIN
6	6:57335587...58075261	p11.2	LOSS	LOSS	LOSS	LOSS
7	7:61091237..62439460	q11.1-q11.21	GAIN		GAIN	
7	7:98820572..102185532	q21.3-q22.1		LOSS	LOSS	LOSS
8	8:6755220..8042158	p23.1	LOSS	LOSS	LOSS	LOSS
9	9:39131199...71033904	p13.1-q12	LOSS			
9	9:91735900..92122168	q21.33-q22.32		GAIN	GAIN	
9	9:130513305..138069659	q33.1-q34.3	GAIN			
9	9:136583961..138069659	q34.11-q34.3		LOSS	LOSS	LOSS
10	10:38598310...43015352	p11.21-q11.21	LOSS			
10	10:46812978..49450532	q11.21-q11.22	LOSS	LOSS	LOSS	LOSS
10	10:87865548..88179055	q23.1-q23.2		LOSS	LOSS	LOSS
10	10:131479757..133626641	q26.2-q26.3		LOSS	LOSS	LOSS
11	11:17520419..19540446	p15.1		LOSS	LOSS	LOSS
13	13:20904235..113346314	q11-q34		GAIN	GAIN	GAIN
13	13:50698010...51585238	q14.3		GAIN	GAIN	AMP
13	13:110995727..111374279	q34	GAIN	GAIN	GAIN	GAIN
14	14:50264879..51754207	q22.1	GAIN			
15	15:20094045..32954812	q11.1-q15.1	LOSS	LOSS	LOSS	LOSS
16	16:11139..31764125	p13.3-q11.2	GAIN	GAIN	GAIN	GAIN
16	16:48900991..84593836	p11.2-q24.3	LOSS	LOSS	LOSS	LOSS
17	17:9455707.15687248	P12				LOSS
17	17:16917282..18755715	p11.2			LOSS	LOSS
17	17:36690553..49204340	q12-q21.33		GAIN	GAIN	AMP
17	17:729302663..78900648	q25.1-q25.3		LOSS	LOSS	
19	19:960519..2970392	p13.3	GAIN			
19	19:28680998..32819119	p12-q13.11	LOSS	LOSS	LOSS	LOSS
19	19:54392659..54877591	q13.41-q13.42		LOSS	LOSS	LOSS
19	19:8629145..9060080	p13.2	LOSS	LOSS	LOSS	LOSS
20	20:90210..59535518	p13-q13.33		GAIN	GAIN	GAIN
20	20:29421720..29996640	q11.21			GAIN	GAIN
22	22:17724207..49794172	22q	LOSS	LOSS	LOSS	LOSS

5.4.3 Analysis of case 3 (pure tubular carcinoma)

Morphology

This is an example of pure tubular carcinoma in which > 95% of the tumour showed tubules, low mitosis and mild pleomorphism (M1, T1, and P1). Extensive columnar cell changes (CCC) without atypia, columnar cell hyperplasia without atypia and ductal carcinoma in situ (mainly cribriform pattern) were intimately coexistence with invasive TC. All these lesions had same the cytoplasmic and nuclear features.

Immunohistochemical profile

The aforementioned lesions showed strong positive staining for CK18+, CK19+, CK8+, ER+, PR+, Bcl2, MUC-1+ and negative expression for p53, CK5/6, and CK14 with no HER-2 over-expression. E-Cadherin immunocytochemistry staining showed strong membrane positive reactivity in all of them.

Genome profiles

Three components were separately laser microdissected including CCC/CCH without atypia, DCIS, and invasive tubular carcinoma

This case showed fewer genetic changes compared to the previous two cases. The genomic patterns (**Figures 5-36, 5-37 and 5-38 and Table 5-5**) were of simplex, characterized by broad segments of duplication at 1q+ and deletion at 16q with occasional amplification at 7p12.3-12.2, 7p11.2 and 18q21.1 in the invasive component. Pearson's correlation performed with normalized Log2 ratios revealed remarkable similarity in the genomic profiles CCL vs. DCIS: r=0.717; CCL vs. invasive; r=0.670; DCIS vs. invasive: r=0.832. The common genetic changes among CCL, DCIS and invasive component were gains of 1q21.1-44 (gain of whole long arm; 1q+), 7q11.21 and 18q21.1 and losses of 1p36.32,

1p36.2, 1p36.11, 2p25.1, 4p16.2-14.2, 5q13.1-13.2, 7p13, 9p34.11-34.3 and 16p11.2-q24.3. Invasive lesion showed amplification at 7p11.2 (*VWC2, ZPBP, IKZF1, DDC, FINGNL1 and RB10*), 7p12.3 (*EGFR, LANCL2, VOPP1, SEPT14, ZNF713, MRPS17, GBAS, PSPH, CCT6A, SUMF2, PHKG1, CHCHD2*) and 18q21.1 (*PAS2, KATNAL2, HDLD2, IER3PI*). In the unselected BC series there was significant correlation between copy number changes and gene expression of (*PHKG1, CCT6A* and *SUMF2*); p=0.04.

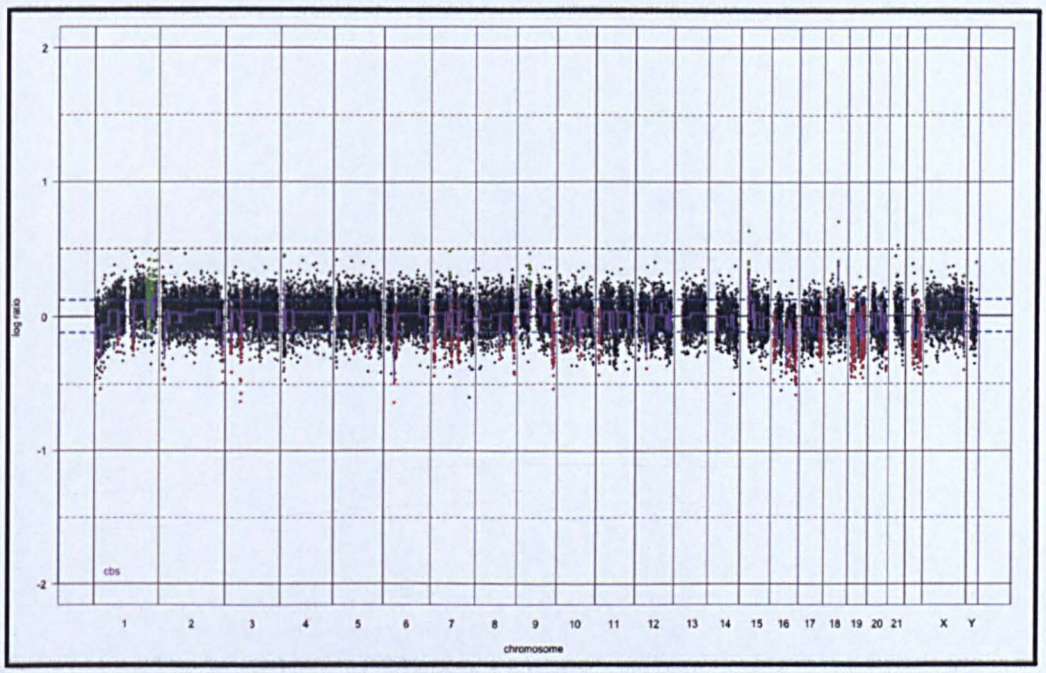

Figure 5-36: Genome plot of columnar cell lesion which has been dissected from case 3 showing gain 1q, 7q and 18q and loss of 1p, 16q and 19q

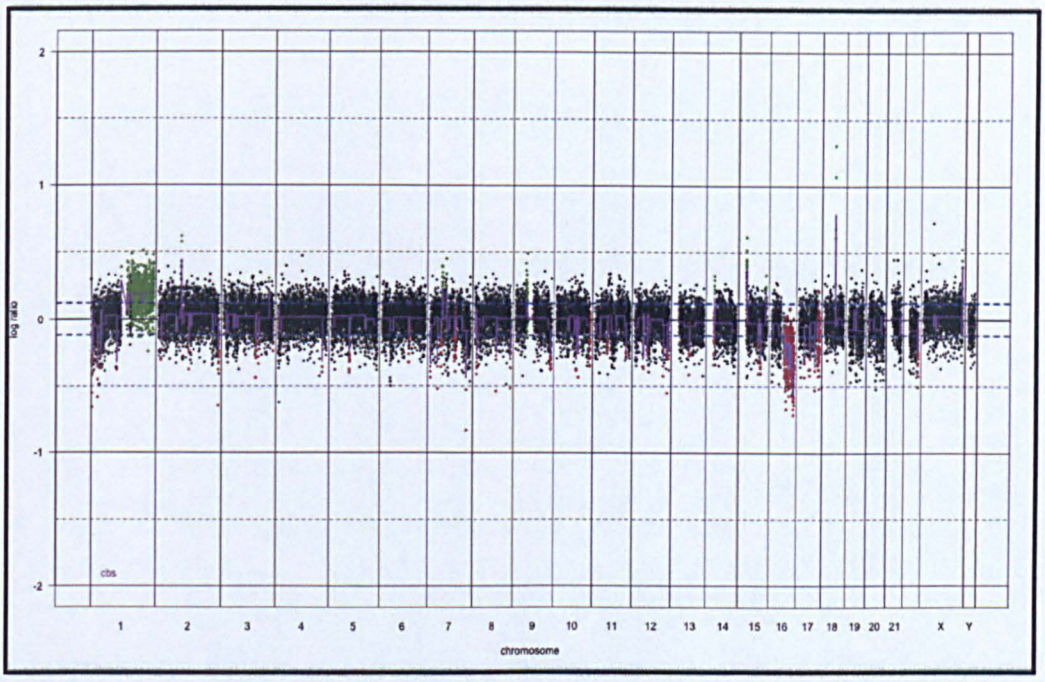

Figure 5-37: Genome plot of ductal carcinoma in situ which has been dissected from case 3 showing gain/amplification 1q, 7p, 7q and 18q and loss of 1p, 16q and 17.

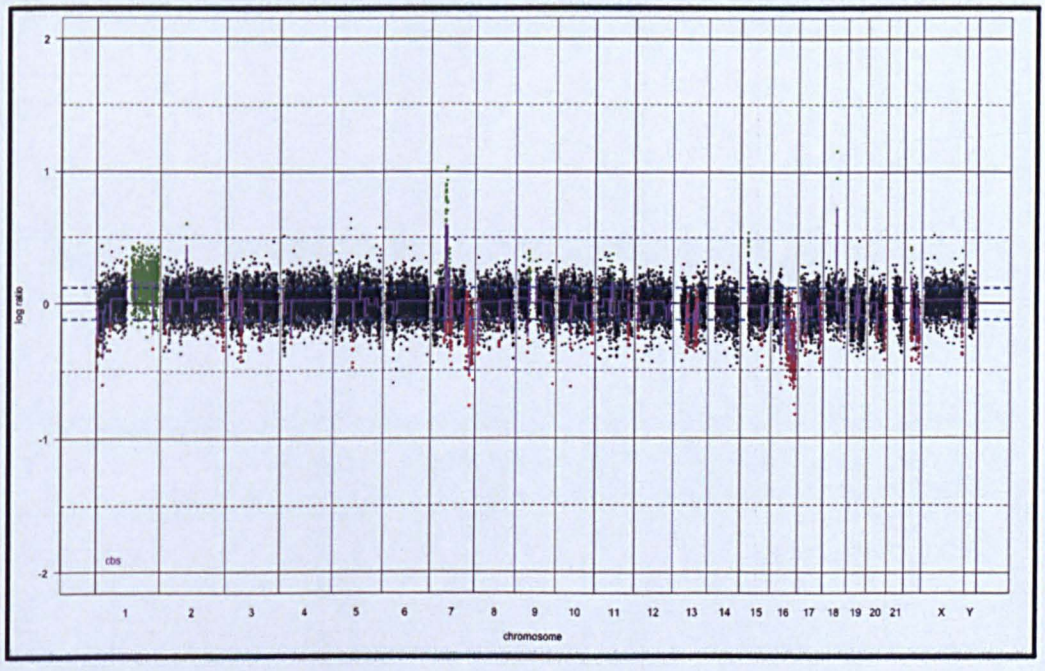

Figure 5-38: Genome plot of invasive tubular carcinoma which has been dissected from case 3 showing gain/amplification 1q, 7p, 7q and 18q and loss of 1p, 16q and 17.

Table 5-5: Genetic Changes of case 3: columnar cell lesion (CCL), ductal carcinoma in situ (DCIS) and tubular carcinoma (TC)

chrom	map	Cytogenetic Band	CCL-3	DCIS-3	TC-3
1	1:2697923..3757389	p36.32	LOSS	LOSS	LOSS
1	1:4114075..5665582	p36.2	LOSS	LOSS	LOSS
1	1:25312395..25779600	p36.11	LOSS	LOSS	LOSS
1	1:104025830..104426934	p21.1		LOSS	
1	1:120436410..246624589	p12-q44	Gain	GAIN	GAIN
2	2:10224532..10608610	2p25.1	LOSS	LOSS	LOSS
4	4:9371304....23169797	p16.2-p15.2	LOSS	LOSS	LOSS
5	5:69035579..70388712	q13.1-q13.2	LOSS	LOSS	LOSS
7	7:44083631..45018187	p13	LOSS	LOSS	LOSS
7	7:48747468..50823472	p12.3-p12.2		GAIN	AMP
7	7:54988969..56402107	p11.2		GAIN	AMP
7	7:64877310..65190324	q11.21	GAIN	GAIN	GAIN
7	7:98820572..102185532	q21.3-q22.1	LOSS	LOSS	
8	8:6755220..8042158	p23.1		LOSS	LOSS
9	9:136583961..138069659	q34.11-q34.3	LOSS	LOSS	LOSS
10	10:46812978..49450532	q11.21-q11.22			LOSS
10	10:87865548..88179055	q23.1-q23.2		LOSS	
10	10:131479757..133626641	q26.2-q26.3		LOSS	LOSS
11	11:80636716..133454282	q14.1-q25		LOSS	LOSS
16	16:48900991..84593836	p11.2-q24.3	LOSS	LOSS	LOSS
17	17:729302663..78900648	q25.1-q25.3	LOSS	LOSS	LOSS
18	18:44404930..44713872	q21.1	GAIN	AMP	AMP
19	19:8629145..9060080	p13.2	LOSS		
19	19:54392659..54877591	q13.41-q13.42	LOSS		

5.4.4 Analysis of case 4 (pure tubular)

Morphology

This is another example of pure tubular carcinoma in which >90% of the tumour showed tubules, low mitosis and mild pleomorphism (M1, T1, and P1). There were extensive areas of columnar cell changes with and without atypia and minimal low grade ductal carcinomas with cribriform and micropapillary patterns.

Immunohistochemical profile

The aforementioned lesions showed strong positive staining for CK18+, CK19+, CK8+, ER+, PR+, Bcl2, MUC-1+ and negative expression for p53, CK5/6, and CK14 with no HER-2 over-expression. E-Cadherin immunocytochemistry staining showed strong membrane positive reactivity in all lesions.

Genome profiles

CCL without atypia and invasive carcinoma were subjected to aCGH. Similar to previous cases, the genomic patterns (**Figures 5-39 and 5-40 and Table 5-6**) were of a simplex pattern. Pearson's correlation performed with normalized Log2 ratios revealed remarkable similarity in the genomic profiles of CCL and TC (r =0.679). The common genetic changes were gains of 1p36.31, 1p12-42 (gain of whole long arm; 1q+), 3p21.31-p21.1, 9q33.1-34.3, 13q34, 16p13.3-q11.2 and losses of p34.3, 4p16.2-14.2, 6p11.2, 8p23.1, 9q13.1-q12, 15q11.1-q15.1 and 16p11.2-q24.3. TC showed amplification at p12 (start at 1:120436410 and end at 20650514. Three genes located on this locus: *ADAM30, NOTCH2 and PHGDH* which their gene expressions related to low grade tumours (www.oncomine.com). However, only *PHGDH* showed a significant correlation between copy number changes and mRNA expression, p=0.005 (gene expression array of unselected cases).

Table 5-6: Genetic changes of case 4: Columnar cell lesion (CCL) and tubular carcinoma (TC)

chrom	map	Cytogenetic Band	CCL-4	TC-4
1	1:2277295..2485326	p36.33-p36.32		GAIN
1	1:4114075..5665582	p36.2 (AJAP1)	LOSS	
1	1:5873942...6950771	p36.31	GAIN	GAIN
1	1:7038707..12129387	p36.23-p36.22		GAIN
1	1:23800462..24461606	p36.12-p36.11		GAIN
1	1:29549713..31394713	p35.3-p35.2	LOSS	
1	1:34515166..35375482	p34.3	LOSS	LOSS
1	1:120436410..24662788	p12-q42	GAIN	AMP
2	2:87128774..98327997	2q11.2		LOSS
3	3:46851921..53308680	p21.31-p21.1	GAIN	GAIN
3	3:183258533..195960808	q26.33-q29		GAIN
4	4:9371304....23169797	p16.2-p15.2	LOSS	LOSS
5	5:65203593..68826309	q12.3		GAIN
5	5:176368478..180676573	q35.2-q35.3	GAIN	
6	6:57335587...58075261	p11.2	LOSS	LOSS
7	7:44083631..45018187	p13		GAIN
7	7:61091237..62439460	q11.1-q11.21	GAIN	
8	8:6755220..8042158	p23.1	LOSS	LOSS
8	8:143743728..144743580	q24.3		GAIN
9	9:39131199...71033904	p13.1-q12	LOSS	LOSS
9	9:130513305..138069659	q33.1-q34.3	GAIN	GAIN
11	11:46261972..48165018	p11.2		GAIN
11	11:49003873..49980055	p11.2-q12.1		LOSS
11	11:60817912..64500237	q12.2-q14.1		GAIN
11	11:80636716..133454282	q14.1-q25		LOSS
11	11:129590768..130258566	q24.3		GAIN
12	12:5972109..7247166	p13.31		GAIN
12	12:121193338..125667418	q24.23-q24.31		GAIN
13	13:110995727..111374279	q34	GAIN	GAIN
14	14:50264879..51754207	q22.1	GAIN	
14	14:99683934..100817227	q32.2-q32.33		GAIN
15	15:20094045..32954812	q11.1-q15.1	LOSS	LOSS
16	16:11139..31764125	p13.3-p11.2-p11.2-q11.2	GAIN	GAIN
16	16:48900991..84593836	p11.2-q24.3	LOSS	LOSS
17	17:2256623..5083694	p13.3-p13.2		GAIN
17	17:16917282..18377155	p11.2		GAIN
17	17:729302663..78900648	q25.1-q25.3		GAIN
18	18:14304059..14984939	p11.21		LOSS
19	19:960519..2970392	p13.3	GAIN	GAIN
19	19:2795315..8663945	p13.2-q12		GAIN
19	19:45182685..51060676	q13.31-q13.42		GAIN
20	20:29421720..29996640	q11.21		LOSS
21	21:10907345..15399525	p11.2-q11.2		LOSS
21	21:43466719...45929047	q22.3		GAIN

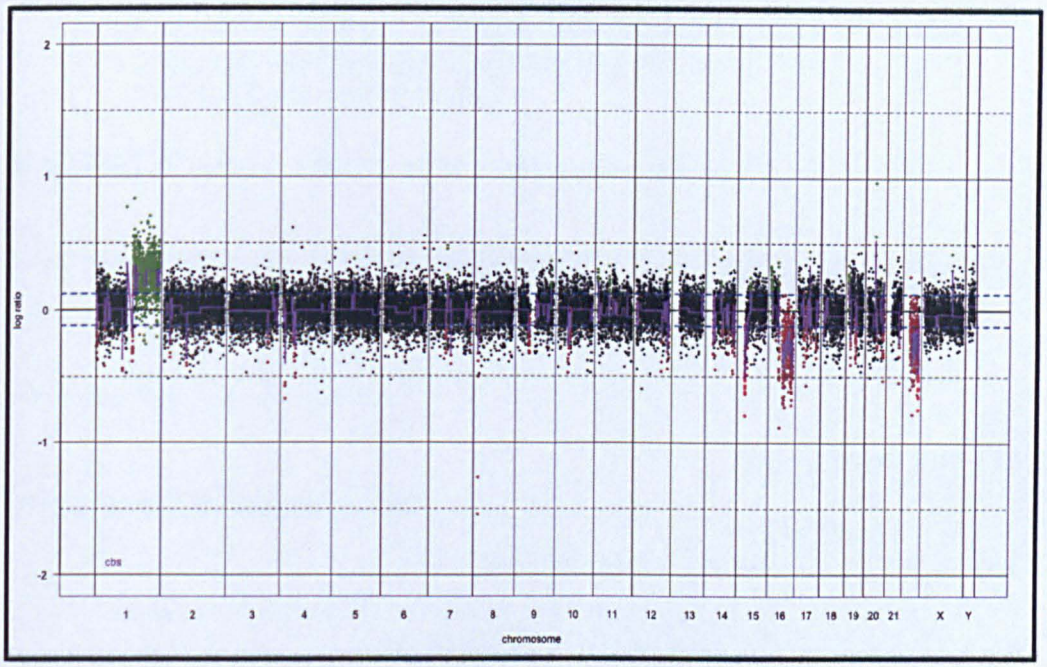

Figure 5-39: Genome plot of columnar cell lesion which has been dissected from case 4 showing gain 1q and loss of 1p, and 16q.

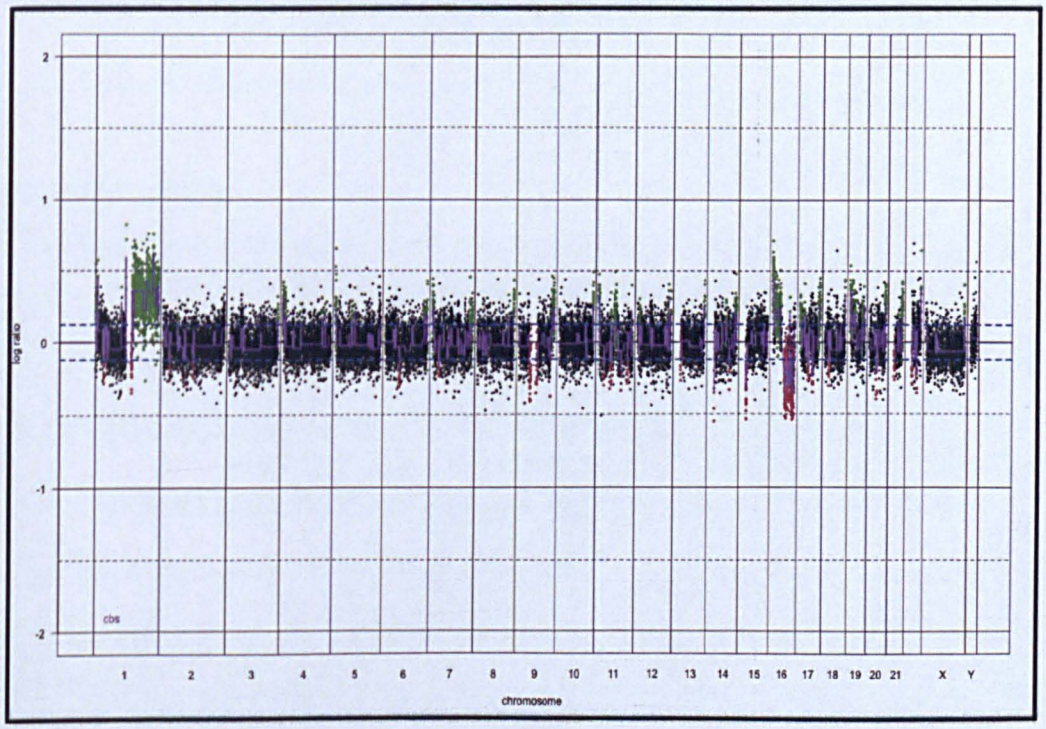

Figure 5-40: Genome plot of invasive tubular carcinoma which has been dissected from case 4 showing gain/amplification 1q, 16p, and 19p loss of 1p, and 16q.

5.4.5 Analysis of case 5 (pure tubular carcinoma associated with lobular neoplasia)

Morphology

This is an example of pure tubular carcinoma (M1, T1, and P2) which showed extensive areas of lobular neoplasia and low/intermediate grade DCIS with cribriform, micropapillary, and solid patterns.

Immunohistochemical profile

The aforementioned lesions showed strong positive staining for CK18+, CK19+, CK8+, ER+, PR+, Bcl2, MUC-1+ and negative expression for p53, CK5/6, and CK14 with no HER-2 over-expression. E-Cadherin immunocytochemistry staining showed strong membrane positive reactivity in TC and all patterns of DCIS. Lobular neoplasia was negative for E-Cadherin.

Genome profiles

TC, LN and DCIS were laser microdissected and subjected to aCGH. The genomic patterns **(Figures 5-41, 5-42 and 5-43 and Table 5-7)** of these lesions were of "sawtooth", characterized by many narrow segments of gains and losses, often alternating, more or less affecting all the chromosomes without copy number amplification. Pearson's correlation revealed remarkable similarity in the genomic profiles of TC vs. DCIS (r =0.820), TC vs. LN (r=0.714) and DCIS vs. LN (r=802). The common genetic changes were involving most of the chromosomes. LN showed amplification at 8p21.3-21.2. Both LN and DCIS showed 19p3 amplification.

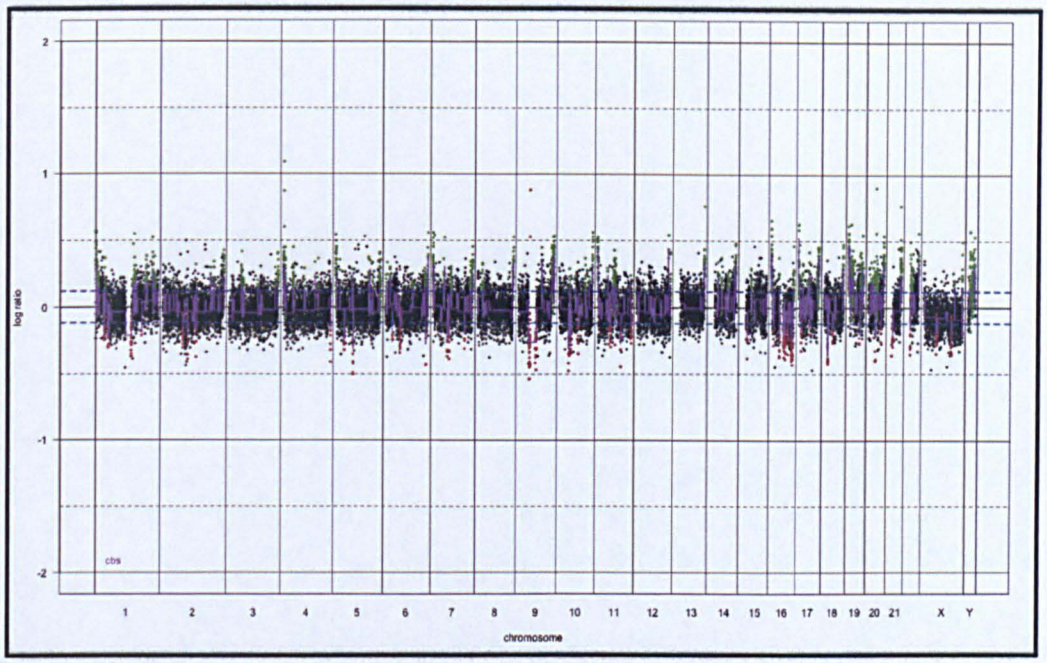

Figure 5-41: Genome plot of ductal carcinoma in situ which has been dissected from case 5 showing genetic changes of most of the chromosomes

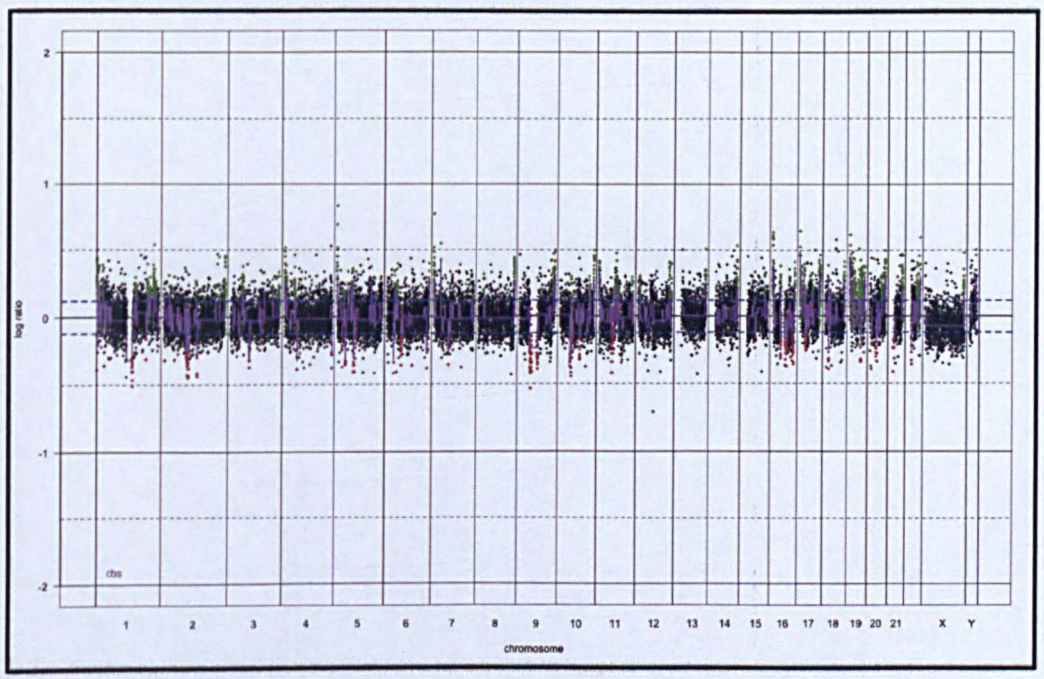

Figure 5-42: Genome plot of tubular carcinoma which has been dissected from case 5 showing genetic changes of most of the chromosomes

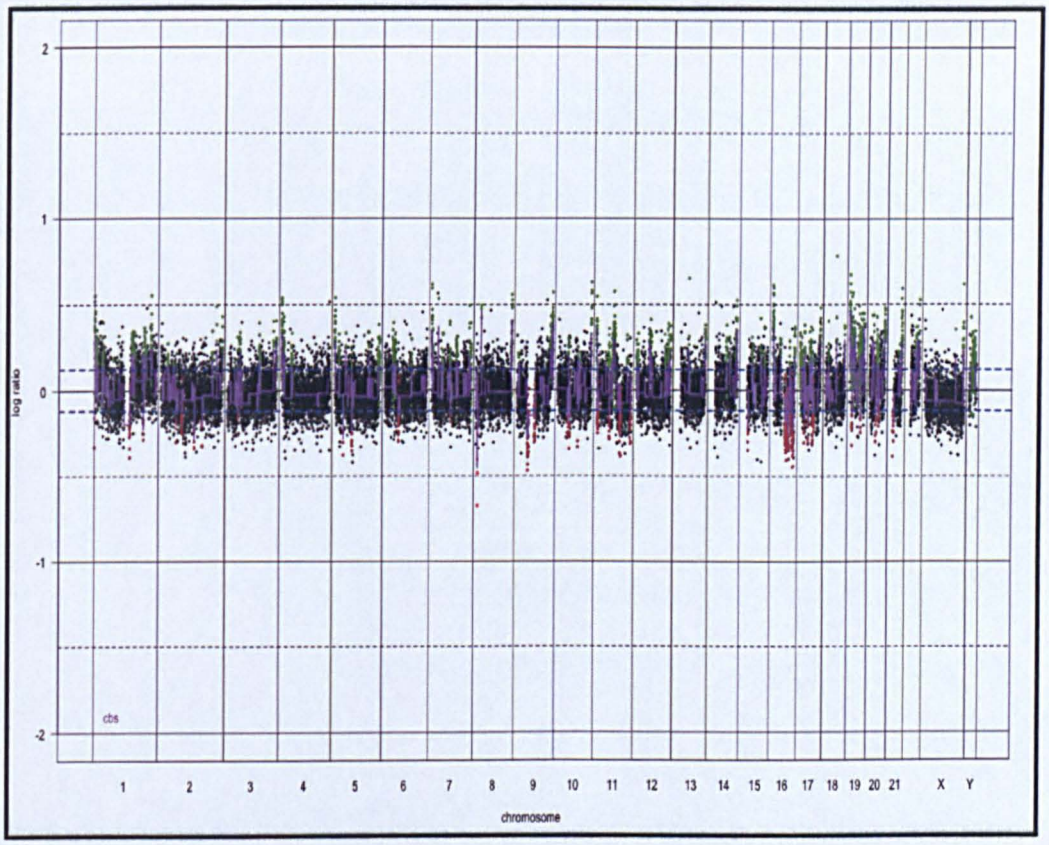

Figure 5-43: Genome plot of lobular neoplasia which has been dissected from case 5 showing genetic changes of most of the chromosomes

Table 5-7: Genetic changes of case 5: ductal carcinoma in situ (DCIS), lobular neoplasia (LN) and tubular carcinoma (TC)

chromosome	Map	Cytogenetic Band	DCIS-5	TC-5	LN-5
1	1:2277295..24461606	p36.33-p36.32	GAIN	GAIN	GAIN
1	1:25312395..25779600	p36.11			GAIN
1	1:29549713..31394713	p35.3-p35.2		LOSS	
1	1:34515166..35375482	p34.3	LOSS	LOSS	LOSS
1	1:150269698..156948996	q21.3-q22-q23.1	GAIN	GAIN	GAIN
1	1:159793016..182853014	q23.3-q25-q31.3			GAIN
1	1:206559883..225499515	q32.1-q32.2-q41			GAIN
1	1:225593333...236748304	q42	GAIN	GAIN	GAIN
1	1:236749347..246624589	q43-q44			GAIN
2	2:10092490..10608610	2p25.1			GAIN
2	2:79440056..80833098	2p12	LOSS		LOSS
2	2:87128774..98327997	2q11.2		LOSS	
2	2:132279581..132994118	2q21.1-q21.2	LOSS	LOSS	LOSS
3	3:9467084.10540466	p25.3	GAIN	GAIN	GAIN
3	3:46851921..53308680	p21.31-p21.1	GAIN	GAIN	GAIN
3	3:56708117..58368941	p14.3-p14.2	GAIN		
3	3:125828183..129284640	p21.31-p21.1			GAIN
3	3:183258533..195960808	q26.33-q29	GAIN	GAIN	GAIN
4	4:38594738..41243420	p14-p13	GAIN	GAIN	GAIN
5	5:34060230..34334851	p13.3	LOSS	LOSS	LOSS
5	5:43351415..43702315	5p12		GAIN	GAIN
5	5:65203593..68826309	q12.3	GAIN	GAIN	
5	5:69035579..70388712	q13.1-q13.2	LOSS	LOSS	LOSS
5	5:176368478..180676573	q35.2-q35.3	GAIN	GAIN	GAIN
6	6:17526937..18404236	p23-p22.3	GAIN	GAIN	GAIN
6	6:42373615..44434337	p21.1		GAIN	GAIN
6	6:57335587...58075261	p11.2	LOSS	LOSS	LOSS
6	6:61959143..62918629	q12	LOSS	LOSS	
6	6:160773903..161249786	q25.3-q26	LOSS	LOSS	
7	7:5155898...6721092	7p22.1	GAIN		GAIN
7	7:44083631..45018187	p13	GAIN	GAIN	GAIN
7	7:72815547..75193290	q11.22-q11.23	GAIN		GAIN
7	7:98820572..102185532	q21.3-q22.1	GAIN		GAIN
8	8:6755220..8042158	p23.1			LOSS
8	8:21864085..23175482	p21.3-p21.2	GAIN	GAIN	AMP
8	8:143743728..144743580	q24.3	GAIN	GAIN	GAIN
9	9:39131199...71033904	p13.1-q12	LOSS	LOSS	LOSS
9	9:91735900..92122168	q21.33-q22.32	GAIN		
9	9:130513305..138069659	q33.1-q34.3	GAIN	GAIN	GAIN
10	10:38598310...43015352	p11.21-q11.21	LOSS	LOSS	LOSS
10	10:43498972..44019673	q11.21	GAIN	GAIN	GAIN
10	10:46812978..49450532	q11.21-q11.22	LOSS	LOSS	LOSS
11	11:4551894...8684969	p15.5-p15.4			LOSS
11	11:46261972..48165018	p11.2			GAIN
11	11:49003873..49980055	p11.2-q12.1	LOSS	LOSS	LOSS
11	11:60817912..64500237	q12.2-q14.1	GAIN		GAIN
11	11:80636716..133454282	q14.1-q25			LOSS
11	11:129590768..130258566	q24.3	GAIN	GAIN	
12	12:5972109..7247166	p13.31		GAIN	GAIN
12	12:48027380..55251462	q13.11-q13.2			GAIN
12	12:121193338..125667418	q24.23-q24.31	GAIN	GAIN	GAIN
14	14:50264879..51754207	q22.1	GAIN		
14	14:63767854..78287450	q23.2-q24.1	GAIN		GAIN
14	14:99683934..100817227	q32.2-q32.33	GAIN		GAIN
15	15:20094045..32954812	q11.1-q15.1	LOSS		LOSS
16	16:11139..31764125	p13.3-p11.2-p11.2-q11.2	GAIN	GAIN	GAIN
16	16:48900991..84593836	p11.2-q24.3	LOSS	LOSS	LOSS
17	17:2256623..5083694	p13.3-p13.2	GAIN	GAIN	
17	17:6879623..8614953	p13.2-p13.1		GAIN	GAIN
17	17:9455707.15687248	P12	LOSS		
17	17:16917282..18377155	p11.2	GAIN		GAIN
17	17:18276146..18755715	p11.2			LOSS
17	17:36690553..49204340	q12-q21.33	GAIN		GAIN
17	17:729302663..78900648	q25.1-q25.3	GAIN	GAIN	
18	18:14304059..14984939	p11.21		LOSS	
18	18:44404930..44713872	q21.1			GAIN
18	18:74032492..74812028	q23	GAIN	GAIN	
19	19:960519..2970392	p13.3	AMP	GAIN	AMP
19	19:2795315..8663945	p13.2-q12	GAIN	GAIN	GAIN
19	19:43266180..43833261	q13.13-q13.2	LOSS	LOSS	LOSS
19	19:45182685..51060676	q13.31-q13.42	GAIN	GAIN	GAIN
19	19:54392659..54877591	q13.41-q13.42	GAIN	GAIN	GAIN
19	19:8629145..9060080	p13.2		LOSS	LOSS
20	20:29421720..29996640	q11.21	LOSS	LOSS	LOSS
21	21:10907345..15399525	p11.2-q11.2	LOSS	LOSS	LOSS
21	21:43466719...45929047	q22.3	GAIN	GAIN	GAIN

5.4.6 Analysis of case 6 and 7 (classic ILC and LN)

Theses two cases showed classic invasive lobular carcinoma (M1, P2, and T3) with extensive areas of lobular neoplasia. Both ILC and LN components were laser microdissected and subjected to aCGH **(Figures 5-44, 5-45, 5-46 and 5-47 and Tables 5-8 and 5-9).**

There was marked similarity of the genomic profiles, of ILCs of case 6 and (r=0.850) which is higher than that recorded for ILC and LN from the same patients (r=0.627). Both invasive components had amplification at 19p3 and 8p12 or p21.

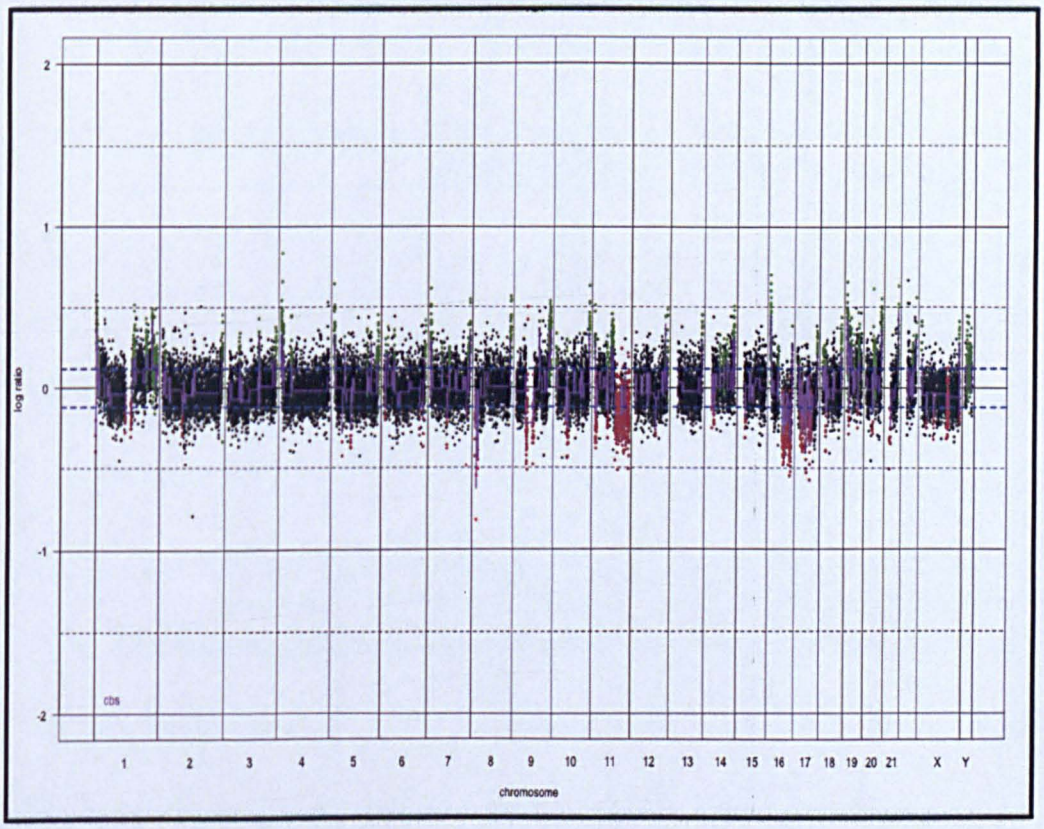

Figure 5-44: Genome plot of lobular neoplasia which has been dissected from case 6 showing genetic changes of most of the chromosomes including gain of 1q, 11p, 16p, and 19p and loss of 8p, 9p, 10p, 11q, 16q, and 17q

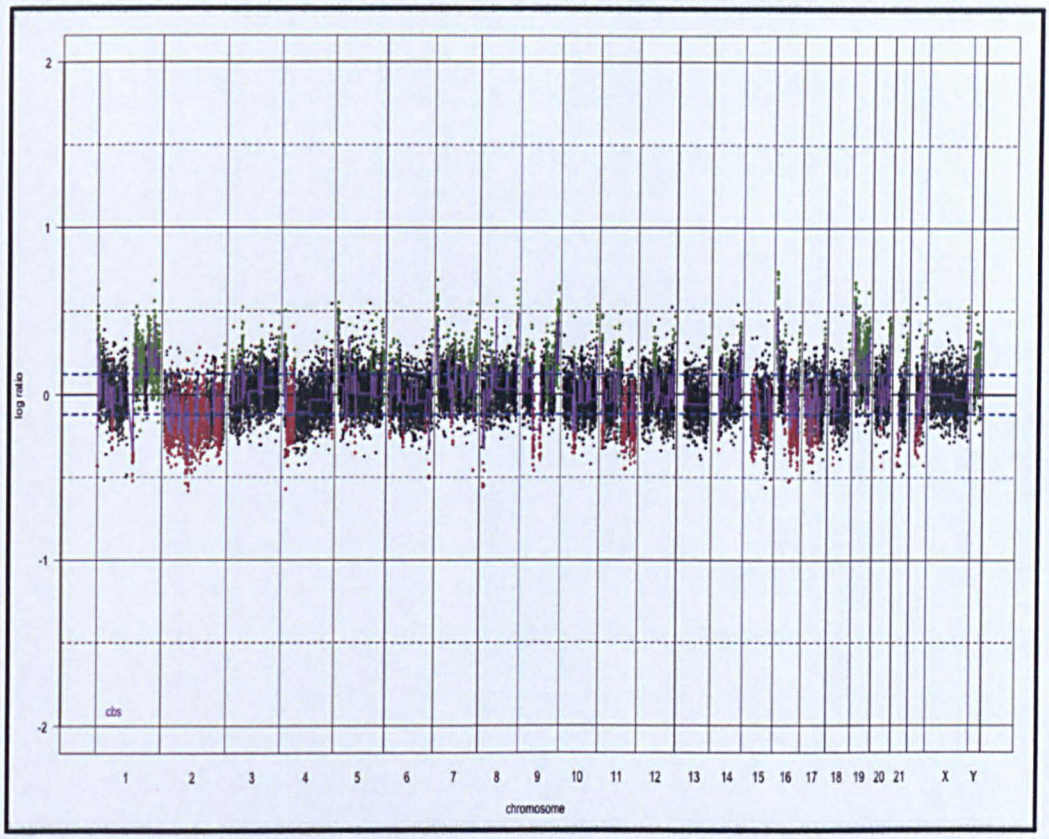

Figure 5-45: Genome plot of lobular carcinoma which has been dissected from case 6 showing genetic changes of most of the chromosomes including gain of 1q, 11p, 16p, and 19p and loss of 8p, 9p, 10p, 11q, 16q, and 17q

Table 5-8: Genetic changes of case 6; lobular neoplasia and invasive lobular carcinoma (ILC)

chrom	map	Cytogenetic Band	LN-6	ILC-6
1	1:2277295..3757389	p36.33-p36.32	GAIN	GAIN
1	1:5873942..12129387	p36.31	GAIN	GAIN
1	1:23800462..25779600	p36.12-p36.11	GAIN	GAIN
1	1:34515166..35375482	p34.3		LOSS
1	1:145190320..246624589	q21.1-q44	GAIN	GAIN
2	2:10092490..10608610	2p25.1	GAIN	GAIN
2	2:79440056..80833098	2p12	LOSS	LOSS
2	2:87128774..98327997	2q11.2		LOSS
2	2:132279581..132994118	2q21.1-q21.2		LOSS
3	3:9467084.10540466	p25.3	GAIN	GAIN
3	3:46851921..53308680	p21.31-p21.1	GAIN	GAIN
3	3:56708117..58368941	p14.3-p14.2		GAIN
3	3:125828183..129284640	p21.31-p21.1	GAIN	GAIN
3	3:183258533..195960808	q26.33-q29	GAIN	GAIN
4	4:9371304....23169797	p16.2-p15.2		LOSS
4	4:38594738..41243420	p14-p13	GAIN	
5	5:34060230...34334851	p13.3	LOSS	LOSS
5	5:43351415..43702315	5p12	GAIN	GAIN
5	5:65203593..68826309	q12.3		GAIN
5	5:69035579..70388712	q13.1-q13.2	LOSS	LOSS
5	5:176368478..180676573	q35.2-q35.3	GAIN	GAIN
6	6:17526937..18404236	p23-p22.3	GAIN	GAIN
6	6:42373615..44434337	p21.1	GAIN	GAIN
6	6:57335587...58075261	p11.2	LOSS	LOSS
6	6:160773903..161249786	q25.3-q26	LOSS	LOSS
7	7:5155898...6721092	7p22.1	GAIN	GAIN
7	7:44083631..45018187	p13	GAIN	GAIN
7	7:72815547..75193290	q11.22-q11.23	GAIN	GAIN
7	7:98820572..102185532	q21.3-q22.1	GAIN	GAIN
8	8:6755220..8042158	p23.1	LOSS	LOSS
8	8:21864085..23175482	p21.3-p21.2		GAIN
8	8:39937888..58230037	p12-q11.21		AMP
8	8:143743728..144743580	q24.3	GAIN	GAIN
9	9:39131199...71033904	p13.1-q12	LOSS	LOSS
9	9:91735900..92122168	q21.33-q22.32	GAIN	GAIN
9	9:130513305..138069659	q33.1-q34.3	GAIN	GAIN
10	10:38598310...43015352	p11.21-q11.21	LOSS	LOSS
10	10:43498972..44019673	q11.21	GAIN	GAIN
10	10:46812978..49450532	q11.21-q11.22	LOSS	LOSS
11	11:4551894...8684969	p15.5-p15.4	LOSS	LOSS
11	11:46261972..48165018	p11.2		GAIN
11	11:49003873..49980055	p11.2-q12.1	LOSS	LOSS
11	11:60817912..64500237	q12.2-q14.1	GAIN	GAIN
11	11:80636716..133454282	q14.1-q25	LOSS	LOSS
12	12:48027380..55251462	q13.11-q13.2	GAIN	GAIN
12	12:121193338..125667418	q24.23-q24.31	GAIN	GAIN
14	14:50264879..51754207	q22.1	GAIN	GAIN
14	14:63767854..78287450	q23.2-q24.1	GAIN	GAIN
14	14:99683934..100817227	q32.2-q32.33	GAIN	GAIN
15	15:20094045..32954812	q11.1-q15.1	LOSS	LOSS
16	16:11139..31764125	p13.3-p11.2-p11.2-q11.2	GAIN	GAIN
16	16:48900991..84593836	p11.2-q24.3	LOSS	LOSS
17	17:6879623..8614953	p13.2-p13.1	GAIN	GAIN
17	17:9455707.15687248	P12	LOSS	LOSS
17	17:18276146..18755715	p11.2	LOSS	LOSS
18	18:14304059..14984939	p11.21	LOSS	LOSS
18	18:74032492..74812028	q23	GAIN	
19	19:960519..2970392	p13.3	GAIN	AMP
19	19:2795315..8663945	p13.2-q12	GAIN	GAIN
19	19:8629145..9060080	p13.2	LOSS	LOSS
19	19:43266180..43833261	q13.13-q13.2	LOSS	
19	19:45182685..51060676	q13.31-q13.42	GAIN	GAIN
20	20:29421720..29996640	q11.21	LOSS	LOSS
21	21:10907345..15399525	p11.2-q11.2	LOSS	LOSS
21	21:43466719...45929047	q22.3	GAIN	GAIN

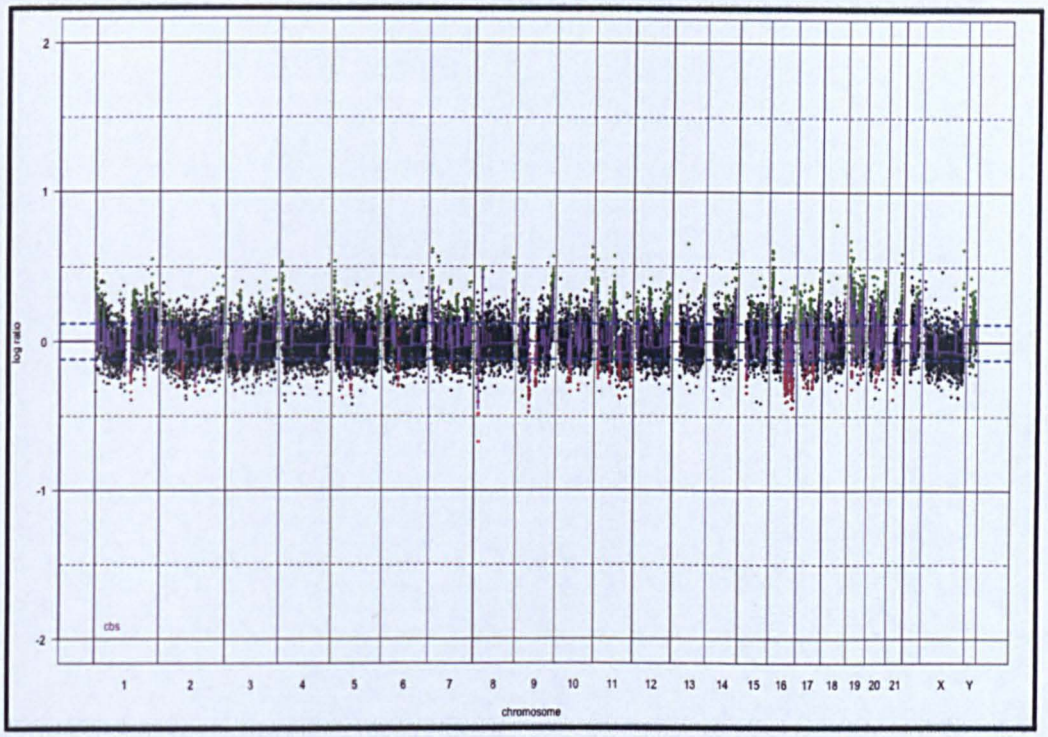

Figure 5-46: Genome plot of lobular neoplasia which has been dissected from case 7 showing genetic changes of most of the chromosomes including gain of 1q and loss of 16q

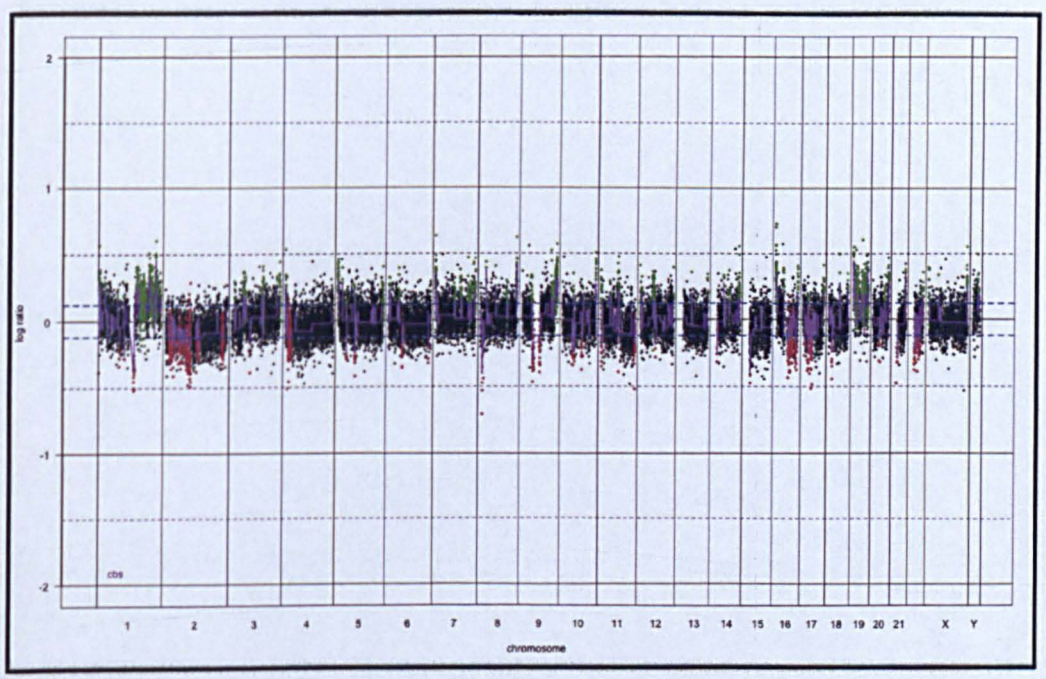

Figure 5-47: Genome plot of invasive lobular carcinoma which has been dissected from case 7 showing genetic changes of most of the chromosomes including gain of 1q and loss of 16q.

Table 5-9: Genetic changes of case 7: invasive lobular (ILC) lobular neoplasia (LN)

chrom	map	Cytogenetic Band	LN-7	ILC-7
1	1:2277295..3757389	p36.33-p36.32	GAIN	GAIN
1	1:5873942...6950771	p36.31	GAIN	GAIN
1	1:7038707..12129387	p36.23-p36.22	GAIN	GAIN
1	1:23800462..25779600	p36.12-p36.11	GAIN	GAIN
1	1:34515166..35375482	p34.3	LOSS	LOSS
1	1:145190320..148644689	q21.1-q21.2		GAIN
1	1:150269698..246624589	q21.3-q44	GAIN	GAIN
2	2:10092490..10608610	2p25.1	GAIN	GAIN
2	2:79440056..80833098	2p12	LOSS	LOSS
2	2:87128774..98327997	2q11.2		LOSS
2	2:132279581..132994118	2q21.1-q21.2	LOSS	LOSS
3	3:9467084.10540466	p25.3	GAIN	GAIN
3	3:46851921..53308680	p21.31-p21.1	GAIN	GAIN
3	3:56708117..58368941	p14.3-p14.2		GAIN
3	3:125828183..129284640	p21.31-p21.1	GAIN	GAIN
3	3:183258533..195960808	q26.33-q29	GAIN	GAIN
4	4:9371304....23169797	p16.2-p15.2		LOSS
4	4:38594738..41243420	p14-p13	GAIN	GAIN
5	5:34060230...34334851	p13.3	LOSS	LOSS
5	5:43351415..43702315	5p12	GAIN	GAIN
5	5:65203593..68826309	q12.3		GAIN
5	5:69035579..70388712	q13.1-q13.2	LOSS	LOSS
5	5:176368478..180676573	q35.2-q35.3	GAIN	GAIN
6	6:17526937..18404236	p23-p22.3	GAIN	GAIN
6	6:42373615..44434337	p21.1	GAIN	GAIN
6	6:57335587...58075261	p11.2	LOSS	LOSS
6	6:160773903..161249786	q25.3-q26		LOSS
7	7:5155898...6721092	p22.1	GAIN	GAIN
7	7:44083631..45018187	p13	GAIN	GAIN
7	7:72815547..75193290	q11.22-q11.23	GAIN	GAIN
7	7:98820572..102185532	q21.3-q22.1	GAIN	GAIN
8	8:6755220..8042158	p23.1	LOSS	LOSS
8	8:21864085..23175482	p21.3-p21.2	AMP	GAIN
8	8:143743728..144743580	q24.3	GAIN	GAIN
9	9:39131199...71033904	p13.1-q12	LOSS	LOSS
9	9:130513305..138069659	q33.1-q34.3	GAIN	GAIN
10	10:38598310...43015352	p11.21-q11.21	LOSS	LOSS
10	10:43498972..44019673	q11.21	GAIN	GAIN
10	10:46812978..49450532	q11.21-q11.22	LOSS	LOSS
11	11:4551894...8684969	p15.5-p15.4	LOSS	LOSS
11	11:46261972..48165018	p11.2	GAIN	GAIN
11	11:49003873..49980055	p11.2-q12.1	LOSS	LOSS
11	11:60817912..64500237	q12.2-q14.1	GAIN	GAIN
11	11:80636716..133454282	q14.1-q25	LOSS	LOSS
12	12:5972109..7247166	p13.31	GAIN	GAIN
12	12:48027380..55251462	q13.11-q13.2	GAIN	GAIN
12	12:121193338..125667418	q24.23-q24.31	GAIN	GAIN
14	14:50264879..51754207	q22.1		GAIN
14	14:63767854..78287450	q23.2-q24.1	GAIN	GAIN
14	14:99683934..100817227	q32.2-q32.33	GAIN	GAIN
15	15:20094045..32954812	q11.1-q15.1	LOSS	LOSS
16	16:11139..31764125	p13.3-p11.2-p11.2-q11.2	GAIN	GAIN
16	16:48900991..84593836	p11.2-q24.3	LOSS	LOSS
17	17:6879623..8614953	p13.2-p13.1	GAIN	GAIN
17	17:16917282..18377155	p11.2	GAIN	GAIN
17	17:18276146..18755715	p11.2	LOSS	LOSS
17	17:36690553..49204340	q12-q21.33	GAIN	GAIN
18	18:14304059..14984939	p11.21		LOSS
18	18:44404930..44713872	q21.1	GAIN	GAIN
19	19:960519..2970392	p13.3	AMP	GAIN
19	19:2795315..8663945	p13.2-q12	GAIN	GAIN
19	19:8629145..9060080	p13.2	LOSS	LOSS
19	19:43266180..43833261	q13.13-q13.2	LOSS	LOSS
19	19:45182685..51060676	q13.31-q13.42	GAIN	GAIN
19	19:54392659..54877591	q13.41-q13.42	GAIN	GAIN
20	20:29421720..29996640	q11.21	LOSS	LOSS
21	21:10907345..15399525	p11.2-q11.2	LOSS	LOSS
21	21:43466719...45929047	q22.3	GAIN	GAIN

5.4.7 Analysis of case 8 and 9 (Classic ILC and tubular carcinoma)

Theses two cases showed classic invasive lobular carcinoma (case 8) and pure tubular carcinoma (case 9). The genetic changes and genome plots (**Figures 5-48 and 5-49 and Table 5-10**) were summarized in table (4-10) and figure (4-13). ILC showed amplification at 1q31.1, 1q32.2, 1q41, 8p12-11.21 and 13q11.34.

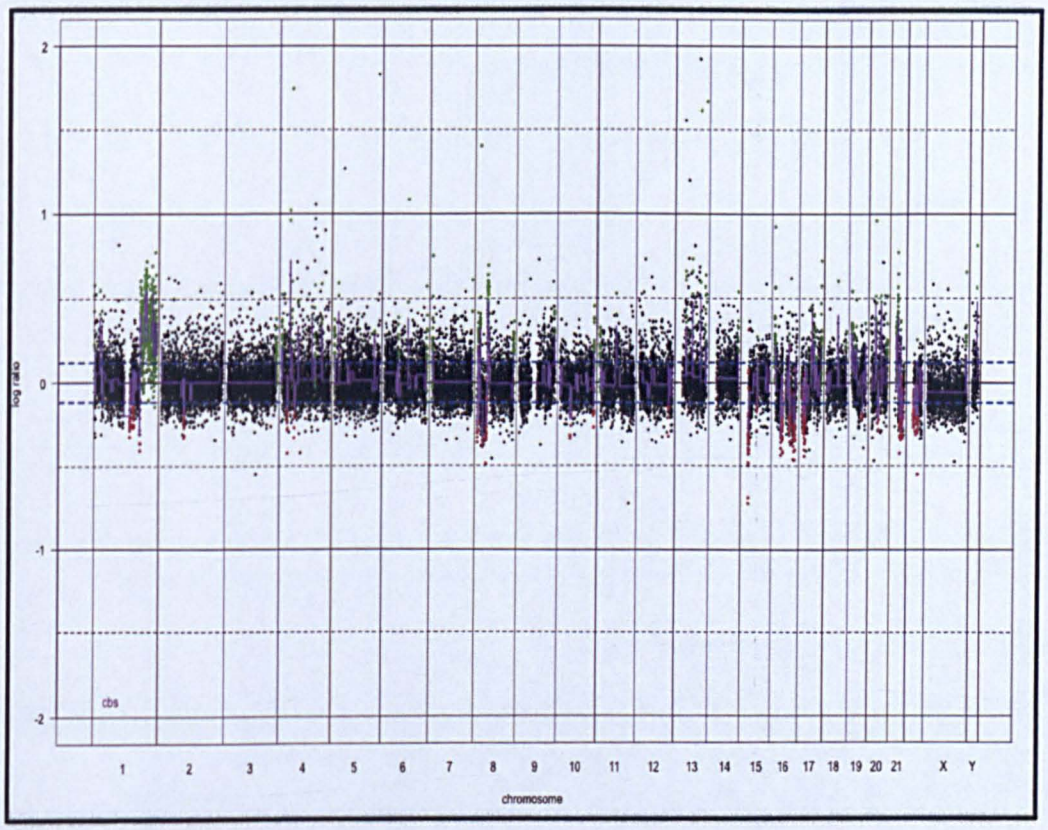

Figure 5-48: Genome plot of invasive lobular carcinoma which has been dissected from case 8 showing gain/amplification of 1q, 8p and 13q and loss of 15p, 16q, 17p 19q and 20q

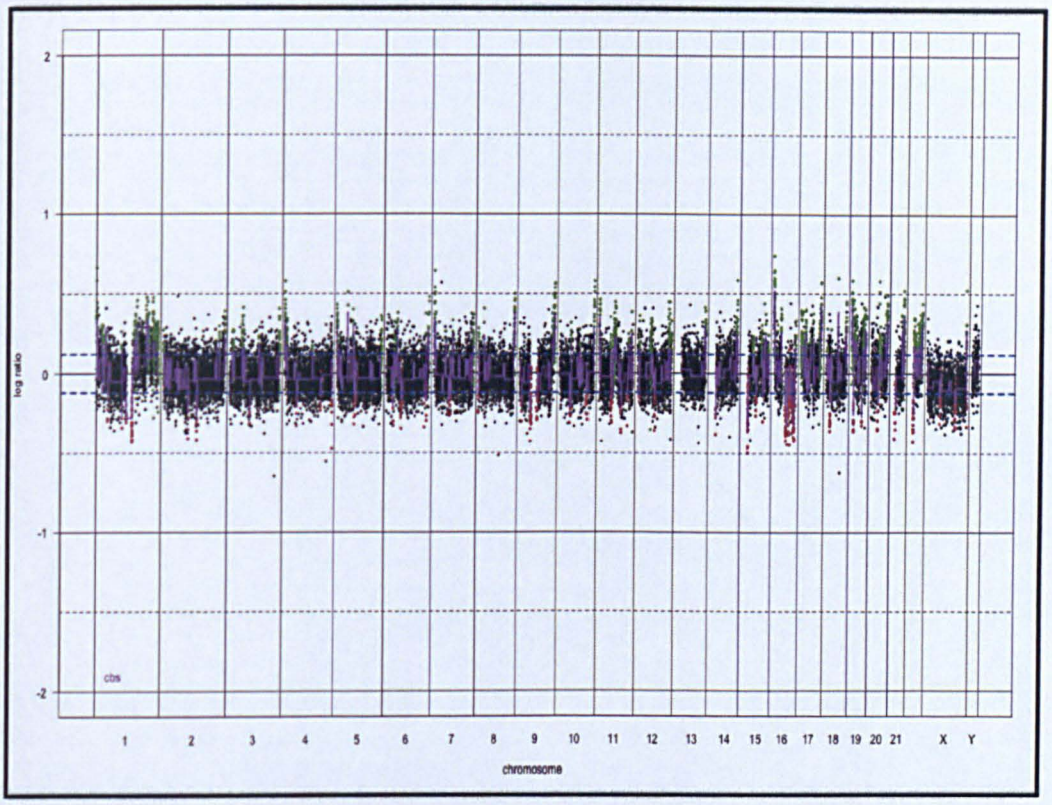

Figure 5-49: Genome plot of invasive tubular carcinoma which has been dissected from case 8 showing genetic changes of most of the chromosomes including gain of 1q and 16p and loss of 16q

Table 5-10: Genetic changes of case 8 (ILC) and 9 (TC)

chrom	map	Cytogenetic Band	ILC-8	TC-9
1	1:2277295..3757389	p36.33-p36.32	GAIN	GAIN
1	1:7038707..12129387	p36.23-p36.22		GAIN
1	1:23800462..24461606	p36.12-p36.11	GAIN	GAIN
1	1:25312395..25779600	p36.11	GAIN	
1	1:34515166..35375482	p34.3	LOSS	LOSS
1	1:150269698..246624589	q21.3-q44	AMP	GAIN
2	2:87128774..98327997	2q11.2		LOSS
2	2:132279581..132994118	2q21.1-q21.2		LOSS
3	3:9467084.10540466	p25.3		GAIN
3	3:46851921..53308680	p21.31-p21.1		GAIN
3	3:183258533..195960808	q26.33-q29	GAIN	GAIN
4	4:9371304....23169797	p16.2-p15.2	LOSS	
4	4:38594738..41243420	p14-p13	GAIN	
5	5:43351415..43702315	5p12		GAIN
5	5:65203593..68826309	q12.3		GAIN
5	5:176368478..180676573	q35.2-q35.3	GAIN	
6	6:42373615..44434337	p21.1		GAIN
6	6:57335587...58075261	p11.2	LOSS	LOSS
6	6:61959143..62918629	q12		LOSS
6	6:160773903..161249786	q25.3-q26		LOSS
7	7:44083631..45018187	p13		GAIN
8	8:21864085..23175482	p21.3-p21.2		GAIN
8	8:39937888..58230037	p12-q11.21	AMP	
8	8:143743728..144743580	q24.3	GAIN	GAIN
9	9:39131199...71033904	p13.1-q12		LOSS
9	9:130513305..138069659	q33.1-q34.3	GAIN	GAIN
10	10:38598310...43015352	p11.21-q11.21	LOSS	LOSS
10	10:43498972..44019673	q11.21		GAIN
11	11:46261972..48165018	p11.2		GAIN
11	11:49003873..49980055	p11.2-q12.1		LOSS
11	11:60817912..64500237	q12.2-q14.1		GAIN
11	11:80636716..133454282	q14.1-q25		LOSS
12	12:5972109..7247166	p13.31		GAIN
12	12:48027380..55251462	q13.11-q13.2	GAIN	
12	12:121193338..125667418	q24.23-q24.31		GAIN
13	13:20904235..113346314	q11-q34	AMP	
13	13:110995727..111374279	q34		GAIN
14	14:99683934..100817227	q32.2-q32.33		GAIN
15	15:20094045..32954812	q11.1-q15.1	LOSS	
16	16:11139..31764125	p13.3-p11.2-p11.2-q1	GAIN	GAIN
16	16:48900991..84593836	p11.2-q24.3	LOSS	LOSS
17	17:2256623..5083694	p13.3-p13.2		GAIN
17	17:6879623..8614953	p13.2-p13.1		GAIN
17	17:9455707.15687248	P12	LOSS	
17	17:16917282..18377155	p11.2		GAIN
17	17:36690553..49204340	q12-q21.33	GAIN	
17	17:729302663..78900648	q25.1-q25.3		GAIN
18	18:14304059..14984939	p11.21		LOSS
18	18:44404930..44713872	q21.1	GAIN	
18	18:74032492..74812028	q23		GAIN
19	19:960519..2970392	p13.3	GAIN	GAIN
19	19:2795315..8663945	p13.2-q12		GAIN
19	19:8629145..9060080	p13.2		LOSS
19	19:43266180..43833261	q13.13-q13.2	LOSS	LOSS
19	19:45182685..51060676	q13.31-q13.42		GAIN
19	19:54392659..54877591	q13.41-q13.42		GAIN
20	20:29421720..29996640	q11.21	LOSS	LOSS
21	21:10907345..15399525	p11.2-q11.2		LOSS
21	21:43466719...45929047	q22.3		GAIN

5.4.8 Chromosomal regions frequently affected in LNGBN family

LNGBN family showed recurrent gains at 1p12-q44 (100%), 16p13.3-11.2, 1p36.21-35.3, 13q11-34, 20q13-33 (>60%) and losses at 16q11.2-24.3 (100%), 1p35.1-34.3, 4q13-22.3 and 9p13.1-q12 (>80%), **(Figures 5-50, 5-51 and 5-52).**

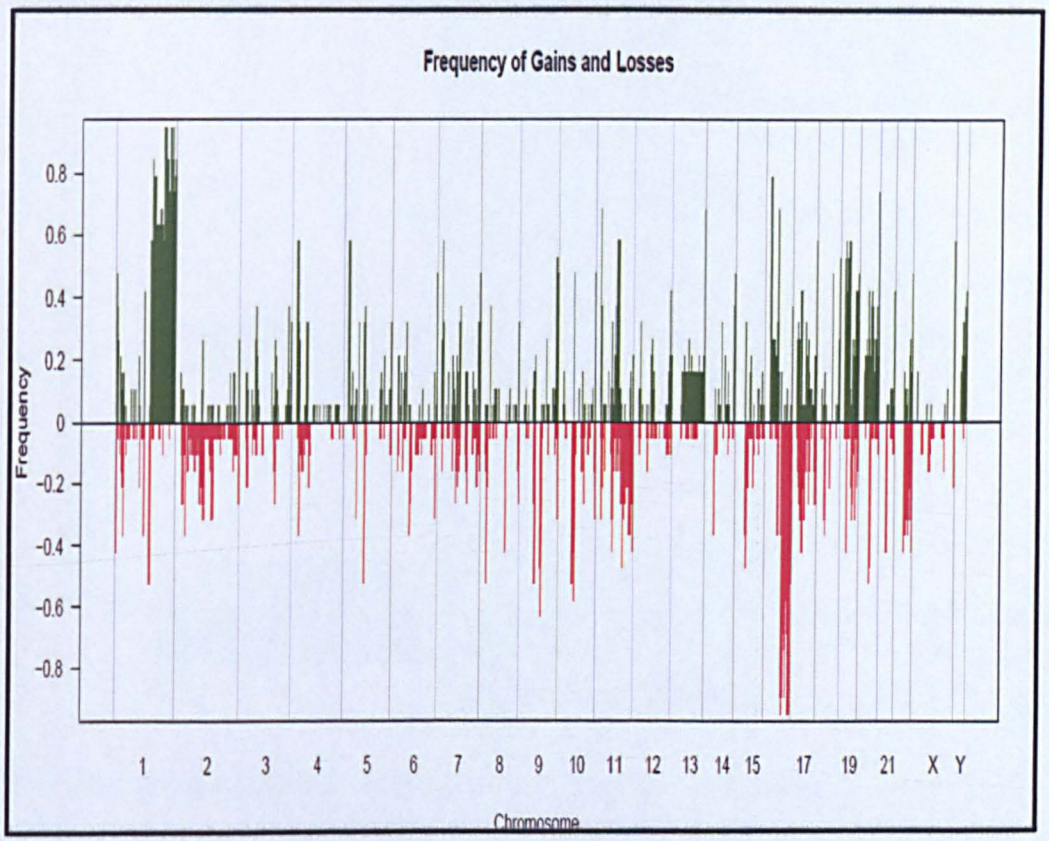

Figure 5-50: The proportion of low nuclear grade neoplastic lesions in which each clone is gained (green bars) or lost (red bars) is plotted (Y axis) for each BAC clone according to genomic location X axis.

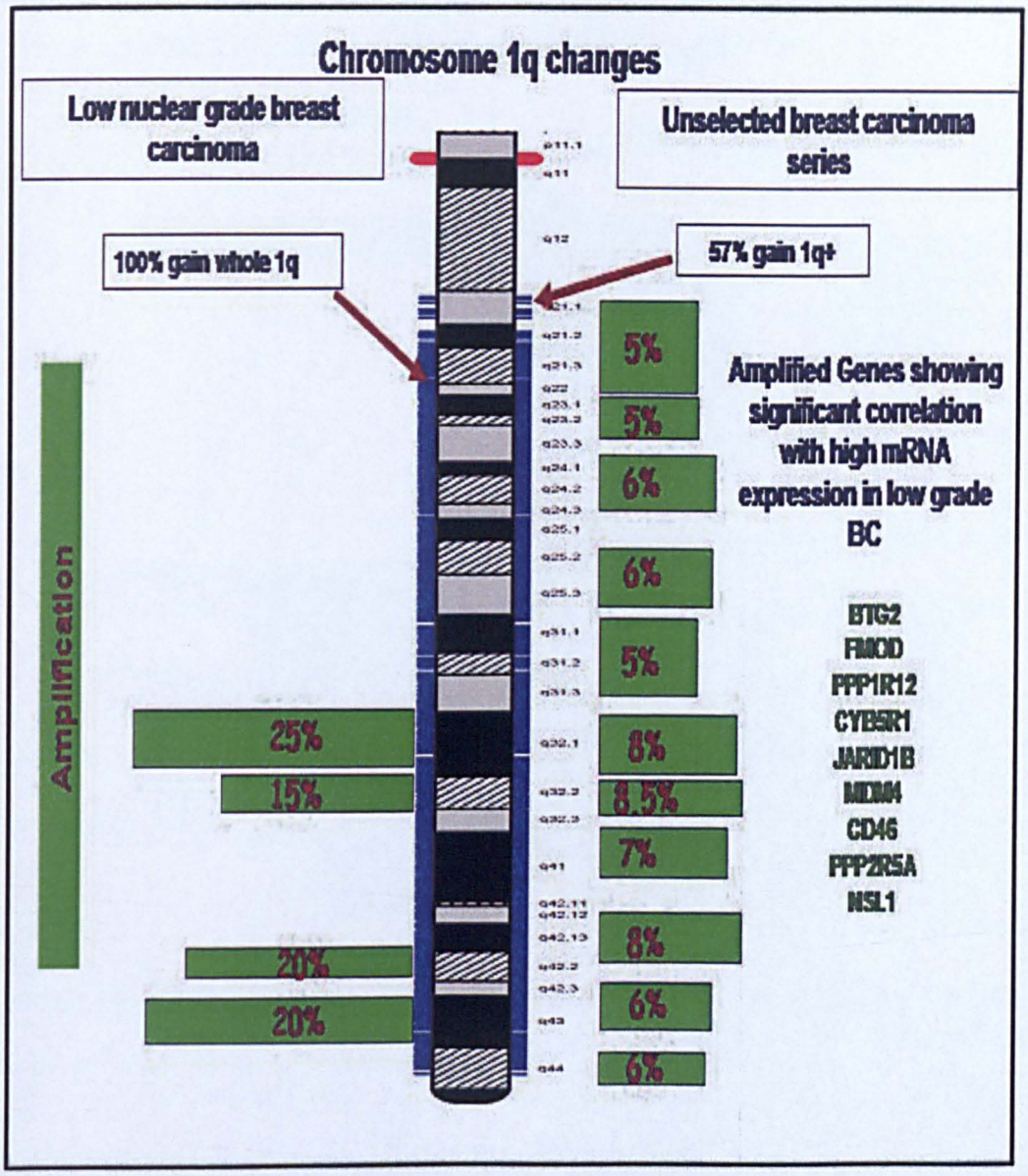

Figure 5-51: Common genetic changes on 1q in both low nuclear grade and unselected breast cancer series

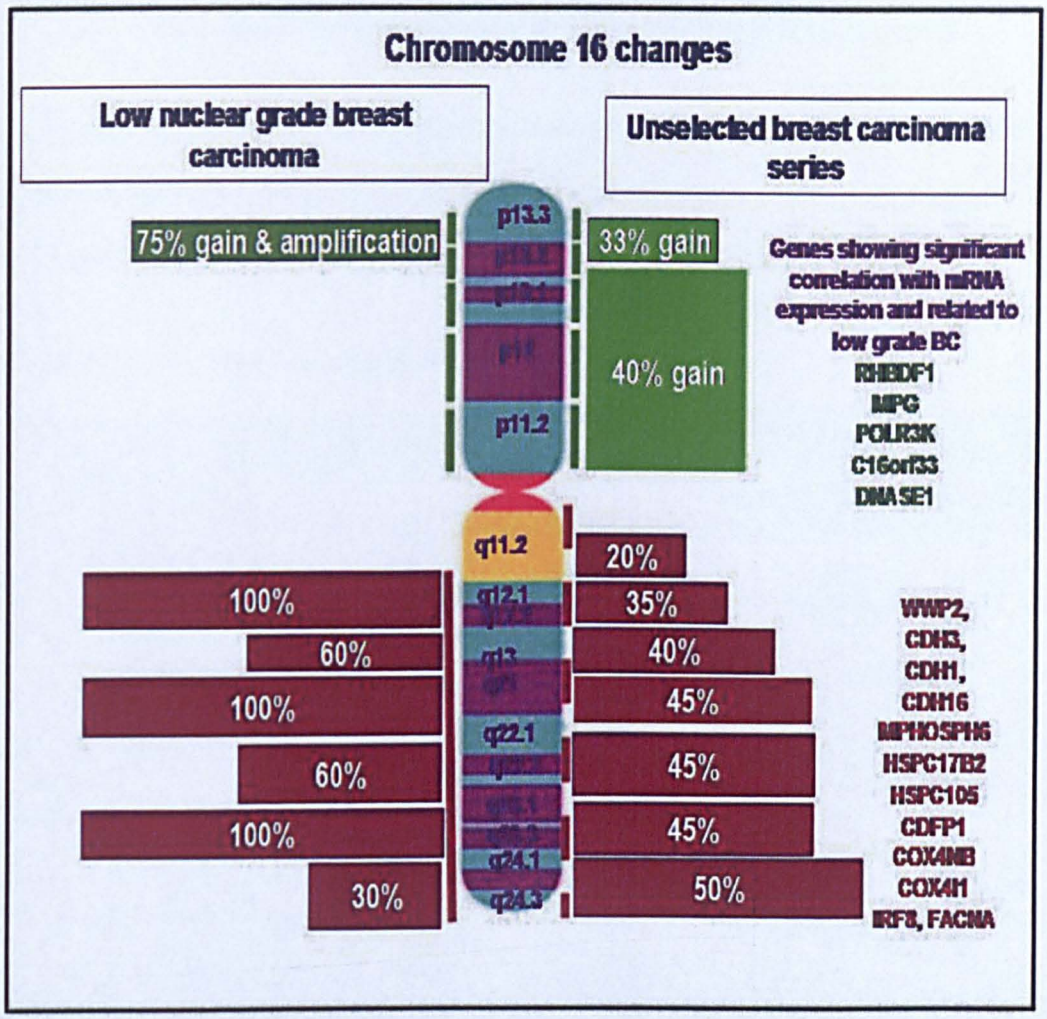

Figure 5-52: Common genetic changes on chromosome 16 in both low nuclear grade and unselected breast cancer series.

5.4.9 Common genetic changes of columnar cell lesions

All columnar cell lesions showed simplex pattern genome plot including gain of 1q whole arm and loss of 16q whole arm. None of CCL showed amplification. Common genetic changes of columnar cell lesions were summarized in (**Table 5-11**).

Table 5-11: Common genetic changes of columnar cell lesions

chromosome	map	Cytogenetic Band	Genetic changes	%
1	1:2697923..3757389	p36.32	LOSS	100
1	1:4114075..5665582	p36.2	LOSS	100
1	1:5873942...6950771	p36.31	GAIN	50
1	1:34515166..35375482	p34.3	LOSS	50
1	1:120436410..246624589	p12	GAIN	100
1	1:236749347..	q43-q44	GAIN	100
3	3:46851921..53308680	p21.31-p21.1	GAIN	75
4	4:9371304....23169797	p16.2-p15.2	LOSS	100
5	5:176368478..180676573	q35.2-q35.3	GAIN	75
6	6:57335587...58075261	p11.2	LOSS	75
7	7:61091237..62439460	q11.1-q11.21	GAIN	75
8	8:6755220..8042158	p23.1	LOSS	75
9	9:130513305..138069659	q33.1-q34.3	GAIN	75
16	16:48900991..84593836	p11.2-q24.3	LOSS	100
18	18:44404930..44713872	q21.1	GAIN	50
19	19:28680998..32819119	p12-q13.11	LOSS	75
19	19:8629145..9060080	p13.2	LOSS	75

5.4.10 Frequently amplified regions in LGBN family

The most common amplified regions in LGBN family were 1q42.13 (4 cases out of 9), 19p13.3 (3 cases out of 9), 1p12, 1q32.1, and 1q21.1 (2 cases out of 9). None of the columnar cell lesions showed recurrent amplification. Common amplified genes are listed in (**Tables 5-12, 5-13, 5-14, 5-15, 5-16, 5-17 and 5-18**).

Table 5-12: list of genes that were relevant to low grade breast cancer

Gene	Location	Function	Overexpression and breast cancer	References
ARF1	1q42-13	Involved in protein trafficking and signal transduction.	ER+ breast cancer	184, 185
OBSCN	1q42-13	Involved in myofibrillogenesis.	Low grade/ER+ breast cancer. Overexpression was associated with low risk of 5 years distant metastases	176, 186, 187
PNPEP	1q32.1	Involved in intracellular transport.	ER+	176, 186-191
PPP1R12B	1q32.1	It regulates myosin phosphatase activity and augments Calcium sensitivity of the contractile apparatus.	Low grade	176, 186-191
CYB5R1	1q32.1	Involved in desaturation and elongation of fatty acids, cholesterol biosynthesis, drug metabolism, and, in erythrocyte, methemoglobin reduction.	ER+	176, 186, 191
BTG2	1q32.1	It is p53 inducible antiproliferative gene that modulates transcription regulation modulated by ESR1.	ER+/low grade, wild type p53 and good prognosis	176, 186-194
FMOD	1q32.1	It may participate in the assembly of the extracellular matrix as it interacts with type I and type II collagen fibrils and inhibits fibrillogenesis in vitro. It may also regulate TGF-beta activities by sequestering TGF-beta into the extracellular matrix	ER+/low grade, wild type p53 and good prognosis	176, 186-195
MDM4	1q32.1	Inhibits p53- and p73-mediated cell cycle arrest and apoptosis and inhibits degradation of MDM2. MDM4 can reverse MDM2-targeted degradation of p53 while maintaining suppression of p53 transactivation and apoptotic functions	ER+ and amplified in 5% of breast cancers	176-183, 186-191
MUC1	1q22	Its protein serves a protective function by binding to pathogens and also functions in a cell signaling capacity. Overexpression, aberrant intracellular localization, and changes in glycosylation of this protein have been associated with carcinomas. Multiple alternatively spliced transcript variants that encode different isoforms of this gene have been reported.	ER+ and marker of luminal restrictive progenitor cells	196-198
MAPKAPK2	1q32.1	In conjunction with p38 MAP kinase, this kinase is known to be involved in many cellular processes including stress and inflammatory responses, nuclear export, gene expression regulation and cell proliferation. Heat shock protein HSP27 was shown to be one of the substrates of this kinase in vivo. Two transcript variants encoding two different isoforms have been found for this gene	ER+	176, 186-191, 199-201
NOTCH2	1p12	It functions as a receptor for membrane-bound ligands Jagged1, Jagged2 and Delta1 to regulate cell-fate determination. Upon ligand activation through the released notch intracellular domain (NICD) it forms a	Overexpressed in BC	176, 186-191, 202-205

		transcriptional activator complex with RBP-J kappa and activates genes of the enhancer of split locus. It affects the implementation of differentiation, proliferation and apoptotic programs		
TRAF3IP3	1q32.2	The gene encodes a protein that mediates cell growth by modulating the c-Jun N-terminal kinase signal transduction pathway. The encoded protein may also interact with a large multiprotein assembly containing the phosphatase 2A catalytic subunit	ER+/low grade, wild type p53 and good prognosis	176, 186-191, 206
IRF2BP2	1q42.3	This gene encodes an interferon regulatory factor-2 (IRF2) binding protein that interacts with the C-terminal transcriptional repression domain of IRF2. Alternative splicing results in multiple transcript variants encoding distinct isoforms	ER+/low grade	176, 186-191, 207
CCND1	11q13.3	It is essential for the control of the cell cycle at the G1/S (start) transition	ILC, ER+ and low grade	100
FADD	11q13.3	It is an apoptotic adaptor molecule that recruits caspase-8 or caspase-10 to the activated Fas (CD95) or TNFR-1 receptors. The resulting aggregate called the death-inducing signaling complex (DISC) performs caspase-8 proteolytic activation.	Ductal carcinoma	202, 208, 209
MKNK2	19q13.3	MAP kinase-interacting kinase-2 (Mnk2) is one of the downstream kinases activated by MAP kinases. It phosphorylates the eukaryotic initiation factor 4E (eIF4E), although the role of eIF4E phosphorylation and the role of Mnk2 in the process of protein translation are not well understood	ER+/low grade, wild type p53 and good prognosis	176, 186-191, 202, 210, 211
NME3	16p13.3	Probably has a role in normal hematopoiesis by inhibition of granulocyte differentiation and induction of apoptosis	Luminal cancers	212, 213

Candidate amplified genes on chromosome 1

The most frequently amplified region among LNGBC was 1q42.13 starting at (228270361) and ending at (228683467). This region contains 15 genes (**Table 5-12**) and only 6 of them showed significant correlation between copy number changes and mRNA expressions (*ARF1, C1orf35, GUK1, OBSCN, TRIM11 and HIST3H2A)* [176]. However, according to the meta-analysis of publicly available gene expression data, *ARF1* and *OBSCN* were the only relevant genes as overexpression of *ARF* and *OBSCN*-mRNAs was more common in low grade/ER positive breast cancer [176-186]. Moreover, overexposing of *OBSCN* was associated with low risk of 5-year distant metastases [176, 187].

The second most common amplified region on chromosome 1 was 1q32.1 which was commonly amplified in luminal cancer [38]. Genes showed correlation between copy number change and their gene expression are presented in (**Table 5-13**). Meta-analysis of gene expression data bases has demonstrated that *RNPEP, PPPIR12B, CYB5R1, BTG2, FMOD,*

MDM4, LGTN1 and MAPKAPK2 are associated with ER+ and low grade phenotype [176-202]. Interestingly, *MDM4* is one of the major regulator genes of the most important tumour suppressor genes in human cancer; p53. For that reason we decided to explore this further by exploring the role of MDM4 in BC and details are shown at the end of this chapter. Overexpression of *NOTCH2, TRAF3IP3 and IRF2BP2* genes that located on 1p12, p32.2 and p42.3, showed significant association with ER positive expression [176-202].

Table 5-13: List of genes on 1q42.13 that were frequently amplified in low nuclear grade breast neoplasia and the correlation between their copy number changes and both mRNA expression and traditional clinicopathological features in breast cancer.

ch	start	end	Band	Gene	Correlation with gene expression	Correlation	No of cases	No of lesions
1	228270361	228286912	q42.13	ARF1	YES (p=2E-6)	ER+	4	5
1	228288429	228293112	q42.13	C1orf35	YES (p=2E-6)	High grade	4	5
1	228294380	228297013	q42.13	MRPL55	NA	NA	4	5
1	228327663	228336685	q42.13	GUK1	YES (p=2E-6)	High grade	4	5
1	228337415	228347523	q42.13	GJC2	NA	NA	4	5
1	228351787	228353213	q42.13	C1orf148	NA	NA	4	5
1	228353429	228369957	q42.13	C1orf69	NA	NA	4	5
1	228391204	228401365	q42.13	C1orf145	NA	NA	4	5
1	228395861	228566575	q42.13	OBSCN	YES (p=2E-6)	- ER+ - Low grade -Good prognosis -Free metastases	4	5
1	228581381	228594517	q42.13	TRIM11	YES (p=2E-6)	NA	4	5
1	228595636	228604583	q42.13	TRIM17	NA	NA	4	5
1	228612546	228613026	q42.13	HIST3H3	YES (p=2E-6)	NA	4	5
1	228645065	228645560	q42.13	HIST3H2A	NA	NA	4	5
1	228645808	228646259	q42.13	HIST3H2BB	NA	NA	4	5
1	228675094	228683467	q42.13	RNF187	NA	NA	4	6

Table 5-14: List of genes on 1q32.1 that were frequently amplified in low nuclear grade breast neoplasia and the correlation between their copy number changes and both mRNA expression and traditional clinicopathological features in breast cancer

Ch	start	end	Band	Gene	Correlation with gene expression	Correlations	No of cases	No of lesions
1	200708686	200829829	q32.1	CAMSAP1L1	NA	NA	2	4
1	200842083	200843306	q32.1	GPR25	NA	NA	2	4
1	200860639	200884863	q32.1	C1orf106	NA	NA	2	4
1	200938520	200992828	q32.1	KIF21B	NA	NA	2	4
1	201008640	201081694	q32.1	CACNA1S	YES (p=0.005)	NA	2	4
1	201103901	201140702	q32.1	TMEM9	NA	NA	2	4
1	201159953	201198080	q32.1	IGFN1	NA	NA	2	4
1	201252580	201302115	q32.1	PKP1	NA	NA	2	4
1	201328136	201346808	q32.1	TNNT2	NA	NA	2	4
1	201349970	201368669	q32.1	LAD1	NA	NA	2	4
1	201372896	201398994	q32.1	TNNI1	NA	NA	2	4
1	201434622	201438365	q32.1	PHLDA3	NA	NA	2	4
1	201452658	201478584	q32.1	CSRP1	NA	NA	2	4
1	201592601	201796097	q32.1	NAV1	NA	NA	2	4
1	201798288	201853422	q32.1	IPO9	NA	NA	2	4
1	201857817	201861426	q32.1	SHISA4	NA	NA	2	4
1	201865584	201915716	q32.1	LMOD1	NA	NA	2	4
1	201924619	201939787	q32.1	TIMM17A	NA	NA	2	4
1	201951766	201975262	q32.1	RNPEP	YES (p=0.001)	ER +	2	4
1	201977073	201986304	q32.1	ELF3	YES (p=0.001)	NA	2	4
1	202092029	202098634	q32.1	GPR37L1	NA	NA	2	4
1	202101977	202113866	q32.1	ARL8A	YES (p=0.001)	NA	2	4
1	202116141	202130709	q32.1	PTPN7	NA	NA	2	4
1	202163118	202288889	q32.1	LGR6	NA	NA	2	4
1	202300786	202311094	q32.1	UBE2T	NA	NA	2	4
1	202317836	202557697	q32.1	PPP1R12B	YES (p=0.003)	Low grade	2	4
1	202559724	202679551	q32.1	SYT2	NA	NA	2	4
1	202696533	202778563	q32.1	KDM5B	NA	NA	2	4
1	202848088	202858263	q32.1	RABIF	NA	NA	2	4
1	202860230	202897764	q32.1	KLHL12	NA	NA	2	4
1	202909963	202927700	q32.1	ADIPOR1	YES (p=0.003)	NA	2	4
1	202931004	202936404	q32.1	CYB5R1	YES (p=0.003)	ER+	2	4
1	202976534	202993197	q32.1	TMEM183A	NA	NA	2	4
1	202995626	203047864	q32.1	PPFIA4	YES (p=0.0007)	NA	2	4
1	203052257	203055377	q32.1	MYOG	NA	NA	2	4
1	203059782	203136533	q32.1	ADORA1	YES (p=0.0007)	NA	2	4

Ch	start	end	Band	Gene	Correlation with gene expression	Correlations	No of cases	No of lesions
1	203136939	203144942	q32.1	MYBPH	NA	NA	2	4
1	203148059	203155922	q32.1	CHI3L1	NA	NA	2	4
1	203185207	203198860	q32.1	CHIT1	NA	NA	2	4
1	203274664	203278725	q32.1	BTG2	YES (p=5E-6)	- ER+ - Low grade - Good prognosis -Wild type p53	2	4
1	203309753	203320289	q32.1	FMOD	YES (p=5E-6)	- ER+ - Low grade - Good prognosis -Wild type p53	2	4
1	203444883	203460475	q32.1	PRELP	NA	NA	2	4
1	203463271	203478077	q32.1	OPTC	NA	NA	2	4
1	203595928	203713207	q32.1	ATP2B4	NA	NA	2	4
1	204001575	204010393	q32.1	C1orf157	NA	NA	2	4
1	204042246	204096867	q32.1	SOX13	YES (p=5E-6)	NA	2	4
1	204100190	204121307	q32.1	ETNK2	NA	NA	2	4
1	204123944	204135465	q32.1	REN	YES (p=5E-6)	NA	2	4
1	204159469	204165628	q32.1	KISS1	NA	NA	2	4
1	204167288	204183220	q32.1	GOLT1A	YES (p=5E-6)	NA	2	4
1	204187982	204329044	q32.1	PLEKHA6	NA	NA	2	4
1	204372494	204380944	q32.1	PPP1R15B	NA	NA	2	4
1	204391770	204463852	q32.1	PIK3C2B	YES (p=5E-6)	NA	2	4
1	204485511	204598840	q32.1	MDM4	YES (p=5E-6)	ER+	2	4
1	204586298	204654597	q32.1	LRRN2	NA	NA	2	4
1	204797804	204991950	q32.1	NFASC	NA	NA	2	4
1	205012340	205047136	q32.1	CNTN2	NA	NA	2	4
1	205052258	205053588	q32.1	TMEM81	NA	NA	2	4
1	205055270	205091143	q32.1	RBBP5	NA	NA	2	4
1	205111632	205180727	q32.1	DSTYK	NA	NA	2	4
1	205197038	205242465	q32.1	TMCC2	NA	NA	2	4
1	205271187	205290888	q32.1	NUAK2	NA	NA	2	4
1	205305220	205326166	q32.1	KLHDC8A	NA	NA	2	4
1	205350506	205419059	q32.1	LEMD1	NA	NA	2	4
1	205473723	205501921	q32.1	PCTK3	NA	NA	2	4
1	205538112	205572045	q32.1	MFSD4	NA	NA	2	4
1	205585237	205602000	q32.1	ELK4	NA	NA	2	4
1	205626981	205649630	q32.1	SLC45A3	NA	NA	2	4
1	205681947	205719361	q32.1	NUCKS1	YES (p=0.0003)	NA	2	4
1	205737115	205744610	q32.1	RAB7L1	YES (p=0.0003)	NA	2	4
1	205758224	205782198	q32.1	SLC41A1	NA	NA	2	4
1	205797154	205819260	q32.1	PM20D1	NA	NA	2	4
1	205882176	205912588	q32.1	SLC26A9	NA	NA	2	4

Ch	start	end	Band	Gene	Correlation with gene expression	Correlations	No of cases	No of lesions
1	206137335	206155066	q32.1	FAM72A	NA	NA	2	4
1	206224347	206231639	q32.1	AVPR1B	NA	NA	2	4
1	206238872	206306131	q32.1	C1orf186	NA	NA	2	4
1	206317459	206332104	q32.1	CTSE	NA	NA	2	4
1	206515187	206637783	q32.1	SRGAP2	NA	NA	2	4
1	206643796	206670222	q32.1	IKBKE	NA	NA	2	4
1	206664449	206671061	q32.1	C1orf147	NA	NA	2	4
1	206680879	206762615	q32.1	RASSF5	NA	NA	2	4
1	206764977	206785904	q32.1	LGTN	YES (p=0.0003)	Low grade	2	4
1	206800108	206857758	q32.1	DYRK3	NA	NA	2	4
1	206858289	206907626	q32.1	MAPKAPK2	YES (p=0.0003)	ER+	2	4
1	206940947	206945839	q32.1	IL10	NA	NA	2	4
1	206972215	207016325	q32.1	IL19	NA	NA	2	4
1	207038699	207042568	q32.1	IL20	YES (p=0.0003)	NA	2	4

Table 5-15: List of genes on p12, q32.2 and q42.3 that were frequently amplified in low nuclear grade breast neoplasia and the correlation between their copy number changes and both mRNA expression and traditional clinicopathological features in breast cancer

Ch	start	end	Band	Gene	Correlation with gene expression	Correlations	No of cases	No of lesions
1	120454178	120612276	p12	NOTCH2		Overexpression in BC	2	4
1	207191866	207206101	q32.2	C1orf116	YES (p=0.0003)	NA	2	4
1	207217194	207226325	q32.2	YOD1	NA	NA	2	4
1	207226620	207254368	q32.2	PFKFB2	NA	NA	2	4
1	209757045	209787283	q32.2	CAMK1G	NA	NA	2	4
1	209788220	209825820	q32.2	LAMB3	NA	NA	2	4
1	209848670	209849732	q32.2	G0S2	NA	NA	2	4
1	209859510	209908295	q32.2	HSD11B1	NA	NA	2	4
1	209929399	209955665	q32.2	TRAF3IP3	YES (p=0.0003)	- ER+ - Low grade - Good prognosis - Wild type p53	2	4
1	209955661	209957904	q32.2	C1orf74	NA	NA	2	4
1	209961262	209979479	q32.2	IRF6	YES (p=0.0003)	NA	2	4
1	210001333	210030908	q32.2	C1orf107	YES (p=0.0003)	NA	2	4
1	234527059	234614849	q42.2	TARBP1	YES(p=1.1E-9)	NA	2	4
1	234740017	234745271	q42.3	IRF2BP2	YES (p=5E-7)	- ER+ - Low grade -	2	4
1	235272662	235292256	q42.3	TOMM20	YES (p=5E-7)	NA	2	4
1	235294950	235324573	q42.3	RBM34	NA	NA	2	4

Candidate genes of chromosome 19

aCGH of 2 cases of ILC and DCIS of another case showed amplification of 19p13.3 region. *CNN2, ABCA7, HMHA1, C1orf23, CIRBP, and C19orf24 genes* showed significant correlation between their copy number changes and gene expression [176]. Interestingly, meta-analysis showed that overexpression of mRNA of these genes was related to either ILC and/or DCIS. *MKNK2* [174-180] is another gene showing correlation between its copy number and mRNA expression. MKNK2 overexpression commonly occurred in ER+, low grade tumours that lack p53 mutation [191].

Candidate genes of chromosome 11

Two cases of ILC carcinoma showed amplification at q13.3 which is the home of cyclin D1 gene *(CCND1), PPFIA1, DHCR7 and FADD* genes that showed upregulation in relation to amplification [202]. *CCND1* is commonly overexpressed in ILC and we confirmed its role in the development of LNGBN earlier in this chapter and in Chapter 3.

Candidate genes of chromosome 16

16p13+, 1q+ and 16q- is the common genetic changes triad of low grade/ER+. Among genes on 16p13 regions that have shown significant correlation between copy number changes and mRNA was *NME3* genes [176-202] which is one of ER responsive genes and is commonly overexpressed in the luminal BC subclass [213].

Table 5-16: List of frequently amplified genes on chromosome 19 of low nuclear grade breast neoplasia, correlation of copy number changes of each genes and mRNA expression in unselected breast cancer and associations of each gene expression and clinicopathological parameters.

Ch	start	end	Band	Gene	Correlation with gene expression	Correlations	No of cases	No of lesions
19	496454	505340	p13.3	MADCAM1	NA	NA	3	3
19	507497	519653	p13.3	C19orf20	NA	NA	3	3
19	531733	542084	p13.3	CDC34	NA	NA	3	3
19	544027	549919	p13.3	GZMM	NA	NA	3	3
19	571325	583492	p13.3	BSG	NA	NA	3	3
19	589893	617157	p13.3	HCN2	NA	NA	3	3
19	617223	633568	p13.3	POLRMT	NA	NA	3	3
19	639895	643703	p13.3	FGF22	NA	NA	3	3
19	647530	663227	p13.3	RNF126	NA	NA	3	3
19	676389	683392	p13.3	FSTL3	NA	NA	3	3
19	685548	695483	p13.3	PRSSL1	NA	NA	3	3
19	708953	748328	p13.3	PALM	NA	NA	3	3
19	751133	764318	p13.3	C19orf21	NA	NA	3	3
19	797392	812327	p13.3	PTBP1	NA	NA	3	3
19	825097	832017	p13.3	AZU1	NA	NA	3	3
19	840985	848175	p13.3	PRTN3	NA	NA	3	3
19	852291	856242	p13.3	ELANE	NA	NA	3	3
19	859665	863606	p13.3	CFD	NA	NA	3	3
19	867964	893218	p13.3	MED16	NA	NA	3	3
19	896503	913225	p13.3	C19orf22	NA	NA	3	3
19	917342	921014	p13.3	KISS1R	NA	NA	3	3
19	926037	972781	p13.3	ARID3A	NA	NA	3	3
19	984328	994569	p13.3	WDR18	NA	NA	3	3
19	1000437	1E+06	p13.3	GRIN3B	NA	NA	3	3
19	1009650	1E+06	p13.3	C19orf6	NA	NA	3	3
19	1026298	1E+06	p13.3	CNN2	NA	Overexpressed in ILC	3	3
19	1040102	1E+06	p13.3	ABCA7	NA	Overexpressed in ILC and DCIS	3	3
19	1066025	1E+06	p13.3	HMHA1	NA	Overexpressed in ILC	3	3
19	1086578	1E+06	p13.3	POLR2E	NA	NA	3	3
19	1104043	1E+06	p13.3	GPX4	NA	NA	3	3
19	1107634	1E+06	p13.3	SBNO2	NA	NA	3	3
19	1205798	1E+06	p13.3	STK11	NA	NA	3	3
19	1229178	1E+06	p13.3	C19orf26	NA	NA	3	3
19	1241749	1E+06	p13.3	ATP5D	NA	NA	3	3
19	1248552	1E+06	p13.3	MIDN	NA	NA	3	3
19	1267471	1E+06	p13.3	C19orf23	NA	Overexpressed in ILC	3	3

Ch	start	end	Band	Gene	Correlation with gene expression	Correlations	No of cases	No of lesions
19	1269267	1E+06	p13.3	CIRBP	NA	Overexpressed in ILC and DCIS	3	3
19	1275520	1E+06	p13.3	C19orf24	NA	Overexpressed in ILC	3	3
19	1285892	1E+06	p13.3	MUM1	NA	NA	3	3
19	1286168	1E+06	p13.3	EFNA2	NA	NA	3	3
19	1383883	1E+06	p13.3	NDUFS7	NA	NA	3	3
19	1397089	1E+06	p13.3	GAMT	NA	NA	3	3
19	1407584	1E+06	p13.3	DAZAP1	NA	NA	3	3
19	1438363	1E+06	p13.3	RPS15	NA	NA	3	3
19	1450148	1E+06	p13.3	APC2	NA	NA	3	3
19	1473203	1E+06	p13.3	C19orf25	NA	NA	3	3
19	1481427	1E+06	p13.3	PCSK4	NA	NA	3	3
19	1491067	1E+06	p13.3	REEP6	NA	NA	3	3
19	1505023	2E+06	p13.3	ADAMTSL5	NA	NA	3	3
19	1524073	2E+06	p13.3	PLK5P	NA	NA	3	3
19	1554669	2E+06	p13.3	MEX3D	NA	NA	3	3
19	1576678	2E+06	p13.3	MBD3	NA	NA	3	3
19	1597180	2E+06	p13.3	UQCR	NA	NA	3	3
19	1609293	2E+06	p13.3	TCF3	NA	NA	3	3
19	1753662	2E+06	p13.3	ONECUT3	NA	NA	3	3
19	1782076	2E+06	p13.3	ATP8B3	NA	NA	3	3
19	1815245	2E+06	p13.3	REXO1	NA	NA	3	3
19	1852398	2E+06	p13.3	KLF16	NA	NA	3	3
19	1876976	2E+06	p13.3	FAM108A1	NA	NA	3	3

Table 5-17: List of frequently amplified genes on chromosome 11 of low nuclear grade breast neoplasia, correlation of copy number changes of each genes and mRNA expression in unselected breast cancer and associations of each gene expression and clinicopathological parameters.

Ch	start	end	Band	Gene	Correlation with gene expression	Correlations	No of cases	No of lesions
11	68522090	68609399	q13.3	CPT1A	NA	NA	2	2
11	68658747	68671303	q13.3	MRPL21	NA	NA	2	2
11	68671319	68708069	q13.3	IGHMBP2	NA	NA	2	2
11	68747490	68748455	q13.3	MRGPRD	NA	NA	2	2
11	68771863	68780850	q13.3	MRGPRF	NA	NA	2	2
11	68816350	68858072	q13.3	TPCN2	NA	NA	2	2
11	69061622	69064753	q13.3	MYEOV	NA	NA	2	2
11	69455873	69469241	q13.3	CCND1	confirmed	Confirmed	2	2
11	69468073	69490165	q13.3	ORAOV1	NA	NA	2	2
11	69513007	69519106	q13.3	FGF19	NA	NA	2	2
11	69587797	69590171	q13.3	FGF4	NA	NA	2	2
11	69624736	69634192	q13.3	FGF3	NA	NA	2	2
11	69924664	70035633	q13.3	ANO1	NA	NA	2	2
11	70049269	70053508	q13.3	FADD	YES(p=2.7E-7)	Ductal carcinoma	2	2
11	70116823	70230500	q13.3	PPFIA1	YES(p=2.7E-7)	Ductal carcinoma	2	2
11	70244612	70282689	q13.3	CTTN	NA	NA	2	2
11	70313961	70963623	q13.4	SHANK2	NA	NA	2	2
11	71145457	71159477	q13.4	DHCR7	YES (p=0.03)	Ductal carcinoma	2	2
11	71164217	71212579	q13.4	NADSYN1	NA	NA	2	2
11	71238302	71280091	q13.4	KRTAP5-10	NA	NA	2	2

Table 5-18: List of frequently amplified genes on chromosome 16 of low nuclear grade breast neoplasia, correlation of copy number changes of each genes and mRNA expression in unselected breast cancer and associations of each gene expression and clinicopathological parameters.

Ch	start	end	Band	Gene	Correlation with gene expression	Correlations	No of cases	No of lesions
16	475619	572478	p13.3	RAB11FIP3	NA	NA	2	2
16	577856	604634	p13.3	SOLH	NA	NA	2	2
16	610422	619494	p13.3	C16orf11	NA	NA	2	2
16	617011	634108	p13.3	PIGQ	NA	NA	2	2
16	640176	679271	p13.3	RAB40C	NA	NA	2	2
16	680932	684116	p13.3	WFIKKN1	NA	NA	2	2
16	684429	686347	p13.3	C16orf13	NA	NA	2	2
16	691849	698474	p13.3	C16orf14	NA	NA	2	2
16	699363	717829	p13.3	WDR90	NA	NA	2	2
16	718133	724170	p13.3	RHOT2	NA	NA	2	2
16	725706	728267	p13.3	RHBDL1	NA	NA	2	2
16	730115	732767	p13.3	STUB1	YES (p=1.15E-6)	NA	2	2
16	734648	740444	p13.3	WDR24	NA	NA	2	2
16	742500	755829	p13.3	FBXL16	NA	NA	2	2
16	765173	767478	p13.3	METRN	NA	NA	2	2
16	771158	772589	p13.3	FAM173A	NA	NA	2	2
16	772582	776846	p13.3	CCDC78	NA	NA	2	2
16	776958	797295	p13.3	HAGHL	NA	NA	2	2
16	779771	790997	p13.3	NARFL	NA	NA	2	2
16	812637	818865	p13.3	MSLN	NA	NA	2	2
16	819428	833370	p13.3	MSLNL	NA	NA	2	2
16	834975	838383	p13.3	RPUSD1	YES (p=0.006)	NA	2	2
16	838046	848074	p13.3	CHTF18	NA	NA	2	2
16	848044	850733	p13.3	GNG13	NA	NA	2	2
16	903638	1020984	p13.3	LMF1	NA	NA	2	2
16	1031808	1036979	p13.3	SOX8	NA	NA	2	2
16	1122756	1131437	p13.3	SSTR5	NA	NA	2	2
16	1138226	1146244	p13.3	C1QTNF8	NA	NA	2	2
16	1203241	1271771	p13.3	CACNA1H	NA	NA	2	2
16	1271658	1275256	p13.3	TPSG1	NA	NA	2	2
16	1278336	1280214	p13.3	TPSB2	YES (p=1.15E-6)	ILC	2	2
16	1290678	1292555	p13.3	TPSAB1	YES (p=1.15E-6)	ILC	2	2
16	1306060	1308609	p13.3	TPSD1	NA	NA	2	2
16	1307043	1326838	p13.3	PRSS29P	NA	NA	2	2
16	1359180	1375390	p13.3	UBE2I	YES (p=1.15E-6)	IDC	2	2
16	1383654	1399440	p13.3	BAIAP3	YES (p=1.15E-6)	NA	2	2

Ch	start	end	Band	Gene	Correlation with gene expression	Correlations	No of cases	No of lesions
16	1399243	1401875	p13.3	C16orf42	NA	NA	2	2
16	1401932	1413351	p13.3	GNPTG	YES (p=1.15E-6)	NA	2	2
16	1413206	1464705	p13.3	UNKL	NA	NA	2	2
16	1469754	1479345	p13.3	C16orf91	NA	NA	2	2
16	1484386	1494557	p13.3	CCDC154	NA	NA	2	2
16	1494935	1525085	p13.3	CLCN7	NA	NA	2	2
16	1535940	1538910	p13.3	C16orf38	NA	NA	2	2
16	1543364	1560453	p13.3	TELO2	NA	NA	2	2
16	1560428	1662109	p13.3	IFT140	NA	NA	2	2
16	1583658	1605577	p13.3	TMEM204	NA	NA	2	2
16	1662338	1736716	p13.3	CRAMP1L	NA	NA	2	2
16	1728278	1752072	p13.3	HN1L	NA	NA	2	2
16	1756221	1820317	p13.3	MAPK8IP3	NA	NA	2	2
16	1820322	1821710	p13.3	NME3	YES (p=1.15E-6)	Luminal carcinoma	2	2
16	1821891	1823151	p13.3	MRPS34	YES (p=1.15E-6)	IDC	2	2
16	1823229	1830628	p13.3	EME2	YES (p=1.15E-6)	NA	2	2
16	1826714	1832581	p13.3	SPSB3	YES (p=1.15E-6)	NA	2	2
16	1832933	1839191	p13.3	NUBP2	NA	NA	2	2
16	1840416	1843734	p13.3	IGFALS	NA	NA	2	2
16	1859108	1877195	p13.3	HAGH	YES (p=1.15E-6)	NA	2	2
16	1877225	1890201	p13.3	FAHD1	YES (p=1.15E-6)	NA	2	2
16	1883989	1922102	p13.3	C16orf73	NA	NA	2	2
16	1961464	1968441	p13.3	HS3ST6	NA	NA	2	2
16	1988211	1993327	p13.3	SEPX1	NA	NA	2	2
16	1993976	2004671	p13.3	RPL3L	NA	NA	2	2
16	2009517	2011976	p13.3	NDUFB10	YES (p=1.15E-6)	NA	2	2
16	2012062	2014827	p13.3	RPS2	NA	NA	2	2
16	2017274	2018976	p13.3	RNF151	YES (p=1.15E-6)	NA	2	2
16	2022064	2028751	p13.3	TBL3	NA	NA	2	2
16	2028919	2031550	p13.3	NOXO1	NA	NA	2	2
16	2034150	2037746	p13.3	GFER	YES (p=1.15E-6)	NA	2	2
16	2039968	2044275	p13.3	SYNGR3	NA	NA	2	2
16	2047768	2059763	p13.3	ZNF598	YES (p=1.15E-6)	NA	2	2
16	2069521	2070755	p13.3	NPW	NA	NA	2	2
16	2089816	2097867	p13.3	NTHL1	NA	NA	2	2
16	2097981	2138721	p13.3	TSC2	YES (p=1.15E-6)	NA	2	2
16	2138711	2185899	p13.3	PKD1	NA	NA	2	2
16	2198645	2204140	p13.3	RAB26	NA	NA	2	2
16	2205799	2228129	p13.3	TRAF7	NA	NA	2	2
16	2227184	2246465	p13.3	CASKIN1	NA	NA	2	2
16	2259254	2261011	p13.3	C16orf79	NA	NA	2	2

Ch	start	end	Band	Gene	Correlation with gene expression	Correlations	No of cases	No of lesions
16	2261603	2264822	p13.3	PGP	NA	NA	2	2
16	2273567	2285743	p13.3	E4F1	NA	NA	2	2
16	2286468	2288709	p13.3	DNASE1L2	NA	NA	2	2
16	2289900	2301603	p13.3	DCI	NA	NA	2	2
16	2303124	2318114	p13.3	RNPS1	NA	NA	2	2
16	2325879	2390747	p13.3	ABCA3	NA	NA	2	2

Table 5-19: List of frequently amplified genes on chromosome 1 of low nuclear grade breast neoplasia, correlation of copy number changes of each genes and mRNA expression in unselected breast cancer and associations of each gene expression and clinicopathological parameters.

Ch	start	end	Band	Gene	Correlation with gene expression	Correlations	No of cases	No of lesions
18	44392060	44497466	q21.1	PIAS2	NA	Invasive Ductal carcinoma	2	3
18	44526787	44627658	q21.1	KATNAL2	NA	NA	2	3
18	44542731	44544607	q21.1	TCEB3CL2	NA	NA	2	3
18	44548658	44550534	q21.1	TCEB3CL	NA	NA	2	3
18	44554573	44556449	q21.1	TCEB3C	NA	DCIS	2	3
18	44558943	44561992	q21.1	TCEB3B	NA	DCIS	2	3
18	44633782	44676871	q21.1	HDHD2	NA	NA	2	3
18	44681415	44702745	q21.1	IER3IP1	NA	NA	2	3
19	1905371	1926011	p13.3	SCAMP4	NA	Overexpressed BC	2	2
19	1905417	1913444	p13.3	ADAT3	NA	NA	2	2
19	1941161	1981309	p13.3	CSNK1G2	NA	NA	2	2
19	1952526	1954548	p13.3	C19orf34	NA	NA	2	2
19	1985447	2015702	p13.3	BTBD2	NA	NA	2	2
19	2037481	2051243	p13.3	MKNK2	NA	- ER+ - Low grade - Good prognosis - Wild type p53	2	2

5.4.11 Genetic alteration of tubular carcinoma and invasive lobular carcinoma

Several prevalent alterations (>70%) were common to both TC and ILC: gains of 1q+ whole arm, 16p13.3-q11.2+, 1p36.33-32+, 3p21, 8q24.3+, 9q33.1-34.3+, 19q13.3+, 19p13.2 11+, 11q14.1-25, 20q11.21 and 21q22.3 and losses of 16q whole are, 1p34.3, 6p11.2, 19p13.2, 4p16.2-p15.2, 9p13.1-q12, 11q14.1-q25 and 20q11.21 (Table 4-20). Chromosomal changes differentially associated with tubular carcinoma compared to ILC were summarized in Table and included gains of 1p36.11, 3p21.31-p21.1, 12q13.11-q13.2 and losses of 11p15.5-p15.4. Compared with tubular carcinoma, ILC harboured gains of 1p36.23-p36.22, 1p12 (NOTCH2), 1q21.1, 5q12.3, 75p13, 12q24.23-q24.31, 13q34, 17p13.3-p13.2, 17q25.1-q25.3, 19q13.31-q13.42 and losses of 2q11.2, p11.21, q11.21-q11.22, p11.2-q12.1 and p11.2-q11.2.

Table 5-20: Comparison between genetic characteristics of both tubular carcinoma and invasive lobular carcinoma

ch	map	Cytogenetic Band	Genetic changes	Number of TC count	Number of ILC
1	1:150269698..246624589	q21.3-q44	GAIN	5	4
16	16:11139..31764125	p13.3- q11.2	GAIN	4	4
3	3:46851921..53308680	p21.31-p21.1	GAIN	4	3
1	1:2277295..2485326	p36.33-p36.32	GAIN	3	4
1	1:2697923..3757389	p36.32	GAIN	3	4
8	8:143743728..144743580	q24.3	GAIN	3	4
9	9:130513305..138069659	q33.1-q34.3	GAIN	3	4
19	19:960519..2970392	p13.3	GAIN	3	4
1	1:5873942...6950771	p36.31	GAIN	3	3
1	1:23800462..24461606	p36.12-p36.11	GAIN	3	3
1	1:145190320..148644689	q21.1-q21.2	GAIN	3	3
3	3:183258533..195960808	q26.33-q29	GAIN	3	3
12	12:5972109..7247166	p13.31	GAIN	3	3
19	19:2795315..8663945	p13.2-q12	GAIN	3	3
21	21:43466719...45929047	q22.3	GAIN	3	3
16	16:48900991..84593836	p11.2-q24.3	LOSS	5	3
1	1:34515166..35375482	p34.3	LOSS	4	3
6	6:57335587...58075261	p11.2	LOSS	4	3
19	19:8629145..9060080	p13.2	LOSS	3	3
4	4:9371304.....23169797	p16.2-p15.2	LOSS	3	3
9	9:39131199...71033904	p13.1-q12	LOSS	3	3
11	11:80636716..133454282	q14.1-q25	LOSS	3	3
20	20:29421720..29996640	q11.21	LOSS	3	3
1	1:25312395..25779600	p36.11	GAIN	0	3
3	3:125828183..129284640	p21.31-p21.1	GAIN	0	3
12	12:48027380..55251462	q13.11-q13.2	GAIN	0	4
11	11:4551894...8684969	p15.5-p15.4	LOSS	0	3
1	1:7038707..12129387	p36.23-p36.22	GAIN	3	0
1	1:120436410..120650514	p12 (NOTCH2)	GAIN	3	0
1	1:144452745..145210875	q21.1	GAIN	3	0
5	5:65203593..68826309	q12.3	GAIN	3	0
7	7:44083631..45018187	p13	GAIN	3	0
12	12:121193338..125667418	q24.23-q24.31	GAIN	3	0
13	13:110995727..111374279	q34	GAIN	3	0
17	17:2256623..5083694	p13.3-p13.2	GAIN	3	0
17	17:729302663..78900648	q25.1-q25.3	GAIN	3	0
19	19:45182685..51060676	q13.31-q13.42	GAIN	3	0
2	2:87128774..98327997	2q11.2	LOSS	3	0
18	18:14304059..14984939	p11.21	LOSS	3	0
10	10:46812978..49450532	q11.21-q11.22	LOSS	3	0
11	11:49003873..49980055	p11.2-q12.1	LOSS	3	0
21	21:10907345..15399525	p11.2-q11.2	LOSS	3	0

5.4.12 MDM4 is subject to early genetic changes in BC development

As has been demonstrated in section 5.4 most low nuclear grade breast carcinoma cases (>85%) showed gain in 1q+ especially at 1q31-32 locus and 15% of our LNGBC had amplification at 1q32 region. Moreover MDM4 which is one of the main regulatory genes of p53 maps to this region and is frequently amplified/overexpressed in 65% of retinoblastoma [181-183]. Subsequently, we hypothesised that it may be a candidate oncogene in BC and we tested this hypothesis on several levels:

1- Copy number changes in two independent data sets in which the results were validated by gene expression array.
2- Immunohistochemistry for protein expression
3- Clinical outcome of a large BC cohort with long follow up

Copy number changes in high grade BC series and unselected series:

We found the MDM4 locus showed gain in 40% and 57% of high grade BC series and unselected BC series, respectively. Moreover, the MDM4 locus was amplified in 8% and 10% of high grade BC[138] and unselected BC series [176].

Integrated aCGH and expression analysis

In both high grade and unselected BC series [176], MDM4 mRNA expression levels displayed a statistically significant correlation with copy number (Spearman's r= 0.58172, adjusted p value = 0.00012). In addition, 4 out of 48 cases of the high grade series (3 luminal and 1 basal-like breast cancers) displayed MDM4 gene amplification and these cases harboured significantly higher levels of MDM4 mRNA expression (Mann-Whitney U test, adjusted p

value = 0.00934). In addition, mRNA expression showed a statistically significant correlation with ER protein expression ($p < 0.0001$).

MDM4 protein expression

There was no expression of MDM4 protein in normal breast tissue while 17% BC of the Nottingham series showed overexpression of MDM4. MDM4 overexpression was statistically significant (<0.0001) associated with small size, low grade, ER+ **(Figures 5-53 and 5-54)** and normal expressions of p53, ATM and BRCA1. In low grade breast cancer we found MDM4 overexpressed in 30% of cases and in cases showing coexistent precursors (columnar cell lesion, DCIS, and LN) with invasive component, MDM4 expression was identical in both lesions **(Figure 5-55)**.

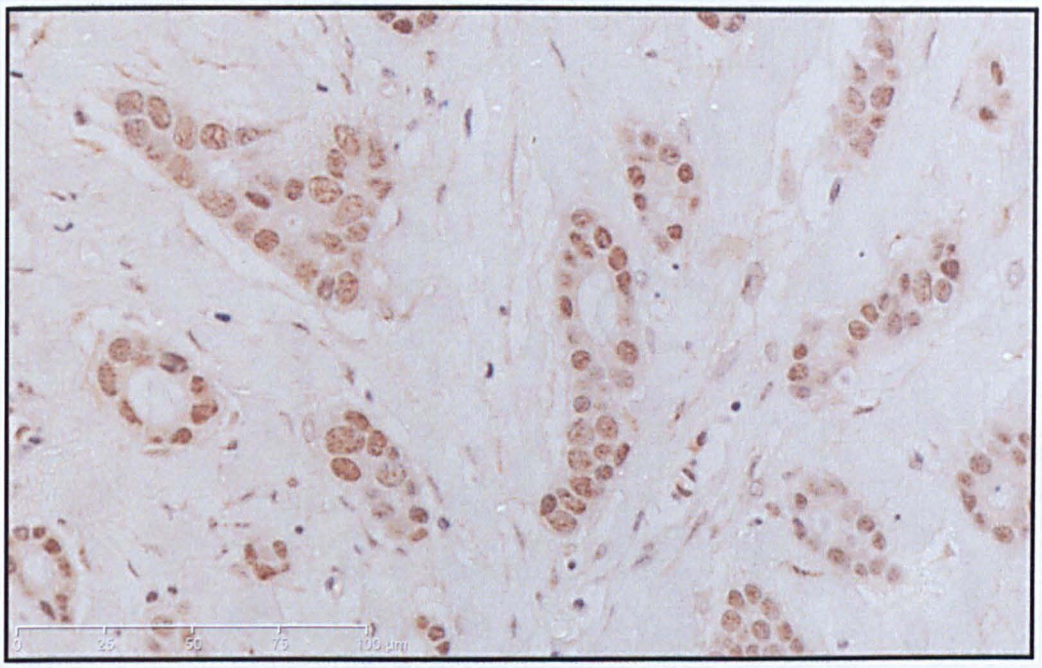

Figure 5-53: Tubular carcinoma showing positive nuclear staining of MDM4

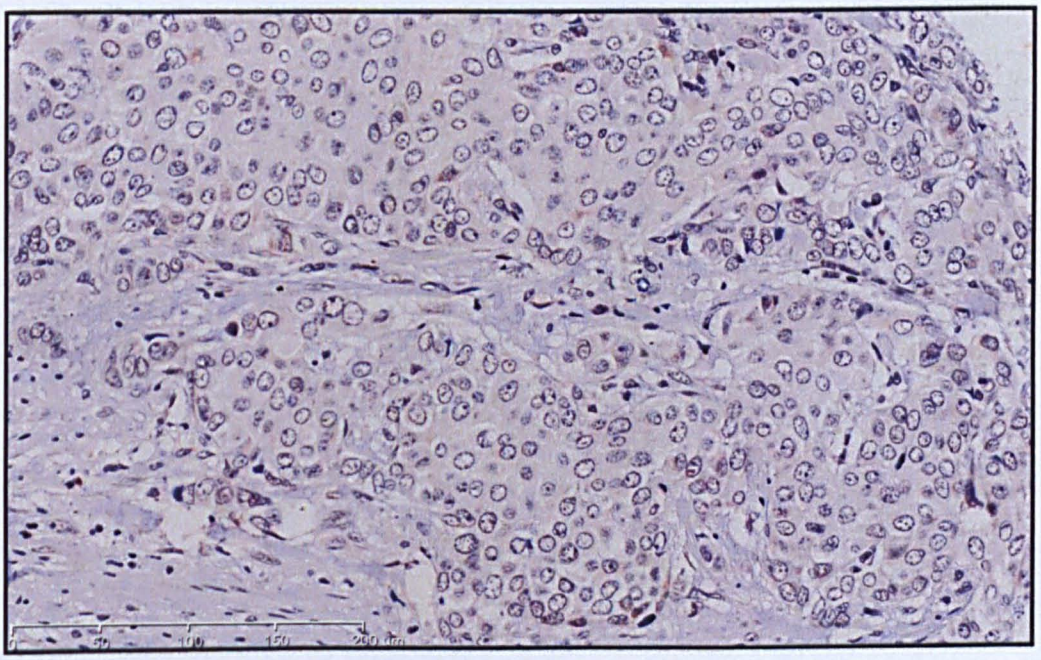

Figure 5-54: High grade breast carcinoma showing no MDM4 staining

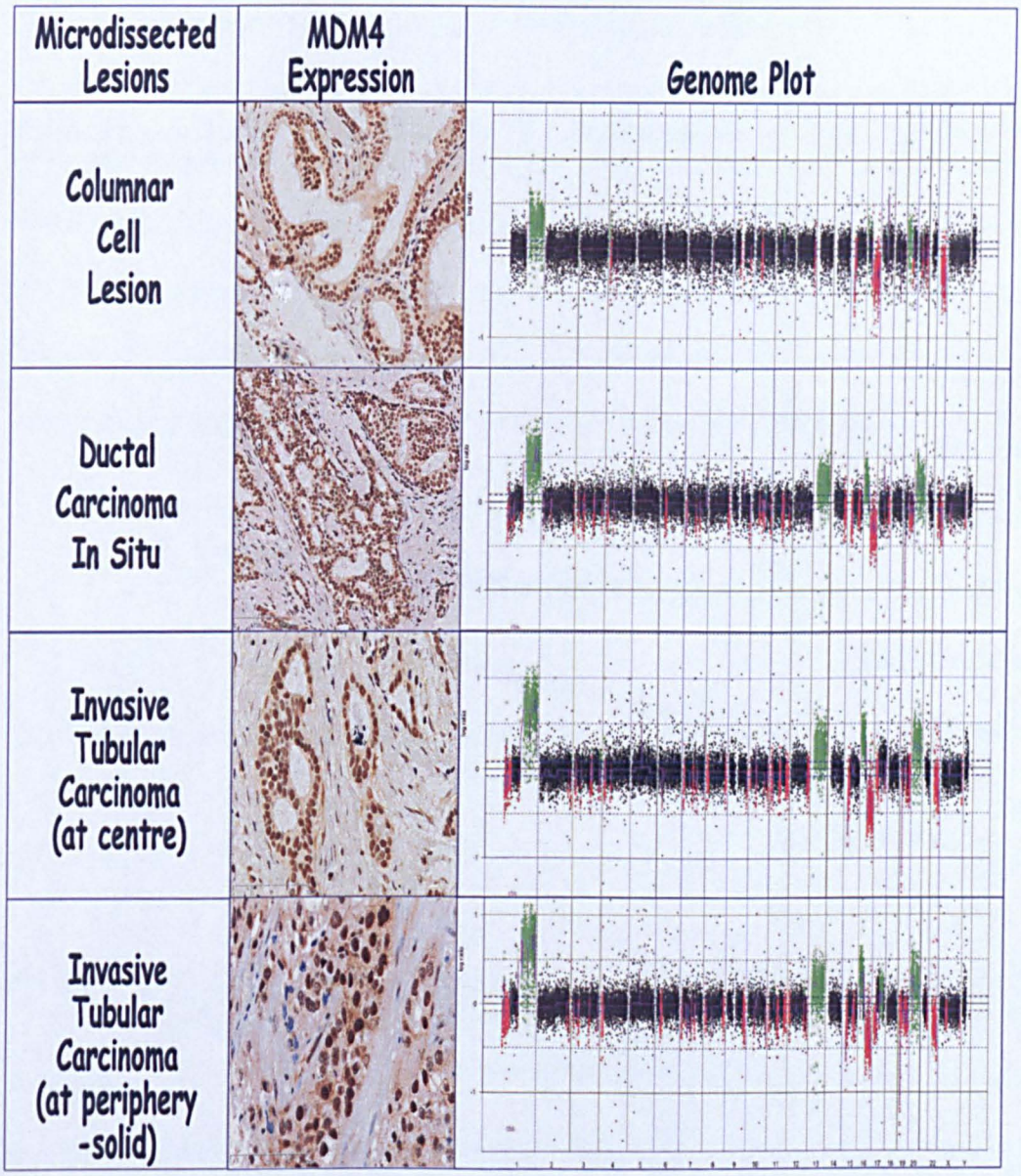

Figure 5-55: Genome plots and MDM4 immunohistochemistry staining of different components of case 2.

The genome plots showing high gain at MDM4 locus on 1q32 which was correlated to MDM 4 overexpression.

Clinical outcome of MDM4 overexpression

Absence of MDM4 over-expression was strongly associated with an adverse outcome at 10 years with a significant increase in the hazard of death, recurrence and DM in the whole Nottingham BC cohort (**Figures 5-56 and 5-57**). Furthermore, the clinical outcomes of MDM4 overexpression of 301 patients with early stage small tumours (LN-negative with tumour size ≤ 2cm) who did not receive any AT were investigated. Consistently, patients with MDM4 overexpression had a better prognosis (**Figures 5-58 and 5-59**).

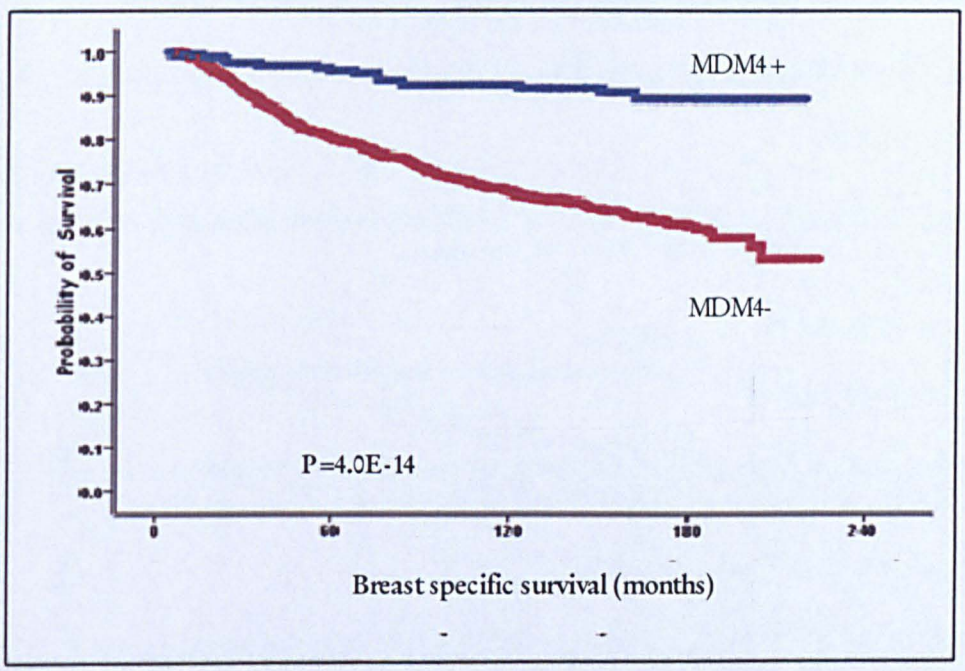

Figure 5-56: Breast cancer specific survival curve of Nottingham whole patient's cohort

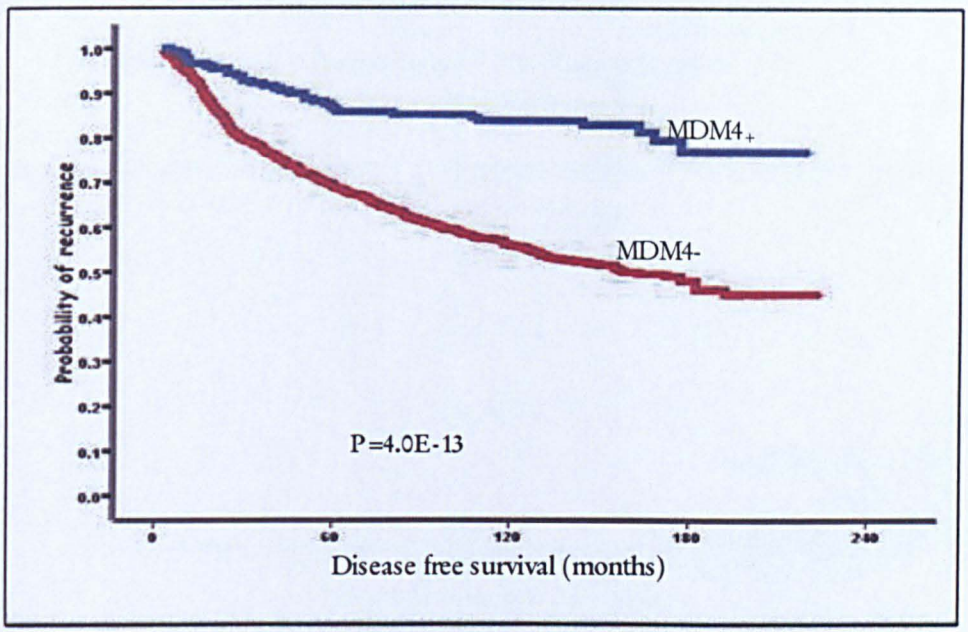

Figure 5-57: Disease free survival curve of Nottingham whole patient's cohort

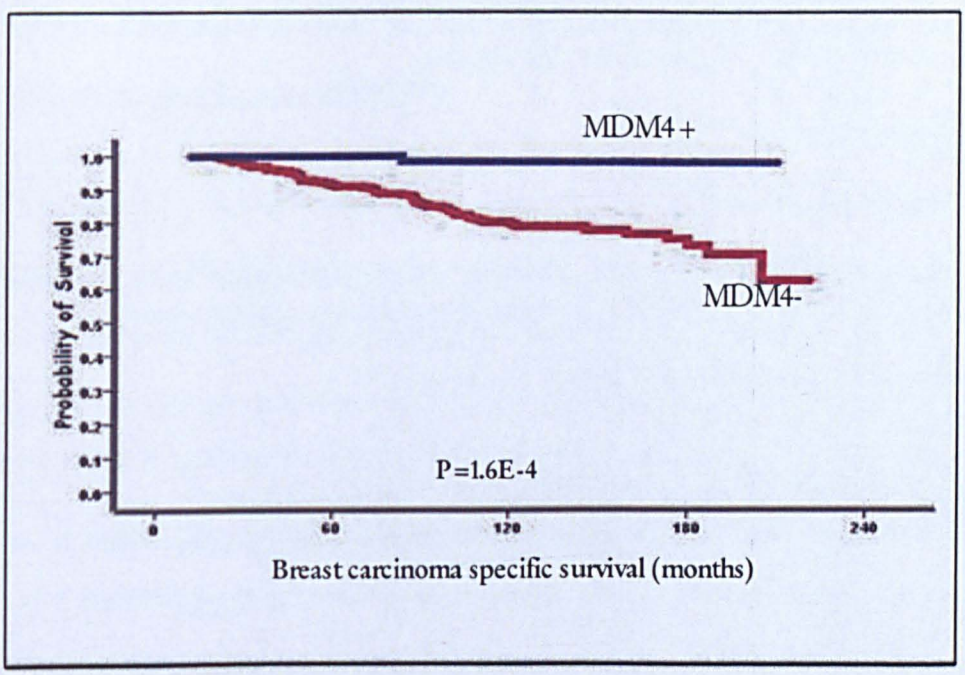

Figure 5-58: Breast carcinoma specific survival curve of small size early stage adjuvant therapy-non treated patients

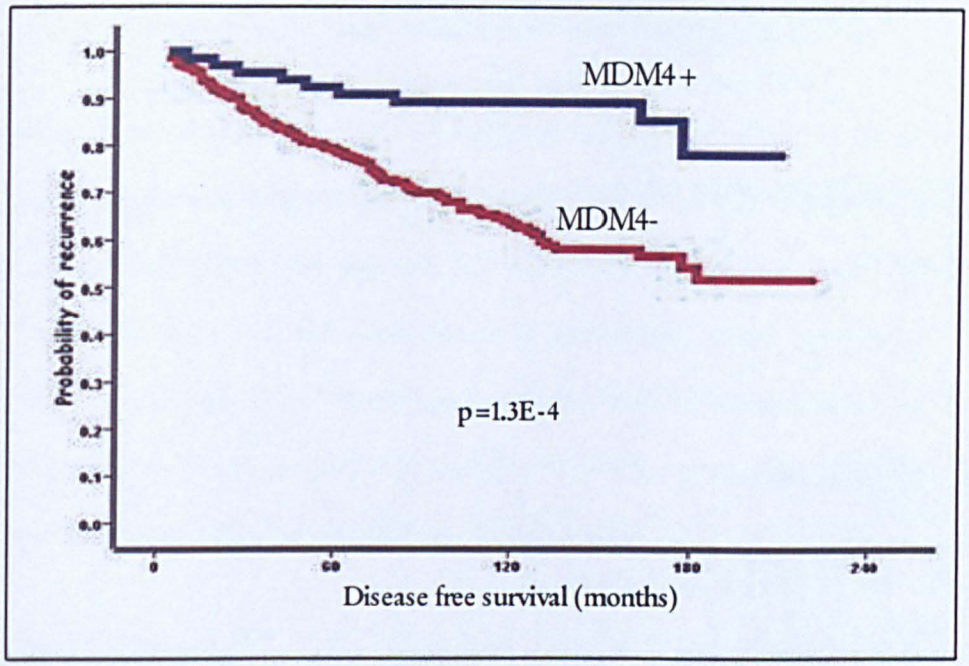

Figure 5-59: Disease free survival curves of small size early stage adjuvant therapy non treated patients

Prognostic significance of MDM4

Multivariate Cox regression models were also used to assess and compare the prognostic performance of MDM4 overexpression to that of validated prognostic indicators including: stage, size, grade, ER, PR, p53, Bcl2, CK5/6 and HER-2 overexpression. We found that the MDM4 overexpression was an independent prognostic marker (**Table 5-20**).

Table 5-21: Multivariate Cox regression analysis of MDM4 overexpression including validated prognostic factors: size, stage, grade, Bcl2, p53, ER, PR, and HER-2 overexpression

MDM4 overexpression	HR	95% CI	p
Risk of death	0.29	0.17-0.49	6.4E-6
Risk of relapse	0.40	0.27-0.58	2.9E-6
Risk of DM	0.37	0.24-0.59	2.2E-5

MDM4 overexpression and clinical outcome of hormone therapy

To evaluate whether the expression of MDM4 had different clinical outcomes in specific AT settings, we investigated the clinical outcomes and survivals of Nottingham high risk patients (n=309; NPI≥3.4) and ER+ who had received HT. We found that patients with Absence of MDM4 had the worst outcome (**Figure 5-60**). Moreover, when we compared the survival of high risk HT-treated patients to those of HT untreated for MDM4 negative subgroup, we found patients with negative MDM4 expression who received HT had a better outcome than those who did not (**Figure 5-61**).

In summary, MDM4 is an independent prognostic and predictor of BC and its overexpression could represent a novel molecular mechanism by which low nuclear grade breast neoplasia family escapes p53-dependent growth control, providing new avenues for therapeutic intervention.

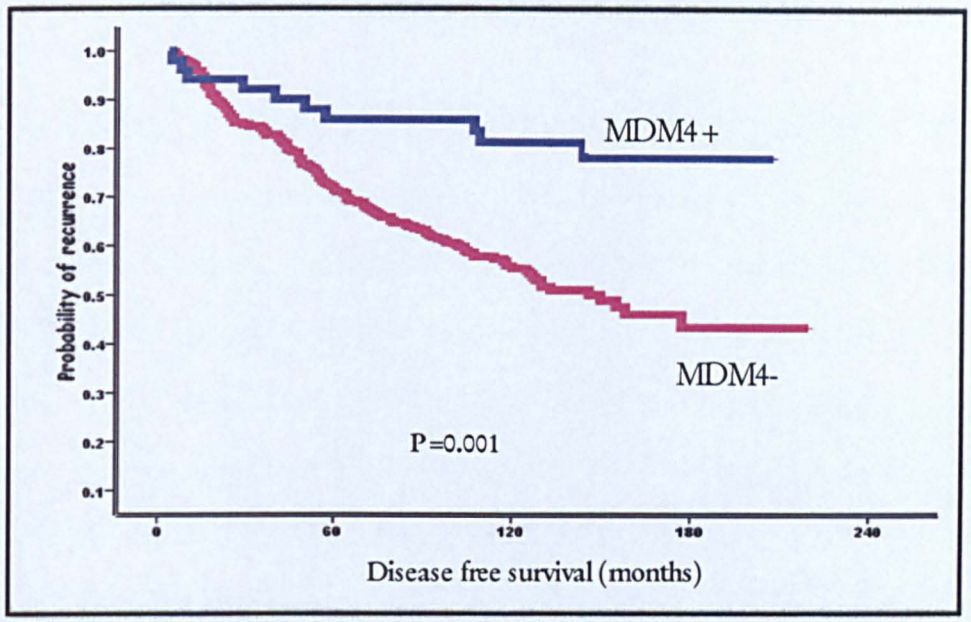

Figure 5-60: Disease free survival of high risk Nottingham patients with positive oestrogen receptors and NPI >3.4 who received adjuvant hormone therapy.

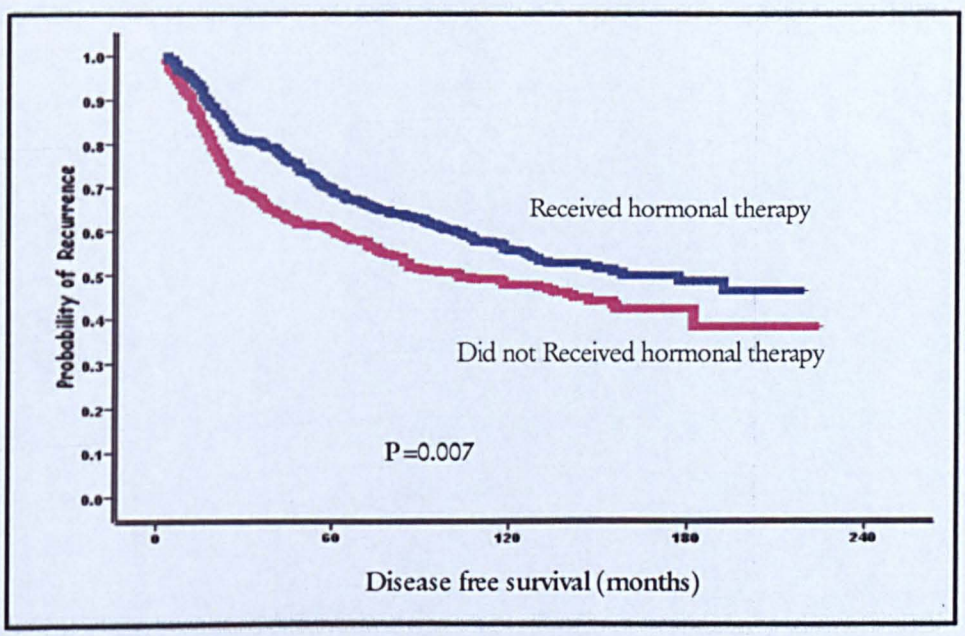

Figure 5-61: Disease free survival of high risk Nottingham patients with positive oestrogen receptors and NPI >3.4 who were negative for MDM4

5.5 Discussion

In this chapter we used aCGH to define the genetic profiles of some lesions of low nuclear grade breast neoplasia including invasive tubular and invasive lobular carcinoma and their matched co-existing precursor lesions: columnar cell lesions low/intermediate grade DCIS and lobular neoplasia. We found that the genomic profiles of these lesions showed remarkable similarity supporting their monoclonality from a common cell of origin. Moreover, our results provide substantial evidence that CCLs are the early non obligate precursor lesions for some tubular and lobular carcinomas in the low-grade molecular pathway of BC in agreement with other studies [52, 69, 71, 75, 85].

Previously, recurrent loss of heterozygosity (LOW) at 11q21-23.2, 16q23.1-24.2, and 3p14.2 was observed in CCL and in adjacent DCIS [52, 69, 71, 75, 85]. Moreover, in agreement with Simpson et al (2005) [71] , we found that the morphologic classification of CCL closely mirrored the level of genetic instability seen with comparative genomic hybridization (CGH), such that a stepwise increase in the mean number of genomic changes coincided with a rise in severity of the morphologic classification. According to Simpson et al 2005 [71], lesions categorized as CCC with or without atypia (category 1 and 6) showed a lower level of copy number changes relative to CCH (category 2). The genetic complexity further increased with the presence of either cytologic or architectural atypia (categories 3 and 4), and then further still in category 5 with the combination of cytologic and architectural atypia showing equivalence at the molecular level to that observed in DCIS. In agreement with others [52, 69, 71, 75, 85], our study has shown CCC/CCH without atypia and FEA forms a biologic continuum that merges into low-grade DCIS and lobular neoplasia. Interestingly, in view of their consistence to harbour recurrent chromosomal abnormalities, CCLs could be considered clonal and neoplastic lesions rather than hyperplastic proliferative lesions. Moreover, in addition to the common genetic changes they shared, CCC/CCH without

atypia, FEA, DCIS, LN, TC and classic ILC is associated with distinct and progressively greater molecular alterations as previous reported [58, 81, 89, 105, 106, 151, 152]. Moreover, we found that the genetic profiles of CCC/CCH without atypia are more advanced than we have thought. However, further studies including a larger number of cases and lesions not associated with invasive carcinoma is warranted.

Although the number of samples is small for each category, the similarity in genomic profiles among representative lesions is dramatic and could provide insight into some of the earliest events leading to invasive breast cancer.

For instance, most of the lesions (>75%) included in this study showed a characteristic rearrangement in chromosome 16 (loss of 16q arm) and concomitant gain of 16p which is coupled with converse rearrangement of chromosome 1 (gain of the 1q whole arm and loss of 1p) and chromosome 8 (8p loss and 8q gain, in agreement with previous studies [55, 52, 71, 81]. In the literature, gain of 1q is one of the most common acquired genetic abnormalities in human cancer [214]. There are several putative mechanisms underlying gain of 1q in breast cancer including duplication, isochromomsome formation or unbalanced translocations[214-223]. The current data indicate that near centromeric regions of both 1q and 16q is breakprone [215-216]. The reasons behind this phenomenon are presently unknown although it has been hypothesized that demethylation of the pericentric heterochromatin is associated with decondensation and subsequent instability of satellite sequences[219-223]. Satellite sequence instability could be responsible for 1q and 16q rearrangements (unbalance translocation) that are commonly reported in low grade (near-diploid) breast cancer[219]. In fact, these chromosomal imbalances seem to play a pivotal role in breast cancer development and might relate to particular clinicopathological characteristics (ER positive cancer) [215-216].

In addition, we found in agreement with others, that one of the common genetic changes in LNGBC involved 11q with 2 narrow (<2 Mb) amplicons at 11q13 and one at 11q15 [100, 202-213] suggesting the important role of 11q13 in the progression of LNGBC. *CCND1* maps to one of these loci and we validated its amplification by using CISH technique. Furthermore, we found that there was a significant correlation between copy number changes and protein expression by IHC in agreement with what we have previously demonstrated in Chapter 3.

Genetic alterations at chromosome 1 is a hallmark of low nuclear grade breast neoplasia as all LNGBN lesions showed one or more events including gain of 1q+ and 1p36. Actually chromosome 1q harbours more than one gene in both ER and p53 network. Among these genes are *MDM4, TP73, MUC1, RNPEP, PPPIR12B, CYB5R1, BTGG2, FMOD, LGTN1* and *MAPKAPK2*[2]. For instance, we found in this study that MDM4 was overexpressed and amplified in a subset of ER+/LNGBC in agreement with recent published reports [181, 182]. In fact, MDM4 overexpression could be an alterative mechanism by which LNGBC could escape the suppressor neoplastic effect of p53. Moreover, we found that MDM4 is an independent prognostic factor and predictive marker which could have therapeutic implications similar to its brother MDM2 [182].

By using comparative analysis with high grade and unselected BC series in which CGH data were validated at mRNA expression by gene expression array, we have suggested a list of target genes on the loci that showed recurrent amplification/high gain in our LNGBC. Furthermore using meta-analysis gene expression data in wwww.oniscomine.org data bases we found a number of genes that their mRNA over-expression are related to ER+, low grade tumour and absence of p53.

Previously in the introduction, we described ER+ luminal restrictive progenitor cells that perceived to reside in the lumina layer of the TDLUs. One of the characteristic of this cell is its positive expression for MUC1+. MUC1 maps to 1q22: the region that showed high

gain in all of our samples. Given that the immunohistochemical profiles of all LNGBN are identical to that of the ER+ luminal restricted progenitor cell (ESR+, MUC1+, ER+, CK19+, CK18+ and CK5/6-) of normal TDLUs, we could claim that the common cell of origin of LNGBN could be that cell. Subsequently, ER+ luminal restricted progenitor cells could acquire stochastic genetic and epigenetic hits such as *CCND1* and *MDM4* amplifications that lead to the activation of the 'luminal A' pathway and that these events determine the phenotype of the pre-invasive and invasive lesions. Furthermore, these hits may be an early event in the progression of 'luminal A' tumours and once committed to this specific 'molecular pathway', progression to a 'high grade' (basal-like or HER-2+) phenotype would be an unlikely biological phenomenon.

LNGBN family showed morphological diversity between some family members, for example low grade DCIS versus LCIS and invasive tubular carcinoma versus classical invasive lobular carcinoma. E-cadherin (*CDH1)* is a TSG localised on chromosome 16q21 and is frequently lost in ILC. It is recognised that CCLs, ADH/low grade DCIS, TC, ICC, low grade IDC, and TLC are positive for E-cadherin, and in contrast LN and ILC lack expression of this tumour suppressor gene and adhesion molecule. Given that, most of the LNGBN family were associated with loss of the whole 16q arm, we speculate that loss of normal *CDH1* gene expression, which is associated with the development of lobular differentiation [2-10, 34], is a secondary epigenetic rather than a genetic event which confers particular morphological and behavioural characteristics to these members of the LNGBN family.

In conclusion, given that the morphological and immunohistochemical features of CCL cells are almost identical to those seen in ADH/ low grade DCIS and LN, and that the molecular genetic changes of CCL are similar to those found in matched low grade breast cancers our findings suggest that CCL is a common non-obligate precursor of LGBC and

ILC. Taken together, these lesions may represent a family of precursor, in situ and invasive neoplastic lesions belonging to the luminal 'A' subclass of breast cancer. Cyclin D1 and MDM4 are among early genetic changes that activate luminal "A" pathway and drive progression of LNGBN family.

Chapter 6:

The Biological, clinical and prognostic implications of p53 transcriptional pathways in breast cancers

6.1 Abstract

In Chapter 5 we have shown that MDM4 was amplified in ~10% and overexpressed in up to 17% of BC, respectively. In addition, we found that MDM4 was an independent prognostic and predictive marker in BC. MDM4 is one of the main regulatory gene of the tumour suppressor gene *TP53*. Subsequently, in this study, we hypothesised that the functional status of p53 transcriptional pathways, rather than p53 protein expression alone, could accurately discriminate between low and high risk breast carcinoma (BC) and inform about individuals tumour biological behaviour. A well characterised series of 990 BC with long term follow-up was immunohistochemically profiled for p53, its main regulators and downstream genes. Results were validated in an independent series of patients (n=245) uniformly treated with adjuvant anthracycline-based chemotherapy. Eleven p53 transcriptional phenotypes were identified with just 2 main clinical outcomes: (a) Low risk/good prognosis group (active/partially inactive p53 pathways) defined as p53±/MDM4+/MDM2±/Bcl2±/p21±, p53-/MDM4-/MDM2+/Bcl2+/p21± and p53±/MDM4-/MMD2-/Bcl2+/p21±. These tumours had favourable clinicopathological characteristics including ER+ and long survival after systemic adjuvant-therapy (AT). (b) High risk/poor prognosis group (completely inactive p53 pathways) defined as p53±/MDM4-MDM2-/Bcl2-/p21-, p53-/MDM4-MDM2+/Bcl2-/p21-, p53±/MDM4-/MDM2-/Bcl2-/p21+. These tumours were characterised by aggressive clinicopathological

characteristics and showed a shorted survival when treated with AT. Completely inactive p53 pathways but intact p21 axis p53±/MDM4-/MDM2-/Bcl2-//p21+ had the worst prognosis particularly patients who received AT. Multivariate Cox regression models including validated prognostic factors for both test and validation series revealed that the functional status of p53 transcriptional pathways was an independent prognosticator for BC specific survival (HR: 2.64 and 4.5, $p<0.001$, respectively) and disease-free survival (HR: 1.93 and 2.5, $p<0.001$, respectively). In conclusion, p53 functional status determined by assessment of p53 regulatory and downstream targets provides independent prognostic value and may help determine more adequate therapeutic regimens for specific subgroups of breast cancer patients.

6.2 Introduction

The *TP53* gene encodes a nuclear transcription factor, p53, which is regarded as a guardian of the genome. p53 transactivates numerous target genes [177] (**Figure 6-1**), and plays pivotal roles in the regulation of cell cycle arrest, apoptosis, DNA repair, angiogenesis and differentiation [177-180].

Although 25% of breast cancer (BC) harbours *TP53* mutation [180, 225, 226], the biological role and clinical importance of p53 alterations in BC may have been underestimated [180, 224, 225] due to several reasons: 1) conflicting published data about its prognostic implications [180], 2) extensive p53 network [179] and 3) technical problems associated with surrogate markers to identify *TP53* gene defects, as most of detecting tests lack sensitivity and specificity [178]. For instance, p53 immunostaining has been used as a surrogate marker for the existence of *TP53* gene mutations which subsequently, translated into a non-functional p53 [178]. Both concepts have several pitfalls. First, about 30% of BC carrying *TP53* point missense mutations do not express p53 immunohistochemically, especially those associated with therapy resistance [226-227]. Second, null p53 mutation (nonsense, frame shift, deletions, insertions, and splicing junction mutations) may not produce p53 protein at all [228]. Third, some mutations of *TP53* could generate abnormal p53 protein that keeps most of its biological function [177-228]. Lastly, the biological functions of wild-type *TP53* might be disrupted by alterations in other proteins e.g., oestrogen receptor (ER) [229-232], MDM2 [233-236], MDM4 [181-183] and ATM [102, 237] (**Table 6-1**).

In the vast majority of studies addressing p53 dysfunction in BC, nuclear immunohistochemical expression of p53 was used as a surrogate marker of *TP53* mutation [177-180, 224-228]. Despite lacking sensitivity and specificity, numerous studies have demonstrated that p53 immunohistochemistry is a prognostic factor in BC and that it may determine the

sensitivity to specific therapeutic agents [177-180, 224-229]. In fact, there is accumulating evidence suggesting that p53 dysfunction could be responsible for the development of antiestrogen therapy resistance of ER+ tumours [230] , whereas in ER- tumours p53 mutation is considered as a key predictor for chemotherapy failure [178, 180, 224, 229].

Given that >70% of BC and more than 97% of low nuclear grade breast neoplastic family have wild-type p53 as shown in Chapter 2, we could claim that p53 dysfunction as a tumour suppressor gene in the majority of BC especially low nuclear grade may be due to other mechanisms rather than mutation.

In Chapter 5, using array comparative genomic hybridization (copy number changes), gene expression array (mRNA expression), immunohistochemistry (protein expression) and clinical outcome, we have identified that MDM4 as one of the amplified target genes that has independent prognostic and predictive implication on breast cancer. MDM4 is one of the main regulatory genes of p53.

In fact, analysis of the transcript profiles of primary breast tumours of known p53 status have shown that the transcriptional profile of p53 is a more definitive indicator of p53 function than its mutational status [181]. Moreover, an immunohistochemical panel combining p53, with two of its down-stream targets, namely p21 and MDM2, has proven to be more sensitive and specific to detect p53 pathway dysfunction than immunohistochemical assessment of p53 itself [228].

In this study, we hypothesised that the functional status of p53 transcriptional pathways rather than p53 immunohistochemistry expression alone could accurately determine clinical outcome in a large unselected series of BC and in a series of patients uniformly treated with adjuvant anthracycline-based chemotherapy.

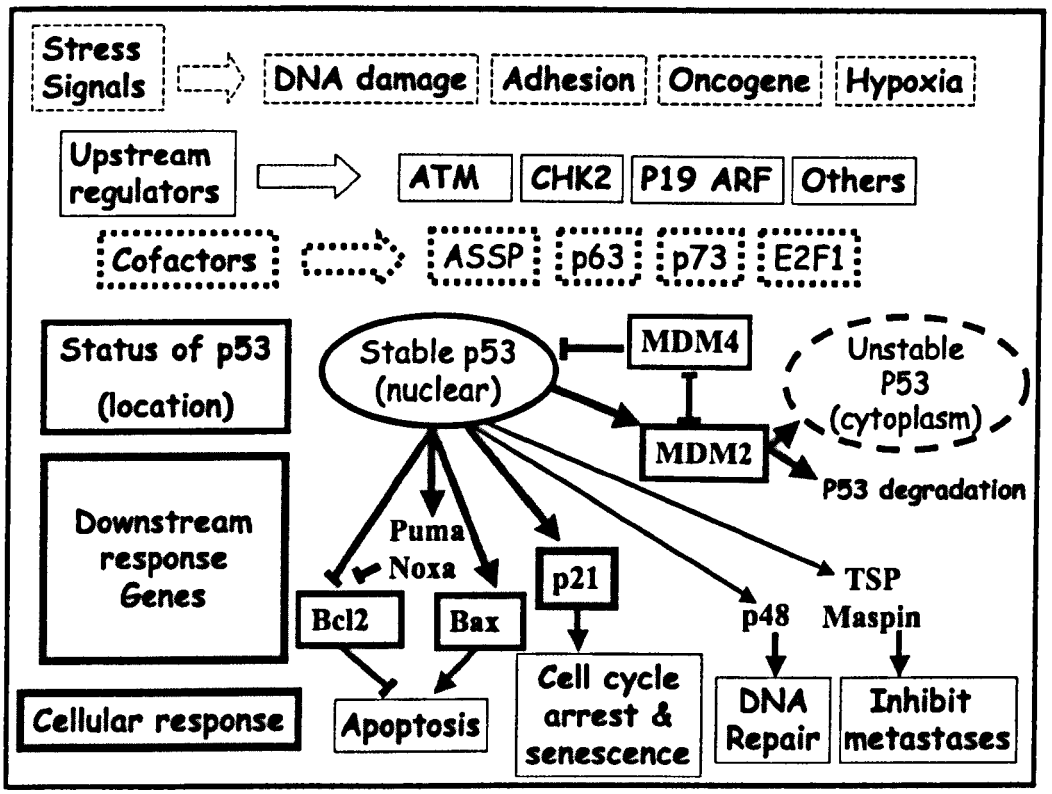

Figure 6-1: p53 network illustrating the interaction between p53 and MDM2: murine double minute 2 (MDM2), murine double minute 4 (MDM4), ataxia telangiectasia mutated (ATM), p21 and Bcl2.

In response to cellular stress (such as DNA damage, oncogenes or hypoxia), p53 is phosphorylated at specific serine/threonine residues which prevents the MDM2-p53 interaction, and thus p53 is stabilized and activated. Therefore oncogene stress signals result in increased proliferation and eventually malignant transformation if upstream activators of p53 (such as ARF, CHK2, or ATM), p53 itself (e.g. mutation), regulators of p53 (e.g. MDM2 or MDM4) or p53 downstream signalling components (p53 target genes: Bcl2, Puma, Noxa, Bax, p21, p48) are inactivated. It should be noted that p53 controls apoptosis by induction of pro-apoptotic genes such as Puma, Noxa and Bax and by suppressing anti-apoptotic genes such as Bcl2.

Table 6-1: Hypothesis and theories of immunohistochemistry detection of the functional status of p53 transcription pathways

Markers	IHC assay	Theory	Clinical outcome: Hypothesis
P53	Negative (-)	❖ Wild type (WT) p53 protein is short lived as activated WT p53 induces the transcription of MDM2, which binds to p53 and leads to its destruction	➢ **Good prognosis:** active WT p53 transcriptional pathways
		❖ Null mutations or deletion of p53 result in absence, or premature stop codons and shortened protein products that often may not be detectable by IHC	➢ **Poor prognosis:** completely inactive p53 transcriptional pathways due to null mutant TP53
		❖ Inactivation of WT p53 rather than mutation e.g.; upstream and/or down stream regulators e.g., MDM2, MDM4, ATM, BRCA1…etc.	➢ **Good prognosis:** partially inactive p53 transcriptional pathways ➢ **Poor prognosis:** completely inactive p53 transcriptional pathways
	Positive (+)	❖ Continuous exposure to stress such as DNA damage, resulting in stabilization and intracellular accumulation of WT TP53	➢ **Good prognosis:** active p53 transcriptional pathways
		❖ point missense mutations of TP53 produce abnormal proteins which are resistant to degradation leading to intracellular accumulation of abnormal p53	➢ **Good prognosis:** partially inactive p53 transcriptional pathways ➢ **Poor prognosis:** completely inactive p53 transcriptional pathways due to point missense mutant TP53
MDM2	Over-expression (+)	Through an auto-regulatory feedback loop with MDM2, activated TP53 induces the transcription of MDM2, which binds to and inactivates WT TP53	
		❖ Overexpression of MDM2 due to ER dependent transactivation of MDM2 inactivate TP53 apoptotic pathway	➢ **Good prognosis:** partially inactive p53 transcriptional pathways
		❖ ER and TP53 independent transactivation of MDM2 e.g., MDM2 gene amplification, overexpression of MDM2 mRNA splice variant	➢ **Poor prognosis:** completely inactive p53 transcriptional pathways due to inappropriate p53 degradation
MDM4	Over-expression (+)	❖ Down regulation of TP53-p21 cell growth axis ❖ Up regulation of TP53 apoptotic activity pathway	➢ **Good prognosis:** partially inactive p53 transcriptional pathways
Bcl2	Positive (+)	❖ Bcl2 is a direct downstream responsive gene of ER and p53. Retention of Bcl-2 expression inhibits apoptosis, inhibit cell cycle progression at G0/G1, extends cell survival but does not promote cell proliferation.	➢ **Good prognosis:** partially inactive p53 transcriptional pathway with cell cycle progression delay
P21	Positive (+)	❖ P21 protein expression is increased by normal TP53 activity leading to cell cycle arrest and tumour growth inhibition	➢ **Good prognosis:** active TP53 mediated cell cycle arrest pathway
		❖ TP53 independent expressed p21 concomitantly prevent apoptosis, promotes growth "cell survival promoter", and induces differentiation by direct interaction with ER-α.	➢ **Poor prognosis:** completely inactive p53 pathway with TP53-independent, inappropriate activation of p21 axis

IHC: immunohistochemistry

6.3 Material and Methods

6.3.1 Nottingham/Tenovus population study

We studied a series of primary operable invasive BC derived from the Nottingham Tenovus (Nottingham/Tenovus) Primary Breast Carcinoma Series of women age ≤70 years, Nottingham City Hospital (1989-1999). Out of 1100 tumours consecutively accrued, 990 cases were included in this study based on the following inclusion criteria: i) complete clinical and therapeutic data available and ii) successful analysis for all markers required for this study. The clinicopathological characteristics of our cohort are summarised in **(Table 6-2)**. Median follow up was 111 months (range 1 to 233).

All patients received a standardised approach for diagnosis and treatment. Adjuvant systemic therapies (AT) were scheduled on the basis of prognostic and predictive factor status including Nottingham Prognostic index (NPI) [137], oestrogen receptor-α (ER-α) status, and menopausal status. Patients within the good prognostic group (NPI ≤3.4) did not receive AT. Hormonal therapy (HT) was prescribed to patients with ER-α+ tumours and NPI scores of >3.4 (moderate and poor prognostic groups). Pre-menopausal patients within the moderate and poor prognostic groups were candidates for CMF (Cyclophosphamide, Methotrexate, and 5-Flourouracil) chemotherapy; and patients with ER-α+ tumour were also offered HT. Conversely, postmenopausal patients with moderate or poor NPI and ER-α+ were offered HT, while ER-α- patients received CMF if fit.

Exploratory subgroup analysis of the p53 pathway surrogates was also performed in LN negative cases vs. LN positive cases, AT untreated cases vs. AT-treated cases and in ER+ high risk patients (NPI >3.4) who received HT vs. HT naïve cases.

Table 6-2: Clinicopathological characteristics of the Nottingham/Tenovus and RMH/Breakthrough series

Variable	Nottingham/Tenovus Series n=990		RMH/Breakthrough Series n=245	
	n*	Cases (%)	n*	Cases (%)
Menopausal status	984			
Pre-menopausal		388 (39)		NA
Postmenopausal		596(61)		NA
Tumour histological grade	983		240	
G1		150 (15)		23 (10)
G2		294 (30)		69 (29)
G3		539 (55)		148 (62)
Lymph node stage	984		237	
Negative		601(61)		38 (35)
Positive		383(39)		154 (65)
Survival **	949		244	
Alive and well		567 (60)		179
Dead from disease		297 (31)		42
Dead from other causes		85 (9)		NA***
Adjuvant systemic therapy (AT)	973		245	
No AT		377 (39)		0 (0)
Hormone therapy (HT) alone		382 (39)		0 (0)
Chemotherapy alone		182 (19)		53 (22)
Hormone + chemotherapy		32 (3)		192 (78)
Tumour size (cm)	983		243	
T1 (≤ 2)		576 (59)		127 (52)
T2 (>2.0-5)		394 (40)		100 (41)
T3 (>5)		13 (1)		16 (7)

* Number of cases for which data were available.

** Survival data for Nottingham/Tenovus series were available for up to 20 years and for RMH/Breakthrough series for up to 10 years.

***: Deaths of causes other than breast cancer were censored at last follow up.

6.3.2 Validation study

We used a series of 245 invasive breast carcinomas diagnosed and managed at the Royal Marsden Hospital and Breakthrough breast cancer research centre (RMH/Breakthrough) between 1994 and 2000. Patients were selected on the basis of being eligible for therapeutic surgery and receiving standard anthracycline-based AT. All patients were primarily treated with surgery followed by anthracycline-based chemotherapy. HT was prescribed for patients with ER+ tumours (tamoxifen alone in 96.4% of the patients for the available follow-up period). Complete follow-up was available for 244 patients, ranging from 0.5 to 125 months (median = 67 months, mean = 67 months). The characteristics of this cohort are described elsewhere [107] and summarised in (**Table 6-2**).

6.3.3 Survival data

Survival data including breast cancer specific survival (BCSS) time, disease-free survival (DFS), development of loco-regional and distant metastases (DM) was maintained on a prospective basis. BCSS was expressed as the number of months from diagnosis to the occurrence of BC related-death. DFS was defined as the number of months from diagnosis to the occurrence of local recurrence (LR), local LN relapse or DM relapse. DM-free survival (MFS) was defined the number of months from diagnosis to the occurrence of DM relapse.

6.3.4 Immunohistochemical assay

In both series, tumours were arrayed in tissue micro arrays (TMAs) constructed with 2 replicate 0.6 mm cores from the centre and periphery of the tumours for each marker which were considered to be sufficiently representative. The TMAs were immunohistochemically profiled for a panel of antibodies including p53 and some of its transcriptional targets (e.g. MDM2, MDM4, Bcl2 and p21). Details of antibodies, antigen

retrieval, immunohistochemical methods and some results of the above immunohistochemical analyses have already been reported elsewhere [87, 104, 106, 107, 138] and are summarised in (**Table 6-3**). A cut-off value for each marker was selected as previous published [87, 100, 102, 104, 105, 106, 107, 138, 139] and was confirmed by testing the different values against outcome at 10 years using Cox regression. Positive and negative (omission of the primary antibody and IgG-matched serum) controls were included in each run.

In Nottingham/Tenovus series, HER-2 expression was assessed according to the new ASCO/ CAP guidelines [109] by using IHC and fluorescence in situ hybridisation (FISH); FISH was performed for HER-2 IHC score 2+ cases using a HER-2 and a centromere 17 (CEP17) specific probe (Vysis, IL, USA), according to the supplier's instructions as previously described in chapter 3.

For the TMA constructed with cases from RMH/Breakthrough, immunohistochemistry was performed with antibodies raised against the following markers: ER, progesterone receptor (PR), HER-2, EGFR, Ck 5/6, Ck 14, Ck 17, Cyclin D1, KI67, p53, and topoisomerase II α, as reported elsewhere [107, 138]. TMA sections were also subjected to chromogenic in situ hybridisation (CISH) with SpotLight probes for *CCND1*, *MYC*, *HER2*, *TOP2A*, and chromosome 8-centromere as previously reported [138]. The immunohistochemical and CISH scoring was performed by at least 2 observers who were blinded to the results of the patients' outcome in two different settings for each marker. There was substantial to excellent intra-observer and inter-observer agreements ($k > 0.6$; Cohen's kappa and multi-rater kappa tests, respectively)

Table 6-3: Primary antibodies, clone, source, optimal dilution and scoring system used for each immunohistochemical marker

Antibody	Clone	Source	Dilution	Distribution	Cut-offs	Ref.
Mouse MAb anti p53	DO7	Novocastra	1: 50	Nuclear	>10% (negative) 10-20 (low) >20% (High)	87, 102, 104-107
Affinity purified rabbit anti-HdmX/MDM4	IHC-00108	Bethyl Labs	1:250	Nuclear	0% (negative) <1-20% (low) >20% (overexpression)	183
Mouse MAb anti-MDM2	IB10	Novocastra	1:50	Nuclear	≥10% (overexpression)	182
Mouse MAb anti-Bcl2	124	Dako-Cytomation	1:100	Cytoplasm	>10% (positive	87, 104, 106, 107
BRCA1	MS110	Oncogen Research	1:150	Nuclear	<25% (negative)	87, 102, 104, 106, 107
Rabbit MAb anti-ATM	Y170	Abcam	1:100	Nuclear	<25% (negative) ≥75%	102, 104
Mouse MAb anti-21	EA10	Abcam	1:25	Nuclear	≥10% (positive)	104, 106, 107, 139
Mouse MAb anti-27	SX53G8	Dako-Cytomation	1:50	Nuclear	≥10% (positive)	104, 106, 107
Mouse MAb anti-vimentin	Vim 3B4	Dako-Cytomation	1:250	Cytoplasm	≥10% (positive)	104, 106
Rabbit anti-Bax	Polyclonal	Abcam	1:1000	Cytoplasm	≥10% (positive)	106
Mouse MAb anti-ER-α	1D5	Dako-Cytomation	1:200	Nuclear	≥3 (positive)	87, 104, 107
Mouse MAb anti-PR	PgR	Dako-Cytomation	1:150	Nuclear	≥3 (positive)	87, 104, 107
Mouse MAb anti-EGFR	31G7	Zymed	1:50	Membrane	0 or +1 (negative) +2 or +3 (positive)	104, 107
Mouse MAb anti-CK14	LL002	Novocastra	1:40	Cytoplasm	≥10% (positive)	87, 104, 107
Mouse MAb anti-CK5/6	D5/161B4	Chemicon	1:60	Cytoplasm	≥10% (positive)	87, 104, 107
Mouse MAb anti-CK17	E3	Dako-Cytomation	1:100	Cytoplasm	≥10% (positive)	107
Mouse MAb anti-CK18	DC10	Dako-Cytomation	1:100	Cytoplasm	≥10% (positive)	87, 104
Rabbit antihuman HER-2	polyclonal	Dako-Cytomation	1:100	Membrane	See text	104, 107, 109
Mouse MAb anti-Ki-67	MIB1	Dako-Cytomation	1:300	Nuclear	<10% (low) 10-30% (moderate) >30% (high)	107, 138
Mouse MAb TOP2A	KiS1	D Dako-Cytomation	1:150	Nuclear/ cytoplasm	>25% (positive)	107, 138

All sections were pre-treated with microwave antigen retrieval using 0.1% citrate buffer (pH 6) except for HER-2 (no pre-treatment) and EGFR (pre-treated with protease for 10 minutes).

MDM2: murine double minute 2, MDM4: murine double minute 4, ATM: ataxia telangiectasia mutated; BRCA1: Breast cancer 1, ER: oestrogen receptor, PR; progesterone receptor, Ck: cytokeratin, EGFR; epidermal growth factor, TOP2A; Topoisomerase II alpha, MAb: Monoclonal antibody.

6.3.5 Statistical analysis

Data management and analysis were performed using both SPSS software (SPSS, version16 Chicago, IL) and STATA software (STATA, version 10, StataCorp LP, Texas, USA). Where appropriate, Pearson's Chi-square, Fisher's exact, x^2 for trend, Student's t and ANOVAs one way tests were used. Cumulative survival probabilities were estimated using the Kaplan–Meier method and differences between survival rates were tested for significance using the log-rank test. Multivariate analysis for survival was performed using the Cox hazard model. The proportional hazards assumption was tested using standard log-log plots. When appropriate, variables were assessed in univariate analysis as a continuous and categorical variable and the two models were compared using an appropriate likelihood ratio test. Hazard ratios (HR) and 95% confidence intervals (95% CI) were estimated for each variable. All tests were two-sided with a 95% CI and a conservative p value <0.01 was considered significant.

6.4 Results

6.4.1 Clinical significance of p53 protein expression

Only 220/990 (22%) and 33/180 (18%) of Nottingham/Tenovus and RMH/Breakthrough cases; respectively, showed positive p53 protein expression (p53+) which was strongly associated ($p<0.001$) with unfavourable clinicopathological parameters including high LN stage, high grade, large tumour size, HER-2 overexpression/ *HER-2* gene amplification, basal-like phenotype (ER-/HER-2- with Ck5+ or Ck14+ or EGFR+), and triple-negative phenotype (ER-/PgR-/HER-2-). Moreover, in both Nottingham/Tenovus and RMH/Breakthrough series, p53+ was associated with reduced BCSS, DFS and MFS (log-rank test; $p<0.0001$; **(Figure 6-2)**. However, in multivariate Cox regression analysis including validated markers associated with outcome, p53 was no longer an independent predictor of BCSS, DFS **(Table 6-4)** or MFS (data not shown).

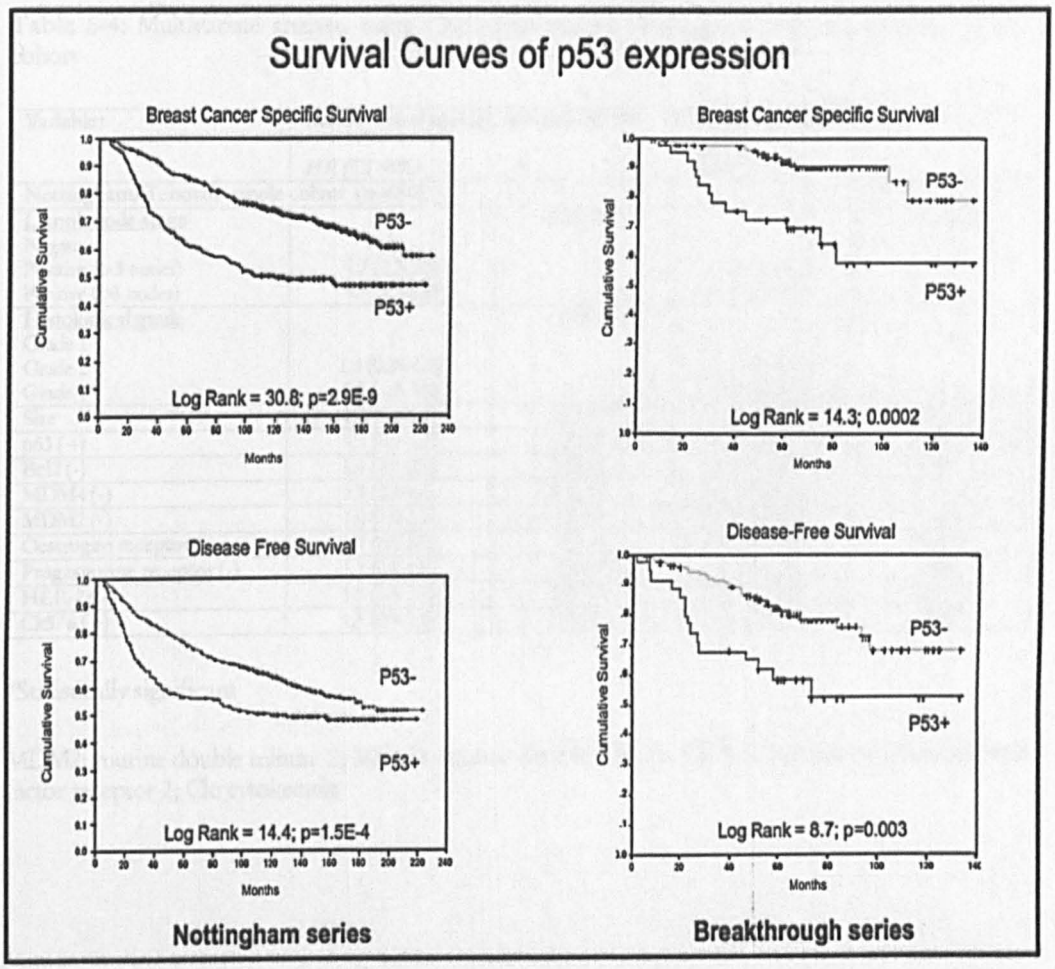

Figure 6-2: Kaplan–Meier survival curves of cases from both the Nottingham/Tenovus (left upper and lower) and the RMH/Breakthrough series (right upper and lower) stratified according to negative and positive p53 expression.

Table 6-4: Multivariate analysis using Cox regression in Nottingham/Tenovus patients' whole cohort

Variables	Breast cancer specific survival (BCSS)		Disease Free Survival (DSF)	
	HR (CI 95%)	*P*	*HR (CI 95%)*	*P*
Nottingham/Tenovus' whole cohort (n=990)				
Lymph node stage		3.3E-15*		6.2E-15*
Negative	1		1	
Positive (1-3 nodes)	1.7 (1.3-2.3)		1.3 (1.1-1.7)	
Positive (>3 nodes)	4.7 (3.3-6.8)		3.9 (2.8-5.5)	
Histological grade		0.001*		
Grade 1	1		1	0.298
Grade 2	1.4 (0.76-1.6)		1.02 (0.7-1.5)	
Grade 3	2.3 (1.2-3.9)		1.25 (0.8-1.9)	
Size	1.2 (1.1-1.4)	0.007*	1.2 (1.1-1.3)	0.01*
p53 (+)	1.3 (0.9-1.7)	0.105	1. 3 (1.0-1.7)	0.091
Bcl2 (-)	1.5 (1.1-2.0)	0.010*	1.3 (1.1-1.7)	0.01*
MDM4 (-)	3.8 (2.1-6.6)	4.7E-6*	2.7 (1.8-4.0)	1.3E-5*
MDM2 (-)	1.0 (1.0-1.1)	0.365	1.0 (1.0-1.1)	0.263
Oestrogen receptor (-)	1.4 (0.9-2.0)	0.110	1.6 (1.1-2.2)	0.007*
Progesterone receptor (-)	1.1 (0.8-1.6)	0.513	1.0 (0.8-1.6)	0.841
HER-2 (+)	1.9 (1.4-2.7)	2.0E-4*	1.9 (1.4-2.6)	1.6E-4*
Ck5/6 (+)	1.3 (0.9-1.8)	0.159	1.6 (1.2-2.3)	0.002*

*Statistically significant

MDM2: murine double minute 2; MDM4: murine double minute; HER-2; Human epidermal growth factor receptor 2; Ck: cytokeratin

6.4.2 Clinical outcome of p53 transcription pathway status

By exploring clinicopathological significance of the main p53 transcription pathways (MDM4, MDM2, Bcl2 and p21) with regard to p53 protein expression, BC patients were stratified into 6 statistically prognostic groups (BCSS: log rank 135, p= 1.4E-27 and DFS: log-rank test 102.7, p=1.4E-20) that ranged from excellent to extremely poor (**Figures 6-3, 6-4 and 6-5**). The robustness of this model was further confirmed in RMH/Breakthrough series (log-rank test; BCSS: p<0.00009, DFS: p=0.00003 and MFS: p=0.00002). Our exploratory analyses revealed that the subclassification of BC according to p53 pathway six prognostic subgroups was proven to be significant in LN-negative patients (BCSS: log rank 79.5, p=1.1E-15 and DFS: log rank 60.1, p=4.6E-12), in LN-positive patients [BCSS: log rank 60.9, p=7.9E-12 and DFS: log rank 4.3, p=3.0E-8], patients who received no AT (BCSS: log rank 59.7, p= 1.4E-11 and DFS: log rank 47.3, p= 4.9E-9) and those with ER+ tumours who received HT (BCSS: log rank 31.0, p= 9.3E-6 and DFS: log rank 28.5, p= 2.9E-5).

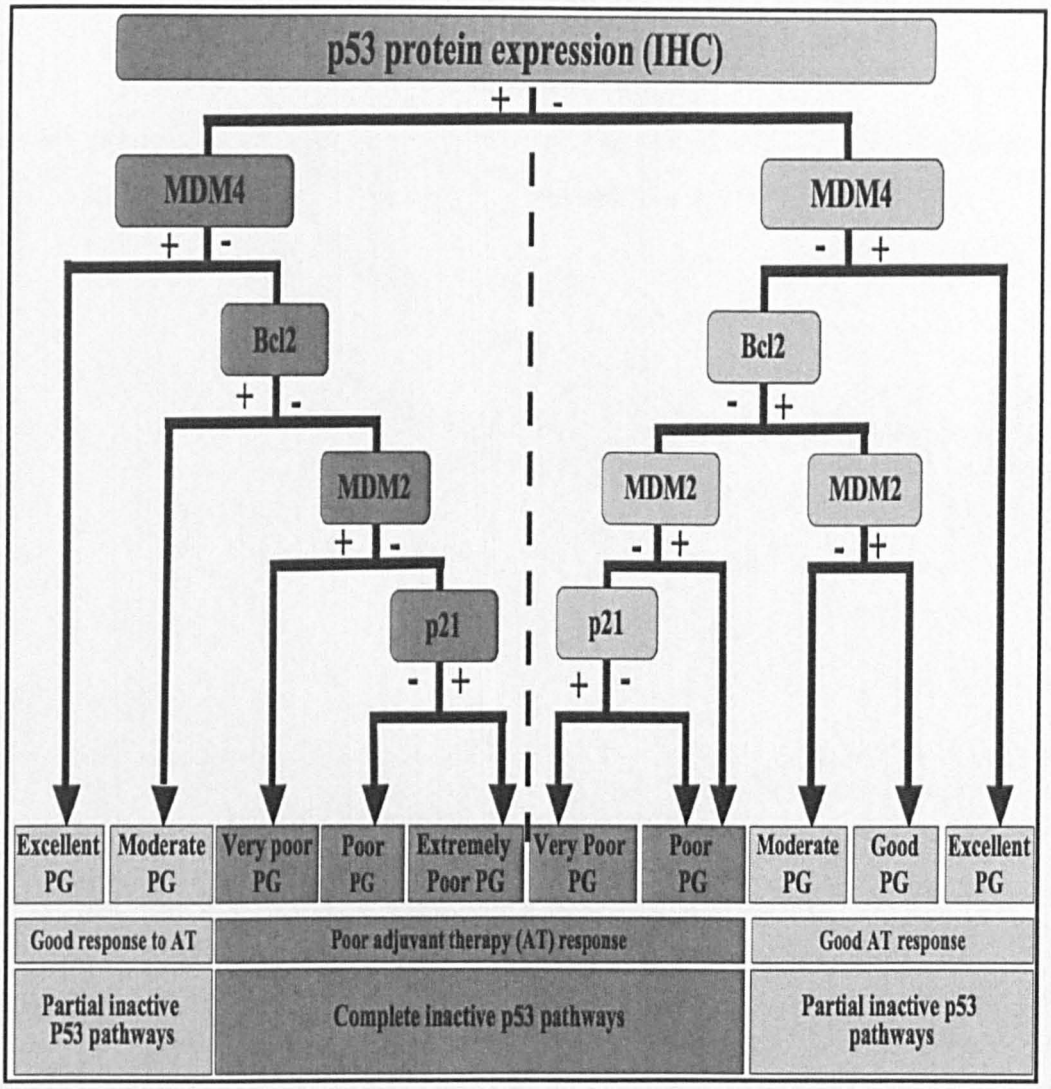

Figure 6-3: Classification of breast carcinoma according to co-expression of p53 and its main regulator and target downstream: MDM4, MDM2, Bcl2 and p21.

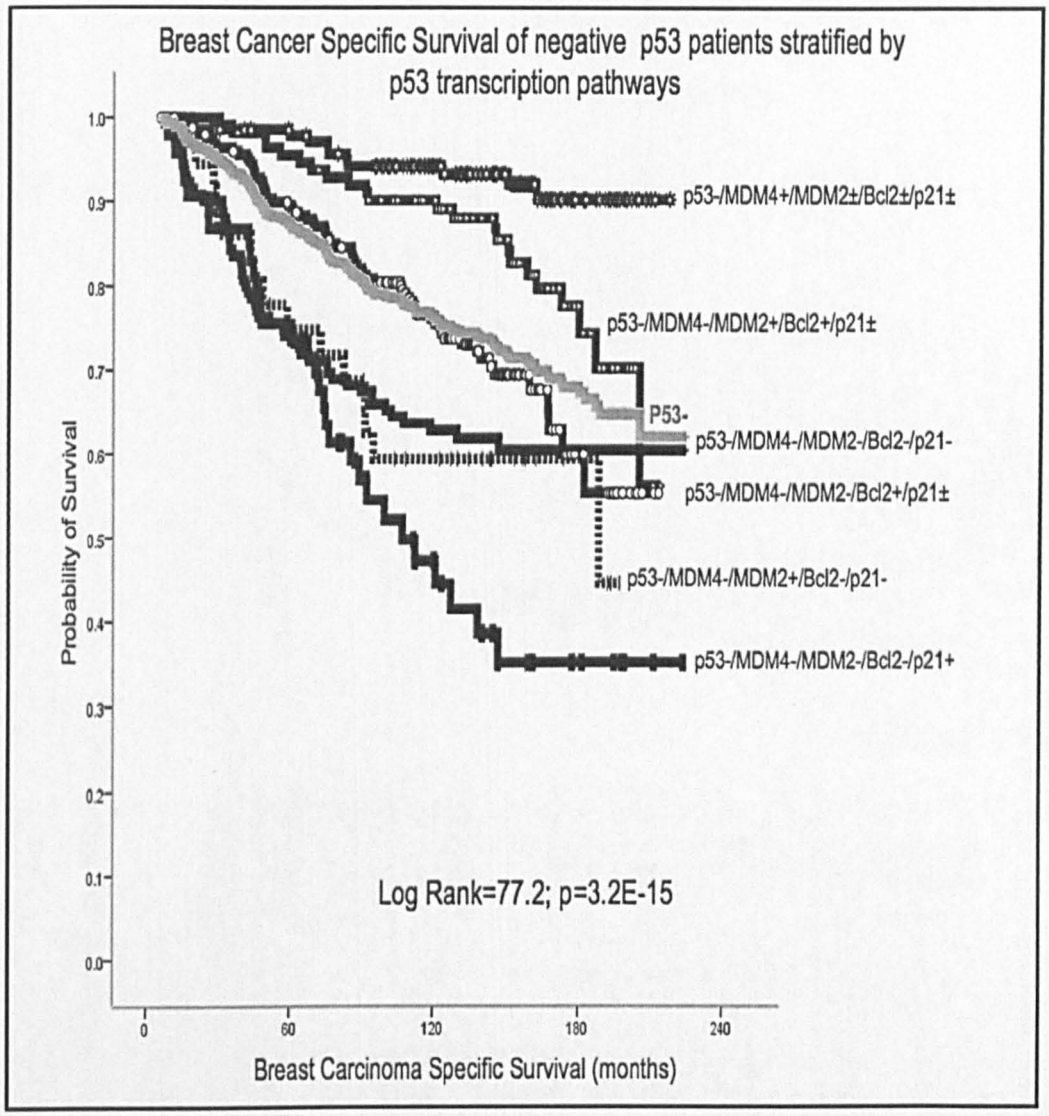

Figure 6-4: Kaplan–Meier survival curves of breast cancer specific survival of p53 negative breast cancers patients stratified according to the p53 transcription pathways.

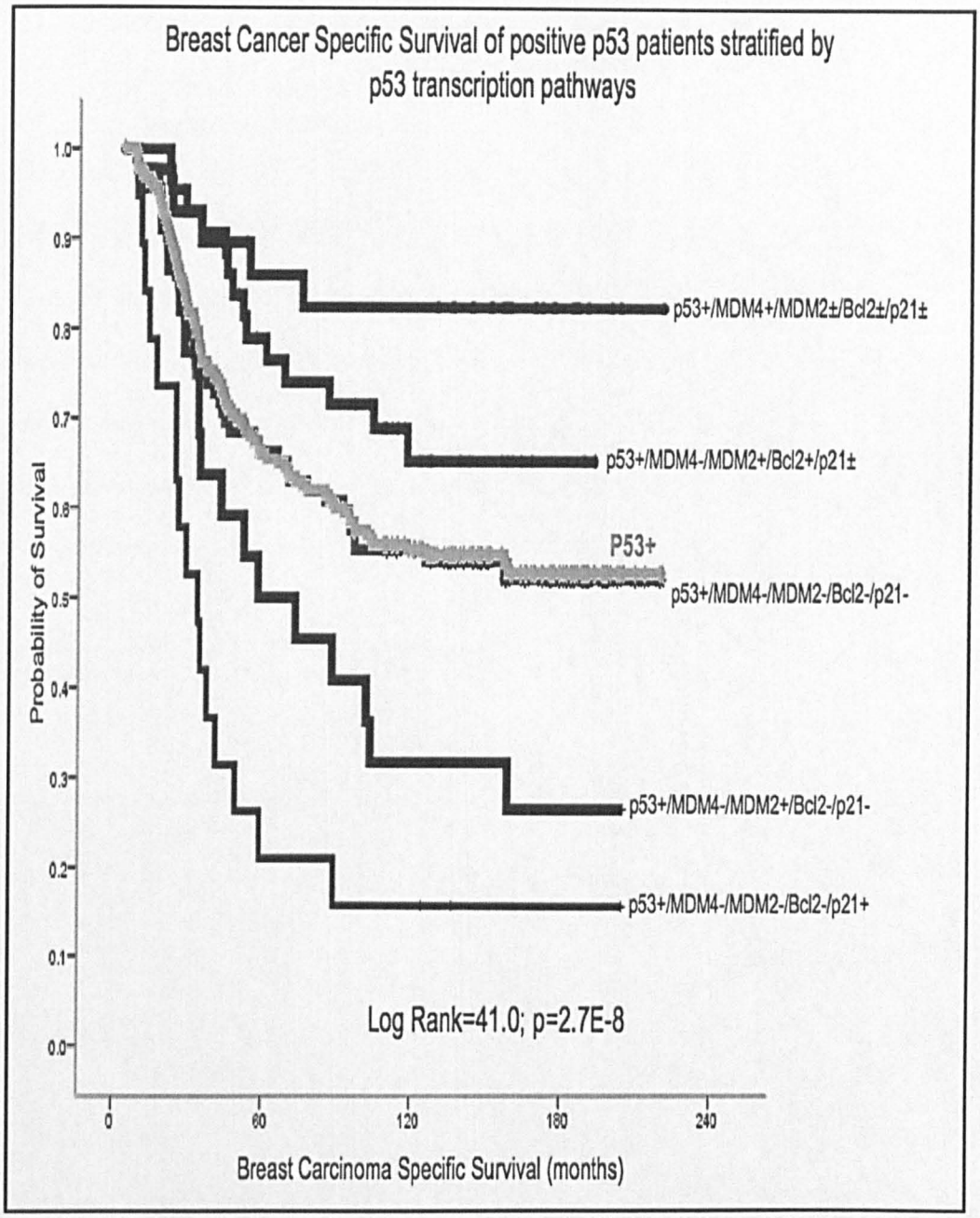

Figure 6-5: Kaplan–Meier survival curves of breast carcinoma specific survival of p53 positive breast carcinoma patients stratified according to the p53 transcription pathways.

6.4.3 Prognostic independence of functional p53 transcription pathway phenotypes

To assess the prognostic importance of these phenotypes, a multivariate Cox regression model was used to compare their performance to the validated prognostic indicators assessed in Nottingham/Tenovus whole patient cohort (**Table 6-5**) and in patients who had not received any AT subgroup (data not shown). We found the functional status of p53 transcription pathways remained significantly associated with BCSS, DFS (**Table 6-5**) and MFS (data not shown). A similar analysis of the RMH/Breakthrough cohort revealed similar results for BCSS (p=0.002), DFS (p=0.003) and MFS (p=0.0005).

Table 6-5: Cox regression model showing independence of p53 transcription pathways as a prognostic factor in Nottingham/Tenovus whole breast carcinoma series

Factor	Breast Carcinoma Specific Survival (BCSS) 10 years			Disease Free survival (DFS) 10 years		
	HR	(CI 95%)	p	HR	(CI 95%)	p
P53 trascription opathwayys			7.6E-12*			2.4E-9*
P53±/MDM4+/MDM2±/Bcl2±/p21±	1.0			1.0		
P53-/MDM4-/MDM2+Bcl2+/p21±	2.7	(1.3-5.4)		2.4	(1.4-3.9)	
P53±/MDM4-/MDM2-/Bcl2+p21±	3.3	(1.8-5.9)		2.2	(1.5-3.4)	
P53±/MDM4-/MDM2-/Bcl2-/p21-	3.6	(2.0-6.7)		2.8	(1.8-4.3)	
P53-/MDM4-/MDM2+/Bcl2-/p21-	4.6	(2.1-10.0)		2.5	(1.3-4.7)	
P53+/MDM4-/MDM2+/Bcl2-/p21-	8.5	(3.9-18.4)		5.9	(3.0-11.2)	
P53-/MDM4-/MDM2-/Bcl2-/p21-	6.1	(3.0-12.4)		3.7	(2.1-6.5)	
P53+/MDM4-/MDM2-/Bcl2-/p21-	14.7	(6.6-32.7)		8.6	(4.3-168)	
Lymph node (LN)stage			1.6E-15*			8.4E-15*
Negative	1.0			1.0	1	
1-3 LNs+	1.8	(1.4-2.4)		1.3	(1.1-1.7)	
>3 LNs+	4.9	(3.4-7.0)		3.9	(2.8-5.4)	
Histological grade			0.001*			0.272
Grade1	1.0			1.0		
Grade 2	1.3	(0.7-2.5)		1.0	(0.7-1.6)	
Grade 3	2.2	(1.2-3.9)		1.2	(0.8-1.9)	
Size	1.3	(1.1-1.54)	0.001*	1.2	(1.1-1.4)	0.003*
HER-2 overexpression	1.8	(1.3-2.6)	0.001*	1.9	(1.3-2.6)	2.5E-4*
Ck5/6+	1.3	(0.9-1.9)	0.108	1.6	(1.2-2.2)	0.001*
Eostrogen receptor(-)	1.2	(0.8-1.8)	0.273	1.6	(1.2-2.3)	0.009*
Progesterone receptor(-)	1.1	(0.8-1.6)	0.476	0.9	(0.7-1.2)	0.772

* Statistically significant

MDM2: murine double minute 2; MDM4: murine double minute; HER-2: Human epidermal growth factor receptor 2; Ck: cytokeratin

To examine the prognostic significance of functional status of p53 transcriptional status, the p53 transcription pathway phenotypes were reduced into 2 groups according to the status of p53 transcriptional activity a) active/partially inactive p53 transcription pathway including p53±/MDM4+/MDM2±/Bcl2±/p21±, p53+/MDM4-/MDM2+/Bcl2+/p21± and p53±/MDM4-/MDM2-/Bcl2+/p21± and b) completely inactive p53 transcriptional pathways (two or more inactive p53 transcriptional pathways) including p53±/MDM4-/MDM2-/Bcl2-/p21-, p53-/MDM4-/MDM2+/Bcl2-/p21-, p53±/MDM4-/MDM2-/Bcl2-/p21+ and p53+/MDM4-/MDM2+/Bcl2-/p21-. In both Nottingham/Tenovus and RMH/Breakthrough series, the completely inactive p53 pathways showed a worse clinical outcome (**Figure 6-6**). Our exploratory analyses revealed that the function status of p53 transcription pathway i.e. active/partially inactive vs. completely inactive pathway status, was proven to be significant in LN-negative patients (BCSS: log rank 5.4, p=2.3E-13 and DFS: log rank 36.5, p=1.5E-9), in LN-positive patients [BCSS: log rank 31.2, p=2.3E-8 and DFS: log rank 19.2, p=1.3E-5], patients who received no AT (BCSS: log rank 40.9, p= 1.7E-10 and DFS: log rank 32.7, p= 1.9E-8) and those with ER+ tumours who received HT ($p<0.0001$) (BCSS: log rank 13.6, p= 2.2E-4 and DFS: log rank 142.2, p= 1.6E-4).

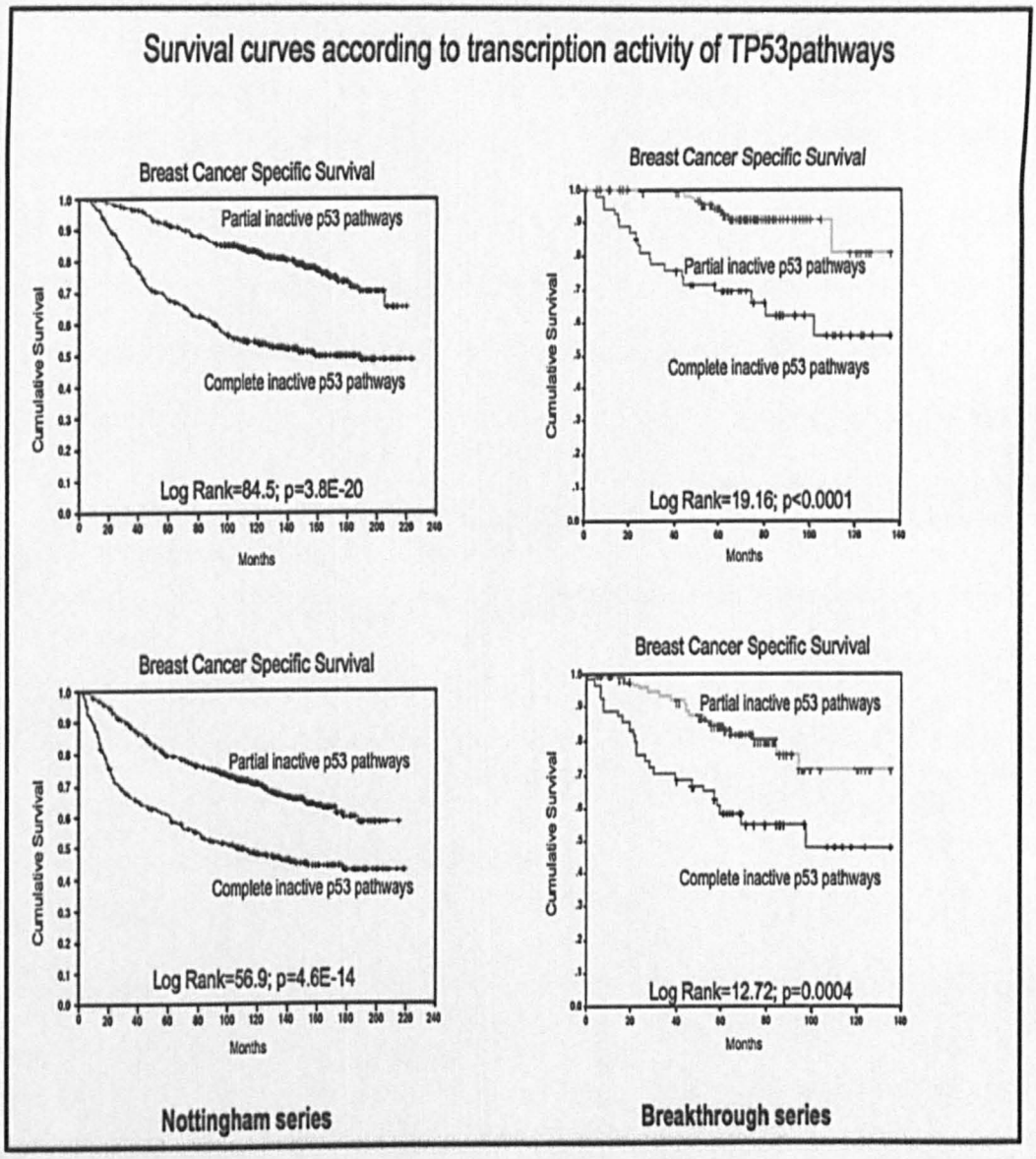

Figure 6-6: Kaplan–Meier survival curves (breast cancer specific survival and disease free survival) of both Nottingham/Tenovus (left upper and lower) and RMH/Breakthrough series (right upper and lower) stratified according to partially inactive and completely inactive p53 pathways.

In Multivariate Cox regression analysis of Nottingham/Tenovus series, the completely inactive p53 transcriptional status was an independent predictor of outcome and more powerful than NPI for BCSS: HR 2.64, 95% (CI) 1.61-4.32, p<0.0001 vs. HR 1.71, 95% (CI) 1.36-2.15, p<0.0001, respectively, and for DFS: HR 1.93, 95% (CI) 1.33-2.81, p=0.001 vs. HR 1.46, 95% (CI) 1.22-1.75, p<0.0001, respectively. These profiles were also shown to be independent predictors of BCSS, DFS and MFS in the RMH/Breakthrough series **(Table 6-6).**

Table 6-6: Cox regression model showing independence of the status of p53 transcription activity as a prognostic factor in RMH/Breakthrough series

Factor	Breast Carcinoma Specific Survival (BCSS) 10 years			Disease Free survival (DFS) 10 years		
	HR	(CI 95%)	p	HR	(CI 95%)	p
P53 trascription activity			0.001*			0.007*
Active/partially inactioc	1			1		
Completely inactive	4.5	(1.856-11.017)		2.5	(1.286-4.806)	
Lymph node (LN) stage			0.008*			0.002*
Negative (LN-)	1			1		
Positive (LN+)	4.2	(1.457-12.275)		3.4	(1.539-7.317)	
Histological grade			0.5			0.161
Grade1	1			1		
Grade 2	1.04	(0.114-9.455)		2.7	(0.337-21.749)	
Grade 3	1.9	(0.235-15.281)		4.8	(0.628-36.140)	
Size	1.01	(0.997-1.035)	0.096	1.02	(1.002-1.028)	0.0261

* Statistically significant

We investigated the clinical outcome of 274 early stage small tumours (lymph node negative with primary tumour size ≤ 2cm) from Nottingham/Tenovus patients who did not receive any AT. Consistent with the findings in the other groups, patients with partially inactive p53 pathways had a longer BCSS and DFS than cases with completely inactive p53 pathways [(HR 3.97, 95% (CI) 2.2-7.2, p<0.0001) and (HR 2.5, 95% (CI) 1.6-3.9, p<0.0001), respectively], **(Figure 6-7).**

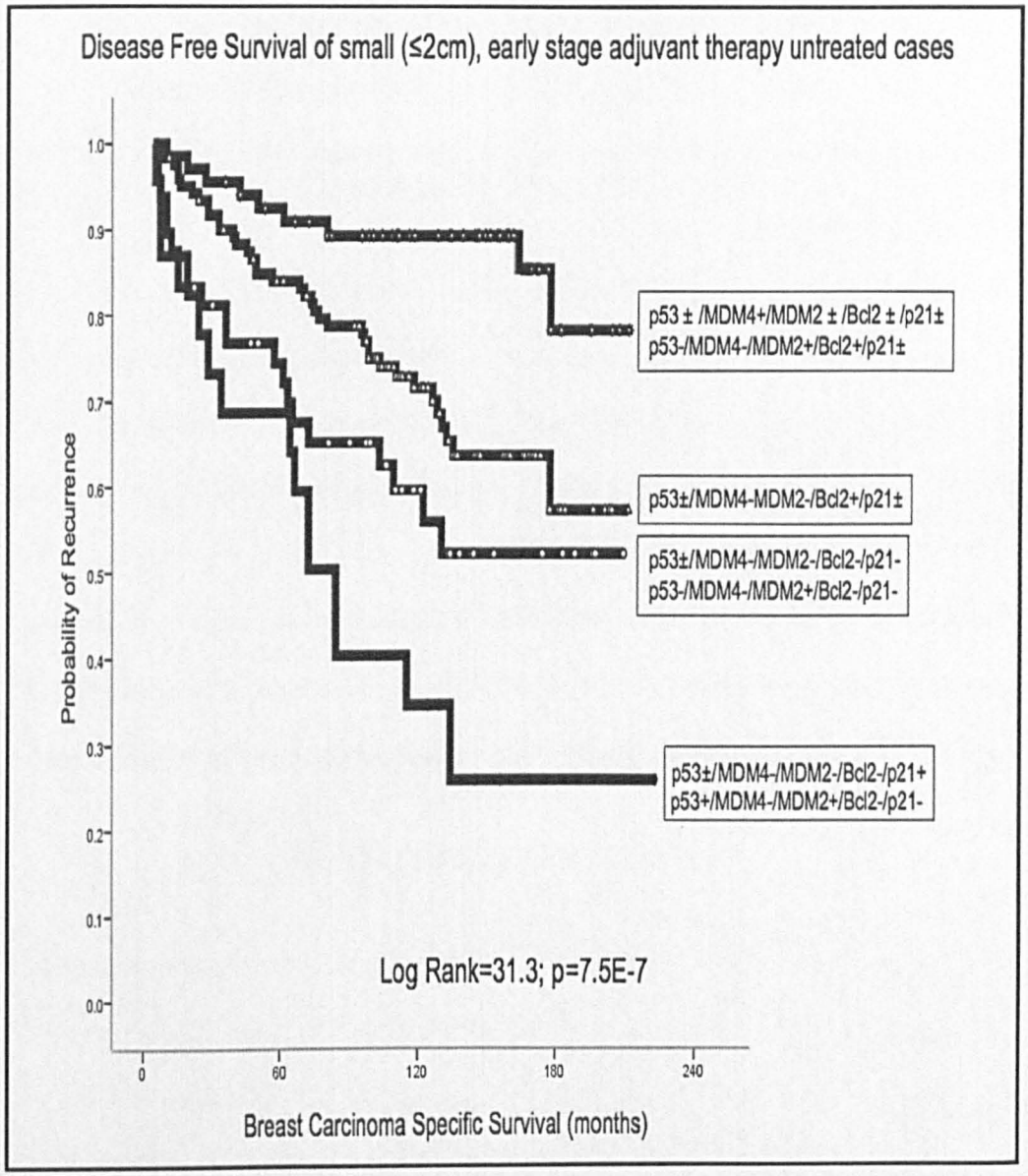

Figure 6-7: Kaplan–Meier survival curves of disease-free survival of breast small early stage breast cancer patients who received no systemic adjuvant therapy stratified according to p53 transcription pathways.

6.4.4 Clinicopathological features of different *TP53* transcription pathway phenotypes

MDM4 overexpression phenotypes

It was found that 182/990 (18%) of Nottingham/Tenovus cohort showed MDM4-overexpression which was associated with favourable clinicopathological features: ER+, PR+, AR+, small tumour size, and low grade with longer BCSS and DFS (data not shown). Tumours with MDM4-overexpression displayed high expression of MDM2, Bcl2, p21 and low Bax indicating partially inactive p53 transcription pathways. BCSS, DSF and MFS of cases with concomitant expression of p53 and MDM4 (p53+/MDM4+/MDM2±/Bcl2±/p21±) were similar to those with a p53-/MDM4+ phenotype, despite the fact that the latter group included a higher percentage of ER+ ($p<0.0001$) and low grade cancers ($p<0.0001$).

MDM2 overexpression phenotypes

MDM2-overexpression was found in 26% (253/990) and 37% (66/180) of Nottingham/Tenovus and RMH/Breakthrough patients; respectively and according to co-expression of p53, MDM4, Bcl2 and p21, it comprised a blend of 4 different phenotypes with statistically significant different clinical outcomes ranging from excellent to very poor prognosis ($p<0.0001$):

a) Patients with tumours displaying a concomitant MDM4+ and MDM2+ phenotype (p53-/MDM4+/MDM2+/Bcl2±/p21±) showed both excellent prognosis and favourable clinicopathological characteristics indistinguishable from those with exclusive MDM4-overexpression (p53±/MDM4+/MDM2-/Bcl2±/p21±).
b) Patients with tumours harbouring p53-/MDM4-/MDM2+/Bcl2+/±p21 had a relatively good outcome, however compared with those from the p53-/MDM4+

/MDM2+/Bcl2±/p21± subtype, these patients showed a relatively worse prognosis (HR=2.5, p=0.01), higher frequency of ATM- (p=0.004) and ER+ (p=0.001)

c) Patients with p53-/MDM4-/MDM2+/bcl2-/p21- tumours displayed a shorter BCSS and DFS (Fig 3) and more aggressive clinicopathological features compared to the p53-/MDM4-/MDM2+/Bcl2+/p21± subgroup.

d) Patients with p53+/MDM4-/MDM2+/Bcl2-/p21- tumours showed clinico-pathological features identical to those with (p53+/MDM4-/MDM2-/Bcl2-/p21-) and those (p53-/MDM4-/MDM2+/Bcl2-/p21-).

Negative MDM4 and MDM2 phenotypes

When Nottingham/Tenovus cases with concomitant negative expression of MDM4 and MDM2 were stratified according to p53, Bcl2 and p21 co-expressions, 6 phenotypes with 4 clinical outcomes ranged from moderate to extremely poor prognosis were identified:

a) Patients with p53-/MDM4-/MDM2-/Bcl2+/p21± tumours were characterised by moderate prognosis and favourable clinicopathological features. Compared to patients with tumours displaying a p53-/MDM4-/MDM2-/Bcl2-/p21- phenotype, they were associated with slightly better prognosis (HR=1.47, p=0.035), lower histological grade (p<0.0001), higher frequency of ER+ (p<0.0001), PR+ (p<0.0001), and lower frequency of basal-like (p<0.0001) and triple-negative phenotypes (p<0.0001). However compared to those with p53-/MDM4-/MDM2+/Bcl2+/p21± tumours, these cases displayed shorter BCSS, DFS, and DM formation times (data not shown), higher grade (p<0.0001), and higher frequency of Bax- (p=0.001).

b) Patients with p53+/MDM4-/MDM2-/Bcl2+/p21± cancers showed clinical outcomes and pathological features similar to those with p53-/MDM4-/MDM2-/Bcl2+/p21± tumours.

c) Patients with tumours displaying a p53-/MDM4-/MDM2-/Bcl2-/p21- phenotype were associated with poor prognosis and unfavourable clinicopathological features, similar to those with p53-/MDM4-/MDM2+/Bcl2-/p21- tumours.

d) Patients with p53+/MDM4-/MDM2-/Bcl2-/p21- tumours, apart from the clinicopathological features of high p53 protein expression (i.e. higher grade, ER-, basal-like and triple negative phenotypes), showed poor clinical outcome and clinicopathological features similar to those present in subjects with p53-/MDM4-/MDM2+/Bcl2-/p21- tumours.

MDM4-/MDM2-/Bcl2- phenotype with high p21

Patients with p53-/MDM4-/MDM2-/Bcl2-/p21+ tumours, compared to those with a p53-/MDM4-/MDM2-/Bcl2-/p21- phenotype, showed shorter BCSS, DFS and MFS (HR; 1.6, 95% CI; 1.04-2.56, p=0.03) but a higher frequency of ER+ (p=0.009). On the other hand, patients with p53+/MDM4-/MDM2-/Bcl2-/p21+ tumours, compared to those with a p53+/MDM4-/MDM2-/Bcl2-/p21- phenotype, showed a shorter BCSS: HR 3.0, 95% CI 1.7-5.5, p=1.6E-4; DFS: HR 2.4, 95% CI 1.4-4.2, p=0.002 and MSF: HR 2.4, 95% CI 1. 4-4.3, p=0.003 and higher frequency of HER-2 overexpression (p=0.004). On the other hand, when compared to those with a p53-/MDM4-/MDM2-/Bcl2-/p21+ phenotype, patients with p53+/MDM4-/MDM2-/Bcl2-/p21+ tumours were significantly more frequently ER- (p=0.001).

6.4.5 Clinicopathological features of completely inactive p53 transcription pathway

In both Nottingham/Tenovus and RMH/Breakthrough series, a completely inactive p53 transcription pathway was strongly associated with aggressive clinicopathological features, active progressive cell cycle and more genetic instability including: higher grade, Bcl2-, p21-, p27-, ER-, PR-, p53+, *HER-2* gene amplification, EGFR+, basal Ck+, higher proliferation index (MIB1), basal-like phenotype and triple negative (**Tables 6-7 and 6-8**). In the Nottingham/Tenovus series completely inactive p53 transcription pathways were associated with larger tumour size and higher LN stage as well; it should be noted that similar associations were not expected to be found in the RMH/Breakthrough series, given that it is composed solely of patients who received AT.

Table 6-7: The clinicopathological features of p53 transcription pathways status in Nottingham/Tenovus series

Variable	P53 transcription status		X^2
	Active/partially inactive (N=608) n (%)	Completely inactive (N = 382) n (%)	*P value*
Size			3.7E-10*
≤2cm	391 (65)	185 (48)	
>2cm	213 (34.5)	186(49)	
>5cm	3 (0.5)	10 (3)	
Lymph node Stage			
Negative	376 (63)	225 (59)	1.2E-5*
Positive (1-3 nodes)	201 (33)	110 (29)	
Positive (>3 nodes)	25 (4)	47 (12)	
Grade			3.8E-30*
Grade 1	134 (22)	16 (4)	
Grade 2	224 (37)	70 (18)	
Grade 3	244 (41)	295 (78)	
Bax (+)	186 (34)	76 (26)	0.024
p27 (+)	169 (36)	45(15)	1.5E-10*
BRCA1 (-)	113 (14)	127 (27)	2.8E-9*
ATM (-)	243 (40)	229 (60)	0.01*
MIB1(+)	274(45)	302(79)	1.2E-14*
ER(+)	503 (86)	155(42)	2.2E-14*
PgR(+)	423 (72)	159 (28)	3.2E-14*
Ck18(-)	29(5)	81 (23)	2.0E-14*
Ck5/6(+)	55(9)	111(29)	1.4E-14*
EGFR (+)	92 (16)	96 (27)	1.0E-04*
Vimentin	23 (5)	79 (25)	1.7E-14*
HER-2(+)	28 (5)	85 (12)	5.0E-7*
Basal like phenotype	37 (6)	110 (31)	1.6E-14*
Triple negative phenotype	47 (8)	161 (44)	1.3E-14*

* Statistically significant.. MDM2: murine double minute 2; MDM4: murine double minute 4; ATM: ataxia telangiectasia mutated; BRCA1: Breast cancer 1; ER: oestrogen receptor; PgR; progesterone receptor; Ck: cytokeratin; EGFR: epidermal growth factor; TOP2A: Topoisomerase II alpha.

Table 6-8: The clinicopathological features of p53 transcription pathways status in RMH/Breakthrough series

Variable	P53 transcription status		
	Active/partially inactive (N=124) n (%)	Completely inactive (N=56) n (%)	X^2 p
Size			0.310
≤2cm	68 (55)	27 (48)	
>2cm	46 (37)	27 (49)	
>5cm	9 (7)	2 (4)	
Lymph node Stage			
Negative	44 (37)	23 (42)	0.616
Positive	74 (63)	32 (38)	
Grade			0.002*
Grade 1	15 (12)	3 (6)	
Grade 2	42 (35)	7 (13)	
Grade 3	65 (53)	44 (81)	
MIB1(+)	52 (49)	25 (79)	5E-4*
ER(+)	115 (93)	33(59)	1.7E-7*
PgR(+)	105 (85)	30 (54)	2.6E-5*
Ck5/6(+)	5 (4)	13 (25)	0.00017*
EGFR(+)	4(3)	13 (23)	7.0E-04*
HER-2(+)	13(10)	13 (25)	0.036
HER-2 CISH(+)	11(9)	15 (28)	0.002*
TOP2A(+)	58 (48)	35 (66)	0.032
TOP2A CISH	7 (6)	10 (11)	0.012
Basal like phenotype	5 (4)	15 (27)	<0.0001*
Triple negative phenotype	6 (5)	14 (25)	0.0002*

* Statistically significant. MDM2: murine double minute 2; MDM4: murine double minute 4; ATM: ataxia telangiectasia mutated; BRCA1: Breast cancer 1; ER: oestrogen receptor; PR: progesterone receptor; Ck: cytokeratin; EGFR: epidermal growth factor; TOP2A: Topoisomerase II alpha.

6.4.6 P53 status and clinical outcome in specific AT settings

To evaluate whether the status of p53 transcription pathways had different clinical outcomes in specific AT settings, we investigated the clinical outcome and survival of Nottingham/Tenovus high risk patients (n=309; NPI≥3.4 and ER+) and (n=152; NPI ≥3.4 and pre-menopausal) who had received HT and CMT-chemotherapy, respectively. We found that patients with phenotypes (p53±/MDM4-/MDM2±/Bcl2-/p21-) and (p53±/MDM4-/MDM2-/Bcl-/p21±) had the worst outcomes in both HT and CMT-chemotherapy treated patients (data not shown). Completely inactive p53 pathways in HT or CMF-chemotherapy treated patients had shorter BCSS: HR 2.1, 95% CI 1.4-3.1, p=2.5E-4 and HR 1.8, 95% CI 1.1-2.9, p=0.026, respectively; DFS: HR 2.0, 95% CI 1.4-2.8, p=2.0E-4 and HR 1.8, 95% CI 1.1-2.6, p=0.01, respectively and MFS: HR 2.0, 95% CI 1.4-2.9, p=3E-4 and HR 1.7, 95% CI 1.03-2.8, p=0.036, respectively.

Poor outcome of completely inactive p53 pathways was confirmed in the RMH/Breakthrough series which comprised patients that were uniformly treated with anthracycline-based chemotherapy (**Figure 6-7**)

6.5 Discussion

Almost half of human cancers retain the wild-type *TP53*, indicating that the p53 pathway is inactivated by alterations other than mutation of *TP53* itself [102, 177-181, 227-228-232]. Specific post-translational modifications of p53 [18, 225, 234] and p53-independent pathways, e.g., ER-α, can modulate the activity of p53 transcription pathways [230-232, 234, 235]. Depending on which upstream or downstream components within the p53 transcription pathway have been inactivated [177-180], variable patterns of association between p53 and a number of other co-regulatory and effectors proteins have been documented [177-180]. In our study we identified two main groups of p53 transcription pathways regardless of the expression level of p53: (a) Low risk, with active or partially inactive p53 transcription pathway, which was associated with tumours displaying favourable clinical parameters, good prognosis and had significantly longer BCSS and DFS after AT. (b) High risk, with completely inactive p53 pathway, which was characterised by aggressive clinicopathological features, and poor prognosis and worse outcome even in AT treated patients.

6.5.1 Completely inactive p53 transcription pathways

As we have shown, regardless of p53 levels, patients with a completely inactive p53 pathway exhibited unfavourable clinicopathological features, bad prognosis and poor outcome even after receiving AT. In a high proportion of cancers lacking point missense *TP53* mutation, p53 function could be inactivated by other recognised mechanisms including null mutations, MDM2 overexpression, and/ or alteration of p53 upstream regulators or co-activator (e.g. ATM) [102, 177-180, 228-231]. For instance, TP53 null mutations destabilise p53 and are associated with absence of p53, MDM2, Bcl2 and p21 [228]. In leukaemia, ATM has been shown to represent an alternative regulatory mechanism of p53 inactivation [102, 177-180]. In agreement with others [102, 177-180], we found 60% of tumours with completely inactive p53 were associated with loss of ATM expression suggesting that ATM in BC may be a

mechanism by which a subset of BC escape tumour suppressor effect of p53 [237, 238]. Another transcriptional co-activator for p53 is BRCA1 which stimulates transcription from p53-resposive promoters [102, 88, 180]. We found down-regulation of BRCA1 was statistically significant ($p<0.0001$) associated with the completely inactive p53 transcription pathways implying a further mechanism whereby p53 function can be inhibited in BC.

Genetic changes at chromosome 17, where the *TP53* gene is located, have been reported in more than half of high grade BC [225]. We found complete inactivation of *TP53* was associated with *HER-2* amplification.

6.5.2 Clinical outcome diversity of MDM2/MDM4 over-expression and TP53/ER crosstalk networks

The significance of MDM2/MDM4 with respect to cancer diagnosis and prognosis is unclear, as MDM2-overexpression has been reported to correlate with poor prognosis in some studies, however with good prognosis in others [179-180, 234, 235, 238]. Indeed we found that MDM2-overexpression is associated with both good and poor prognosis depending on co-expression of p53, MDM4, Bcl2 and on p53 dependent and independent transactivation of MDM2 [177-180, 234, 235, 238]. In BC, overexpression of multiple-MDM2-mRNA variants has been shown to correlate with absence of ER and worse outcome, while MDM2 overexpression occurred only in ER-α positive tumour, and was associated with a favourable prognosis [234]. In addition, in tissue culture model systems, it was shown that ER-dependent p53- independent transactivation of MDM2 in BC cells could only occur in cell lines that were ER-α positive [234, 235]. Moreover, it has been suggested that Bcl2, p21 and MDM2 could be p53-independent direct transcriptional regulators of ER [179, 180, 230, 231, 234, 235, 238]. In accord with these observations, we found MDM2-overexpression subgroups with better prognosis were associated with normal expression of p53 and strongly correlated to

the presence of Bcl2 and ER, while those with poor prognosis were strongly correlated to presence of abnormal p53 protein expression and absence of Bcl2, p21, and ER.

6.5.3 P21 expression and worst prognosis and poorest outcome after AT treatment

We found that p21+ expression is not significantly associated with clinical outcome in BC although p21+ was statistically associated with recognised favourable clinical parameters. However, tumours with p53-/MDM4-/MDM2-/p21+ and p53+/MDM4-/MDM2-/Bcl2-/p21+ phenotypes, despite showing ER+ and HER-2 overexpression, respectively, had a very poor prognosis and the shortest BCSS and DFS after receiving AT, in agreement with previous reports on p21 [239-242]. In fact, data from colorectal cancer cell lines and mouse model studies showed that the growth and proliferation of tumour cells with intact checkpoint functions (p21+/+) was not inhibited by γ-irradiation and chemotherapeutic agents, whereas γ-irradiation and chemotherapeutic agents successfully inhibited checkpoint-deficient cells (p21-/-) [240-242]. In addition, recent anti-sense studies for p21 gene suppression reported increased radio- and chemo-responsiveness by enhancing apoptosis [243]. Moreover, critical roles of p21 in concomitantly preventing apoptosis, promoting growth "cell survival promoter", and inducing differentiation through direct interaction with ER, have been recently proposed [243].

6.5.4 p53 transcriptional pathways, clinical outcome and management of BC

In BCs, only a minority of patients (< 20% of those receiving AT fully benefit from the different AT regimens currently in use) [178, 180, 227, 232, 235]. There is evidence to support a critical role of wild-type p53 in modulating response to AT by triggering either apoptosis or cell-cycle arrest [177-227, 232, 233] .However, it is also obvious that AT may also induce apoptosis via a p53-independent pathway [239] and mutant *TP53* has been claimed to interfere with p53-independent apoptosis [239]. In agreement with other studies [177-227, 230, 232, 233] we have demonstrated a significantly worse BCSS and DFS in completely inactive p53 transcription pathways with either high or low p53 expression patients even after receiving AT compared with patients with active or partially inactive TP53 pathways. Moreover, we found that patients with p53-independent p21 and MDM2 expression given AT had the shortest BCSS and DFS especially ER-α + patients. This study was not designed to address the associations between p53 transcriptional pathways and response to adjuvant endocrine or chemo-endocrine therapies. However, our results provide evidence to suggest that the functional status of p53 transcriptional pathways may predict the clinical outcome in both adjuvant systemic therapy naïve patients and those treated with endocrine and/ or chemotherapy (both CMF and anthracycline-based regimens). In fact, interfering with p53 itself or its downstream transcriptional targets may provide interesting therapeutic avenues. Preclinical gene therapy studies have demonstrated that *TP53* correction results in an increase in radio- and chemotherapy sensitivity and anti-tumourigenic effects in several types of cancer [177, 180, 224-232, 233, 235, 243] .

In conclusion, we have shown that the phenotypic patterns of p53 functional transcriptional pathways rather than its expression alone provide important information about BC behaviour. This information may assist routine clinical decision-making. Future

studies testing the prognostic and predictive information provided by the p53 transcriptional pathway subgroups in prospectively accrued material from clinical trials are warranted.

Chapter 7:

Discussion

Frequently, pathologists observe a collection of co-existing subtle pathological changes in breast tissue samples representing 'precursor' lesions. These are challenging to identify, classify and manage and currently, we cannot predict which precursors will progress into cancer but studies suggest that between 1–30% lesions develop a subsequent tumour event within a decade [66-67]. In contrast to the 'stochastic' model of ontogenesis where transformation results from random mutations and subsequent clonal selection, tumours nowadays are considered as a multi-step clonal disease and its progression is dependent on acquiring further genetic and epigenetic changes in stem or progenitor cells that lead to activation of oncogenes and inactivation of tumour suppressor genes [27-30, 62-65]. In this model, cancer originates in tissue stem or progenitor cells probably through dysregulation of self-renewal pathways and this leads to expansion of this cell population that may undergo additional genetic and epigenetic change [62]. The nature of these genetic and epigenetic changes, and the type of progenitor they target, probably contribute to the cellular heterogeneity found in tumours [27-30, 62-65]. The transformation of progenitor cells into neoplastic cells may be due to deregulation of self-renewal, differentiation, membrane transport activity, telomerase activity and anti-apoptotic pathways, contributing to the ability to migrate and metastasis [27-30, 62-65]. Currently the precise cell lineages involved in the earliest oncogenic events involving progenitor transformation and formation of precursor lesions en route to invasive cancer development is not known.

In this study, we noticed that some columnar cell lesions associated with ADH and/or /ALH progressed into invasive special types of breast cancer: TC, TLC and/or classic ILC, within 5-15 years of the initial diagnosis. This led us to conduct a comprehensive morphological study to determine the morphological features and frequency of putative precursor lesions involved in the development of some pure forms of special types of

breast carcinoma. Subsequently, we identified the LNGBN family that included low nuclear grade breast carcinoma (LNGBC; tubular, cribriform, low grade invasive ductal carcinoma, classical lobular and tubulolobular carcinoma) and their putative precursor lesions; low nuclear grade intraepithelial neoplasia (flat epithelial atypia (FEA), atypical ductal hyperplasia (ADH), low/intermediate ductal carcinoma in situ (DCIS), and lobular neoplasia (LN), (**Figure 7-1**).

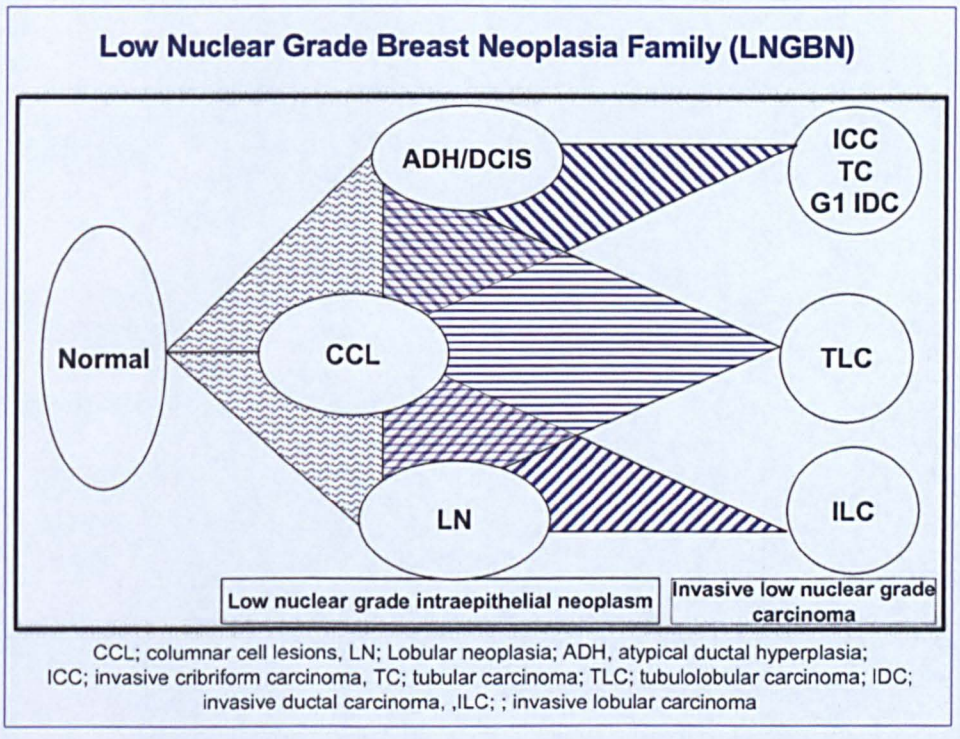

Figure 7-1: Evolutionary pathways of low grade breast neoplasia.

Our proposal of the LNGBN family was based on a) remarkable similarity of nuclear and cytoplasmic morphological features between putative precursor lesions and either co-existing or consequent invasive carcinoma, b) intimate topographic distribution of putative precursor lesion and either co-existing or consequent invasive carcinoma, c) the significant coexistence of columnar cell lesions (CCLs), lobular neoplasia (LN) and atypical ductal hyperplasia/low grade ductal carcinoma in situ (ADH/low grade DCIS) with invasive tubular carcinoma (TC), tubulolobular carcinoma (TLC) and classic invasive lobular carcinoma (ILC).

In addition, we proposed an evolutionary and biological pathway for the development of this LNGBN family in which FEA was considered as the very early non obligate common precursor (**Figures 7-2 and 7-3**).

Lesions		Reported Genetic Changes						Reference
		Loss			Gain			
CCC ↓		-16q	-19q	-11q	+16p +7	+19	+20 +15q	71
CCC with atypia ↓	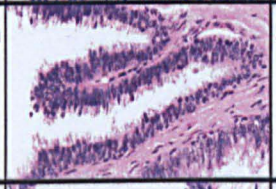	-16q	-17p -22 -12q		+16p +7			71 75
CCH with atypia ↓	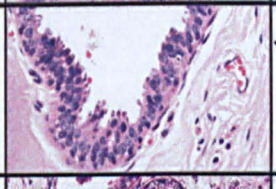	-16q	-17p -22 -12q		+16p +7	+8q		71
CCH complex architectural & atypia ↓	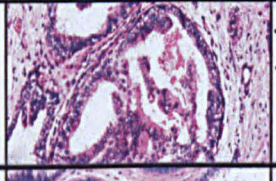	-16q -6q	-17p -22 -12q		+16p +7 +17q	+8q +19	+15q +12p +3p +3q	71
ADH ↓		-16q -6q -8p	-17p -22q 12q	-11q -1p -13q -11q	+17q	+1q +8q	+12q +6q +3q +2p	81 89
Low grade DCIS ↓	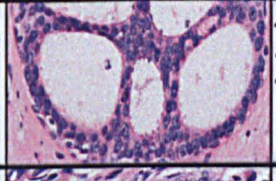	-16q -6q -8p	-17p -19q -22 -12q	-13q -14q -11q	+16p +7p +17q	+8q +19 +1q	+15 +20 +12p +3p	71 81
Tubular Carcinoma	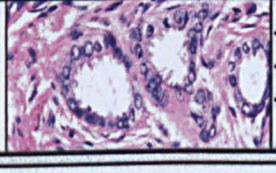	-16q -6p -8p	-17p	-11q	-16p +7 +17q	+8q +19 +1q	+20	60 90

Figure 7-2: The proposed evolutionary pathway of tubular carcinoma based on histological evidence and the reported genetic changes for each stage

Lesions		Reported Genetic Changes						Reference
		Loss			Gain			
CCC ↓	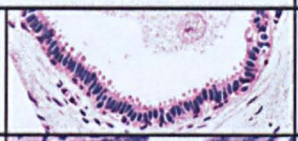	-16q		-11q -19q	+16p +7		+19 +20 +15q	71
CCH ↓	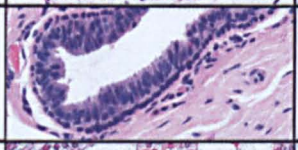	-16q	-17p -22 -12q	-11q -1p	+16p +7			71
CCH with atypia ↓	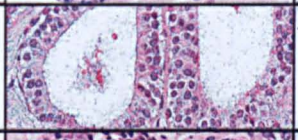	-16q	-17p -22 -12q		+16p +7	+8q		71
LN ↓	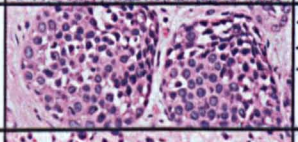	-16q -16p -8p	-17p -22q 12q	-11q -1p -13q -11q	+17q	+1q +8q	+12q +6q +3q +2p	60 81 82
ILC	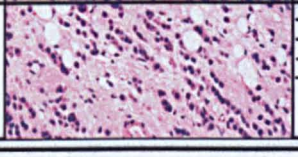	-16q -16p -6q -8p	-17p -22q -12q	-19p -11q -1p -13q -17q	+16p +7p +17q	+1q +8q	+19 +20q +3q	60 81 82

Figure 7-3: The proposed evolutionary pathway of ILC through CCLs based on histological evidence and the reported genetic changes for each stage

Moreover, we have used custom-made tissue microarrays (TMA) with high throughput immunohistochemistry (IHC) to investigate a panel of biological markers including cell cycle, proliferation, apoptosis, differentiation and hormone receptor regulator proteins and a number of putative tumour suppressor and oncogenes. We found that CCL, ADH/low grade DCIS, LN and invasive low grade breast cancers have remarkably similar immunophenotype and that this phenotype is very similar to the immunophenotype of the luminal "A" BC subclass and is distinct from that have seen in high grade breast cancers. The luminal "A" BC subclass is characterised by high expression of oestrogen and progesterone receptors, MUC1, ESA, and luminal CK (CK18/19).

Interestingly, we found the low nuclear grade breast neoplasia family have a similar immunohistochemistry profile to the ER+ luminal restricted progenitor cell of normal terminal duct lobular units and we speculated that the LNGBN family may arise from the luminal restricted progenitors cell (ER+/MUC-1+) which might further acquire stochastic genetic and epigenetic hits that lead to the activation of the luminal 'A' pathway. This finding supports our proposal of FEA as a common non-obligate precursor of TC and ILC. Furthermore, the similarity in the genomic profiles of CCLs and matched co-existing DCIS, LN and invasive carcinoma supports a common cell of origin of this family and gives substantial evidence that CCLs are the early non-obligate precursor lesions of tubular and invasive lobular carcinoma.

We found one of the remarkable features of the LNGBN family is low mitotic index and positive expression of cell cycle/apoptosis regulator Bcl2. Subsequently, we hypothesised that a grading system based on balance between "M" as a proliferation marker and "Bcl2" as a cell cycle/apoptosis regulator would be capable of accurately discriminating between low and high-grade tumours and providing a more objective and clinically valuable measure of tumour grade with prognostic significance for invasive BC in general and particularly in moderately differentiated, small and ER negative (ER-) cancers. Moreover, we found the balance between mitotic index and Bcl2 protein expression is an independent predictor of

outcome in a population based cohort and accurately reclassified most patients with NGS-G2 including (97%) of ILC into low grade like risk group. In addition, we showed the M/Bcl2 balance identified prognostically significant subgroups in a cohort of patients treated with adjuvant anthracycline-based chemotherapy. The use of this simple and objective grading system instead of NGS may help improve on the prognostic ability of current algorithms for clinical decision making (e.g. NPI). We further substantiate our proposal of LNGBN by exploring the genomic profiles of matched coexisting different members of LNGBN family which exhibit remarkable genetic similarity.

Whether the LNGBN family is a continuum through which BC progresses or merely the end point of distinct genetic pathways has been debated [140] and it is not clear whether BC develops along two (low versus high) or three (grades 1 versus 2 versus 3) distinct pathways. In our study, the large majority of BC cases exhibited one of the two predominant forms comprising either LNGBC (NGS-G1-like) or high (NGS-G3-like) grade biological characteristics, supporting the view that genetic pathways model of grade origin. Tumours with intermediate prognosis (NGS-G2-like) may arise as homogenous tumours that are truly border-line between low and high grade, or could rather reflect a heterogeneous composition of both low and high grade cell types. Genetic analysis of LNGBC suggests the majority of these tumours constitute the end of the spectrum of low grade cancers as they often harbour deletion of 16q and gains of 1q [56, 60, 81].

Interestingly, we found that LNGBN tumours were either arrested in G0/G1 or out-of-cell cycle state. On the contrary, most basal-like and HER-2+ tumours were NGS G3-like phenotypes with actively progressive cell cycle suggesting that once BC committed to a specific evolutionary/molecular pathway, progression or cross over to other high grade pathways would be an unlikely biological phenomenon. However, the progression of a subset of low nuclear grade with luminal phenotype to luminal BC of a higher grade would be a possibility [140] and could be due to acquisition of additional genetic or epigenetic

aberrations (e.g., p53 mutation, gene amplifications), which lead to more active cell cycle progression and increased proliferation.

Meta-analysis of publicly available gene expression data [176-191] demonstrated that most of the genes associated with histological grade are involved in cell cycle regulation, proliferation, apoptosis, p53 and ER signalling networks. In agreement with these studies, we found that most candidate genes associated with the progression of LNGBN family are involved in cell cycle regulation, proliferation, apoptosis, p53 and ER signalling networks. Among these genes was MDM4 which demonstrated independent prognostic and predictive power. In addition our results showed that these markers faithfully identified women who were at high risk and who would benefit from different protocols of adjuvant therapy. Given that most of the LNGBN family have wild type p53, and both functional MDM4 and Bcl2 expression among p53 network led us to hypothesise that the functional status of p53 transcriptional pathways rather than p53 immunohistochemistry expression alone could accurately determine clinical outcome in a large unselected series of BC and in a series of patients uniformly treated with adjuvant anthracycline-based chemotherapy. Depending on which upstream or downstream components within the p53 transcription pathway have been inactivated. We recognized variable patterns of association between p53 and a number of other co-regulatory and effectors proteins. Subsequently, we identified two main groups of p53 transcription pathways regardless of the expression level of p53: (a) Low risk, with active or partially inactive p53 transcription pathway, which was associated with tumours displaying favourable clinical parameters, good prognosis and had significantly longer BCSS and DFS after AT; (b) High risk, with completely inactive p53 pathway, which was characterised by aggressive clinicopathological features, poor prognosis and worse outcome even in AT treated patients.

Chapter 8:

Conclusions, Key Points an Future Directions

The co-localisation of lobular neoplasia (ALH and LCIS) with columnar cell lesions, and ADH and low grade DCIS has been described with or without coexisting low grade or lobular invasive breast cancer. The concept of a low grade (luminal A type) family of invasive, in situ and their precursors is emerging which includes columnar cell lesions, ADH/ low grade DCIS, lobular neoplasia, classical lobular carcinoma and tubular carcinoma

In summary, our results suggest that 1) Tubular and lobular breast carcinoma arise as members of a low nuclear grade breast neoplasia (LNGBN) family, 2) CCLs are early non-obligate precursor components of the LNGBN family, 3) The common cell of origin of the LNGBN family may be the oestrogen receptor-alpha (ER α) positive luminal restricted progenitor cell (ER+/MUC1+ cells) of the terminal duct lobular unit that might acquire stochastic genetic and epigenetic changes that eventually lead to activation of the luminal "A" pathway, 4) Cyclin D1 and MDM4 are oncogenes that potentially lead to activation of the luminal pathway and progression of the LNGBN family, 5) An alteration of E-cadherin (*CDH1*) appears to be a secondary event resulting in the characteristic morphology of both in situ and invasive lobular lesions, 6) A biological grading system dependent on the balance between Bcl2 protein expression and mitotic figures could accurately reclassify patients with intermediately differentiated, small early stage or ER α negative breast cancers into two groups of low versus high risk of death and recurrence, and 7) The functional status of p53 transcriptional pathways can be assessed using immunohistochemistry protein expression of p53 downstream/regulator genes to accurately discriminate between low and high grade breast carcinoma and to assist routine clinical decision-making.

The future goals should focus on the development of a rapid, inexpensive prognostic clinical test that will provide individual risk information for all women diagnosed with precursor lesions.

This goal could be achieved by translating our genomic findings into a series of actions:

a) Substantiate our study findings of genomic change, using aCGH, in LNGBN by including additional candidate precursor lesions in a larger patient cohort with and without invasive cancer

b) Validate our genomic findings by detecting gene amplification/loss using fluorescence in situ hybridisation (FISH) and chromogenic in situ hybridisation (CISH) techniques, with emphasis on ER/p53 cross-talk network and cell cycle regulator genes

c) Investigate the prone chromosomal sites on 1q and 16q; other molecular techniques such as spectral karyotyping (SKY), muti-colour chromosome painting, second generation sequencing or methylation strategies could be used to investigate reciprocal translocation, subtle rearrangements or demethylation.

d) Develop a biological mouse model to investigate how human breast cells acquire cancer properties and to provide insights for predicting the development of tumour formation. A transplantable human-mouse (HIM) xenograft model could be generated from patients' precursor lesions before treatment as described by Ding et al 2010 [244]. Cells from precursor lesions could be implanted into the mammary fat pad and be followed up to detect further host-tumour pathological changes using histologic technique. Full genome sequencing could be performed on precursor lesions, early passage xenograft (harvested 101 days after initial engrafting into the mouse host) and for any new pathological lesions. DNA samples could be prepared from the aforementioned stages for sequence coverage and mutation analysis. In addition, these xenografts could be used to knockout one or more of the suppressor genes e.g. E-cadherin, p53 etc and/or to induce overexpression of one of the oncogenes to examine their role in the progression of

breast cancer. In addition, we can use one of the breast cancer transgenic mouse models whose oncogenesis is induced by expression of the polyoma virus middle T oncoprotein (PyMT mice) to analyze a series of biomarkers that are associated with the progression of human breast cancers especially cell proliferation, differentiation, and apoptosis markers. Previously, this mouse model of mammary carcinogenesis proved to represent a powerful model to study the causal events associated with tumour progression to malignancy and metastasis[245]

e) Clinical follow up of cases diagnosed with exclusive CCLs without ADH/ALH to estimate the risk of progression

f) Develop routine immunohistochemical (IHC) techniques to identify candidate markers which would assist in decision-making regarding the clinical management of preinvasive lesions and would tell a woman diagnosed with one of the precursor lesions about her risk of future breast cancer.

g) Develop clinical trials for our new biological grading system, MDM4 and p53 transcription activity.

Chapter 9:

References

1. American Cancer Society. Breast Cancer Facts & Figures 2009-2010. Atlanta: American Cancer Society, Inc (2009).

2. Ferlay J, Bray F, Pisani P et al. Globocan 2002: cancer incidence, mortality and prevalence worldwide. IARC Cancer Base 2004; 5(v2.0).

3. Veronesi U, Boyle P, Goldhirsch A et al. Breast cancer. Lancet 2005; 365: 1727-41.

4. Boyle P and J Ferlay. Cancer incidence and mortality in Europe, 2004. Annals of Oncology 2005; 16(3): 481-488.

5. Office for National Statistics, Cancer Statistics registrations: Registrations of cancer diagnosed in 2004, England. Series MB1 no.35.National Statistics: London (2007).

6. ISD Online. Information and Statistics Division, NHS Scotland (2007).

7. Welsh Cancer Intelligence and Surveillance Unit. Cancer Incidence in Wales (2007).

8. Northern Ireland Cancer Registry. Cancer Incidence and Mortality (2007)

9. Office for National Statistics. Mortality statistics: cause. England and Wales. London: The Stationery Office (2003).

10. Ellis IO, Galea M, Broughton N et al. Pathological prognostic factors in breast cancer. II: histological type: Relationship with survival in a large study with long-term follow-up. Histopathology 1992; 20: 479-89.

11. Wellings SR, Jensen HM, Marcum RG. An atlas of subgross pathology of the human breast with special reference to possible precancerous lesions. J Natl Cancer Inst 1975; 55: 231–273.

12. Dimri G, Band H, Band V. Mammary epithelial cell transformation: insights from cell culture and mouse models. Breast Cancer Res 2005; 7: 171-179.

13. Anbazhagan R, Osin PP, Bartkova J et al. The development of epithelial phenotypes in the human fetal and infant breast. J Pathol 1998; 184:197-206.

14. Nathan B, Anbazhagan R, Clarkson P et al. Expression of BCL-2 in the developing human fetal and infant breast. Histopathology 1994; 24:73–76.

15. Naccarato AG, Viacava P, Vignati S et al. Bio-morphological events in the development of the human female mammary gland from fetal age to puberty. Virchows Arch 2000; 436:431-8.

16. Woodward WA, Chen MS, Behbod F et al. On mammary stem cells. Cell Sci 2005; 118:3585-3594.

17. Polyak K. Breast cancer: origins and evolution. J Clin Invest 2007;117:3155-63

18. Clarke RB, Howell A, Potten CS et al. Dissociation between steroid receptor expression and cell proliferation in the human breast. Cancer Res 1997; 57:4987-91.

19. Gusterson BA, Ross DT, Heath VJ et al. Basal cytokeratins and their relationship to the cellular origin and functional classification of breast cancer. Breast Cancer Res 2005; 7:143-148.

20. Russo J, Mailo D, Hu YF et al. Breast differentiation and its implication in cancer prevention. Clin Cancer Res 2005 5; 11:931s-6s.

21. Russo J, Russo IH. Breast development, hormones and cancer. Adv Exp Med Biol 2008; 630:52-6.

22. Sabourin JC, Martin A, Baruch J et al. bcl-2 expression in normal breast tissue during the menstrual cycle. Int J Cancer 1994;59:1-6

23. Böcker W, Moll R, Poremba C et al. (2002). Common adult stem cells in the human breast give rise to glandular and myoepithelial cell lineages: a new cell biological concept. Lab Invest 82: 737-746.

24. Stingl J, Raouf A, Joanne T et al. Epithelial Progenitors in the Normal Human Mammary Gland. J Mammary Gland Biol Neoplasia 2005; 10:49-59.

25. Böcker W. and Buerger H. Evidence of progenitor cells of glandular and myoepithelial cell lineages in the human adult female breast epithelium: a new progenitor (adult stem) cell concept. Cell Profil 2003, 36: 73-84.

26. Nielsen TO, Hsu FD, Jensen K et al. Immunohistochemical and clinical characterization of the basal-like subtype of invasive breast carcinoma. Clin Cancer Res 2004 15; 10: 5367-74.

27. Liu S, Dontu G, Wicha MS. Mammary stem cells, self-renewal pathways, and carcinogenesis. Breast Cancer Res 2005; 7: 86-95.

28. Sherley JL. Asymmetric cell kinetics genes: the key to expansion of adult stem cells in culture. Stem Cells 2002; 20:561-572.

29. Behood F, Rosen JM. Will cancer stem cells provide new therapeutic targets? Carcinogenesis 2005; 26:703-711.

30. Charafe-Jauffret E, Monville F, Ginestier C et al. Cancer Stem Cells in Breast: Current Opinion and Future Challenges. Pathobiology 2008;75:75–84

31. Clarke RB, Spence K, Anderson E et al. A putative human breast stem cell population is enriched for steroid receptor-positive cells. Dev Biol 2005; 277:443-56.

32. Clayton H, Titley I, Vivanco M. Growth and differentiation of progenitor/stem cells derived from the human mammary gland. Exp Cell Res 2004; 297:444-60.

33. Dontu G, Al-Hajj M, Abdallah WM et al. Stem cells in normal breast development and breast cancer. Cell Prolif 2003, 36(Suppl 1):59-72.

34. Dontu G, El-Ashry D, Wicha MS et al. Breast cancer, stem/progenitor cells and the oestrogen receptor. Trends Endocrinol Metabol 2004; 15:193-197.

35. Dontu G, Liu SL, Wicha MS et al. Stem cells in mammary development and carcinogenesis - Implications for prevention and treatment. Stem Cell Reviews 2005; 1:207-213.

36. Dontu G. Breast cancer stem cell markers - the rocky road to clinical applications. Breast Cancer Res 2008;10:110

37. Stingl J, Eaves CJ, Kuusk U et al. Phenotypic and functional characterization in vitro of a multipotent epithelial cell present in the normal adult human breast.. Differentiation 1998; 63:201-213.

38. Stingl J and Caldas C. Molecular heterogeneity of breast carcinomas and the cancer stem cell hypothesis. Nature Reviews Cancer 2007; 7:791-799

39. Gudjonsson T, Villadsen R, Nielsen HL et al. Isolation, immortalization, and characterization of a human breast epithelial cell line with stem cell properties. Genes Dev 2002; 16:693-706.

40. Molyneux G, Regan J and Smalley MJ. Mammary stem cells and breast cancer. Cell Mol Life Sci 2007; 64: 3248 – 3260.

41. Al-Hajj M, Wicha MS, Benito-Hernandez A et al. Prospective identification of tumorigenic breast cancer cells. Proc Natl Acad Sci U S A. 2003 ;100:3983-8

42. Honeth G, Bendahl PO, Ringnér M et al. The CD44+/CD24- phenotype is enriched in basal-like breast tumors. Breast Cancer Res 2008; 10:R53.

43. Shipitsin M, Campbell LL, Argani P et al. Molecular definition of breast tumor heterogeneity. Cancer Cell. 2007 Mar;11(3):259-73.

44. Liu R, Wang X, Chen GY et al. The prognostic role of a gene signature from tumorigenic breast-cancer cells. N Engl J Med. 2007 Jan 18;356(3):217-26.

45. Jacquemier J, Ginestier C, Rougemont J et al. Protein expression profiling identifies subclasses of breast cancer and predicts prognosis. Cancer Res 2005; 65:767-779.

46. Sorlie T, Perou CM, Tibshirani R et al. Gene expression patterns of breast carcinomas distinguish tumour subclasses with clinical implications. Proc Natl Acad Sci USA 2001; 98: 10869-10874.

47. Weigelt B, Horlings HM, Kreike B et al. Refinement of breast cancer classification by molecular characterization of histological special types. J Pathol 2008; 216:141-50.

48. Sotiriou C, Wirapati P, Loi S et al. Gene expression profiling in breast cancer: understanding the molecular basis of histologic grade to improve prognosis. J Natl Cancer Inst 2006; 98: 262-272.

49. Ellsworth RE, Hooke JA, Love B et al. Correlation of levels and patterns of genomic instability with histological grading of invasive breast tumours. Breast Cancer Res Treat 2008; 107:259-265.

50. Ivshina A V, George J, Senko O et al. genetic reclassification of histologic grade delineates new clinical subtypes of breast cancer. Cancer Res 2006; 66: 10292-10301.

51. Ma XJ, Salunga R, Tuggle JT et al. Gene expression profiles of human breast cancer progression. PNAS 2003; 100 5974–5979.

52. Simpson PT, Reis-Filho JS, Gale T et al. Molecular evolution of breast cancer. J Patho 2005; 205:248-254.

53. Pasqualini JR and Chetrite GS. The enzymatic systems in the formation and transformation of estrogens in normal and cancerous human breast: Control and potential clinical applications. In: Pasqualini JR, ed. Breast cancer. Prognosis, treatment and prevention. New York: Informa healthcare 2008;11-49

54. Chin K, DeVaries S, Fridlyyand J et al. Genomic and transcriptional aberrations linked to breast cancer pathophysiologies. Cancer Cell 2006; 10:529-541.

55. Hicks J, Krasnitz A, Lakshmi B et al. Novel patterns of genome rearrangement and their association survival in breast cancer. Genome Res 2006; 16:1465-1479

56. Buerger H, Otterbach F, Simon R et al. Different genetic pathways in the evolution of invasive breast cancer are associated with distinct morphological subtypes. J Pathol, 1999; 189: 521-26.

57. Buerger H, Mommers EC, Littmann R et al. Ductal invasive G2 and G3 carcinomas of the breast are the end stages of at least two different lines of genetic evolution. J Pathol 2001; 194: 165-70.

58. Buerger H, Simon R, Schäfer KL et al. Genetic relation of lobular carcinoma in situ, ductal carcinoma in situ, and associated invasive carcinoma of the breast. Mol Pathol 2000; 53: 118-121.

59. Simpson PT, Reis-Filho JS, Lambros MB et al. Molecular profiling pleomorphic lobular carcinomas of the breast: evidence for a common molecular genetic pathway with classic lobular carcinomas. J Pathol 2008; 215: 231-244

60. Reis-Filho JS, Simpson PT, Gale T et al. The molecular genetics of breast cancer: The contribution of comparative genomic hybridization. Pathol Res Pract 2005; 201:713-725.

61. Roylance R, Gorman P, Harris W et al. Comparative genomic hybridization of breast tumors stratified by histological grade reveals

new insights into the biological progression of breast cancer. Cancer Breast Res 1999; 59: 1433-1436

62. Wicha MS, Liu S, Dontu G. Cancer stem cells: an old idea--a paradigm shift. Cancer Res. 2006; 66:1883-90; discussion 1895-6.

63. O'Connell P, Pekkel V, Fuqua S et al. Molecular genetic studies of early breast cancer evolution. Breast Cancer Res Treat. 1994; 32:5-12.

64. Trosko JE, Chang CC, Upham BL et al. Ignored hallmarks of carcinogenesis: stem cells and cell-cell communication. Ann N Y Acad Sci 2004; 1028:192-201.

65. Metsuyanim S, Pode-Shakked N, Schmidt-Ott KM et al. Accumulation of malignant renal stem cells is associated with epigenetic changes in normal renal progenitor genes. Stem Cells 2008; 26:1808-17.

66. Arpino G, Laucirica R, Elledge RM. Pre-malignant and in situ breast disease: biology and clinical implications. Ann intern Med 2005; 143:446-57.

67. Allred DC, Mohsin SK, Fuqua SA. Histological and biological evolution of human premalignant breast disease. Endocr Relat Cancer 2001; 8:47-61.

68. Jones JL. Over diagnosis and over treatment of breast cancer: progression of ductal carcinoma in situ: the pathological perspective. Breast Cancer Res 2006; 8:204.

69. Schnitt SJ, Vincent-Salomon A. Columnar cell lesions of the breast. Adv Anat Pathol 2003; 10:113-124.

70. Vincent-Salomon A. Columnar lesions: a frequent diagnosis in breast pathology! Ann Pathol. 2003; 23:593-596

71. Simpson PT, Gale T, Reis-Filho JS et al. Columnar cell lesions of the breast: The missing link in breast cancer progression? A morphological and molecular analysis. Am J Surg Pathol 2005; 29:734-746

72. Goldstein NS, O'Malley BA. Cancerization of small ectatic ducts of the breast by ductal carcinoma in situ cells with apocrine snouts: a lesion associated with tubular carcinoma. Am J Clin Pathol, 1997; 107: 561-566.

73. Guerra-Wallace MM, Christensen WN, White RL. A retrospective study of columnar alteration with prominent apical snouts and secretions and the association with cancer. Am J Surg Pathol 2004; 188:395-398.

74. Oyama T, Iijima K, Takei H et al. Atypical cystic lobule of the breast: an early stage of low-grade ductal carcinoma in-situ. Breast Cancer. 2000; 7:326-331.

75. Moinfar F, Man YG, Bratthauer GL et al. Genetic abnormalities in mammary ductal intraepithelial neoplasia-flat type ("clinging ductal carcinoma in situ"): a simulator of normal mammary epithelium. Cancer 2000; 88:2072-2082.

76. Sahoo S, Recant WM. Triad of columnar cell alteration, lobular carcinoma in situ and tubular carcinoma of the breast. Breast J 2005; 11:140-142.

77. Tavassoli FA, Hoefler H, Rosai J et al. Intraductal proliferative lesions. In: Tavassoli FA, Devilee P, eds. Pathology and Genetics of Tumours of the Breast and Female Genital Organs. Lyon: IARC Press 2003; 63-73.

78. Bai M, Agnantis NJ, Kamina S et al. In vivo cell kinetics in breast carcinogenesis. Breast Cancer Res 2001; 3:276-83.

79. Liu C, Zhang H, Shuang C et al. Alternations of ER, PR, HER-2/neu, and P53 protein expression in ductal breast carcinomas and clinical implications. Med Oncol 2009. [Epub ahead of print].

80. Livasy CA, Perou CM, Karaca G et al. Identification of a basal-like subtype of breast ductal carcinoma in situ. Hum Pathol 2007; 38:197-204..

81. Reis-Filho JS, Lakhani SR. The diagnosis and management of pre-invasive breast disease: Genetic alterations in pre-invasive lesions. Breast Cancer Res 2003; 5:313-319.

82. Shelley Hwang E, Nyante SJ, Yi Chen Y et al. Clonality of lobular carcinoma in situ and synchronous invasive lobular carcinoma. Cancer 2004; 100:2562-2572

83. Fraser JL, Raza S, Chorni K et al. Columnar alteration with prominent apical snouts and secretions: a spectrum of changes frequently present in breast biopsies performed for microcalcifications. Am J Surg Pathol 1998; 22:1521-1527.

84. Lakhani SR. Molecular genetics of solid tumours: translating research into clinical practice. What we could do now: breast cancer. Mol Pathol 2001, 54:281-284.

85. Rossen PP. Columnar cell hyperplasia is associated with lobular carcinoma in situ and tubular carcinoma. Am J Surg Pathol 1999; 1523:1561.

86. NHSBSP, RCPath. Pathological reporting of breast disease: a joint document incorporating the third edition of the NHS Breast Screening Programme's Guidelines for pathology reporting in breast cancer screening and the second edition of the royal college of pathologists' minimum dataset for breast cancer histopathology. NHSBSP Publication No 58. Sheffield: NHSBSP; 2005.

87. Abd El-Rehim DM, Ball G, Pinder S, et al. High-throughput protein expression analysis using tissue microarray technology of a large well-characterised series identifies biologically distinct classes of breast cancer confirming recent cDNA expression analyses. Int J Cancer 2005; 116:340-350.

88. Fenandez-Aguilar S, Simon P, Buxant F et al. Tubular carcinoma of the breast and associated intra-epithelial lesions: a comparative study with invasive low-grade ductal carcinomas. Virchows Arch 2005; 447:683-687.

89. Gong G, DeVries S, Chew KL et al. Genetic changes in paired atypical and usual ductal hyperplasia of the breast by comparative genomic hybridization. Clin Cancer Res 2001; 7:2410-2414.

90. Waldman FM, Hwang ES, Etzell J et al. Genomic alterations in tubular breast carcinomas. Hum Pathol 2001; 32:222-226.

91. Gunther K, Merkelbach-Bruse, Amo-Takyi BK et al. Differences in genetic alterations between primary lobular and ductal breast cancers detected by comparative genomic hybridization. J Pathol 2001; 193:40-47.

92. Goldstein NS, Kestin LL, Vicini FA. Refined morphologic criteria for tubular carcinoma to retain its favorable outcome status in contemporary breast carcinoma patients. Am J Clin Pathol 2004; 122:728-739.

93. Sullivan T, Raad RA, Goldberg S et al. Tubular carcinoma of the breast: a retrospective analysis and review of the literature. Breast Cancer Res Treat 2005; 93:199-205.

94. Bratthauer GL, Tavassoli FA. Assessment of lesions coexisting with various grades of intraepithelial neoplasia of the breast. Virchows Arc. 2004; 444:340-344.

95. Brogi E, Oyama T, Koerner FC. Atypical cystic lobules in patients with lobular neoplasia. Int J Surg Pathol 2001; 9:201-206.

96. Soslow RA, Carlson DL, Horenstein MG et al. A comparison of cell cycle markers in well-differentiated lobular and ductal carcinomas. Breast Cancer Res Treat 2000; 61:161-171.

97. Vos CB, Cleton-Jansen AM, Berx G et al. E-cadherin inactivation in lobular carcinoma in situ of the breast: an early event in tumorigenesis. Br J Cancer 1997; 76:1131-1133.

98. Wheeler DT, Tai LH, Bratthauer GL et al. Tubulolobular carcinoma of the breast: an analysis of 27 cases of a tumor with a hybrid morphology and immunoprofile. Am J Surg Pathol 2004; 28: 1587-1593.

99. Cleton-Jansen AM, Buerger H, Ter-Haar N et al. Different mechanisms of chromosome 16 loss of heterozygosity in well- versus poorly differentiated ductal breast cancer. Genes Chromosom Cancer 2004; 41:109-116..

100. Reis-Filho JS, Savage K, Lambros MBK et al. Cyclin D1 protein overexpression and CCND1 amplification in breast carcinomas: an immunohistochemical and chromogenic in situ hybridisation analysis. Mod Pathol 2006; 19:999-1009.

101. Man SM, Ellis IO, Sibbering M et al. High levels of allele loss at the FHIT and ATM genes in non-comedo ductal carcinoma in situ and grade 1 tubular invasive breast. J Pathol 1997; 182:A1-A1.

102. Ding SL, Sheu LF, Yu JC et al. Abnormality of the DNA double-strand-break checkpoint/repair genes, ATM, BRCA1 and TP53, in breast cancer is related to tumour grade. Br J Cancer 2004; 90:1995-2001.

103. Shaaban AM, O'Niell PA, Davies MP, et al. Declining estrogen receptor beta expression defines malignant progression of human breast neoplasia. Am J Surg Pathol 2003; 27:1502-1512.

104. Abdel-Fatah TM, Powe DG, Hodi Z. et al. Morphologic and molecular evolutionary pathways of low nuclear grade invasive breast cancers and their putative precursor lesions: further evidence to support the concept of low nuclear grade breast neoplasia family. Am J Surg Pathol 2008; 32: 513-523.

105. Vagunda V, Smardová J, Vagundová M et al. Correlations of breast carcinoma biomarkers and p53 tested by FASAY and immunohistochemistry. Pathol Res Pract 2003; 199: 795-801.

106. Callagy GM, Pharoah PD, Pender SE et al. Bcl2 is a prognostic marker in breast cancer independently of the Nottingham Prognostic Index. Clin Cancer Res 2006; 12: 2468-2475.

107. Tan DS, Marchió C, Jones RL et al. Triple negative breast cancer: molecular profiling and prognostic impact in adjuvant anthracycline-treated patients. Breast Cancer Res Treat; 2008; 111:27-44.

108. Shaaban AM, Green AR, Karthik S et al. Nuclear and cytoplasmic expression of ERbeta1, ERbeta2, and ERbeta5 identifies distinct prognostic outcome for breast cancer patients. Clin Cancer Res 2008;14:5228-35.

109. Wolff AC, Hammond ME, Schwartz JN et al. American Society of Clinical Oncology/College of American Pathologists Guideline Recommendations for Human Epidermal Growth Factor Receptor 2 Testing in Breast Cancer. Clin Oncol 2007; 25:1-28.

110. Allred DC, Harvey JM, Berardo M et al. Prognostic and predictive factors in breast cancer by immunohistochemical analysis. Mod Pathol 1998; 11: 155-168.

111. Aubele MM, Cummings MC, Mattis AE et al. Accumulation of chromosomal imbalances from intraductal proliferative lesions to adjacent in situ and invasive ductal breast cancer. Diagn Mol Pathol 2000; 9:14-19.

112. Böcker W, Buerger H, Schmitz K et al. Ductal epithelial proliferations of the breast: a biological continuum? Comparative genomic hybridization and high-molecular-weight cytokeratin expression patterns. J Pathol 2001; 195:415-421.

113. Jones C, Merrett S, Thomas VA et al. Comparative genomic hybridization analysis of bilateral hyperplasia of usual type of the breast. J Pathol 2003; 199:152-156..

114. Cheng GJ, Li Y, Omoto Y et al. Differential regulation of estrogen receptor (ER) alpha and ER beta in primate mammary gland. J Clin Endocrinol Metab 2005; 90:435-444.

115. Tremblay G, Deschenes J, Alpert L et al. Overexpression of estrogen receptors in columnar cell change and in unfolding breast lobules. Breast J 2005; 11:326-332.

116. Fletcher CDM. Expert Commentary 2002; 83-84.

117. Reis-Filho JS. Re: Korsching et al. The origin of vimentin expression in invasive breast cancer: epithelial-mesenchymal transition, myoepithelial histogenesis or histogenesis from progenitor cells with bilinear differentiation potential? J Pathol 2005; 206: 451-457. J Pathol 2005; 207:367-369.

118. McCarthy A, Savage K, Gabriel A et al. A mouse model of basal-like breast carcinoma with metaplastic elements. J Pathol 2007; 211:389-398.

119. Shaw JA, Udokang K, Mosquera JM et al. Oestrogen receptors alpha and beta differ in normal human breast and breast carcinomas. J Pathol 2002; 198:450-457.

120. Roger P, Sahla ME, Makela S et al. Decreased expression of estrogen receptor beta protein in proliferative preinvasive mammary tumors. Cancer Res 2001; 61:2537-2541.

121. Iwao K, Miyoshi Y, Egawa C et al. Quantitative analysis of estrogen receptor-alpha and -beta messenger RNA expression in breast carcinoma by real-time polymerase chain reaction. Cancer 2000; 89:1732-1738.

122. Alle K, Henshall S, Field A, et al. Cyclin D1 protein is overexpressed in hyperplasia and intraductal carcinoma of the breast. Clin Cancer Res 1998; 4: 847-854.

123. Oh YL, Choi JS, Song SY et al. Expression of p21 (Waf1), p27 (Kip1) and cyclin D1 proteins in breast ductal carcinoma in situ: Relation with clinicopathologic characteristics and with p53 expression and estrogen receptor status. Pathol Int 2001; 51:94-99.

124. Bardin A, Boulle N, Lazennec G et al. Loss of ER beta expression as a common step in estrogen-dependent tumor progression. Endocr Relat Cancer 2004; 11:537-551.

125. Paruthiyil S, Parmar H, Kerekatte V et al. Estrogen receptor beta inhibits human breast cancer cell proliferation and tumor formation by causing a G(2) cell cycle arrest. Cancer Res 2004; 64:423-428.

126. Liu MM, Albanese C, Anderson CM et al. Opposing action of estrogen receptors alpha and beta on cyclin D1 gene expression. J Biol Chem 2002; 277:24353-24360.

127. Luna-More S, Weil B, Bautista D, Garrido E et al. Bcl-2 protein in normal, hyperplastic and neoplastic breast tissues. A metabolite of the putative stem-cell subpopulation of the mammary gland. Histol Histopathol 2004; 19:457-463.

128. Yang QF, Sakurai T, Jing XF et al. Expression of Bcl-2, but not Bax, correlates with estrogen receptor status and tumor

proliferation in invasive breast carcinoma. Pathol Int 1999; 49:775-780.

129. Cuatrecasas M, Santamaria G, Velasco M et al. ATM gene expression is associated with differentiation and angiogenesis in infiltrating breast carcinomas. Histol Histopathol 2006; 21:149-156.

130. Gasco M, Shami S, Crook T. The p53 pathway in breast cancer. Breast Cancer Res 2002; 4:70-76.

131. Sevignani C, Calin GA, Cesari R, et al. Restoration of fragile Histidine triad (FHIT) expression induces apoptosis and suppresses tumorigenicity in breast cancer cell lines. Cancer Res 2003; 63:1183-1187.

132. Elston CW, Ellis IO. Pathological prognostic factors in breast cancer: I. The value of histologic grade in breast cancer-Experience from a large study with long-term follow up. Histopathology 1991; 19:403-410.

133. Rakha EA, El-Sayed ME, Lee AHS et al. Prognostic significance of Nottingham histologic grade in invasive breast cancer. J Clin Oncol 2008; 26:3153-3158

134. Ignatiadis M, Sotiriou C. Understanding the molecular bases of histologic grade. Pathobiology 2008; 75:104-111.

135. Singletary SE, Allred C, Ashley P et al. Revision of the American Joint Committee on Cancer staging system for breast cancer. J Clin Oncol 2002; 20:3628-3636.

136. Desmedt C, Haibe-Kains B, Wirapati P et al. Biological processes associated with breast cancer clinical outcome depends on the molecular subtypes. Clin Cancer Res 2008; 14:5158-5165.

137. Blamey RW, Ellis IO, Pinder SE et al. Survival of invasive breast cancer according to the Nottingham Prognostic Index in cases diagnosed in 1990-1999. Eur J Cancer 2007; 43: 1548-1555.

138. Marchiò C, Iravani M, Natrajan R et al. Mixed micropapillary-ductal carcinomas of the breast: a genomic and immunohistochemical analysis of morphologically distinct components. J Pathol 2009; 218:301-315.

139. Caffo O, Doglioni C, Veronese S et al. Prognostic value of p21 (WAF1) and p53 expression in breast carcinoma: an immunohistochemical study in 261 patients with long-term follow-up. Clin Cancer Res 1996; 2: 1591-1599.

140. Natrajan R, Lambros MB, Geyer FC et al. Loss of 16q in high grade breast cancer is associated with estrogen receptor status: Evidence for progression in tumors with a luminal phenotype? Genes Chromosomes Cancer 2009; 48:351-65.

141. Baak JP, Van diest PJ, Voorhorst FJ et al. Prospective multicenter validation of the independent prognostic value of the mitoyic activity index in lymph node negative breast cancer patients younger than 55 years. J Clin Oncol 2005; 23: 5993-6001.

142. Paik S, Shak S, Tang G et al. A multigene assay to predict recurrence of tamoxifen-treated, node-negative breast cancer. N Engl J Med 2004; 351:2817–2826.

143. Wang Y, Klijn J, Zhang Y et al. Gene-expression profiles to predict distant metastasis of lymph-node-negative primary breast cancer. Lancet 2005; 365:671–679.

144. Reed JC. Bcl-2 and the regulation of programmed cell death. J Cell Biol 1994; 124: 1–6.

145. Quinn CM, Ostrowski JL, Harkins L. Loss of bcl-2 expression in ductal carcinoma in situ of the breast relates to poor histological

differentiation and to expression of p53 and c-erbB-2 proteins. Histopathology 1998; 33:531-536.

146. Sierra A, Castellsagué X, Escobedo A et al. Bcl-2 with loss of apoptosis allows accumulation of genetic alterations: a pathway to metastatic progression in human breast cancer. Int J Cancer 2000; 89:142-147.

147. Teixeira C, Reed JC, Pratt MA. Estrogen promotes chemotherapeutic drug resistance by a mechanism involving Bcl-2 proto-oncogene expression in human breast cancer cells. Cancer Res 1995; 55:3902–3907.

148. O'Reilly LA, Huang DC, Strasser A. The cell death inhibitor Bcl-2 and its homologues influence control of cell cycle entry. EMBO J 1996; 15:6979–6990,

149. William GH, Stoeber K. Cell cycle markers in clinical oncology. Curr opin Cell Biol 2000; 19: 672-679.

150. Nakayama T, Taback B, Turner R et al. Molecular clonality of in-transit melanoma metastasis. Am J Pathol. 2001; 158:1371-8.

151. Werner M, Mattis A, Aubele M et al. 20q13.2 amplification in intraductal hyperplasia adjacent to in situ and invasive ductal carcinoma of the breast. Virchows Archiv 1999;, 435: 469-472.

152. Jeffrey SS, Pollack JR. The diagnosis and management of pre-invasive breast disease: promise of new technologies in understanding pre-invasive breast lesions. Breast Cancer Res 2005; 5: 320-328.

153. Cardoso J, Molenaar L, de Menezes RX, et al. Genomic profiling by DNA amplification of laser capture microdissected tissues and array CGH. Nucleic Acids Res 2004; 32:e146.

154. Johnson NA, Hamoudi RA, Ichimura K et al. Application of array CGH on archival formalin-fixed paraffin-embedded tissues including small numbers of microdissected cells. Lab Invest. 2006 Sep;86(9):968-78.

155. Weigelt B, Horlings HM, Kreike B, et al. Refinement of breast cancer classification by molecular characterization of histological special types. J Pathol. 2008; 216:141-50.

156. Kallioniemi A, Kallioniemi OP, Sudar D, et al. Comparative genomic hybridization for molecular cytogenetic analysis of solid tumors. Science. 1992; 258:818-21.

157. Pinkel D, Segraves R, Sudar D, et al. High resolution analysis of DNA copy number variation using comparative genomic hybridization to microarrays. Nat Genet. 1998; 20:207-11

158. Jobanputra V, Sebat J, Troge J, et al. Application of ROMA (representational oligonucleotide microarray analysis) to patients with cytogenetic rearrangements. Genet Med. 2005; 7:111-8.

159. Pollack JR, Perou CM, Alizadeh AA, et al. Genome-wide analysis of DNA copy-number changes using cDNA microarrays. Nat Genet. 1999; 23:41-6.

160. Solinas-Toldo S, Lampel S, Stilgenbauer S, et al. Matrix-based comparative genomic hybridization: biochips to screen for genomic imbalances. Genes Chromosomes Cancer. 1997; 20:399-407.

161. Inazawa J, Inoue J, Imoto I. Comparative genomic hybridization (CGH)-arrays pave the way for identification of novel cancer-related genes. Cancer Sci. 2004; 95: 559-63.

162. Oostlander AE, Meijer GA, Ylstra B. Microarray-based comparative genomic hybridization and its applications in human genetics. Clin Genet. 2004; 66:488-95.

163. Li MM. Molecular Cytogenetics: Protocols and Applications. Am J Hum Genet. 2003; 72: 1353.

164. Wilkens L, Bredt M, Flemming P. Comparative genomic hybridization (CGH) and fluorescence in situ hybridization (FISH) in the diagnosis of hepatocellular carcinoma. J Hepatobiliary Pancreat Surg 2002; 9:304-11.

165. Bassem A. Bejjani and Lisa G. Shaffer. Application of Array-Based Comparative Genomic Hybridization to Clinical Diagnostics. J Mol Diagn 2006; 8: 528–533.

166. van Beers EH, Joosse SA, Ligtenberg MJ et al. A multiplex PCR predictor for aCGH success of FFPE samples. Br J Cancer 2006; 94, 333-337.

167. Dietrich D, Lesche R, Tetzner R et al. Analysis of DNA methylation of multiple genes in microdissected cells from formalin-fixed and paraffin-embedded tissues. J Histochem Cytochem 2009;57: 477-89.

168. Devries S, Nyante S, Korkola J, Segraves R, et al. Array-based comparative genomic hybridization from formalin-fixed, paraffin-embedded breast tumors. J Mol Diagn. 2005; 7:65-71.

169. Paris PL, Albertson DG, Alers JC, et al. High-resolution analysis of paraffin-embedded and formalin-fixed prostate tumors using comparative genomic hybridization to genomic microarrays. Am J Pathol. 2003; 162:763-70.

170. Santos S, Sá D, Bastos E, Guedes-Pinto H, et al. An efficient protocol for genomic DNA extraction from formalin-fixed paraffin-embedded tissues. Res Vet Sci. 2009; 86(3):421-6.

171. Wang G, Maher E, Brennan C et al. DNA amplification method tolerant to sample degradation. Genome Res 2004; 4:2357-66.

172. Curran S, Murray GI. An introduction to laser based tissue microdissection techniques. In: Murray GI, Curran S, eds. Laser captures microdissection; methods and protocols. New Jersey: Human press 2005; 3-11.

173. Gunnarsson R, Staaf J, Jansson M et al. Screening for copy-number alterations and loss of heterozygosity in chronic lymphocytic leukemia-a comparative study of four differently designed, high resolution microarray platforms. Genes Chromosomes Cancer 2008; 47: 697-711.

174. JMD CME Program in Molecular Diagnostics 2006. The Journal of Molecular Diagnostics 2006; 8. www. imd. amjpatholo..org/ cgi/ issue_pdf/backmatter_pdf/8/5.pdf.

175. Mackay A, Tamber N, Fenwick K et al. A high-resolution integrated analysis of genetic and expression profiles of breast cancer cell lines. Breast Cancer Res Treat. 2009; 118:481-98...

176. Chin SF, Teschendorff AE, Marioni JC et al. High-resolution aCGH and expression profiling identifies a novel genomic subtype of ER negative breast cancer. Genome Biol 207; 8:R215.

177. Vousden KH, Prives C. p53 and prognosis: new insights and further complexity. Cell 2005; 120:7-10.

178. Lønning PE, Knappskog S, Staalesen V et al. Breast cancer prognostication and prediction in the postgenomic era. Ann Oncol 2007; 18:1293-1306.

179. Vogelstein B, Lane D, Levine AJ. Surfing the p53 network. Nature. 2000; 408: 307-310.

180. Børresen-Dale AL. TP53 and breast cancer. Hum Mutat 2003; 21:292-300.

181. Toledo F, Wahi GM. MDM2 and MDM4: p53 regulators and targets in anticancer therapy. Int J Biochem Cell Biol. 2007; 39: 1476-1482.

182. Danovi D, Meulmeester E, Pasini D, et al. Amplification of Mdmx (or Mdm4) directly contributes to tumor formation by inhibiting p53 tumor suppressor activity. Mol Cell Biol. 2004; 24:5835-43.

183. Veerakumarasivam A, Scott HE, Chin SF et al. High resolution array-based Comparative Genomic Hybridization of bladder cancers identifies Mouse Double Minute 4 (MDM4) as an amplification target exclusive of MDM2 and PT53. Clin Cancer Res 2008; 14:2527-2534.

184. Boulay PL, Cotton M, Melançon P et al. ADP-ribosylation factor 1 controls the activation of the phosphatidylinositol 3-kinase pathway to regulate epidermal growth factor-dependent growth and migration of breast cancer cells. J Biol Chem 2008 ;283: 36425-34.

185. Balakrishnan A, Bleeker FE, Lamba S et al. Novel somatic and germline mutations in cancer candidate genes in glioblastoma, melanoma, and pancreatic carcinoma. Cancer Res 2007 ;67:3545-50.

186. Finak G, Bertos N, Pepin F, et al. Stromal gene expression predicts clinical outcome in breast cancer. Nat Med 2008; 14:518-27.

187. Zhang Y, Martens JW, Yu JX, et al. Copy number alterations that predict metastatic capability of human breast cancer. Cancer Res 2009; 69:3795-801.

188. Aurich-Costa J, Cadel S, Gouzy C et al. Assignment of the aminopeptidase B gene (RNPEP) to human chromosome 1 band q32 by in situ hybridization. Cytogenet Cell Genet 1997;79:143-4.

189. Schuetz CS, Bonin M, Clare SE et al. Progression-specific genes identified by expression profiling of matched ductal carcinomas in situ and invasive breast tumors, combining laser capture

microdissection and oligonucleotide microarray analysis. Cancer Res 2006; 66:5278-86.

190. Farmer P, Bonnefoi H, Becette V et al. Identification of molecular apocrine breast tumours by microarray analysis. Oncogene 2005 Jul 7; 24(29):4660-71.

191. Lin CY, Ström A, Vega VB et al. Discovery of estrogen receptor alpha target genes and response elements in breast tumor cells. Genome Biol. 2004; 5:R66.

192. Karmakar S, Foster EA, Smith CL. Estradiol downregulation of the tumor suppressor gene BTG2 requires estrogen receptor-alpha and the REA corepressor. Int J Cancer 2009 ;124:1841-51.

193. Kawakubo H, Brachtel E, Hayashida Tet al. Loss of B-cell translocation gene-2 in estrogen receptor-positive breast carcinoma is associated with tumor grade and overexpression of cyclin d1 protein. Cancer Res 2006;66:7075-82.

194. Boiko AD, Porteous S, Razorenova OVet al. A systematic search for downstream mediators of tumor suppressor function of p53 reveals a major role of BTG2 in suppression of Ras-induced transformation. Genes Dev. 2006;20: 236-52.

195. Mikaelsson E, Danesh-Manesh AH, Lüppert Aet al. Fibromodulin, an extracellular matrix protein: characterization of its unique gene and protein expression in B-cell chronic lymphocytic leukemia and mantle cell lymphoma. Blood 2005;105:4828-35.

196. Yuan S, Shi C, Liu L et al. MUC1-based recombinant Bacillus Calmette-Guerin vaccines as candidates for breast cancer immunotherapy. Expert Opin Biol Ther 2010. [Epub ahead of print]

197. Bitler BG, Goverdhan A, Schroeder JA. MUC1 regulates nuclear localization and function of the epidermal growth factor receptor. J Cell Sci. 2010;123: 1716-23.

198. Khodarev N, Ahmad R, Rajabi H et al. Cooperativity of the MUC1 oncoprotein and STAT1 pathway in poor prognosis human breast cancer. Oncogene 2010 ;29: 920-9.

199. Zhang WH, Poh A, Fanous AA et al. DNA damage-induced S phase arrest in human breast cancer depends on Chk1, but G2 arrest can occur independently of Chk1, Chk2 or MAPKAPK2. Cell Cycle 2008;7:1668-77

200. Salh B, Marotta A, Wagey R et al. Dysregulation of phosphatidylinositol 3-kinase and downstream effectors in human breast cancer. Int J Cancer 2002; 98:148-54.

201. Paine E, Palmantier R, Akiyama SK et al. Arachidonic acid activates mitogen-activated protein (MAP) kinase-activated protein kinase 2 and mediates adhesion of a human breast carcinoma cell line to collagen type IV through a p38 MAP kinase-dependent pathway. J Biol Chem 2000 ;275:11284-90

202. Adélaïde J, Finetti P, Bekhouche I, et al. Integrated profiling of basal and luminal breast cancers. Cancer Res 2007; 67: 11565-75.

203. Fu YP, Edvardsen H, Kaushiva A et al. NOTCH2 in breast cancer: association of SNP rs11249433 with gene expression in ER-positive breast tumors without TP53 mutations. Mol Cancer 2010 ;9: 113-17

204. Parr C, Watkins G, Jiang WG. The possible correlation of Notch-1 and Notch-2 with clinical outcome and tumour clinicopathological parameters in human breast cancer. Int J Mol Med 2004 ;14:779-86.

205. O'Neill CF, Urs S, Cinelli C et al. Notch2 signaling induces apoptosis and inhibits human MDA-MB-231 xenograft growth. Am J Pathol 2007;171:1023-36

206. Ma X, Wang X, Gao X et al. Identification of five human novel genes associated with cell proliferation by cell-based screening from an expressed cDNA ORF library. Life Sci 2007 ;81:1141-51

207. Childs KS, Goodbourn S. Identification of novel co-repressor molecules for Interferon Regulatory Factor-2. Nucleic Acids Res 2003;31: 3016-26.

208. Rosa-Rosa JM, Pita G, González-Neira A et al. A 7 Mb region within 11q13 may contain a high penetrance gene for breast cancer. Breast Cancer Res Treat 2009 ;118:151-9.

209. Lundgren K, Holm K, Nordenskjöld B et al. Gene products of chromosome 11q and their association with CCND1 gene amplification and tamoxifen resistance in premenopausal breast cancer. Breast Cancer Res 2008;10:R81

210. Wang P, Wang X, Wang F et al. Interaction between Mnk2 and CBC(VHL) ubiquitin ligase E3 complex. Sci China C Life Sci 2006 ;49: 265-73

211. Chrestensen CA, Shuman JK, Eschenroeder A et al. MNK1 and MNK2 regulation in HER2-overexpressing breast cancer lines. J Biol Chem. 2007; 282:4243-52.

212. Carinci F, Arcelli D, Lo Muzio L et al. Molecular classification of nodal metastasis in primary larynx squamous cell carcinoma. Transl Res 2007;150: 233-45

213. Mandal S, Davie JR. An integrated analysis of genes and pathways exhibiting metabolic differences between oestrogen receptor positive breast cancer cells. BMC Cancer. 2007; 7: 181.

214. Dutrillaux B, Gerbault-Seureau M, Zafrani B. Characterization of chromosomal anomalies in human breast cancer. A comparison of 30 paradiploid cases with few chromosome changes. Cancer Genet Cytogenet 1990;49:203-17.

215. Tsarouha H, Pandis N, Bardi G et al. Karyotypic evolution in breast carcinomas with i(1)(q10) and der(1;16)(q10;p10) as the primary chromosome abnormality. Cancer Genet Cytogenet 1999;113:156-61

216. Farabegoli F, Hermsen MA, Ceccarelli C et al. Simultaneous chromosome 1q gain and 16q loss is associated with steroid receptor presence and low proliferation in breast carcinoma. Mod Pathol. 2004;17:449-55.

217. Pandis N, Jin Y, Gorunova L et al. Chromosome analysis of 97 primary breast carcinomas: identification of eight karyotypic subgroups. Genes Chromosomes Cancer 1995;12:173–185

218. Texeira MR, Pandis N, Heim S. Cytogenetic clues to breast carcinogenesis. Genes Chromosomes Cancer 2002;33:1–16

219. Davidsson J, Andersson A, Paulsson K et al. Tiling resolution array comparative genomic hybridization, expression and methylation analyses of dup(1q) in Burkitt lymphomas and pediatric high hyperdiploid acute lymphoblastic leukemias reveal clustered near-centromeric breakpoints and overexpression of genes in 1q22-32.3. Hum Mol Genet 2007 ;16:2215-25.

220. Mitelman F, Johansson B, Mertens F. Mitelman Database of Chromosome Aberrations in Cancer. (2010)

221. Narayan A, Ji W, Zhang X, Marrogi A et al. Hypomethylation of pericentromeric DNA in breast adenocarcinomas. Int J Cancer 1998; 77:833–838

222. Wong N, Lam W, Lai P, Pang Eet al. Hypomethylation of chromosome 1 heterochromatin DNA correlates with q-arm copy gain in human hepatocellular carcinoma. Am J Pathol 2001; 159:465–471

223. Sawyer J., Tricot G, Mattox S et al. Jumping translocations of chromosome 1q in multiple myeloma: evidence for a mechanism involving decondensation of pericentromeric heterochromatin. Blood 1998; 91:1732–1741

224. Fitzgibbons PL, Page DL, Weaver D et al. Prognostic factors in breast cancer. College of American Pathologists Consensus Statement 1999. Arch Pathol Lab Med.2000; 124: 966-978.

225. Lacroix M, Toillon RA, Leclercq G. p53 and breast cancer, an update. Endocr Relat Cancer. 2006; 13: 293-325.

226. Sjögren S, Inganäs M, Norberg T et al. The p53 gene in breast cancer: prognostic value of complementary DNA sequencing versus immunohistochemistry. J Natl Cancer Inst 1996; 88:173–182.

227. Geisler S, Lønning PE, Aas T et al. Influence of TP53 gene alterations and c-erbB-2 expression on the response to treatment with doxorubicin in locally advanced breast cancer. Cancer Res 2001; 61:2505–2512.

228. Nenutil R, Smardova J, Pavlova S et al. Discriminating functional and non-functional p53 in human tumours by p53 and MDM2 immunohistochemistry. J Pathol 2005; 207:251-259.

229. Liu W, Konduri SD, Bansal S et al. Oestrogen Receptor- Binds p53 Tumor Suppressor Protein Directly and Represses Its Function. J Biol Chem 2006; 281: 9837-9840.

230. Sayeed A, Konduri SD, Liu W et al. Estrogen receptor alpha inhibits p53-mediated transcriptional repression: implications for the regulation of apoptosis. Cancer Res 2007; 67:7746-55.

231. Rahko E, Blanco G, Bloigu R et al. Adverse outcome and resistance to adjuvant antiestrogen therapy in node-positive postmenopausal breast cancer patients-The role of p53. Breast 2006; 15:69-75.

232. Kandioler-Eckersberger D, Ludwig C, Rudas M et al: TP53 mutation and p53 overexpression for prediction of response to neo-adjuvant treatment in breast cancer patients. Clin Cancer Res 2000; 6:50-56.

233. Miller LD, Smeds J, George J et al. An expression signature for p53 status in human breast cancer predicts mutation status, transcriptional effects, and patient survival. Proc Natl Acad Sci U S A 2005; 102:13550–5.

234. Bertheau P, Espié M, Turpin E et al. TP53 status and response to chemotherapy in breast cancer. Pathobiology 2008; 75: 132-139.

235. Phelps M, Darley M, Primrose JN et al. p53-independent activation of the hDM2-P2 promoter through multiple transcription factor response elements results in elevated hdm2 expression in oestrogen receptor alpha positive breast cancer cells. Cancer Res 2003; 63: 2616 – 2623.

236. Hori M, Shimazaki J, Inagawa S et al. Overexpression of MDM2 oncoprotein correlates with possession of oestrogen receptor alpha and lack of MDM2 mRNA splice variants in human breast cancer. Breast Cancer Res Treat 2002; 71: 77 – 83.

237. Angèle S, Treilleux I, Tanière P et al. Abnormal expression of the ATM and TP53 genes in sporadic breast cancer. Clin Cancer Res 2000; 6:3536-3544.

238. Rayburn E, Zhang R, He J et al. MDM2 and human malignancies: expression, clinical pathology, prognostic markers, and implications for chemotherapy. Curr Cancer Drug Targets 2005; 5:27-41.

239. Yang W, Klos KS, Zhou X et al. ErbB2 overexpression in human breast carcinoma is correlated with p21Cip1 up-regulation and tyrosine-15 hyperphosphorylation of p34Cdc2: Poor responsiveness to chemotherapy with cyclophoshamide methotrexate, and 5-

fluorouracil is associated with Erb2 overexpression and with p21Cip1 overexpression. Cancer 2003; 98:1123–1130.

240. Waldman T, Lengauer C, Kinzler KW et al. Uncoupling of S phase and mitosis induced by anticancer agents in cells lacking p21. Nature 1996; 381: 713–716.

241. Wouters BG, Giaccia AJ, Denko NC et al. Loss of p21Waf1/Cip1 sensitizes tumors to radiation by an apoptosis-independent mechanism. Cancer Res 1997; 57: 4703-4706.

242. Weiss RH, Marshall D, Howard L et al. Suppression of breast cancer growth and angiogenesis by an antisense oligodeoxynucleotide to p21 (Waf1/Cip1). Cancer Lett 2003; 189: 39-48.

243. Maynadier M, Ramirez JM, Cathiard AM et al. Unliganded oestrogen receptor alpha inhibits breast cancer cell growth through interaction with a cyclin-dependent kinase inhibitor (p21 (WAF1). FASEB J 2008; 22: 671-681.

244. Ding L, Ellis MJ, Li S et al. Genome remodelling in a basal-like breast cancer metastasis and xenograft. Nature 2010 ;464:999-1005.

245. Lin EY, Jones JG, Li P et al. Progression to malignancy in the polyoma middle T oncoprotein mouse breast cancer model provides a reliable model for human diseases. Am J Pathol 2003 ;163: 2113-26.